Titre: Title:	Friction and wear of high speed polymer-metal contact
Auteur: Author:	Ibrahim El Fahham
Date:	1997
Type:	Mémoire ou thèse / Dissertation or Thesis
Référence: Citation:	El Fahham, I. (1997). Friction and wear of high speed polymer-metal contact [Ph.D. thesis, École Polytechnique de Montréal]. PolyPublie. https://publications.polymtl.ca/6804/

UNIVERSITÉ DE MONTRÉAL

FRICTION AND WEAR OF HIGH SPEED POLYMER-METAL CONTACT

IBRAHIM EL FAHHAM
DÉPARTEMENT DE GÉNIE MÉCANIQUE
ÉCOLE POLYTECHNIQUE DE MONTRÉAL

THÈSE PRÉSENTÉE EN VUE DE L'OBTENTION
DU DIPLÔME DE PHILOSOPHIAE DOCTOR (Ph.D.)
(GÉNIE MÉCANIQUE)
DÉCEMBRE 1997

UNIVERSITÉ DE MONTRÉAL

ÉCOLE POLYTECHNIQUE DE MONTRÉAL

Cette thèse intitulée:

FRICTION AND WEAR OF HIGH SPEED POLYMER-METAL CONTACT

Présentée par: **EL FAHHAM Ibrahim**

en vue de l'obtention du diplôme de: **Philosophiae Doctor**

a été acceptée par le jury d'examen constitué de:

M. FORTIN Clément, Ph.D., Président

M. GAUVIN Raymond, D. Sc. A., membre et directeur de recherche

M. YELLE Henri, Ph.D., membre et codirecteur de recherche

M. BOUKHILI Rachid, Ph.D. membre

M. CLOUTIER Louis, Ph.D. membre

To my Mother, my Father,
my Sisters and my Brother

To my Loving Family

ACKNOWLEDGMENTS

Thanks to God, master of the universe, who gave me his blessing and the strength to achieve this work.

I would like to thank professor Henri Yelle for his support and his guidance. He gave me graciously from his time and his experience what helped me achieving this work. Working with him was a great and pleasant experience and I am greatly indebted to him for what I have learned. I would also like to thank professor Raymond Gauvin for giving me the opportunity to work in such an intriguing project. He was always there when it was needed, and his critical comment and ultimate viewpoints guided me to establish the structure of my work.

I would also like thank the members of the jury, Professor Clément Fortin, Professor Louis Cloutier and Professor Rachid Boukhili, for accepting to evaluate and critique this thesis.

The success of such projects, depends always on the team spirit and the support of the technical team. This special team includes Jean Marie Béland, Éric Gérard, Richard Dallaire, Jacques Beausoleil, Anne Dionne and François Morin. Their great help and special technical skills were a major pillar in the success of this work.

Finally I would like to thank all my colleagues at École Polytechnique de Montréal, the students and the members of the Center for applied research on Polymers (CRASP), and all my friends for their wonderful support and kindness. The family ambiance and the collaboration of the group helped me considerably in the progress of my research.

RÉSUMÉ

Un tribomètre est réalisé pour étudier le frottement et l'usure du contact polymère-métal à hautes vitesses de glissement. Le tribomètre peut fonctionner à des vitesses allant jusqu'à 60 m/s et des charges jusqu'à 600 N. Il peut aussi soutenir des tests de longue durée avec des surfaces de contact élevées, allant jusqu'à 7 000 mm^2, en contact continu et discontinu.

La charge est appliquée par deux vérins pneumatiques et la force de frottement est mesurée par une cellule de charge de flexion. L'usure est mesurée par perte de poids. L'ordinateur du système permet la surveillance et le contrôle en temps réel de la charge, du coefficient de frottement et de la distribution de température à différents points du contact. Il est muni de systèmes de sécurité contre une usure excessive, une température du contact ou des roulements trop élevés, et une force de frottement élevée. La machine offre aussi la possibilité de faire des essais avec lubrification, en présence de particules abrasives.

Une équation simplifiée est développée pour calculer la chaleur générée par frottement, et dissipée par conduction et convection. L'équation permet de valider les mesures de température de contact en l'appliquant aux données de frottement et de température obtenues lors de différents tests de frottement. Les résultats ont démontré la précision des mesures quand le film de polymère transféré à la surface métallique est mince. La précision des mesures de température augmente avec la vitesse. Dans une autre série de tests, un thermocouple d'une faible épaisseur est inséré sous la surface de l'échantillon en polymère pour évaluer la température réelle du contact. Les tests confirment que la différence entre la température mesurée sous la surface métallique et la température réelle de contact est inférieure à la précision des thermocouples soit ±2°C. D'autre part, le dépôt d'un film épais réduit considérablement la précision de la mesure de température.

Des tests de frottement sont réalisés sur quatre polymères en contact avec l'acier avec une surface relativement élevée, de 2380 mm^2, en contact continu et discontinu. Les matériaux sont le PTFE (Polytétrafluoroéthylène), l'acétal homopolymère, le UHMWPE (polyéthylène à très haute masse moléculaire) et le nylon 6/6. En contact continu, les tests ont démontré que le PTFE a le coefficient de frottement le plus faible et une limite Pv la plus élevée qui dépasse de loin les valeurs rapportées dans la littérature. Le film de transfert instable de ce matériau réduit la force d'adhérence, mais entraîne un taux d'usure très élevé. L'acétal a un coefficient de frottement relativement faible et une limite Pv élevée. Son mécanisme d'usure est similaire à celui du PTFE. Le UHMWPE montre le taux d'usure le plus faible à vitesses modérées, mais sa limite Pv est plus faible que celles du PTFE et de l'acétal. Il dépose un film de transfert très mince qui adhère fortement à la surface métallique, ce qui entraîne un coefficient de frottement relativement faible avec un taux d'usure très faible. Le nylon 6/6 a à la fois le coefficient de frottement le plus élevé et la limite Pv la plus faible. Quand la température du contact se rapproche de sa température de transition vitreuse, le coefficient de frottement atteint des valeurs très élevées. Aussi, à haute vitesse de glissement, la surface du polymère fond; un film de transfert relativement épais est déposé sur la surface métallique, ce qui réduit considérablement la précision des mesures de température.

En général, le coefficient de frottement et le taux d'usure diminuent avec l'augmentation de la vitesse, jusqu'à la limite Pv du matériau. Aussi, le taux d'usure décroît avec l'augmentation de la température de contact. Par ailleurs, les valeurs de limite Pv observées lors des essais sont plus élevées que celles rapportées dans la littérature. La performance des matériaux testés est directement reliée à la nature du film déposé à différentes vitesses et à la stabilité des caractéristiques mécaniques du polymère à différentes températures de contact.

Quand on dépasse les valeurs du Pv limite des matériaux, on constate que le coefficient de frottement ne diminue pas avec l'augmentation de la vitesse et que le taux

d'usure devient excessif. Ceci contredit le modèle du contrôle thermique de frottement qui prévoit une diminution du coefficient de frottement avec l'augmentation de la vitesse de glissement quand la température de contact atteint la température de fusion du matériau. Ceci peut être attribué à la grandeur de la surface de contact et à la distribution non uniforme de l'usure le long de la surface; ceci limite l'effet lubrifiant de la surface fondue. Aussi, la surface réelle de contact augmente à haute température, entraînant une augmentation importante de la force d'adhérence.

En contact discontinu, les valeurs du coefficient de frottement observées sont légèrement plus élevées que celles en contact continu, à l'exception du Nylon 6/6. Les valeurs des limites Pv sont beaucoup plus faibles. De plus, les mécanismes d'usure sont les mêmes que ceux du contact continu pour tous les matériaux, mais avec un taux d'usure plus élevé. La performance unique du UHMWPE en contact discontinu, quand la température du contact dépasse sa température de fusion, mérite une étude plus approfondie.

Finalement, les mécanismes d'usure des polymères, au delà de leur limite Pv, peuvent affecter d'une façon importante la performance des machines dans lesquelles on retrouve de tels contact. Pour le PTFE et l'acétal, le matériau peut subir un taux d'usure élevé avec des débris d'usure relativement petits ou fondre sans déposer un film qui colle sur la surface métallique; ceci n'affectera pas ou peu la surface métallique en contact et peut prendre un certain temps avant de causer une défaillance du contact. Dans le cas du UHMWPE, le matériau maintient sa stabilité pour une certaine période. Après cette période, un taux d'usure très élevé se développe avec l'arrachement de grosses particules de la surface du polymère. Ces particules adhèrent à la surface métallique en contact et les deux surfaces peuvent se souder ensemble après que la machine est arrêtée. Pour le nylon 6/6, un film épais se dépose sur la surface métallique et endommage la surface du polymère; ceci engendre des vibrations dans le système, ce qui peut causer des problèmes mécaniques. Aussi, des grosses particules, résultant de l'accumulation du film déposé, peuvent être projetées de la surface à grandes vitesses et causer aussi certains dommages dans d'autres composantes de la machine.

ABSTRACT

A tribometer is designed to test the friction and wear properties of polymer-metal contact at high sliding speed. The tribometer is capable of running at speeds up to 60 m/s and loads up to 600 N with high rigidity and dynamic stability. The machine has the capacity to withstand long duration tests with large contact area, of up to 7 000 mm^2, in both continuous and discontinuous contact.

The load is applied by two pneumatic cylinders and the friction force is measured using a bending beam load cell. The wear rate is measured by weight. The system computer allows an on line control and monitoring of the load, the coefficient of friction and the temperature distribution at different points of contact. It is also equipped with safety features for high wear rates, excessive temperature rise, high friction force and bearing temperatures. The machine has also the capacity to work under lubricated conditions with and without abrasive particles.

A simplified equation is developed to calculate the heat generated by friction and dissipated by conduction and convection. The equation is also used to validate the temperature measurements of the tribometer by applying it on friction and temperature data from different tests. The correlation between the heat generated and the heat dissipated demonstrated the accuracy of the friction and temperature measurements in the cases where limited film deposition is likely to occur. The accuracy of the temperature measurement increases with increasing the sliding speed. In another test group, a fine thermocouple is inserted under the polymer specimen surface to evaluate the actual contact temperature. The tests confirmed that the difference between the temperature measured under the metallic specimen and the actual contact temperature is in the order of the thermocouples accuracy which is ± 2°C. On the other hand, thick film deposition would affect largely the accuracy of the temperature measurement.

Tests are conducted on four different polymers in contact with steel counterface at relatively large surfaces in both continuous and discontinuous contacts. The materials are PTFE (polytetrafluoroethylene), Acetal homopolymer, UHMWPE (ultrahigh molecular weight polyethylene) and Nylon 6/6. The continuous contact tests demonstrated that PTFE has the lowest friction coefficient and the highest Pv limit, which exceeds largely the limits found in literature. The unstable film transfer of this material decreases the adhesion force but leads to high wear rates. Acetal has also a relatively low coefficient of friction with relatively high Pv limits. Its wear mechanism is similar to PTFE. UHMWPE exhibits the minimum wear rate at moderate speeds but with lower Pv limits than PTFE and Acetal. The thin film transfer of this material adheres perfectly to the metallic surface, leading to a relatively low coefficient of friction and a very low wear rate. Nylon 6/6 has both the highest coefficient of friction and the lowest Pv limits. When the contact temperature reaches the polymer glass transition temperature, very high coefficient of friction is detected. In addition, surface melting is likely to occur at high sliding speed and the thick film deposition of Nylon 6/6 affects largely the temperature measurement.

Generally, the coefficient of friction and the wear rate decrease with increasing speed up to the material Pv limit. It is also concluded that the wear rate decreases with increasing the contact temperature. On the other hand, the Pv limits detected are much larger than that reported in the literature. The performance of those materials was directly related to the nature of the transfer film deposited at different speeds and their mechanical characteristics stability at different contact temperatures.

When exceeding the polymer Pv limits, it is found that the coefficient of friction does not decrease and very high wear rates occur. This contradicts the thermal control regime of friction model, which predicts a decrease in the friction coefficient with increasing speed after polymer surface melting. This contradiction may be attributed to the large contact surface and the nonuniform wear distribution along this surface which limits the lubrication effect of the molten surface. Furthermore, the real surface of contact increases due to the high

temperature developed leading to a significant increase in the adhesion force.

In discontinuous contact, the coefficient of friction is slightly higher, except for Nylon 6/6, whereas the Pv limit is much lower for all tested polymers. On the other hand, it is found that the wear mechanisms are the same as in continuous contact for all polymers, but with higher wear rates. The unique performance of UHMWPE at discontinuous contact, when the contact temperature exceeds its melting point, needs further investigations.

Finally, it is suggested that the wear mechanisms of polymers when exceeding their Pv limits would affect greatly the performance of the machine components involved. For PTFE and Acetal, the material may wear rapidly with relatively small debris or melt without depositing a film on the counterface surface; this would not affect the counterface materials and might take certain time before contact failure occurs. For UHMWPE, the material maintains its stability for a certain time, after which a very high wear rate occurs and large particles are smeared out from the surface. The particles adhere to the counterface surface and both surfaces may weld together after the machine is stopped. As for Nylon 6/6, the large films deposited on the counterface surface, with high polymer surface distortion, induce high vibrations in the system which may cause mechanical problems. The large film deposited may also be projected from the surface, which may cause certain damage to other components of the machine.

CONDENSÉ EN FRANÇAIS

Plusieurs applications tribologiques impliquent des contacts polymère-métal à haute vitesse de glissement. Certaines applications impliquent également des contacts discontinus ou intermittents, où la chaleur générée par frottement est très élevée. On retrouve des exemples de ce mode de contact dans les pneus de voiture et dans les glissières des motoneiges. Dans ce mode de contact, les propriétés mécaniques et les caractéristiques des deux surfaces jouent un rôle très important dans la définition du comportement tribologique du contact. Les coefficients de frottement statique et dynamique des polymères sont généralement plus faibles que ceux de l'acier ainsi que ceux de la plupart des matériaux métalliques. Toutefois, la faible conductivité thermique et la basse température de fusion des polymères limitent leurs performances à hautes vitesses et aux charges élevées sous lesquelles la probabilité d'apparition de fusion de surface et/ou d'usure excessive est augmentée.

La plupart des travaux de recherche portant sur le contact polymère-métal ont été réalisés à des vitesses inférieures à 5 m/s. D'autre part, la majorité des travaux de recherche expérimentaux ont été réalisés sur des machines de type pion sur disque, pour lesquels la surface de contact est très petite. Dans cette gamme de vitesses et d'aires de contact, le polytétrafluoroéthylène (PTFE) possède le coefficient de frottement le plus faible de tous les polymères, et le polyéthylène à très haute masse moléculaire (UHMWPE) démontre le taux d'usure le plus faible avec un coefficient de frottement modéré. Deux autres matériaux se distinguent: le polyamide 6/6 (nylon 6/6) qui possède des propriétés mécaniques intéressantes ainsi qu'une température de fusion assez élevée, et le polyoxyméthylène (acétal) qui démontre une bonne stabilité thermique, conservant ses propriétés mécaniques à des températures approchant son point de fusion. Dans les quelques études réalisées à haute vitesse, des traces de polymère fondu ont été observées sur la surface de contact, avec une

chute du coefficient de frottement. Évidement, dans des conditions semblables, la géométrie des surfaces en contact joue un rôle important dans le dégagement de la chaleur. À la connaissance de l'auteur, aucun résultat concernant la performance du UHMWPE, du PTFE ou de l'acétal, à très haute vitesse n'a été publié, spécialement pour des aires de contact élevées. Aussi, les différents mécanismes d'usure à températures de contact très élevées n'ont pas été étudiés.

L'objectif de ce travail de recherche est de construire un tribomètre capable de réaliser des tests à des vitesses et des charges élevées, avec une aire de contact importante, en contact continu et discontinu. Une fois le tribomètre construit, il permettra de faire des tests pour étudier l'effet de la vitesse, de la charge et de la température du contact sur le coefficient de frottement et l'usure du contact polymère-métal. Il permettra aussi d'étudier les différents mécanismes d'usure à hautes vitesses et températures de contact.

Suite à une étude de la littérature, on conclut que les contacts polymère-métal peuvent être classifiés selon la vitesse de contact en quatre catégories:

- Faibles vitesses: quand la variation de la température de contact est négligeable et n'affecte pas les caractéristiques mécaniques de la surface du polymère. Dans cette gamme de vitesse, le coefficient de frottement est indépendant de la vitesse. Toutefois, le taux d'usure augmente légèrement avec la vitesse.

- Vitesses modérées: quand la température de contact devient relativement élevée. Dans cette gamme de vitesse le coefficient de frottement augmente généralement avec la vitesse, et le taux d'usure diminue avec la vitesse.

- Vitesses élevées: quand la température de contact s'approche du point de fusion du polymère. Une augmentation rapide du coefficient de frottement est généralement observée avec un taux d'usure très élevé.

- Très hautes vitesses: après la fusion du polymère en surface. Dans cette gamme de vitesse, un modèle du contrôle thermique du frottement est proposé dans lequel le coefficient de frottement diminue avec l'augmentation de la vitesse ou de la charge. Ceci est basé sur une température caractéristique qui ne peut être dépassée, et ainsi une valeur maximale de la chaleur générée par frottement. Cette température dépend normalement de la température de fusion du polymère.

Aux vitesses faibles et modérées, on constate que la rugosité joue un rôle important dans le comportement tribologique des polymères. Une valeur optimale entre 0.14 et 0.35 μm Ra est recommandée pour obtenir un coefficient de frottement et un taux d'usure minima. À haute vitesse, l'effet de la rugosité de la surface est négligeable.

Pour simuler une application tribologique, on doit se rapprocher le plus possible des conditions réelles du contact. Ces conditions comprennent la température ambiante, le taux d'humidité, la présence de particules abrasives et/ou de lubrifiant. La vitesse de glissement, la charge, l'aire de contact et le mouvement relatif entre les deux surfaces doivent être déterminés et maintenus dans le modèle de contact.

Dans ce projet, un tribomètre a été conçu et fabriqué pour fonctionner sous charges et vitesses élevées en contact continu et discontinu. La charge est appliquée par deux vérins pneumatiques branchées à une source d'air comprimé. La pression des vérins est contrôlée par deux cartes électroniques. La force de frottement est mesurée par une cellule de charge qui utilise une poutre en flexion. Le taux d'usure est mesuré par perte de poids en utilisant une balance précise à 1.0×10^{-4} gramme. La température de contact et la chaleur dégagée sont évaluées en mesurant la température en différents points sous la surface métallique. L'ordinateur du système permet de contrôler la charge appliquée et d'observer l'évolution du coefficient de frottement et de la température à différents points de contact, en temps réel. Les différents systèmes de mesure du tribomètre sont calibrés et s'avèrent être fiables pour

des tests à des vitesses de 1 à 60 m/s, des charges qui s'élèvent jusqu'à 600 N et des températures de contact jusqu'à 400 °C. Le tribomètre est capable d'accommoder des tests de longues durées avec des aires de contact allant jusqu'à 7000 mm^2.

Le tribomètre peut aussi fonctionner lorsque de l'eau et des abrasifs sont injectés dans le contact. Une charte a été préparée pour déterminer le débit de l'eau à partir de la pression d'entrée de l'eau et de l'air. Le système d'injection d'eau et d' abrasif a été utilisé pour des tests industriels qui ne sont pas rapportés dans ce document à cause d'une entente de confidentialité. Le tribomètre a aussi la capacité de tester différentes combinaisons de matériaux. Plusieurs applications peuvent être étudiées; par exemples les glissières de motoneige, les freins à disques, les pneus et les paliers hydrostatiques ou hydrodynamiques.

Une équation simplifiée de transfert de chaleur est développée, et utilisée pour valider les mesures de température réalisées sur le tribomètre. L'équation développée a été appliquée pour des résultats de frottement et de température obtenus pour différents polymères en contact avec l'acier, à différentes vitesses de glissement. Les résultats ont démontrés que la précision des mesures de frottement et de la température est bonne à condition que le film de polymère déposé sur la surface métallique ne soit pas trop épais; l'erreur de mesure est alors de 2 à 5 %. La précision de mesure de température augmente avec la vitesse. Cette équation permet aussi de calculer la chaleur dissipée par conduction et celle dissipée par convection, ce qui permet de détecter des erreurs éventuelles de mesure de température.

Dans d'autres tests, un thermocouple fin est inséré dans l'échantillon de polymère à 1 mm de sa surface pour mesurer la température réelle de contact à différentes vitesses. Durant ces tests, on laisse l'échantillon de polymère s'user jusqu'à ce que le thermocouple touche la surface métallique. Pour le UHMWPE et l'acétal, les tests ont confirmé que la différence entre la température mesurée sous la surface métallique et la température au contact est de l'ordre de la précision des thermocouples (±2°C). Dans le cas du PTFE, la

différence est légèrement plus élevée; ceci peut être expliqué par son taux d'usure élevé qui isole partiellement la surface métallique. Pour le nylon 6/6, la mesure de température est affectée par le film déposé. La fusion de ce polymère, à des vitesses plus faibles que les autres, dépose sur la surface métallique un film épais et isolant qui affecte les mesures de température.

Trois séries de tests sont réalisées avec quatre polymères pour étudier leur caractéristiques en frottement et en usure à hautes vitesses, en contact continu, et une aire de contact de 2380 mm^2. Les polymères testés sont: le UHMWPE, le PTFE, l'acétal et le nylon 6/6.

Une première série de tests est effectuée à vitesse variable et charge constante. Ces tests sont effectués pour étudier la variation du coefficient de frottement avec la vitesse et déterminer les limites Pv. La procédure suivie est de débuter à une vitesse de 2 m/s, puis d'augmenter la vitesse de 2 m/s à tous les 10 minutes jusqu'à observer un taux d'usure très élevé ou la fusion du polymère sur la surface métallique. La procédure est répétée avec une charge de 120 N et de 200 N pour étudier l'effet de la charge sur le coefficient de frottement.

La deuxième série de tests est effectuée à vitesse et charge constantes. L'objectif est de déterminer le coefficient de frottement et le taux d'usure de chaque matériau à une vitesse et une charge données et d'étudier les mécanismes d'usure de chaque matériau à différentes vitesses. La procédure consiste à démarrer la machine avec un échantillon à une vitesse et une charge données pendant une (1) heure; l'échantillon est pesé avant et après le test. Le test est ensuite continué pendant une deuxième heure avec le même échantillon; une deuxième mesure de poids est faite à la fin. Ces tests sont réalisés à des vitesses de 2, 4, 6, 8, 16 et 30 m/s et une charge uniforme de 200 N.

La troisième série de tests est celle à charge variable et vitesse constante. Cette série est effectuée pour étudier l'effet de la charge sur le coefficient du frottement et sur les limites Pv. La procédure suivie durant ces tests est de commencer avec une charge de 30 N, puis d'augmenter la charge de 30 N à tous les 10 minutes jusqu'à avoir un taux d'usure très élevé ou observer la fusion du polymère sur la surface métallique. La procédure est répétée à 16 m/s puis à 30 m/s pour chaque matériau.

Les tests ont démontré que le PTFE possède le coefficient de frottement le plus faible et la limite Pv la plus élevée. Cependant son taux d'usure est très élevé, spécialement à vitesse modérée. Ce matériau démontre une stabilité élevée jusqu'à la vitesse maximale des tests, avec une limite Pv qui dépasse de loin celle rapportées dans la littérature. Le film de transfert de ce matériau diminue la force d'adhérence entre les surfaces de contact d'où un coefficient de frottement très faible. Cependant, le film se détache facilement de la surface ce qui entraîne un taux d'usure très élevé.

L'acétal a aussi un coefficient de frottement relativement faible avec une limite Pv relativement élevée. Son mécanisme d'usure est similaire que celui du PTFE. Cependant, sa dureté de surface élevée et sa température de fusion plus faible mènent à un coefficient de frottement plus élevé et un taux d'usure et une limite Pv plus faibles que ceux du PTFE.

Le UHMWPE a le taux d'usure le plus faible des quatre matériaux étudiées à vitesse modérée mais aussi une limite Pv plus faible que celle du PTFE et de l'acétal. Ce matériau dépose un film très mince qui adhère fortement à la surface métallique. Ceci entraîne un coefficient de frottement relativement faible avec un taux d'usure minime. Cependant, sa faible limite Pv peut être attribuée à sa température de fusion relativement basse (136 °C). Ce matériau maintient sa structure solide jusqu'à des températures de contact élevées, mais son taux d'usure devient excessif jusqu'à l'endommagement de la surface.

Le nylon 6/6 possède le coefficient de frottement le plus élevé et la limite Pv la plus faible. À faible vitesse, aucun film de transfert n'est observé sur la surface métallique. Son coefficient de frottement élevé pourrait être attribué à sa rigidité et à sa dureté de surface élevée. La température de surface augmente et dépasse sa température de transition vitreuse qui varie entre 55 et 80 °C. Cette transition diminue la rigidité de surface et augmente la surface réelle de contact, ce qui augmente d'avantage son coefficient de frottement. Un film épais de transfert est ainsi déposé sur la surface métallique; celui-ci agit comme un isolant et diminue la dissipation de la chaleur générée par frottement.

La performance tribologique de ces matériaux peut être reliée directement à la nature du film de transfert déposé à différentes vitesses de glissement et la stabilité de leurs propriétés mécaniques à différentes températures de contact.

En général, à hautes vitesses de glissement , le coefficient de frottement diminue avec l'augmentation de la vitesse jusqu'à la limite Pv du matériau. Des coefficients de frottement très faibles sont observés à hautes vitesses. D'autre part, l'effet de la charge sur le coefficient de frottement varie selon le matériau. En ce qui concerne le taux d'usure, il diminue avec l'augmentation de la vitesse jusqu'à la limite Pv du matériau. On constate aussi en général que le taux d'usure diminue avec la température de contact.

En ce qui concerne l'effet de l'aire de contact, on constate que les mécanismes d'usure sont pratiquement les mêmes que ceux rapportés en littérature pour des faibles aires de contact. Cependant, la déformation de la surface du polymère et les particules d'usure sont beaucoup plus grandes; ceci affecte la planéité de la surface métallique et augmente le taux d'usure et le coefficient de frottement. D'autre part, quand la température de contact dépasse le point de fusion du polymère, le coefficient de frottement ne diminue pas avec une augmentation de la vitesse; ceci limite l'application de la théorie du contrôle thermique de frottement quand l'aire de contact est grande. On peut croire que cette contradiction avec les

résultats rapportés dans la littérature est reliée au fait que la distribution de la température sur la surface est non homogène. La déformation de la surface du polymère qui en résulte empêche la formation d'un film homogène de polymère fondu qui serait responsable de la chute du coefficient de frottement tel que rapporté dans la littérature.

Des tests sont aussi réalisés sur les mêmes quatre polymères pour étudier leur comportement tribologique à hautes vitesses en contact discontinu. L'effet de la vitesse et de la nature du contact sur le coefficient de frottement et le taux d'usure sont étudiés. En plus, les limites Pv des matériaux sont comparées avec celles obtenues en contact continu.

En général, le coefficient de frottement est légèrement plus élevé en contact discontinu, sauf pour le Nylon 6/6. D'autre part, les limites Pv sont beaucoup plus faibles en contact discontinu. Ceci peut être relié à la surface métallique plus faible, ce qui limite la dissipation de la chaleur générée par frottement, aussi bien par conduction que par convection. Le PTFE a la limite Pv la plus élevée suivi du UHMWPE, de l'acétal et finalement par le nylon 6/6.

En ce qui concerne le taux d'usure, le PTFE possède le taux d'usure le plus élevé suivi par l'acétal, le nylon 6/6 et enfin le UHMWPE avec un taux d'usure très faible. Les mécanismes d'usure sont les mêmes que ceux en contact continu pour tous les matériaux, mais le taux d'usure est généralement plus élevé en contact discontinu. À haute vitesse, le taux d'usure diminue pour le PTFE mais augmente pour les autres. La performance unique du UHMWPE à des températures au dessus de son point de fusion mériterait une étude plus poussée.

Finalement, les mécanismes d'usure des polymères, au delà de leur limite Pv, peuvent affecter d'une façon importante la performance des machines dans lesquelles on retrouve de

tels contact. Pour le PTFE et l'acétal, le matériau peut subir un taux d'usure élevé avec des débris d'usure relativement petits ou fondre sans déposer un film qui colle sur la surface métallique; ceci n'affectera pas ou peu la surface métallique en contact et peut prendre un certain temps avant de causer une défaillance du contact. Dans le cas du UHMWPE, le matériau maintient sa stabilité pour une certaine période. Après cette période, un taux d'usure très élevé se développe avec l'arrachement de grosses particules de la surface du polymère. Ces particules adhèrent à la surface métallique en contact et les deux surfaces peuvent se souder ensemble après que la machine est arrêtée. Pour le nylon 6/6, un film épais se dépose sur la surface métallique et endommage la surface du polymère; ceci engendre des vibrations dans le système, ce qui peut causer des problèmes mécaniques. Aussi, des grosses particules, résultant de l'accumulation du film déposé, peuvent être projetées de la surface à grandes vitesses et causer aussi certains dommages dans d'autres composantes de la machine.

TABLE OF CONTENTS

LIST OF APPENDICES

LIST OF TABLES

LIST OF FIGURES

NOMENCLATURE

A	surface area (mm^2)
A_{app}	apparent area of contact (mm^2)
B	contact width
C_p	specific heat (kJ/kg.°C)
C_f	coefficient of friction
F	friction force (N)
h	coefficient of heat convection ($W/m^2.°C$)
k	specific wear rate ($mm^3/N.m$)
k_m	coefficient of thermal conductivity of the metallic specimen (W/m.°C)
k_{asb}	coefficient of thermal conductivity of the isolating asbestos film (W/m.°C)
k_{air}	coefficient of thermal conductivity of the air (W/m.°C)
l	contact length (mm)
L	characteristic length of the convection term (mm)
Nu	Nusselt number
P	contact pressure (MPa)
Pr	Prandtl number
Q	heat flux (kW)
R_a	average surface roughness (μm)
Re	Reynolds number
T_{disc}	disc temperature measured under the isolating film (°C)
T_{in}	metallic surface temperature at inlet of the contact zone (°C)

T_m metallic specimen mean temperature (°C)

T_{max} maximum temperature of the metallic surface at the end of the contact zone (°C)

T_{sub} temperature measured under the metallic specimen (°C)

T_{surf} metallic surface temperature (°C)

T_{air} air temperature measured at 2 mm from the metallic surface (°C)

t test duration (s)

t_m metallic specimen thickness (mm)

t_{asb} asbestos film thickness (mm)

v sliding speed (m/s)

V volumetric wear rate (mm^3/s)

V_o output voltage of the pressure control card (Volt)

V_i input voltage of the pressure control card (Volt)

W applied load (N)

α_m thermal diffusivity of the metallic surface (m^2/s)

Δm mass loss (kg)

ν_{air} air dynamic viscosity (m^2/s)

ρ density (kg/m^3)

τ contact period (sec)

INTRODUCTION

Many tribological applications involve a dry metal-polymer contact in high speed sliding. Some applications undergo discontinuous or intermittent contact where very high thermal energy is developed. Examples of such applications are found in tires and snowmobile sliders. In such applications the mechanical and surface properties of both materials play an important role in determining the friction and wear behavior of the contact. The static and dynamic coefficients of friction of polymers are generally lower than steel and most metallic materials. However, their low thermal conductivity and melting temperature restrain their performance at high contact load and sliding speed where surface melting and/or high wear rates are likely to occur.

Most of the research work, in polymer-metal contact were conducted at speeds limited to 5 m/s. On the other hand, the experimental research works are mostly conducted on pin on disk machines, in which the area of contact is very limited. Within this range of speeds and contact area, the polytetrafluoroethylene (PTFE) has the lowest coefficient of friction where the ultrahigh molecular weigh polyethylene (UHMWPE) exhibit the best wear rate with a moderate friction coefficient. In the few available publications at high speed sliding, a model of thermal control of friction is suggested. In this model, the surface of the polymer in contact is considered partially molten. Eventually in such a model, the geometry of the surfaces in contact has major effects on the heat dissipation. There is no available publication on the performance of UHMWPE or PTFE at high speed sliding especially with large contact surfaces. Furthermore, the different wear mechanisms developed when a high contact temperatures is likely to occur are ill studied.

The first objective of this work is to design and construct a tribometer capable of testing metal-polymer contact at speeds from 1 to 60 m/s. The contact area should be

relatively large (between 2 000 to 7 000 mm^2) and of continuous and discontinuous nature. The tribometer should be able to apply normal pressure from 5 to 200 kPa and to measure the friction force in dry, water lubricated and abrasive environments. It must be possible to measure and record the temperature at several points in both the polymer and the metal specimens. Eventually, the tribometer must be stable and safe at such high speeds, loads and aggressive environmental conditions. The first objective completed, research work will be done to study the friction and wear behavior of polymer-metal contact at high speed sliding with large contact surfaces in both continuous and discontinuous contacts. This includes the effect of sliding speed, applied load and contact temperature on the friction coefficient, the Pv limit, the wear rate and the different wear mechanisms. Also, the heat generation and dissipation are to be evaluated to validate the friction and temperature measurements.

In chapter I, a general review of the previous investigations on the tribological behavior of polymers is presented, with special interest on high speed polymer-metal contacts. This includes tribological machines, testing apparatus and different measurement techniques. The different wear mechanisms of polymers for both continuous and discontinuous contacts are discussed, with the effect of different parameters on the wear rate and friction coefficient.

In chapter II, the tribometer design and its load and speed capacities are presented with the friction, the wear and the temperature measurements performed in both continuous and discontinuous contacts. The different calibration procedures are also reviewed.

In chapter III, a one dimensional thermal analysis is presented for the calculation of the contact temperature in the tribometer. The energy equation derived is applied on the friction and the metallic temperature measurements, obtained at different test conditions, to validate the measurement approach. Another measurement technique is used on the polymer surface temperature to investigate the real contact temperature.

Chapter IV presents the results of the tests performed on four different polymers with large contact surfaces in continuous contact. The polymers selected are UHMWPE, PTFE, polyoxymethylene (Acetal) and Nylon 6/6. The effect of speed, load and the large contact surface on the friction coefficient and wear mechanisms is studied. In addition, the limiting Pv value is investigated for each material.

Chapter V reports the results of the tests performed on the same materials but in discontinuous contact. The objective of these tests is to study the effect of the nature of contact on the friction and wear properties of polymers at high sliding speed and load. In addition, the limiting Pv value is investigated for each material and compared with that obtained in continuous contact.

This document will be concluded with a general conclusion and the proposed future research work.

CHAPTER I
LITERATURE REVIEW

1.1 Introduction

Polymers are being used increasingly in tribological applications. Due to their elasticity, polymers are able to accommodate shock loading, shaft misalignment and bending better than metals. Their friction coefficients and wear rates are so low in dry conditions that in fact they are applied to as self-lubricated materials.

However, their low thermal conductivity and softening temperature limit their capacity to work under high speed and load conditions; this can be modified by adding metallic fillers, solid lubricants or high strength fibers. In fact, polymers had been favored in high speed applications such as elastomers in tires and thermoplastics in snowmobile sliders. On the other hand, many high speed applications undergo discontinuous or intermittent contact where very high thermal energy transfer rates are developed; this in a way affects the performance of polymers in such tribological applications.

In this chapter, a general review of the previous investigations on the tribological behavior of polymers is presented, with special emphasis on the high speed polymer-metal contacts. This will include tribological machine, testing apparatus and different measurement techniques. The different wear mechanisms of polymers for both continuous and discontinuous contact are also discussed, with the effect of different parameters on the wear rate and friction coefficient.

1.2 Apparatus

1.2.1 Tribometers

A review of the different mechanisms used to test friction and wear was presented by Hutchings (1992). Budinski (1989) presented another review of the laboratory testing methods for solid friction in which he illustrated the different standard friction tests. In unidirectional sliding applications the pin on disc test was the most common. As an example, three different models of pin on disc machines can be found in the work of Tanaka (1974), Fusaro (1983) and Barrett (1992), which differ according to each application. Tanaka used a conventional pin on disc shown in figure 1.1, to investigate the friction, wear and surface melting of crystalline polymers. His machine had a speed range of 0.1 to 3 m/s. Fusaro's apparatus had a stationary stainless steel pin sliding against a rotating UHMWPE disc. He studied the wear mechanisms and transfer films on the contact for a speed range of 0.003 to 1.7 m/s. The friction specimens were enclosed in a chamber to control humidity. Barrett also used a pin on disc machine to study the effect of surface roughness on the friction and wear of UHMWPE-stainless steel sliding contact. A schematic diagram of his apparatus is shown in figure 1.2, and the speed range used was 1.25 to 10 m/s. Ramasubramanian (1993) used a similar machine, with higher sliding speed (12.4 m/s), to study the effect of fillers on the sliding behavior of UHMWPE-stainless steel contact.

However those machines, according to certain researchers, become unsatisfactory as speed and load increase since the load is applied at a single point. The vibration induced may affect the friction force measurement. Also, in lubricated conditions, the centrifugal forces cause liquids to be flung off the rotating disc leading to fluctuation in the applied load and variations in friction measurements. In their work, Seedhom (1973), Dowson (1974,1982), Atkinson (1978), Brown (1982) and Cooper (1991,1993) used a tri-pin-on-disc tribometer, shown in figure 1.3, which has more dynamic stability. However, most of their tests were

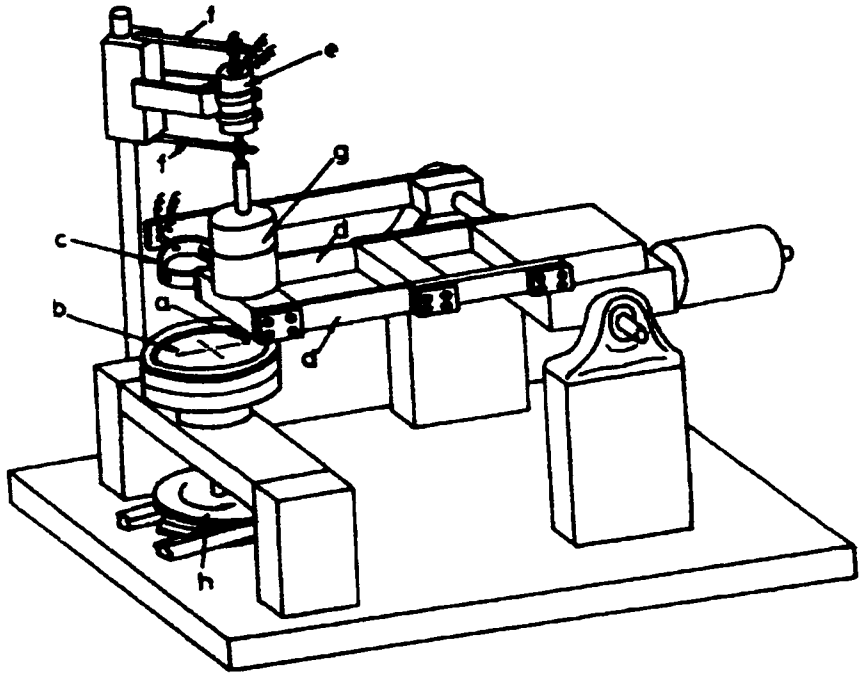

Figure 1.1 Tanaka's pin on disc apparatus (1974)
a- polymer pin; b- glass or steel disk; c- ring shape spring; d- plate sprigs;
e- linear diff. transformer; f- plate sprigs; g- weight; h- driving pulley

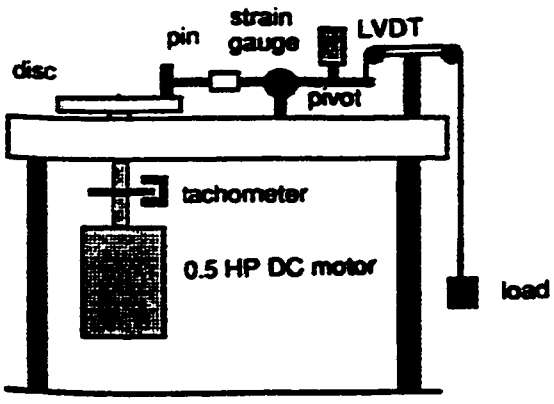

Figure 1.2 Schematic diagram of Barret's pin-on-disc test apparatus (1992)

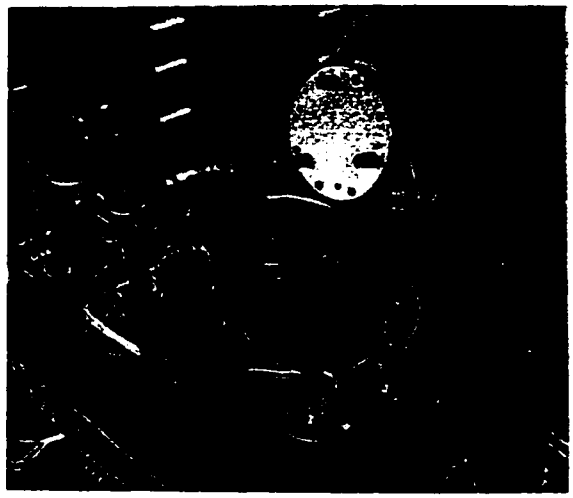

Figure 1.3 The tri-pin on disc machine used by Seedhom, Dowson and others)

done at a sliding speed of 0.24 m/s to simulate the biomechanical behavior of human joints. Thorp (1981,1982) designed a similar tri-pin-on disc tribometer (figure 1.4), which retains more the lubricants at high speed (18 m/s) and load (310 N), although the maximum test speed reported in his results was 12 m/s. He studied the friction of some commercial polymer-based bearing materials against steel.

To model some aspects of the sliding of a tire over a pavement asperity, in locked and partially locked braking, Ettles (1988) conducted experiments of intermittent frictional contact at sliding speeds up to 30 m/s. A glass sphere is loaded for a period 0.5 sec against a rubber surface in a pin on disc apparatus. Clarck (1991) used a specially modified vertical drill stand to study the lubricated wear behavior of five polymeric materials against steel at speeds up to 2.27 m/s with contact pressures up to 5 MPa. The machine is designed to simulate the hydraulically powered stopping equipment. Slifka (1993) used a special tribometer designed to measure the friction coefficient and the wear rate in a controlled atmosphere and temperature. The tribometer uses a ball on flat and a ring on flat contacts and has a speed range of 0.06 - 4 m/s, and a temperature range of 80 - 1030 °K.

Very high speed tests (up to 700 m/s) were conducted by Bowden (1961) who used a steel ball rapidly spinning around its vertical axis, and allowed to fall a short distance and to bounce off an inclined flat solid surface. He used these tests to study the effect of frictional heating on the deformation and surface melting of solids in contact. However, the accuracy of his results is much affected by the time of contact that varied between 30 μs and 140 μs. To simulate the friction of a projectile sliding down a cannon bore, Montgomery (1976) also conducted very high speed tests (up to 560 m/s) in a special machine presented in figure 1.5. To reduce windage losses, high speed tests (> 180 m/s) were conducted under reduced pressure in the test chamber. In both studies, the contact temperature was not reported.

In oscillating motion applications, Lloyd (1988) used a reciprocating pin-on-plate wear machine in his investigation of UHMWPE-stainless steel wear mechanisms at an

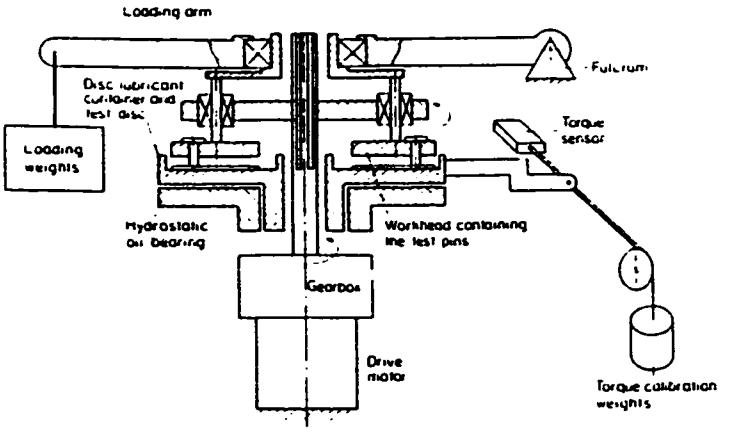

Figure 1.4 Basic design of Thorp's tribometer (1981)

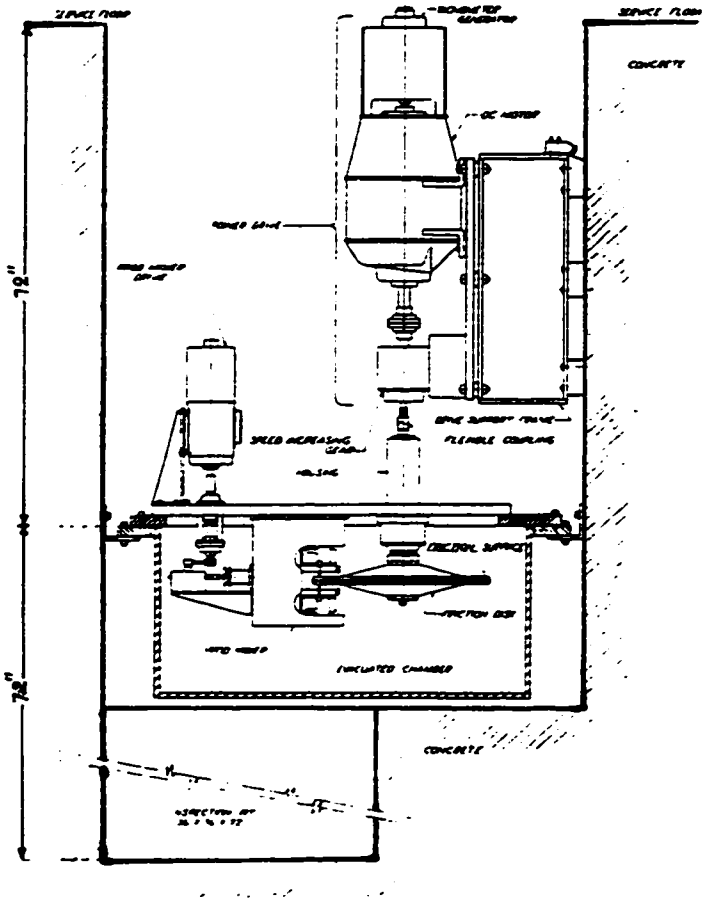

Figure 1.5 Schematic assembly of the friction machine used by Montgomery (1976)

average speed of 0.25 m/s. Blanchet (1989) used a test machine that has a stationary UHMWPE pin in contact with oscillating metallic disc sliding to study the film transfer deposition in oscillatory motion and the maximum average sliding speed was 0.027 m/s. Brown (1982) also used a 9-head reciprocating wear machine in his comparison between the wear rate and mechanisms of unidirectional and reciprocating motions. Benabdallah (1991(a)), in his investigation of the friction characteristics of 3 polymers against stainless steel, used a plane on plane vertical reciprocating apparatus, which fits a universal hydraulic testing machine (MTS). The average sliding speeds varied between 0.01-0.1 m/s. Benabdallah (1991(b)) also used cylinder-on-flat and pin-on-flat tests to investigate the friction and wear of UHMWPE-stainless steel reciprocating contact, and results showed no difference in wear measurement between the two methods. The load was set at 57 N and the speed at 0.025 m/s.

Finally it is important to mention that most ASTM standard tests (1993,1995) for static and dynamic coefficients of friction and wear rate are based on pin on disc machines. In those test recommendations, it is stated that each test is designed for a particular application, and therefore, cannot be taken as a general reference for polymers tribological performance. The standard friction and wear tests have a speed limit of 3 m/s. On the other hand, at high sliding speed and load, the temperature rise affects the rigidity of the pin and alters the contact surface in pin on disc tests. This decreases the precision of the calculated contact pressure and the friction force measurements.

From this review of different tribometers used, it is concluded that the dynamic effects are an important factor in determining the limiting load and speed of a tribometer, especially at high speeds and lubricated conditions. For speeds up to 3 m/s the standard pin on disc tribometers are generally used. When conditions become more severe, special designs or modifications are used to insure the stability of the machine and maintain a proper accuracy of the different parameters measured. On the other hand, the reciprocating tests have a very limited speed range due to the dynamic effects generated from the oscillating motion. It is very important to mention here that most high speed testing machines are

designed for a very specific application with very limited test duration. There is no available standard test for high speed application (>3 m/s).

1.2.2 Parameter measurements

Generally, the tribological behavior of materials is represented by their friction coefficient and specific wear rate. The friction coefficient is usually calculated using Amontons law of friction (Hutchings 1992),

$$C_f = \frac{F}{W} \qquad \textbf{1.1}$$

Where F is the tangential friction force (N) and W is the normal applied load (N).
The specific wear rate k is calculated using the Archard equation (Hutchings 1992):

$$k = \frac{V}{W\,v} \qquad \textbf{1.2}$$

Where V is the volumetric wear rate (mm^3/s) and v is the sliding speed (m/s).

1.2.2.1 Wear measurement

Wear is usually monitored using either volume, weight or displacement measurements. In volume measurement, a sophisticated volumetric analysis is usually needed. The humidity absorption and the presence of foreign particles limit weight measurements especially in lubricated contact. The main disadvantage of both wear and volume measurements is that it must be conducted after the test; hence the wear cannot be monitored during the test. This is the main advantage of displacement tests. On the other hand, the dynamic effects limit the accuracy of the displacement tests, with the necessity of measuring the displacement at different positions of the contact zone.

In volume measurement, Fusaro (1983) calculated the volumetric wear loss of a UHMWPE disc by measuring the cross sectional area of the wear track and multiplied it by

the circumference of the track. In Blanchet (1989), Tetreault (1989) and Barrett's (1992) experiments, the wear was monitored by a linear-variable-displacement transducer LVDT contacting the pin, as shown in figure 1.6. This device can detect the displacement with an accuracy as small as 1 μm. Using LVDT, Blanchet and Tetreault initially loaded the pin for 48 hr until the initially high creep rate diminishes.

However, in most applications, the specific wear rate is determined by weight loss, to avoid creep effects. When a polymer pin wear rate is to be calculated, the pin weight is measured at high accuracy before and after the experiments to evaluate the weight loss. Then the density is used to calculate the volumetric wear loss. In Tetreault's tests (1989) a second pin was used as a reference for humidity absorption. Soak-control specimens were used by Benabdallah (1991(b)) and Clarke (1991) to provide the necessary correction for weight gain due to fluid absorption. Usually the term wear rate is used to denote the specific wear rate.

1.2.2.2 Friction measurement

Generally the load is applied by a pre measured weight as shown in figure 1.1,1.2 and 1.4. The friction force is usually measured by strain gauges as shown in Barrett's apparatus in figure 1.6. Blanchet (1989) used a piezoelectric transducer, and Ramasubramanian (1993) determined the frictional torque by measuring the variations in load current using the two-wattmeter method. On the other hand, Yoon (1997) demonstrated both analytically and experimentally that the pneumatic loading gives the most accurate results, especially when the asperities of the contact induce vibrations and dynamic loading

1.2.2.3 Temperature measurement

Measuring the real contact temperature is one of the most delicate problems in tribology, especially at high sliding speeds. The problem arises from the fact that the real contact area is not accessible for optical or radiation measurements. The temperature is

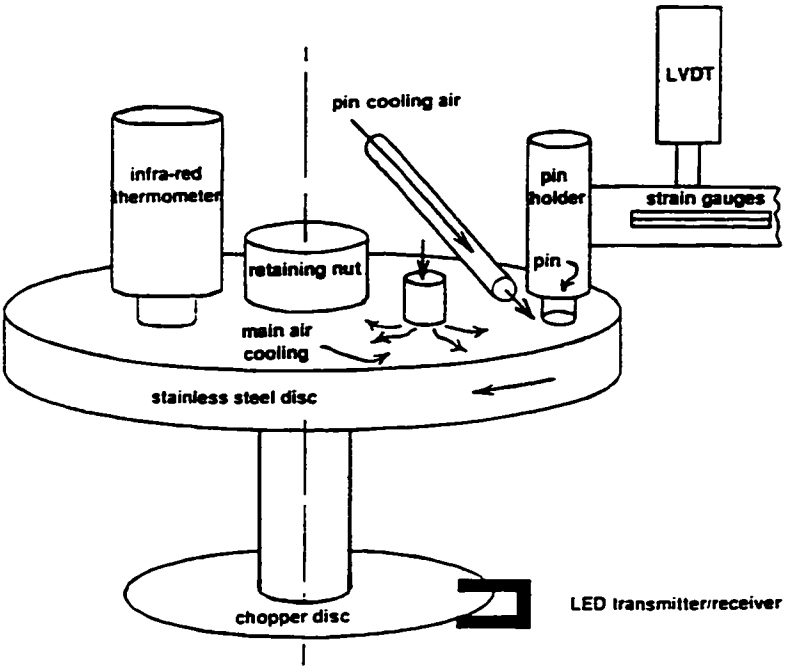

Figure 1.6 Schematic diagram of the temperature control and measurement systems for Barrett's apparatus (1992)

usually measured by embedded thermocouples under the contact surfaces. This problem is more sophisticated in polymer contacts due to their low thermal conductivity and high wear rate at high sliding speeds. On the other hand the real area of contact is difficult to calculate. In most research work, thermocouples are fixed under the metallic surface to predict the metallic surface temperature where thermal analysis and empirical models are used to verify or calculate the real contact temperature.

As an example of such analysis, Challen (1976) developed an equation that gives an estimation of the temperature rise on the surface of an UHMWPE pin sliding against a stainless steel disc in Dowson's tri-pin-on-disc machine, and had the form.

$$T_f = F_p W + F_{tb} T_B$$

$$F_p = \frac{1.65 F_s F_m C_f v^{0.5}}{F_s + F_m} \qquad \textbf{1.3}$$

$$F_{tb} = \frac{F_s - 0.65 F_m v^{-0.5}}{F_s + F_m v^{-0.5}}$$

Where T_f is the contact temperature °C, T_b is the disc surface temperature and F_s and F_m are constants depending on the thermal conductivity and geometry of the surfaces in contact.

Using the previous equation for contact temperature calculation, Barrett (1992) used an IR pyrometer to measure the disc surface temperature. To control the heat dissipation and high temperature at high contact speeds (up to 10 m/s), an air jet cooling system was provided as seen in figure 1.6.

To verify his experimental results, Benabdallah (1991(b)) used the equation developed by Lancaster (1971) for calculating the theoretical mean temperature rise. The equation of Lancaster was presented in the form,

$$\Delta T = \frac{0.236 C_f g H_m^{0.5} W^{0.5} v}{J (K_1 + K_2)} \qquad \textbf{1.4}$$

Where H_m is the plastic hardness (g/cm^2), J the mechanical equivalent of heat ($g.cm^2/s^2$ cal), K_1 and K_2 the thermal conductivity of both materials (cal/cm.s.°C), W the load (g) and v the sliding speed (cm/s). In his tests, he used a very fine thermocouple at a position 0.3 mm away from the rubbing surfaces. He found good agreement between the calculated and the measured contact temperature. Both models assumed a constant ambient temperature.

Kennedy (1981) developed finite element equations to study the surface temperature in both dry and lubricated contacts. He applied his equations on plastic-lined sleeve bearings and found good assent between his analytical predictions and experimental measurements.

It is important to note here that polymer film deposition may partially isolate the metallic surface especially at high speed sliding and/or large surface of contact. Also, it may affect the radiation temperature measurements on the metallic surface since it depends on the emisivity of the surface. Finally, there is no available standard test for measuring the contact temperature in tribological applications.

1.2.2.4 Surface topography

In most applications, a Taylor-Hobson talysurf was used for surface roughness measurements. The Talysurf was also used to describe the surface profile when connected to a trace recorder. The R_a value was always the parameter reported as the surface finish reference in most tribological investigations. More details of the apparatus design and applications are presented in the American National Standard for surface roughness (1985).

1.2.2.5 Surface and subsurface scanning

Generally, a scanning electron microscopy (SEM) is used to study the worn surfaces. This technique can only be used at the end of a wear test since the polymeric wear surface had to be coated with Au/Pd to render it electrically conducting.

Atkinson (1978) used optical microscopy, SEM and Transmission electron microscopy (TEM) in his study of the UHMWPE-stainless steel surfaces. The optical microscopy permitted him to study the surfaces at different stages of the testing period. SEM permitted him to study the pin and counterface surfaces wear and surface fractures. TEM provided sufficient resolution to the fine details.

Marcus (1993) used X-ray spectroscopy and X-ray fluorescence to determine the composition of a commercially filled UHMWPE. A similar investigation is used to study the surface composition of metals and to detect film transfer on the surface.

Cooper (1991) presented a birefringent study of UHMWPE wear specimens to detect the residual strains or deformations of the wear surface. Specimens were carefully sectioned into 30 μm slices and the frigence patterns were viewed in a microscopy set up as a polariscope.

1.3 Materials preparation and specimens

1.3.1 Polymers

In most pin on disc tests the polymeric pin has a conical shape and the surface is always finished by grinding or by using 600 grade emery papers to R_a between 0.15 - 0.2 μm. Before the test, the polymer pin is ultrasonically cleaned in ethanol or alcohol and dried in hot air to remove any dust or greasy contaminants. Then the specimen is weighted or dimension measurements are done. A digital balance is usually used in weight measurement which has an accuracy between 0.1 and 0.01 mg.

In Barrett (1992) tests, the UHMWPE pins were machined into two forms, one with a conical profile with a flat circular end, and the other with a rod-shaped projection from the

main body of the pin. The latter design was intended to provide better cooling of the wearing surface and found to have slightly different wear characteristics from the conical pin.

Fusaro (1983) investigated the effect of the rider geometry and the different combination of the surfaces in contact and compared his results with Jones (1981). He found that the friction coefficient of UHMWPE rider sliding against a stainless steel disc was 3 to 4 times greater than that with stainless steel rider sliding against an UHMWPE disc, whereas the wear rate was approximately the same. Also, to test the different material combination Fusaro (1982) used two combinations, Graphite-fibber-reinforced polyamide (PA/GR) hemispherical rider sliding on stainless steel counterface and the opposite, at different temperatures. At 25 °C, he obtained a coefficient of friction of 0.24 with the first combination and 0.19 with the opposite. At 300 °C he obtained a coefficient of friction as high as 0.76 with the first combination and 0.05 with the opposite. On the other hand when comparing with Atkinson (1978), he found that the wear rate for a tri-pin-on-disc test has 10 times less wear rate than for a single pin on disc test.

Those studies elaborated the importance of maintaining the type and area of the contact surfaces, when simulating a specified friction contact. There is no available information on the effect of the contact area at speed higher than 3 m/s, where the wear rate and different mechanisms would affect the friction and wear properties of the materials.

1.3.2 Metals and ceramics

The surface roughness of metallic and ceramic counterface has a significant effect on the wear rate of polymers. To study this effect, the surfaces were usually diamond polished to obtain the desired surface finish of the test that can be as smooth as $R_a = 0.01$ μm. The same surface cleaning process as for polymeric material was also used. In Barrett (1992) experiments, the discs were prepared to various level of surface roughness by machining to a fine turned finish followed by hand finishing with emery papers. The surface roughness

range was between R_a 0.53 - 0.07 μm. The randomness of the surface roughness was checked by measuring the surface roughness in radial and circumferential directions for each disc.

1.4 Tribological behavior of polymers

1.4.1 The wear mechanisms of polymers

In normal running conditions, the two main mechanisms of wear in polymer- metal contact are adhesion and abrasion (Lloyd, 1988). Adhesion is the main wear mechanism for very smooth surfaces whereas abrasion is that for rougher surfaces. The adhesion wear mechanism in polymers is usually accompanied by film transfer to the counterface as confirmed by the results obtained by Atkinson (1978) in UHMWPE-stainless steel contact. With a constant wear rate, the new surface became progressively smoother. Then a sudden increase in wear rate was detected after a certain sliding distance, which was the result of a surface fatigue mechanism, identified by fine powdery debris particles. This sliding distance depends on the applied load. Krasnov (1996) related the increase of the friction coefficient and the wear rate, detected after a certain running period, to a tribochemical modification in surface composition of UHMWPE.

On the other hand, Hornbogen (1980) stated that the frictional shear force, acting on the surface of polymers, is usually higher than the critical shear stress needed to induce plastic deformation. The resulting deformation energy is dissipated and the surface is modified by molecular rearrangement. The molecules are aligned in the direction of sliding and considerable amounts of work hardening occur in this direction. This can lead to a decrease in the coefficient of friction due to the increase of hardness and a decrease of the real area of contact.

Lancaster (1972) presented a diagram which resumes the changes that occur on a

counterface during sliding on a polymer and their effect on the wear mechanisms (Figure 1.7). According to his diagram, the surface finish is the major factor affecting the wear rate.

Film transfer is another important factor that controls the friction and wear of polymeric materials. Blanchet (1989) explained the transfer film for UHMWPE on a metallic surface as a two-stage process: anchor deposition which is the result of adhesion of small area of polymer-metal contact, and anchor smearing which is a cumulative deformation of these deposited anchors into smoother and more uniform film. The transfer film is directly related to the contact temperature as presented by Watanebe (1986). He found that there is less transfer film at 110 °C than at 25 °C for Nylon sliding against steel.

Eiss (1979) presented an analytical model for predicting the thickness of the transfer film for low-density polyethylene (LDPE), polyvinyl chloride (PVC) and poly-chloride tetrafluoroethylene (PCTFE) on steel counterface. The model used the normal load, the yield strength of the polymer, the apparent area of contact, the bearing area curve for the surface, the polymer density and the shear angle of the polymer to make the transfer prediction. The predicted wear rate was higher than the experimental results by a factor of five, whereas the difference in the film thickness was one order of magnitude higher. There is no available research work about the effect of speed on the film transfer at high speed applications.

Burton (1980) discussed the formation of thermal asperities on the polymer surface when significant frictional heating is observed. He concluded that those asperities may either lead to surface approaching absolute smoothness or correspond to high roughness peaks. The first is the result of the asperity deformation or melting which leads to higher surface smoothness. The second could be explained in two different steps; the first called thermoelastic transition in which the surface changes from nominally flat to highly deformed as a result of plastic deformation and the second, called thermoelastic instability, leading to a change in contact stress distribution that may lead to high wear rate and surface cracking.

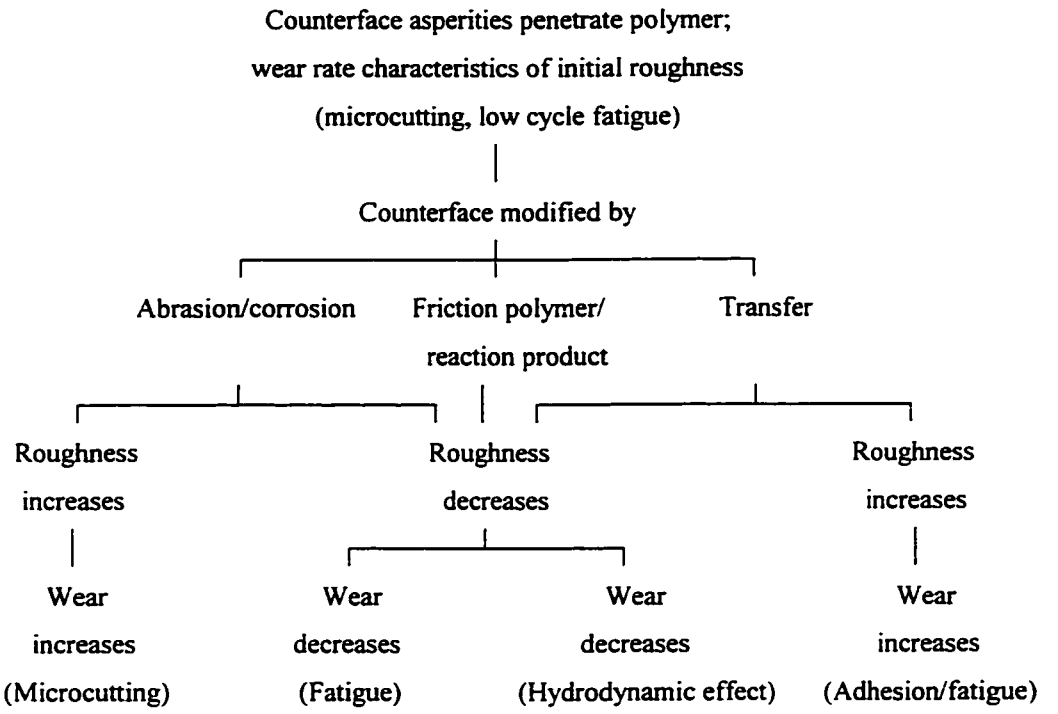

Figure 1.7 Changes occurring to a counterface during sliding, and their effect on the wear of polymers (Lancaster, 1972)

At high sliding speed or load, the high temperature developed due to frictional heating may cause the polymer to degrade (Fusaro, 1990). On the other hand, the molecular chains must have the time to reorient, in order to develop a surface shear film and a transfer film. At high sliding speed the unoriented chains may fracture producing large wear particles and higher wear rates.

Although some research work suggested different explanations for the wear mechanism developed at different sliding speed for a particular set of material, there is no available research that studied the difference in wear mechanisms of different polymers at speeds in which the frictional heat generated may induce a significant temperature rise.

1.4.2 Friction coefficient and wear rate of different polymers

Polymers have generally lower coefficient of friction and wear rates than metals. A typical value of the coefficient of friction of polymers rubbing against steel lies between 0.15 - 0.4, where the wear rate can vary between 10^{-4} to 10^{-11} $mm^3/N.m$.

It is clear that the coefficient of friction and wear rate for a polymer-metal sliding system cannot be regarded as a single-valued material constant since variations in the load, the sliding speed, the geometry and the roughness of the counterface all affect the friction and wear mechanisms. The usual procedure is to publish values of the friction coefficient and the wear rate for polymers at a fixed set of test conditions.

A general review of the performance of commercially available polymeric materials, with their applications and limiting load, speed and Pressure × speed values (Pv), are presented by Lancaster (1971,1973) and Evans (1982) .The performance of a variety of polymers when subjected to different wear mechanisms is studied by Böhm (1990). Another review of wear properties and bearing applications of high density polyethylene (HDPE) and UHMWPE was also presented by Anderson (1982) with a brief comparison with other

common basic materials. Whereas Harschnitz (1992) reviewed some plastic materials for high temperature bearing applications such as polyetheretherketone (PEEK), polyamide-imide (PAI), polyphenylenesulphide (PPS), Nylon 6/6 and has taken Acetal as reference.

Holmberg (1987) studied the friction and wear of 22 commercial polymers materials and found that UHMWPE had the best friction and wear performance over a speed range from 0.1 to 1 m/s. In his comparison between PTFE and UHMWPE sliding against stainless steel, Blanchet (1989) found that PTFE had lower friction coefficient. UHMWPE revealed a better wear rate since the protective transfer film is not easily removed from the counterface by peeling as in PTFE. This confirms the results presented by Lancaster (1971,1973) .

Clarke (1991) investigated the sliding wear behavior of 5 polymer base materials at different speeds and contact pressures. The materials were UHMWPE, Acetal, disulfide filled polyamide (Nylon 6/MoS_2), polyethylene terephtalate (PET) and PA/GR. For low sliding speed and contact pressure, PET exhibits excellent wear resistance where UHMWPE is found to be good under most conditions, especially at high velocities and low pressures.

It is important to note here that the melting index affects the friction and wear behavior of polymers. Studying the effect of melting index on friction and wear of commercial grade polyethylene, Deanin (1980) found that the abrasive wear of low melting index polyethylene (ex. UHMWPE) is two orders of magnitude lower than that of high melting index polyethylene (ex. LDPE).

It is clear from all research available that the UHMWPE exhibits the best wear rate with a moderate coefficient of friction at large range of sliding speed, in both lubricated and dry contacts. PTFE has the smallest coefficient of friction in most applications, but with a relatively high wear rate. Both Nylon and Acetal had a moderate wear rate and friction coefficient. Although some research work has been conducted on polymer composites at high speed sliding, there is no available information about the performance of UHMWPE, Acetal

and PTFE at speeds exceeding 10 m/s.

1.4.3 Effect of different parameters on the friction and wear of polymers

Many parameters affect the tribological performance of polymers when sliding against harder materials. In his study of the wear behavior of UHMWPE, Dumbelton (1976) compared his work with different researches, which were to some extent contradictory with his results. He concluded that difference in testing temperature or type of motion can change the wear rate by up to two orders of magnitude. The friction coefficient and specific wear rate of selected polymers at different speed and contact pressure (Pv values) are presented in Table 1.1 and 1.2.

1.4.3.1 Sliding speed and type of motion

The upper limit of operation of polymers is usually based on a maximum allowable value of Pv. This factor is widely used as a performance criterion for bearing materials and represents a limiting value for the maximum allowable pressure of contact versus speed under normal running condition. This value predict a sudden wear rise and rapid bearing failure if exceeded. This constrains the interface temperature to a limiting value since the power dissipated (C_f Wv) must diffuse through a series of thermal resistance to ambient.

Lancaster (1971) defined the limiting Pv as the value above which the wear rate increases rapidly and the maximum Pv as the maximum value for continuous operation at a specified wear rate. The Pv limit is usually measured by fixing the speed or load and varying the other term gradually, in fixed intervals, until a sharp increase in the wear rate is detected (Lancaster, 1973; Wolverton, 1983). The maximum Pv, or the Pv factor, is determined by measuring the wear rate in constant load and speed tests (Lancaster, 1971). The recommended Pv limits for selected materials are presented in table 1.3.

Table 1.1 Specific wear rate for different materials (x 10^{-6} mm^3/N.m)

Conditions			PTFE	Acetal	UHMWPE	Nylon 6/6	Ref.
Speed (m/s)	Pressure (MPa)	Pv (MPa.m/s)					
0.25	0.28	0.07	20			4	1
0.1	1	0.1	800				2
0.01	1.4	0.014	107	2.8		5.8	3
0.1	5	0.5		1.5	0.5	20	2
0.24	2.5	0.606			0.25		4
0.25	5	1.25		2.1		16	5
0.24	10	2.4			0.2		6
0.24	10	2.4			0.27		4
0.25	10	2.5		12	0.51		7
12.4	0.15	1.86			2.9		4
---	---	---	400	1.25		3.8	8

1) Wolverton (1983); 2) Holmberg (1987); 3) Tanaka (1980); 4) Atkinson (1978); 5) Mens (1991); 6) Dowson (1974); 7) Böhm ((1990); 8) Lancaster (1973)

Table 1.2 Coefficient of friction for different materials

Conditions			PTFE	Acetal	UHMWPE	Nylon 6/6	Ref.
Speed m/s	Pressure MPa	Pv MPa.m/s					
0.25	0.28	0.07	0.06			0.24	1
0.1	5	0.5	0.2	0.6	0.2	0.4	2
0.1	1.5	0.15		0.45		0.57	3
0.1	6.8	0.68			0.14		3
0.25	5	1.25		0.45		0.57	4

1) Wolverton (1983); 2) Holmberg (1987); 3) Blau (1989); 4) Mens (1991)

Table 1.3 Recommended Pv limits for different materials (MPa.m/s)

Speed (m/s)	PTFE	Acetal	UHMWPE	Nylon 6/6
0.05	0.04	0.14	0.07	0.11
0.5	0.06	0.12	0.07	0.09
5	0.09	0.09	Not recommended	0.09
References	1	1	2	1

1) Lancaster (1973); 2) Engineering Plastics (1987)

In polymers, this factor is limited by their low melting temperature and visco-elastic behavior. On the other hand, there are limiting values of load and speed for each material, independently from the Pv factor. For example, at speed up to 0.5 m/s, the limiting Pv factor for UHMWPE in bearing application is approximately 0.07 MPa.m.s^{-1} for dry contacts, whereas the maximum contact pressure and speed are 10 MPa and 2 m/s respectively (Eng. Plastics, 1987). It should be noted here, that the contact pressure is calculated as a function of the apparent area of contact ($P = W/A_{app}$).

At low speed sliding, when the variation of the contact temperature is negligible and does not affect the mechanical characteristic of the polymer surface, the friction coefficient is rather independent of speed as shown in figure 1.8 (Tetrault, 1989). On the other hand the wear rate slightly increases with speed as shown in figure 1.9.

At higher speeds, when the temperature of the surface becomes relatively high, the coefficient of friction generally increases due to the increase of both the real contact surface and the adhesive component of friction. The later can be attributed to the increase of the surface energy. On the other hand, the wear rate generally decreases. This is attributed to the decrease of the surface hardness and rigidity where the ploughing component of abrasive wear is replaced by plastic deformation of the asperities.

At high sliding speed, when the temperature at the interface approaches the softening point of the polymer, a rapid increase in both the coefficient of friction and the wear rate, is detected with material being removed from the molten layer at the surface of the polymer (figure 1.8 and 1.9).

Mc Laren (1965) found that unlike amorphous polymers, linear crystalline polymers show a marked dependence of friction on speed at low speeds. Cross-linked thermosetting polymers (mostly rigid) exhibit the smallest dependence of friction on speed. On the other hand, he declared that the coefficient of friction increases with speed in most polymers to

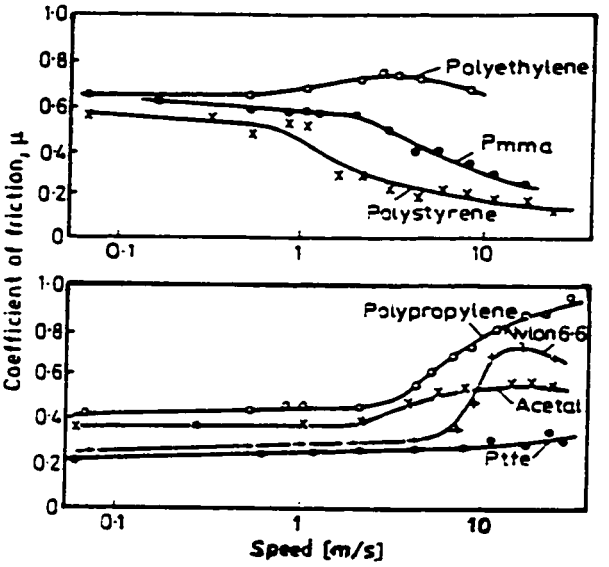

Figure 1.8 Variation of friction coefficient with speed (Lancaster, 1971)

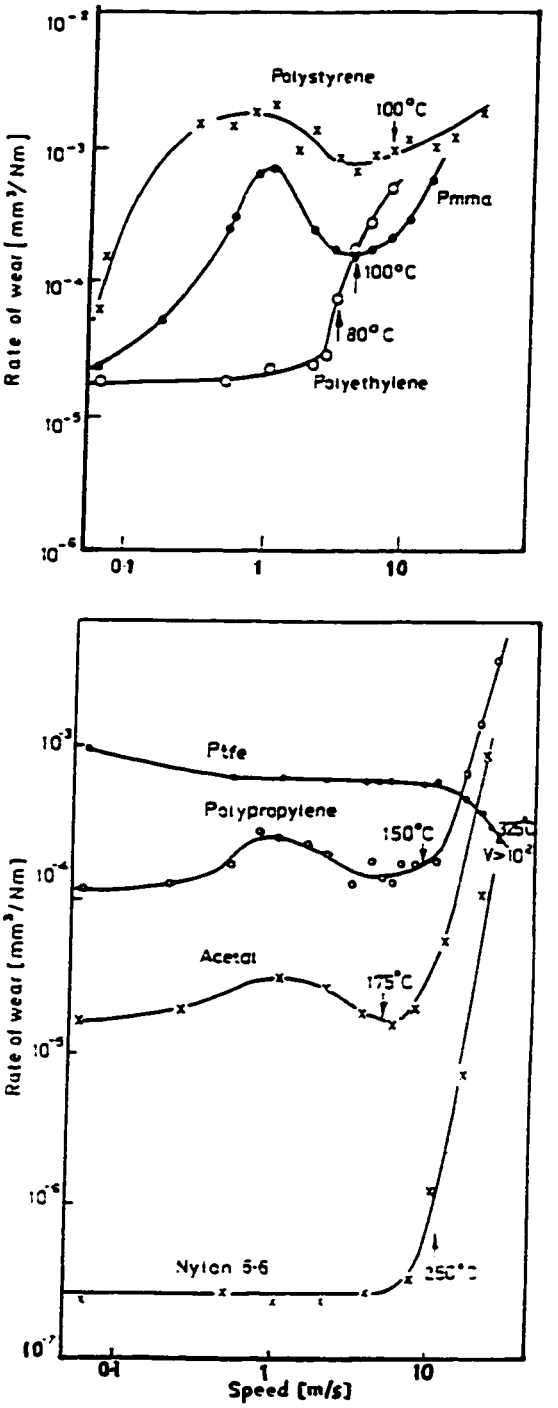

Figure 1.9 Variation of wear rate with speed (Lancaster, 1971)

reach a peak when the temperature reaches the glass transient temperature and then decreases dramatically with increasing speed.

Barrett (1992) discussed the wear behavior of UHMWPE at different sliding speeds. He found that UHMWPE, having very high viscosity, revealed friction characteristics similar to metals up to the melting point where his behavior becomes similar to polymers. At the polymer surface, the straight sharp-edged wear tracks detected at low speed (1.25 m/s) had more irregular forms at high speeds (10 m/s) with smearing of tongues of polymer and irregular wave features. At the surface of the disc, transfer films of the polymer took different forms depending on the speed and surface roughness, from fine powdered (1.25 m/s) to ribbon (5 m/s) and filament debris (10 m/s). The film was about 10 μm in thickness.

On the other hand, Brown (1982) found that the overall wear rates in reciprocating and oscillating motion are lower than that of unidirectional motion for the same conditions of surface roughness sliding speed and load. The wear rate component due to adhesion alone was 2.5 times lower whereas the component due to fatigue was slightly lower. Both reciprocating and oscillating tests had approximately the same wear rates.

Ettles (1988) conducted some experiments to measure the friction of some polymers over four orders of magnitude range of Pv. In his results he showed that an upper bond, he called the friction defined temperature, may be obtained at high Pv values, which was not exceeded as speed and/or load increased. This was characterized by a reduction of friction coefficient with increasing velocity according to $C_f \alpha v^{-1/2}$ (see section 1.4.4).

In summary, the relation between the coefficient of friction and the wear rate with speed can be resumed as presented in figure 1.10 and 1.11. The Pv value is generally used as a guiding factor in the design of tribological applications. However, it is clear that the ambient temperature and the overall heat conduction and convection coefficients of the contact would affect largely the limiting speed and load of a specific application.

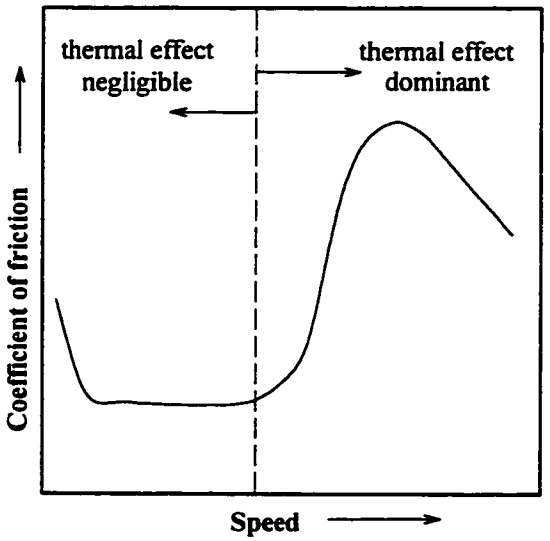

Figure 1.10 Schematic representation of the relation between the coefficient of friction and speed

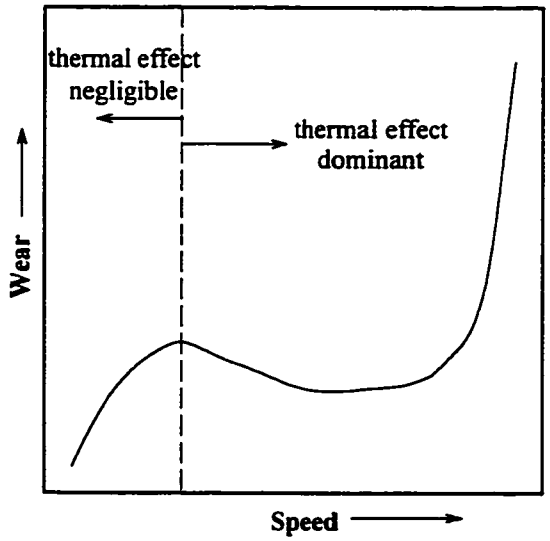

Figure 1.11 Schematic representation of the relation between the wear rate and speed

1.4.3.2 Load and contact pressure

The applied load is generally the parameter reported in the literature. This is because the load is the factor that controls the heat generation and the real area of contact. On the other hand, the friction and wear are independent of the apparent area of contact and hence the contact pressure. Nevertheless, the contact pressure becomes an important parameter when it is in the same order of magnitude of the polymer yield strength.

Atkinson (1978) found that the wear rate was independent of the applied load up to a certain value, where a sudden increase in the wear rate was detected. At high values of applied load and surface roughness, brown colored debris revealed the oxidative degradation of the polymer surface that was the result of the high temperature generated from higher load. This was also confirmed in the tests reported by Ramasubramanian (1993) at higher load.

In a birefringent study of polyethylene (PE) wear specimens, Cooper (1991) found that at high contact pressure (up to 12 MPa) the sub-surface fatigue mechanism dominated the wear process. The micrographs taken in their tests showed subsurface residual strain 5 - 40 μm thick varying with time and normal stress.

Studying the effect of dynamic loading on the performance of UHMWPE-stainless steel contact in a hip joint simulator, Cooper (1993) found that the wear rate variation and surface fluctuation of the polymer under dynamic loading was a result of the initiated subsurface cracking and debris formation.

1.4.3.3 Contact temperature

Thermoplastic polymers generally have low thermal conductivity and low softening temperature. The contact temperature is directly proportional to the frictional heat dissipated, which depends mainly on the applied load and sliding speed as discussed earlier. The

estimated maximum useful temperature of UHMWPE is 80 °C and 130 °C for Nylon 6/6, after which the wear rate increases dramatically (Lancaster, 1971; Fusaro, 1990).

The generation of high temperatures during sliding may also lead to oxidation or other types of degradation of the polymer. In this case, the surrounding environment may be very important (Clark, 1978). At high sliding speed, very high temperature is developed at the contact surface, and the thermal characteristics of the polymer becomes very important. This will be discussed in section 1.4.4. On the other hand the wear rate and friction coefficient decrease at very low temperature. This was identified by Holemberg (1987) in his previously presented study of some commercial polymers at low temperature (-35 °C).

Theories have been developed by Marscher (1982) about the concept of shear heating due to the high rate of strain generated very close to the interface. It was very difficult to apply it quantitatively due to its coupled with the actual amount of local heating.

Finally to demonstrate the discrepancy in the wear results in literature, a very important comparison is presented here between the results of Woltverton (1983) and that of Harschnitz (1992). The first presented a comparison between the wear rate of PA and PEEK at 149 °C (300 °F) and 204 °C (400 °F) and found that at higher temperature the wear factor doubles. The second also presented a comparison between the wear factor at 150 °C and 200 °C for different polymers (PA, PEEK and PAI) and the results showed that the wear factor at 200 °C is lower than that at 150 °C. The later confirms the results presented by Watanebe (1986) in his study of Nylon film transfer on steel at different temperatures.

1.4.3.4 Effect of counterface material

Generally stainless steel is the most favorable material used in tribological application with polymeric materials. This is due to its resistance to oxidization and to prevent any influence on the wear rate by small abrasive particles of rusted iron (Barrett, 1992). For this

reason, the combination of materials favored for total replacement of human joints has been UHMWPE with stainless steel.

In high speed tests of different polymers on glass and steel, Tanaka (1974) found that the melt depth of polymers on glass is comparatively greater and rapidly increases as the speed increases, while that on steel is only several microns and little dependent upon speed. This could be explained by the high thermal conductivity of steel. The friction coefficient of HDPE on steel was slightly lower than that of UHMWPE whereas the wear coefficient of UHMWPE is very small compared with the HDPE.

In his study of the friction and wear behavior of UHMWPE, Tetreault (1989) found that the wear rate when sliding against titanium was much greater than against Co-Cr, where the friction coefficient was about the same ($C_f = 0.2$). This was related to the difference in the film transfer layer on the titanium surface that was rougher and thicker than that deposed on the Co-Cr. While the wear rate, when sliding against heat treated Co-Cr, is greater than against as-cast Co-Cr, under both dry and lubricated conditions. This was attributed to the improved surface finish obtained with the heat treated Co-Cr together with the absence of surface imperfection. The same observations were reported by Martinella (1989), in his investigation on the wear behavior of UHMWPE sliding against Ti6Al4V alloys, ANSI 316L stainless steel and vitallium. No wear was detected on the metallic surfaces where UHMWPE revealed mild wear against Vitallium and SP-lapped TiAl4V, an intermediate wear against ANSI 316L and a severe wear with DP-lapped Twelve. He also related the variation of the wear rate to the nature of film transfer and its roughness that resulted from the different metallic-transfer film bond.

Benabdallah (1991(b)) studied friction and wear of UHMWPE in contact with five alumina and Zirconia based ceramics counterface in lubricated conditions. His results showed that the alumina based ceramic toughened with Zirconia gives best compromise between the wear rate and the friction coefficient. The wear coefficient calculated were

between 10^{-4} and 10^{-5} mm ^{3}/ N.m and coefficient of friction in the range 0.2 to 0.3. On the other hand, for the same materials and surface roughness, Dowson (1982) found a wear rate of about 2 x 10^{-7} mm^3/ N.m in dry conditions. The wear rate was about 4.6 x 10^{-9} mm^3/N.m at lubricated conditions. There were two orders of magnitude difference in both results. Benabdallah explained the high wear rate as a result of the third body wear made of PE transfer and Zirconia particles, which was not detected in Dowson's experiments. Dowson also stated that the wear rate detected is about 50% the wear rate of UHMWPE-stainless steel contact for the same dry test conditions, and 56% in the lubricated test.

From this review, it is concluded that the counterface thermal conductivity, the surface finish, the hardness and the counterface-polymer film transfer bond are the major factors that affect the friction and wear behavior of polymers. Polymer-ceramic contact has better coefficient of friction and wear rate than polymer-metallic contact especially in lubricated conditions. However, their low thermal conductivity limits their application at high temperature and therefore at high sliding speeds. Also, the cost and machinability of the ceramics limit their application in general bearing service.

1.4.3.5 Surface topography and nature of contact

Barrett (1992) studied the effect of surface roughness on wear and friction of UHMWPE-stainless steel contact. He found that an optimum surface counterface roughness between R_a 0.14 - 0.24 μm gave best wear coefficient at all sliding speed, except at 10 m/s where the surface roughness variations have minor influence on the wear rate as shown in figure 1.12. On the other hand, friction was not much influenced by changes in surface roughness (figure 1.13). The wear mechanism also changed with surface roughness and temperature. At low surface roughness a continuous loss of material was detected which increased at high temperatures, where at high surface roughness and temperature a stepped wear characteristics were detected with higher wear rates. For the same combination of material, Lloyd (1988) found that the optimum surface roughness was approximately

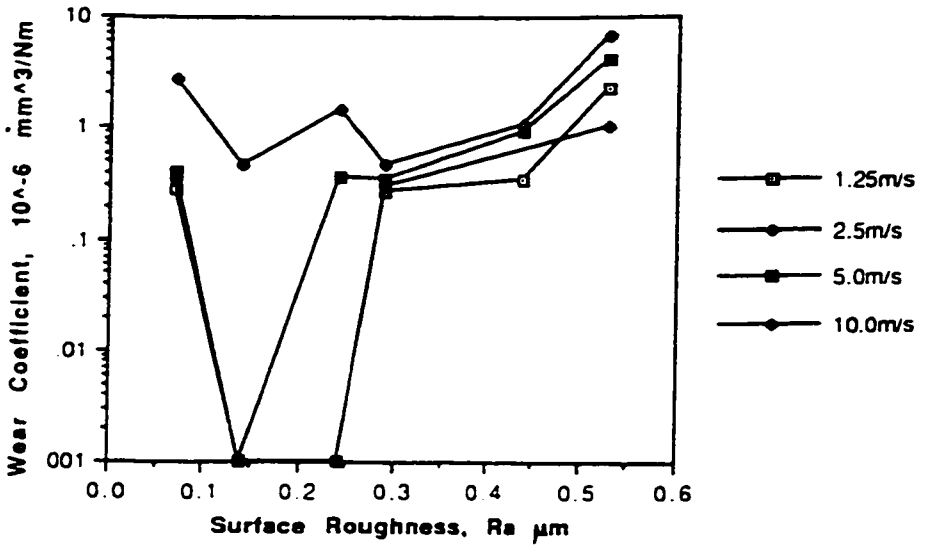

Figure 1.12 Effect of counterface roughness on the wear rate of UHMWPE at various sliding speed (Barrett, 1992)

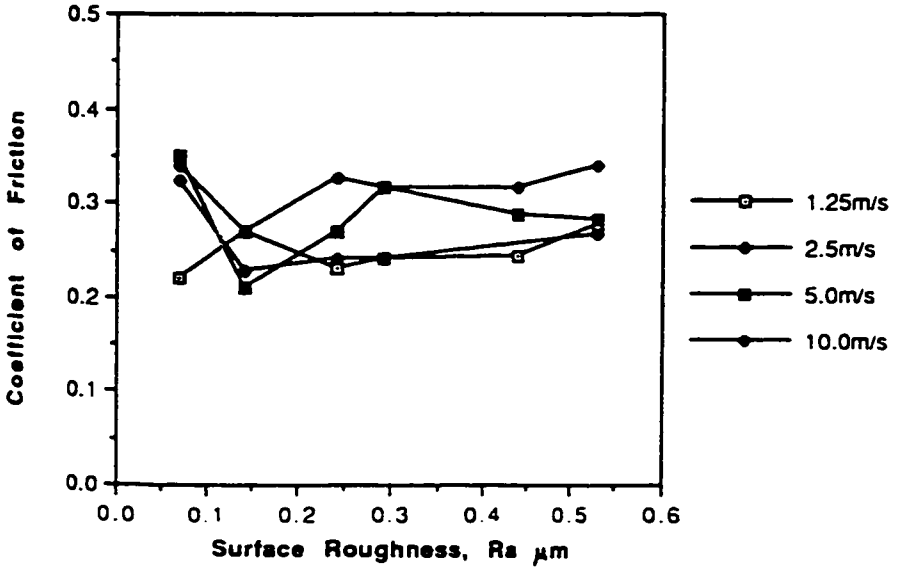

Figure 1.13 Effect of counterface roughness on the friction coefficient of UHMWPE at various sliding speed (Barrett, 1992)

R_a = 0.35 μm. He also found that the relation between the wear rate and the surface roughness, in lubricated contact, can be represented by a log relation in the form $k = 1.1 \times 10^{-8} \exp(7.7 \times R_a)$. In UHMWPE-ceramics contact, the results presented by Benabdallah (1991(b)) at low speed tests (0.025 m/s) confirmed that the roughness of the hard counterface surface has major influence on the wear rate, especially in running-in period.

It is important to note that the effect of surface roughness varies according to each material. For example, Eiss (1983) reported that at a surface roughness of Ra 0.1 μm, the wear rate of Acetal is about 1/9 that of PE. At surface roughness 1.0 μm the wear rate of Acetal is 6 times of PE.

On the other hand, polymers generally exhibit good embeddability. This is an advantage when small particles of dust from atmosphere attend the surface and prevent three body wear. When large particles are involved, wear become more pronounced in the harder surface making scares, which in turn increase the wear rate of the polymer. When a particle was deposited on the wear track, Fusaro (1983) found that a deep groove was worn on the metallic rider revealing a third body wear of the metallic surface caused by embedded particle on the polymer surface. Marcus (1991) studied the effect of grinding direction on the wear of UHMWPE sliding against stainless steel. He found that the wear rate is higher when sliding parallel to the counterface grinding direction than sliding perpendicular to it. He also found that the wear debris and film transfer are more crystalline than the bulk of the worn polymer surface. However, his DSC tests were performed at relatively high heating rate (10 °C/min), which may lead to higher error in percentage crystallization measurement.

Concerning the nature of contact, most high speed applications undergo intermittent or discontinuous contact. The intermittent high temperature developed largely affect the friction coefficient and the wear mechanisms of the polymer in contact.

In discontinuous contact, most of the publications are concentrated on cars and

aircrafts braking systems, in which intermittent slipping at high speed occurs between an elastomer and the pavement, resulting a very high temperature and wear rates. The only available work that had taken into account the effect of discontinuous contact on the thermomechanical wear mechanisms and wear rates was that of Padovan (1994). He studied the wear at intermittently slipping speed interfaces. Using Finite Element analysis, he developed a methodology to model the intermittent wearing process and applied it to define tire wear induced in antilock braking system (ABS) of aircraft. In his study he used a maximum value of the coefficient of friction of about 0.4 in his stick-slip model throughout the friction process. This in a way was very delicate because the coefficient of friction increases dramatically at high temperature especially for rubber. The reported instantaneous temperature reaches values of up to 204°C (400 °F).

Other publications in high speed discontinuous contacts include the friction of the slider with the disc in computers hard disc drives, in which practically no load is applied on the contact. Another application was the turbine blade tip contact with the casing in which very limited contact is induced which normally disappears after the running-in period. There is no available publication on the performance of antifriction materials such as UHMWPE, PTFE, Acetal or Nylon at discontinuous contact especially at high sliding speed.

Finally Brown (1982) studied the effect of molecular orientation on the wear of drawn UHMWPE. Two different mechanisms were used: Tensile drawing and hydrostatic extrusion. He found that the wear rate increases with increasing the degree of orientation when the orientation was perpendicular to the sliding direction. On the other hand a slight decrease in the wear rate was detected when the orientation was parallel to the surface.

1.4.3.6 Additives and fillers

The role of additives or solid lubricants is generally to reduce the adhesive force polymer-counterface. Fillers form a transferred film that remains firmly attached to the hard

counterface and further sliding over these films leads to a very low polymer wear rate (1974). The different fillers, binders and fibre reinforcement used in polymer-based bearing materials and their limitations are presented by Lancaster (1972,1973).

Mens (1991) studied the friction and wear behavior of 18 polymers in contact with steel in dry and water-lubricated pin on disc tests. Six unfilled materials were used in tests including Nylon 6/6, Acetal, PET, PEEK, PPS and polyetherimide (PEI). The same base materials filled with PTFE or PTFE plus glass were then used. In dry contact, Nylon 6/6-PTFE, Acetal-PTFE, PET-PTFE and PEEK-PTFE had k values bellow 1.0×10^{-6} mm^3 / N m and friction coefficients in the range 0.15 - 0.2. PEEK - PTFE has the advantage that it could sustain a relatively high temperature (up to 200°C). In lubricated contact, PA 66, Nylon 6/6-PTFE and Acetal-PTFE had the best wear coefficient. He concluded that the addition of PTFE in dry contact was generally beneficial, where in lubricated contact, PTFE had no effect. The optimum percentage of PTFE in the polymer was studied and found to be about 15%. This is also confirmed by Byett (1992) who was studying the dry sliding behavior of polyamide composites filled with PTFE, UHMWPE and glass fiber. On the other hand, Byett found that the addition of glass fiber decrease significantly the wear rate, which contradicted Mens results who stated that the addition of glass fibre generally produced unfavorable effects in air as well as in water. Marcus (19993) also studied the effect of fillers on wear behavior of UHMWPE. The fillers were glass beads and titanium-based inorganic fillers and it was found that the filled material exhibited lower wear rates than the unfilled material in rough surfaces, where they showed higher wear rates at smooth counterface.

Thorp (1982) tested 7 different commercial thermoplastics bearing materials with UHMWPE, Nylon 6, Nylon 6/6 and Polyurethane base. He found that the UHMWPE filled with silica sand had the lowest coefficient of friction ($C_f = 0.11$) in dry contact for up to 1 m/s. He also studied the effect of film transfer on the abrasive wear of the same commercial polymers (1982). The UHMWPE filled with silica sand also gave the best wear resistant when sliding against emery paper (i.e., at film transfer conditions), where the

Nylon 6 exhibited the best resistant in steel gauze contact (i.e., at no film transfer). Wolverton (1983) studied the tribological properties of reinforced and lubricated thermoplastic composites at elevated temperature. The materials were PTFE, PEEK, PPS and Nylon 6/6 where the fillers studied were glass fibers, bronze, carbon fiber MoS_2 and PTFE. He found that the PTFE composites offer excellent balance of bearing and chemical resistance with high thermal stability. On the other hand the addition of PTFE to a fiber reinforced composite results in improved tribological properties at all temperatures.

Ramasubramanian (1993) investigated the influence of filler concentration on dry sliding behavior of UHMWPE at high sliding velocity of 12.4 m/s. The fillers investigated were graphite, MoS_2 and silica gel. He found that an initial increase in filler content increased the wear rate of polymers with all fillers, followed by a decrease in the wear rate for graphite and MoS_2 as shown in figure 1.14. With graphite, the polymer exhibited the most improved friction and wear behavior due to its homogeneity in the structure unit with the polymer, which leads to the formation of a relatively smooth film transfer.

From this review it is concluded that the use of PTFE as additive or surface coating improves the friction behavior in dry contact. Also Graphite and MoS_2 fillers improve the wear and friction behavior of polymers especially UHMWPE when provided with the right percentage. On the other hand the effect of glass fibers as additive depends largely on testing conditions and the basic material.

1.4.3.7 Lubrication and humidity

Generally, the coefficient of friction is much lower under lubricating conditions and decreases with increasing speed. The wear rate is generally higher under lubricating conditions but also decreases with increasing speed. Tanaka (1980) investigated the friction and wear of semicrystalline polymers sliding against steel in dry and lubricated contacts. His results are presented in figure 1.15 and 1.16. He concluded that the presence of water

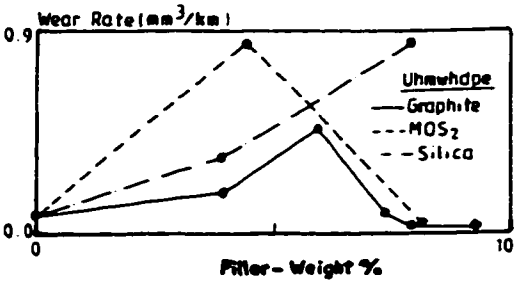

Figure 1.14 Variation in wear rate with % filler for UHMWPE composites (Ramasubramanian, 1993)

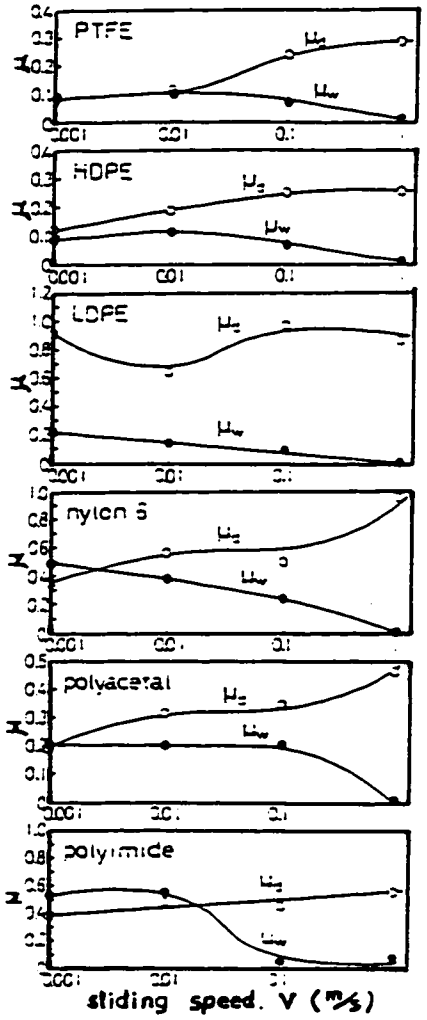

Figure 1.15 Variations of the coefficient of friction (μ) with speed for various polymers at dry and wet conditions (Tanaka, 1980)

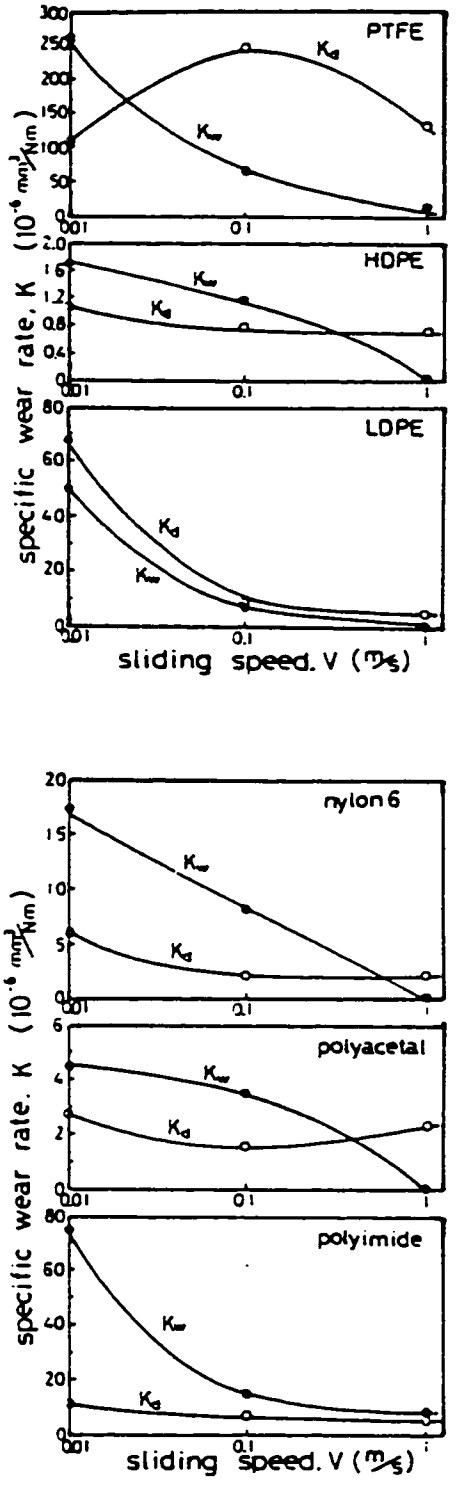

Figure 1.16 Variation of the specific wear rate k with speed for various polymers at dry and wet conditions (Tanaka, 1980)

interface decreases the possibility of transfer film deposition on the harder surface, and hence increases the wear rate at low sliding speed. At high sliding speeds (>1 m/s), the wear rate of most polymers was much higher in dry conditions with higher friction coefficient. Dowson (1982) found that the wear rate of UHMWPE sliding against alumina ceramic in dry contact is about 20 times greater than those experienced by the same materials in wet sliding.

In his study of 5 different polymers in water lubricated conditions, Clarke (1991) found that there was a linear relation between wear volume and sliding speed (i.e., constant wear coefficient) except for UHMWPE, which revealed a decrease in the wear rate with increasing speed. He also suggested that with thermal softening of the surface there was also a partial EHL (elasto-hydrodynamic lubrication) developed by the water film between both surfaces.

Lloyd (1988) suggested that in water lubrication of UHMWPE-stainless steel contact, the asperities of the counterface caused a uniform abrasion of the polymer by ploughing where film transfer were detected on the counterface. This mechanism of two body wear was accompanied by a three body micro cutting wear mechanism where metal fragments become embedded in the polymer surface, which caused also wear to the counterface. On the other hand, on the oil-in-water emulsion lubrication no film transfer was found and a mechanism of stick-slip process was observed. It should be noted here, that Lloyd's tests were done at higher loads than those with Tanaka and Dowson, and therefore, wear particles of the stainless steel counterface were found on the polymer surface.

When comparing with other test results, Fusaro (1983) found that the difference in relative humidity lead to a slight difference in the wear rate with a finite difference in the coefficient of friction. Mc Laren (1965) found that the adsorption of vapors can reduce the friction of polymers by a factor of 50%, where a large increase in friction is observed in the presence of humid air.

From this review it is concluded that the lubrication effect on the wear rate depends on the conditions of film transfer formation, whereas the coefficient of friction always decreases with lubrication. On the other hand the humidity can have different effect depending on the material adsorption capacity and the surface temperature.

1.4.4 Friction and wear at very high speed

In high speed testing, Bowden (1961) found that on steel slides on nylon the coefficient of friction drops from 0.25 at 30 m/s to 0.075 at 675 m/s (nylon Melting point 265 °C). This was explained by the increase in the film temperature to reach the polymer softening temperature. A considerable amount of heat would be absorbed by the molten material and removed by the wiping-off action of the moving surface without reaching the liquid-solid surface interface. The same observations were reported by Montgomery (1976). His steel on lead tests were conducted at very high speed (up to 560 m/s) to simulate the rotating bands in gun pipes (figure 1.17). An initial increase of the friction coefficient is reported just before surface melting occurs. This increase of friction coefficient is assigned to be initiated by the transition from partial contact to full contact; i.e., when the ratio between the real and apparent surface of contact approaches unity. The contact temperatures were not reported in his work due to uncertainty of the results. Recently, Sviridenok (1996) studied the friction of polymers and composites in contact with metals at speeds up to 1000 m/s in electromagnetic fields and the same trend of friction coefficient was reported. This dramatic decrease of friction coefficient with speed was the subject of many investigations conducted by Ettles (1985,1988 1986), Akkok (1987) and others.

Ettles (1985) studied the contact temperature in slider and recording disc transient contact. In this case, asperity contact between sliders and magnetic recording discs occurs at high speed (40 m/s) and low loads (0.015 MPa). He presumed that very high temperature might be developed in the contact resulting in lubrication failure and/or head crash. He then studied the heat generation in rotating band (1985) and braking tires (1986,1988) and found

that very high temperatures are developed at high sliding speed. When the temperature approaches the material softening point, the coefficient of friction decreases with increasing the speed. The maximum temperature reached in rotating band was more than 1050 °C, where in the case of tires it was about 180 °C. On the other hand, Akkok (1987) was studying the friction of glass and nylon on ice, his upper temperature limits were lower than -1°C, therefore the friction coefficient drop begins at relatively low speed of contact (<1 m/s)

Ettles proposed that at severe conditions of dry contact sliding, a regime is eventually initiated in which friction is governed by heat flow. He assumed that when the temperature reaches a certain limit, relative to the material with a lower melting point, the friction coefficient begins to drop with the increase of either the sliding speed or the normal load so that it becomes an independent parameter. Therefore, in a given configuration, a maximum allowable surface temperature can be defined and a maximum heat flux can then be calculated. Further increase in speed or load would lead to a decrease in the friction coefficient to accommodate the constant heat flux as presented in figure 1.18. This theory, usually referenced as the thermal control of friction theory, is originally outlined by Krafft (1955) then developed by Oksanen (1982) and others. Figures 1.19 to 1.24 presents some examples of the thermal control of friction theory applied on different material combinations. More details about this theory are found in appendix I.

1.4.5 Lubrication by a melting solid

At high contact speeds, Wilson (1976) studied the phenomenon of lubrication by a melting solid. He considered the case of two infinite bodies in contact in which melting of only one surface occurs due to frictional heating. He found that the friction coefficient increases with the square root of the sliding speed and decreases with the load. His work is followed by Becego (1981) and Fowler (1993) who developed his model for the cases of finite width and nonisothermal conditions and found similar results.

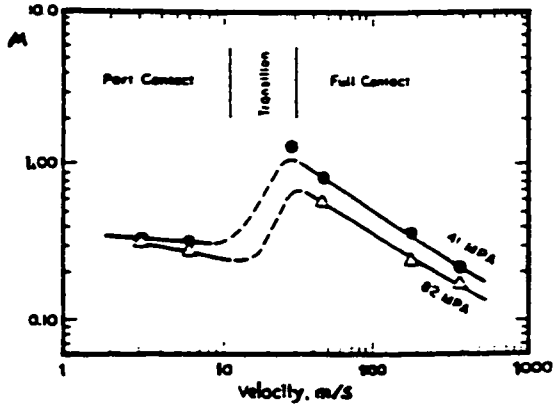

Figure 1.17 Montgomery's results (1976) for copper pins sliding against a disk of gun steel, compiled by Ettles (1985)

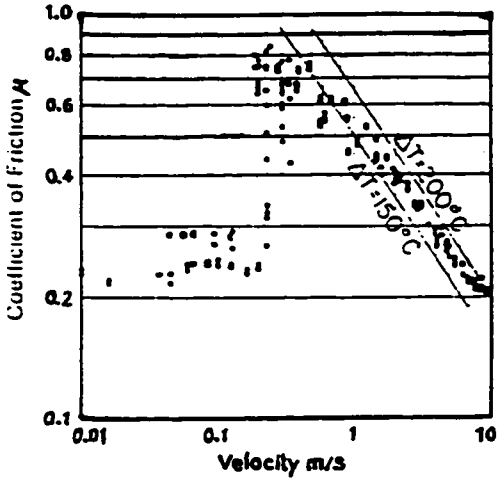

Figure 1.19 The friction coefficient of a steel pin sliding against a nylon 6/6 disc (Ettles, 1988)

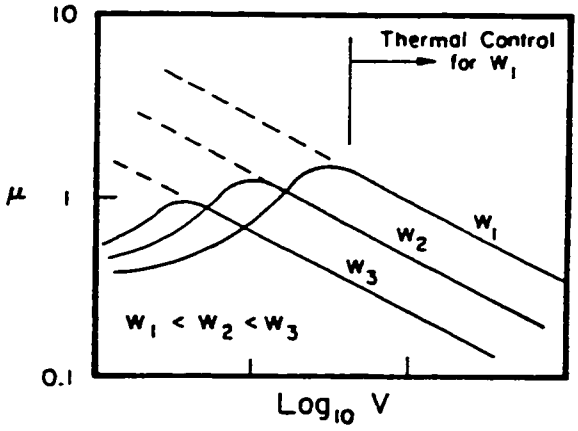

Figure 1.18 Variation of the coefficient of friction with speed and load in thermal control regime as proposed by Ettles (1985)

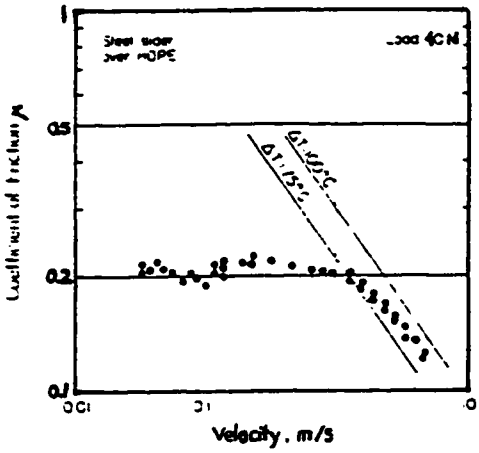

Figure 1.20 The friction coefficient of a steel pin sliding against an HDPE disc (Ettles, 1988)

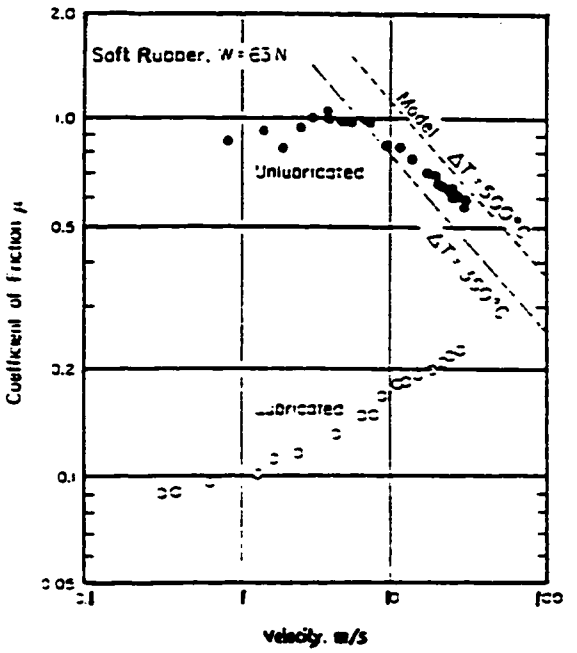

Figure 1.21 The friction coefficient of a glass sphere sliding against soft rubber (Ettles, 1988)

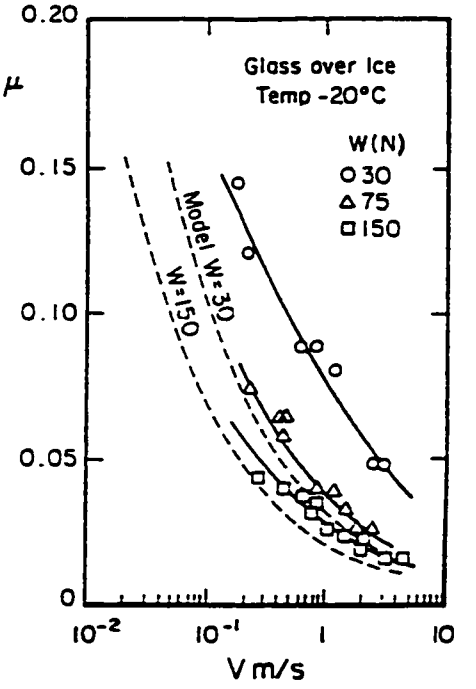

Figure 1.23 The friction coefficient of a glass slider sliding against ice for various loads (Akkok, 1987)

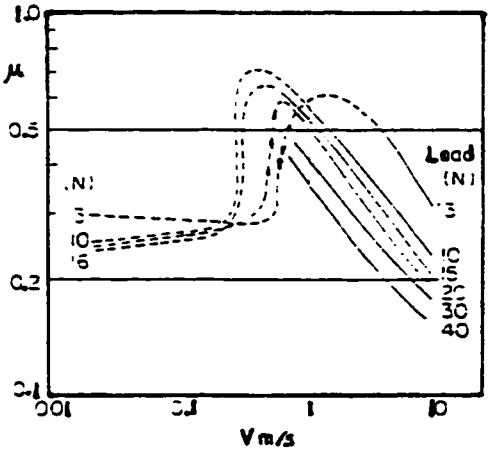

Figure 1.22 The friction coefficient of a steel pin sliding against nylon 6/6 for various loads (Ettles, 1988)

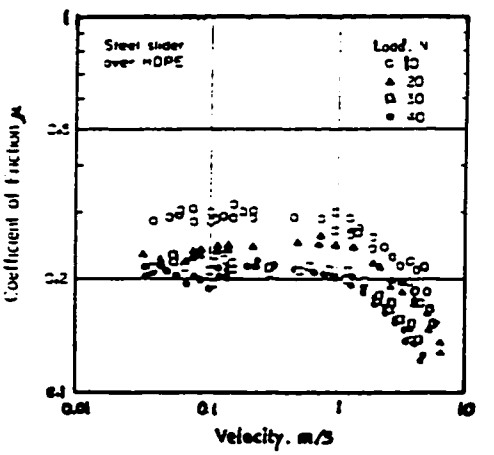

Figure 1.24 The friction coefficient of a steel pin sliding against HDPE for various loads (Ettles, 1988)

Stiffler (1984) studied the friction and wear of a fully melting surface in conducting and nonconducting surfaces for both high and low speed applications. He found that for a highly conducting surface the coefficient of friction decrease with increasing speed while in nonconducting surfaces it increases with increasing speed. In both cases the friction coefficient decreases with the load. He applied his theories on two examples: a copper rotating band melting on a steel gun barrel (conducting surface) and ice skater (non conducting surface) and found good agreement with the experimental results. On the other hand his model also suggested that at low sliding speed the coefficient of friction would increase with speed where at high speed the coefficient of friction would decrease with increasing speed. This theory confirmed the results presented by Mc Laren (1965) for high speed sliding of polymers. He related the effectiveness of friction by melting surface theory to the thickness of the molten surface developed, which must exceed the surface roughness.

Bejan (1989) studied two cases: the first where the melting is due primarily to direct heating (i.e., due to the difference between the solid surface temperature and the melting point of the phase change material), where the melting in second case is caused mainly by the frictional heating of the liquid formed in the relative gap. He found that in the first case the friction coefficient increases linearly with the sliding speed and decrease's mono tonically with the load. In the second case the melting speed becomes very important. In this case, the coefficient of friction increases with the square root of the speed whereas a slight decrease of the coefficient of friction with the load is previewed. Finally the viscosity of the molten surface was considered constant in all the research presented (i.e., independent of the temperature and pressure).

From the previous research work it is concluded that at very high speed application, when the contact temperature exceeds the softening point of the material, the coefficient of friction generally decreases with increasing the Pv value. The coefficient of friction decreases with the load whereas the effect of increasing speed depends on the speed range, the materials in contact and the thickness of the molten surface. On the other hand, it is noted

that in the researches presented, the effect of the wear mechanisms and the variation in surface topography after the surface melting is neglected. The experimental results are very limited and mostly conducted on materials with high melting index.

1.5 Conclusion

From this review, it is concluded that the polymer-metal dry sliding contact can be classified, according to the sliding speed, in four main categories:

- Low speed: when the variation of the contact temperature is negligible and does not affect the mechanical characteristic of the polymer surface. In this zone the friction coefficient is independent of the speed where the wear rate slightly increases with speed.

- Moderate speed: when the temperature of the surface becomes relatively high. In this zone the friction coefficient generally increases with speed where the wear rate generally decreases.

- High speed: when the temperature at the interface reaches the softening point of the polymer. In this zone a rapid increase in both the coefficient of friction and the wear rate is detected.

- Very high speed: after surface melting occurs. A model of thermal control regime of friction is proposed in which the coefficient of friction decreases with increasing the sliding speed and load. This is based on a limiting characteristic temperature of the surfaces, which cannot be exceeded, and therefore a maximum frictional heat generation. This temperature depends on the melting point of the polymeric material in polymer-metal contact. The friction and wear behavior at such high speeds depends largely on the contact surfaces parameters.

Studying the friction and wear behavior of polymers in contact with metallic counterface at different sliding speed the following conclusions can be drawn,

- UHMWPE exhibits the best wear rate with a moderate coefficient of friction over a large range of sliding speed, in both lubricated and dry contacts. PTFE has the smallest coefficient of friction in most applications, but with a high wear rate. It has also a high melting point. Nylon 6/6 has a moderate wear rate, high mechanical strength and a relatively high melting point. However, its high water absorption rate limits its application in lubricated contact. Acetal has both moderate friction coefficient and wear rate. This material has also a relatively high mechanical stability with temperature up to its melting point.

- The counterface surface roughness has a significant effect on polymers friction and wear behavior at low and moderate speeds. An optimum counterface surface roughness between 0.14 and 0.35 μm is recommended in both dry and lubricated conditions. However the effect of surface roughness is limited at high speeds, especially when the contact temperature exceeds the material melting point.

- For most polymers, using PTFE as additive or surface coating improves the friction behavior in dry contact. Also Graphite and MoS_2 fillers improve the wear and friction behavior of polymers when provided with the right percentage.

- Polymers with higher molecular orientation exhibit lower coefficient of friction and wear rate. This explains the superior tribological behavior of crystalline polymers.

- At low speed applications, the wear of polymers increases under lubricated conditions, where, the wear rate is lower in lubricated contacts at high speeds. On the other hand the friction coefficient is always much lower in lubricated conditions.

To simulate a certain tribological contact, the testing conditions must conform with the real conditions of contact. This conditions include the ambient temperature, the percentage humidity, the presence of abrasive particles or wear debris and the lubricated conditions if any. The sliding speed, load and the relative motion between the two contacting surfaces must be determined and maintained in the tribological contact model. There is no standard test for high speed applications.

Finally, there is a lack of information about the tribological behavior of polymers at high speed especially near their melting temperature. Also, the difference in wear mechanisms of different polymers is not studied at high sliding speed. On the other hand, there is no available information on the effect of the contact area at high speed sliding where the wear mechanism would affect the friction and wear properties of the materials.

CHAPTER II
TRIBOMETER AND MATERIALS

2.1 Introduction

Some applications of dry polymer-metal contact include high speed sliding in which speed can reach values of up to 50 m/s. Many of those applications have relatively large contact surfaces in continuous and discontinuous contact. In such applications, very high temperatures are developed in the contact area and surface melting is frequently observed on the polymeric surface. Therefore, the contact temperature and the area of contact have major influence on the wear rate and friction coefficient. To model such high speed contacts, the parameters affecting the heat generation and the conditions of heat transfer must be maintained. Such parameters include the applied load, the contact speed, the contact area and the ambient temperature.

A tribometer is designed to produce a high sliding speed and insures relatively high load and large contact surfaces in both continuous and discontinuous contacts. In the present chapter, the tribometer design, structure and capacity are illustrated. The controlled parameters, such as the applied load and the sliding speed, and the friction, wear and temperature measurement equipments and technics are described. Also, the selected test materials and the specimens preparation are presented. Finally, the different calibration procedures are discussed.

2.2 Tribometer

Our goal is to design a tribometer which has the capacity to test the friction and wear behavior of polymers in contact with steel at high speeds with different geometries of the

surfaces in contact. This tribometer must provide a precise measure of the friction coefficient, the wear rate and the contact temperature.

The design of this tribometer was first initiated with the collaboration of the industry in September 1993. The first model was tested in March 1995. Many load application methods, friction measurements, temperature analysis, and surface finish methods were tested for industrial applications. The tribometer with its testing techniques described in this chapter is the final version which is used in all the tests presented in this document. This machine was designed using AutoCAD© version 12.

2.2.1 Tribometer design

Figure 2.1 presents the general assembly of the tribometer which is based on a milling machine frame. The milling machine construction, with its 1000 kg weight, insures a high rigidity and dynamic stability for high speed (up to 70 m/s) and load (up to 700 N) tests. The metallic specimen is mounted on a 455 mm diameter disc. The disc is rigidly fixed to a disc coupling which in turn is fixed to the shaft using a self-centering shaft-hub locking assembly as shown in figure 2.2. The shaft is driven by a 15-HP brushless DC motor through a poly-V belt drive. To insure maximum rigidity, the shaft is mounted on the machine head and machine base using a set of preloaded tapered roller bearings. The polymer specimen is fixed to an arm which is free to rotate on the shaft using a self aligned deep groove ball bearing. The arm rotation motion is limited by the friction load cell through a flexible connecting road mechanism. The normal load is applied using two pneumatic cylinders connected to an air pressure line through 2 pressure control cards. The pneumatic loading insures a maximum stability for friction measurements. The cylinders are rigidly fixed on the machine frame as shown in figure 2.3.

The friction load cell, the pressure control cards and the thermocouples are all connected, through a 12 bits 333 MHz data acquisition card, to a PC Pentium 133 MHz with

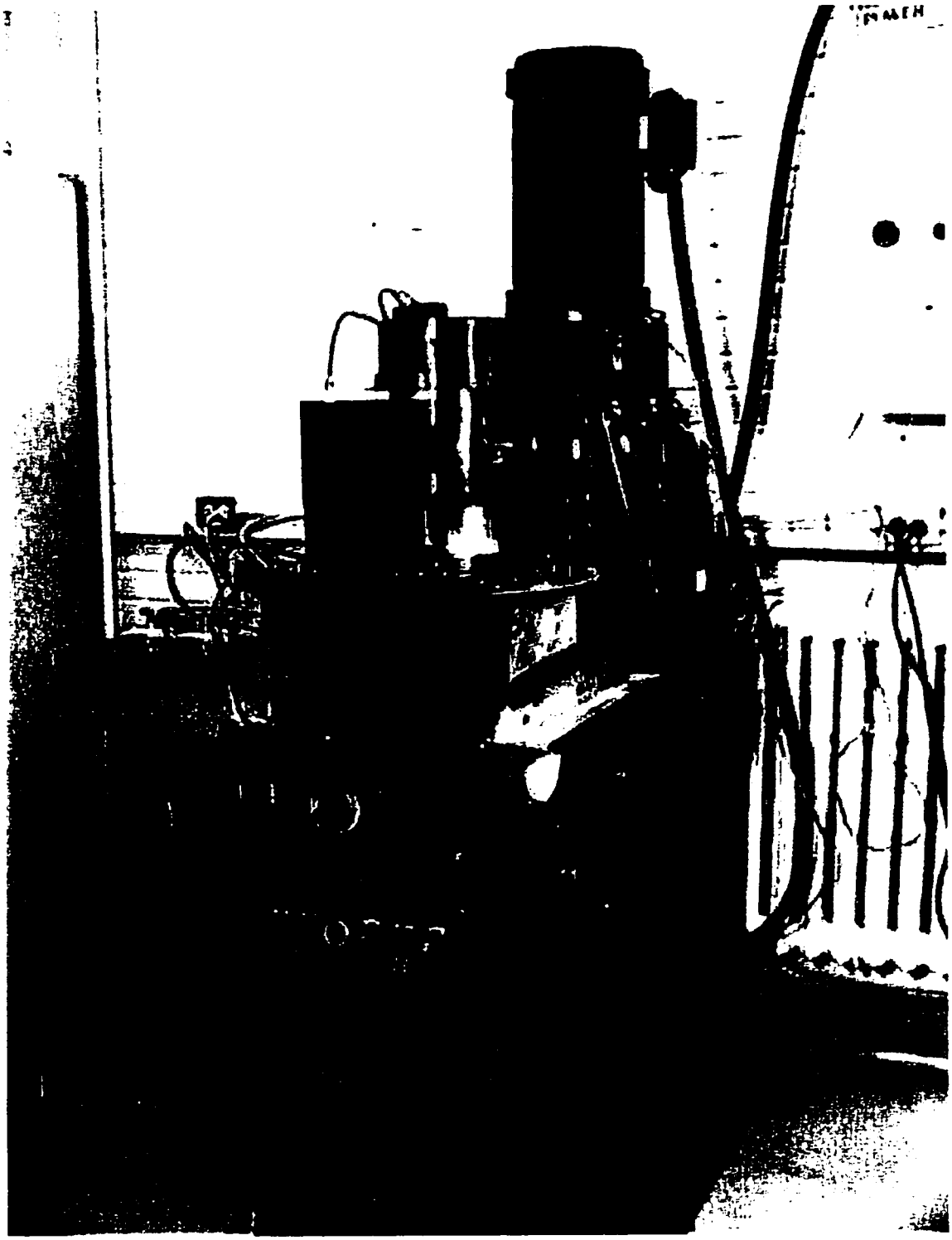

Figure 2.1 General view of the tribometer

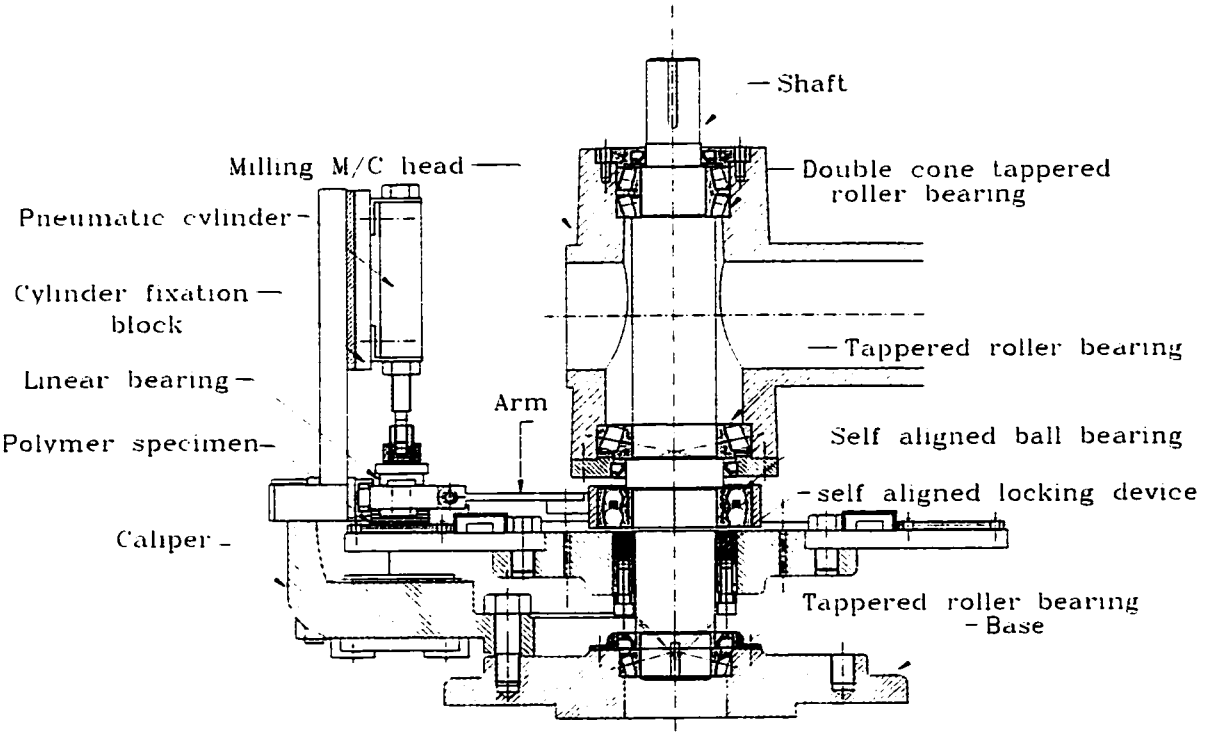

Figure 2.2 General assembly of the tribometer in continuous contact

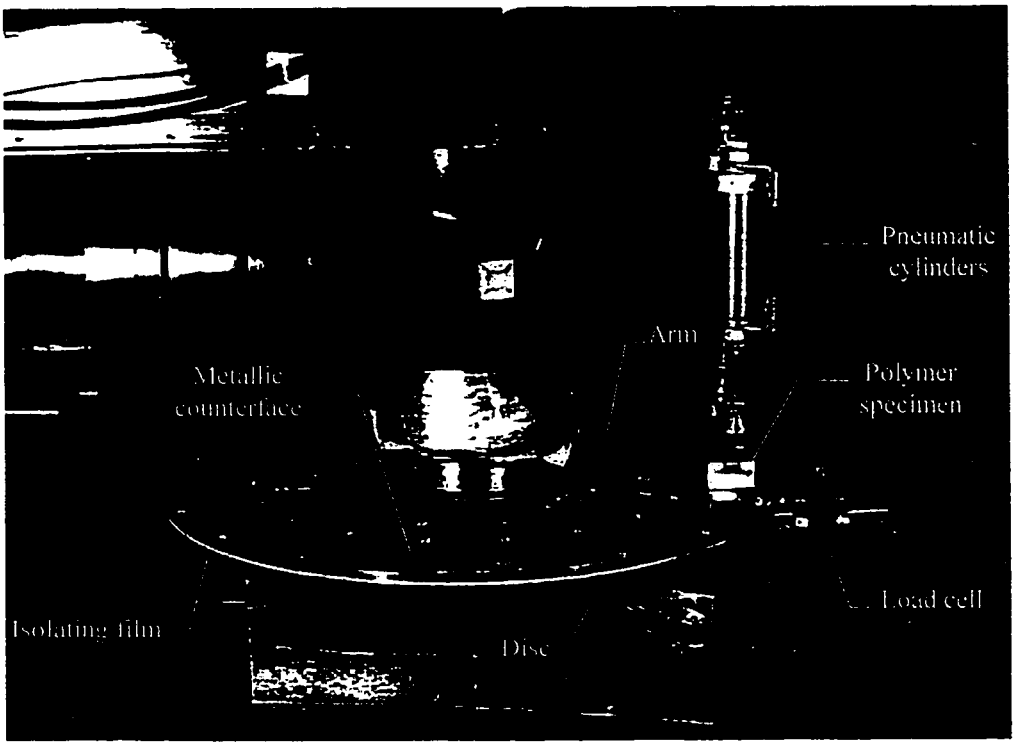

Figure 2.3 Polymer specimen and metallic counterface in continuous contact

16 MB RAM. A control program is designed to analyze the data on line using LABVIEW© version 4.0. Figure 2.4 shows the control panel and figure 2.5 shows the block diagram. The motor is operated using the motor control panel.

The machine is installed in an air-conditioned room to maintain a constant ambient temperature. A steel casing is installed to control the temperature over the contact zone. This casing is connected to a 1/3 HP air pump through a flexible duct (150 mm diameter) to improve the air circulation inside the contact zone (figure 2.6). The casing also serves as a guard from any projected particles.

2.2.2 Polymer-metal contact

2.2.2.1 Continuous contact

In continuous contact, the polymer specimen is fixed to a metallic specimen holder (figure 2.7) which is connected with the piston plate through a linear bearing. A safety arm is installed on each side of the supporting plate to avoid a metal to metal contact between the polymer fixation plate and the metallic counterface.

The metallic counterface (figure 2.8) is prepared from a 455 mm diameter steel ring (ANSI 4130) with 35 R_c surface hardness and with an average surface roughness of R_a = 0.25 μm. The ring has 305 mm inside diameter and a thickness of 6.35 mm. The surface finish is realized after the ring fixation on the disc to insure a homogeneous surface finish and minimum waviness on the surface. The metallic surface finish is reestablished after each test using the mechanism shown in figure 2.9. The lower surface of the ring is thermally isolated from the rotating disc using a 2.5 mm asbestos film as shown in figure 2.3. This isolation permits a precise measurement of the contact temperature and the calculation of the different heat transfer power as will be described in section 2.2.4.3

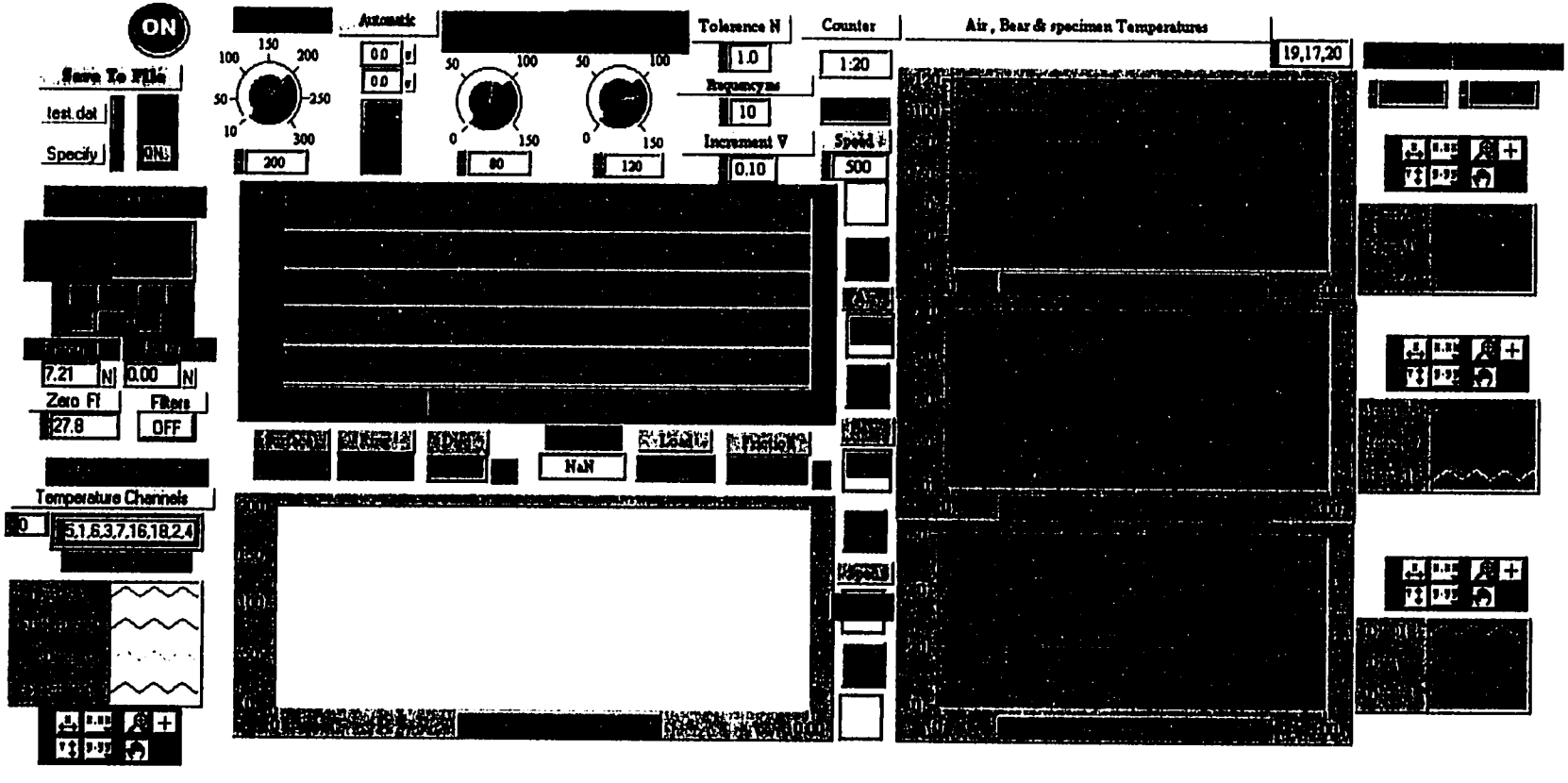

Figure 2.4 Control panel of the system control

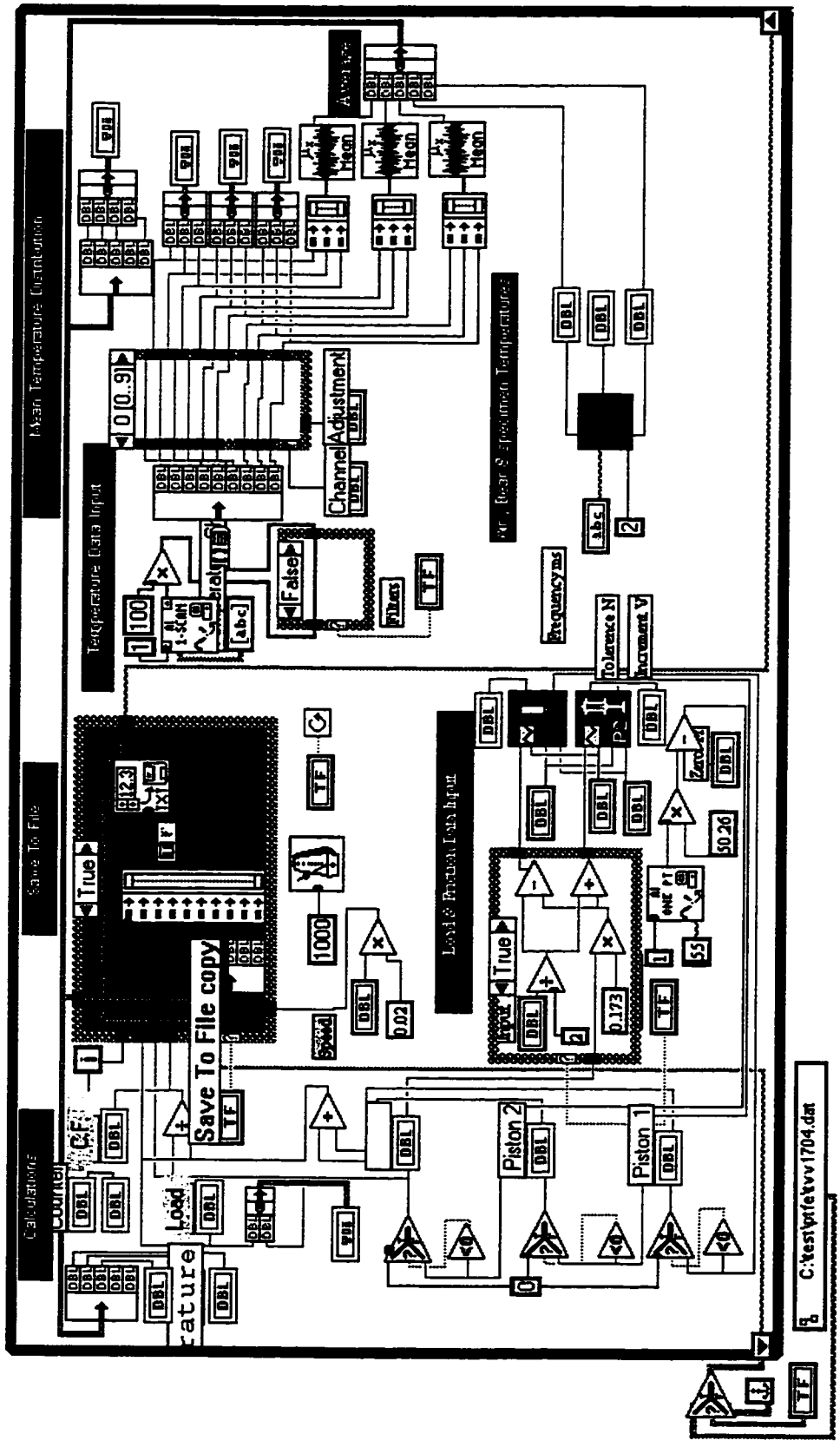

Figure 2.5 Block diagram of the system control

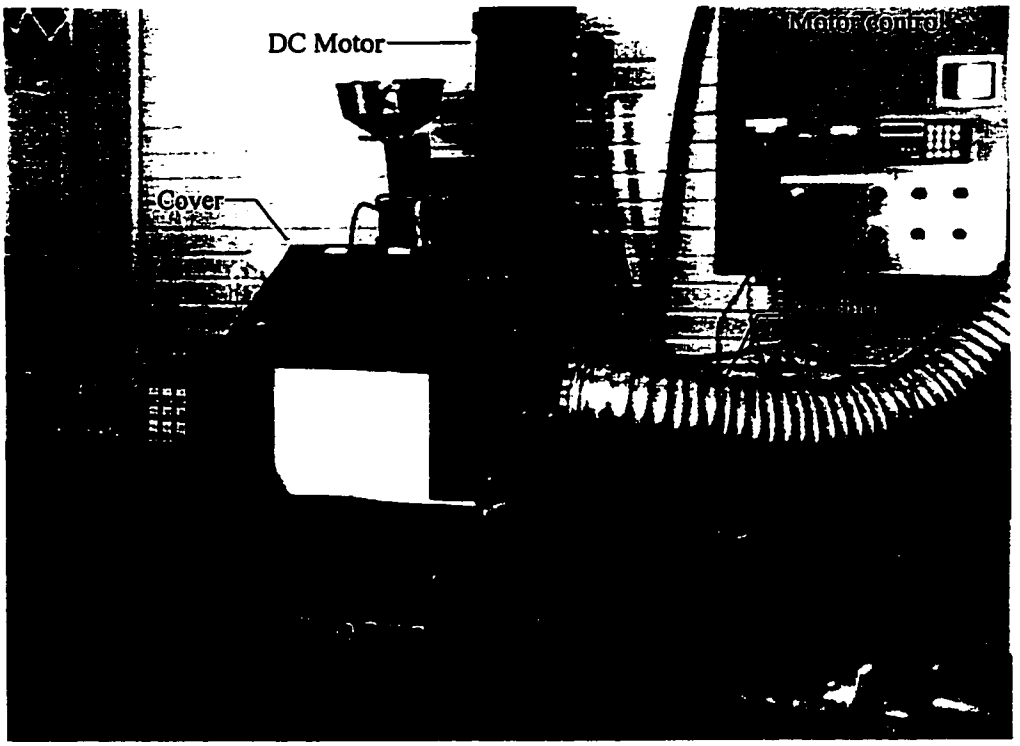

Figure 2.6 The Tribometer casing and the flexible duct for air circulation

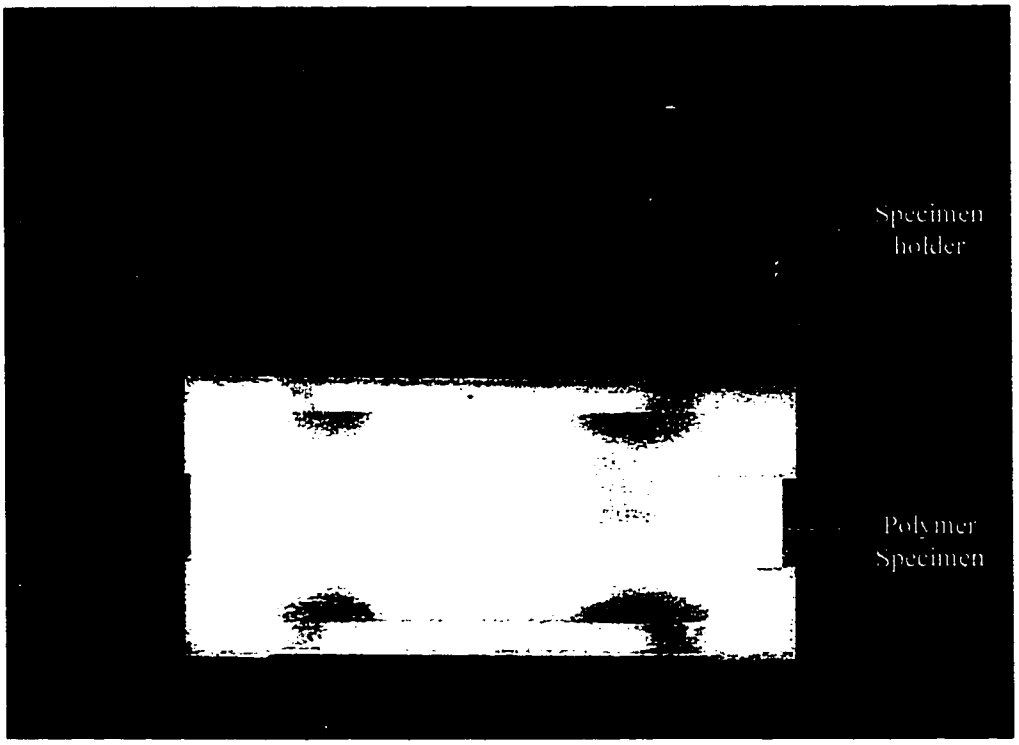

Figure 2.7 The polymer specimen with the specimen holder

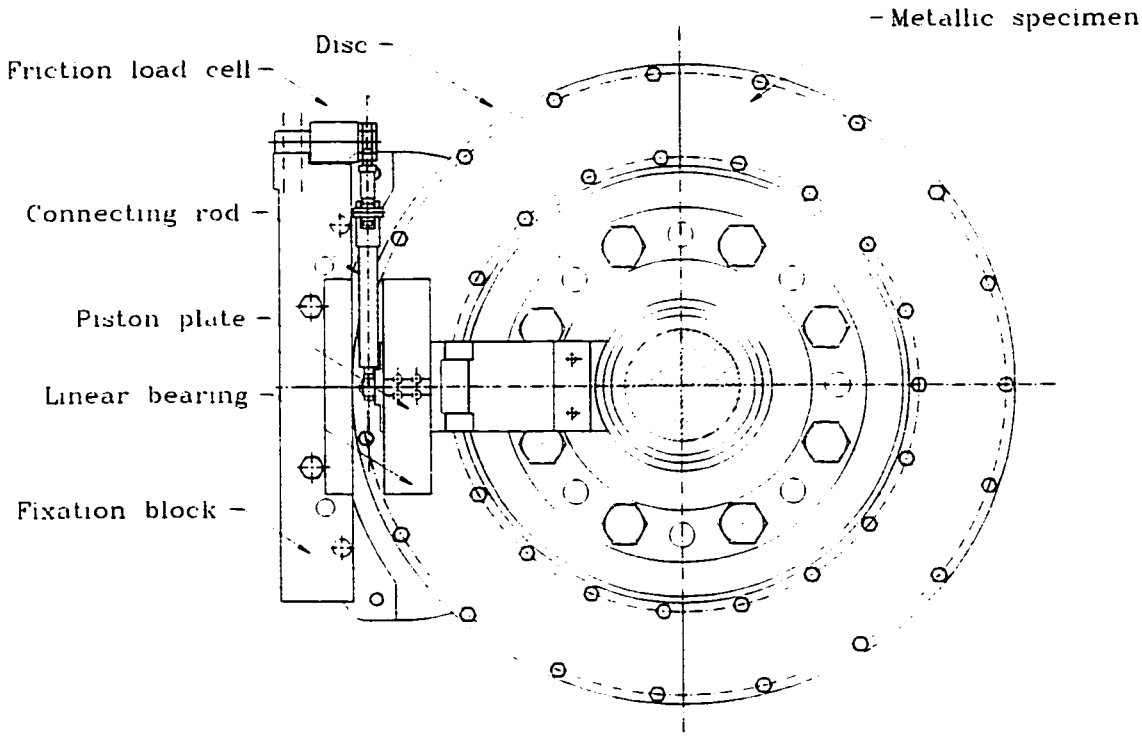

Figure 2.8 The metallic counterface in continuous contact

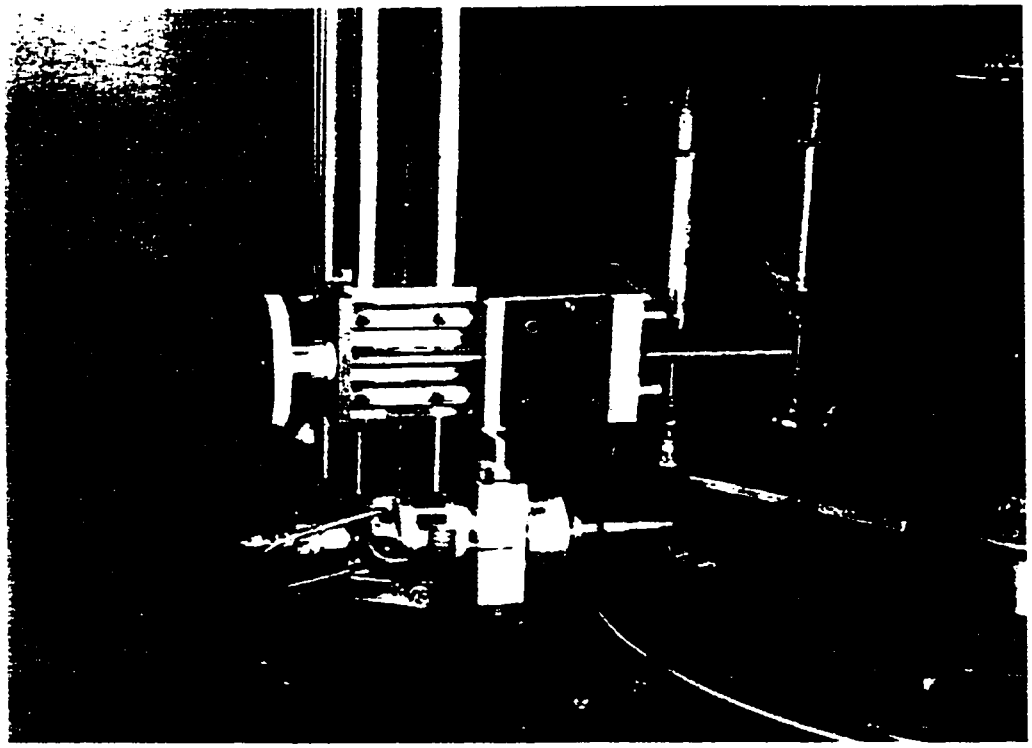

Figure 2.9 System for the metallic counterface surface finish

2.2.2.2 Discontinuous contact

In discontinuous contact the polymer specimen is fixed to a semi circular metallic plate which is in contact with the cylinders pistons through two linear bearings as shown in figure 2.10. Thermocouples are installed under the metallic surface to evaluate the contact temperature.

The metallic counterface is prepared from 19 steel inserts which are fixed on the disc by means of two steel rings (figure 2.11). The polymer specimen length insures the same contact area as in continuous contact. The metallic inserts are 46 mm x 19 mm with 1.6 mm thickness. They are prepared from the same material with the same surface hardness and surface finish of the continuous contact counterface. The same procedure of surface finish is realized as in continuous contact. The lower surface of the inserts and the rings are thermally isolated and thermocouples are installed under the inserts as in continuous contact.

2.2.3 Controlled parameters

To compare the tribological behavior of different materials, the testing parameters and conditions must be maintained identical. The test parameters include the sliding speed, the normal load, the contact area and the relative motion between the materials in contact. The tests are conducted in an air-conditioned room to maintain a constant ambient temperature of 20 °C. The percentage humidity is in general in the range of 25%.

2.2.3.1 Sliding speed

The motor has a speed range of 0 - 3600 r.p.m. The belt transmission speed ratio used in the present document is unity. The motor control panel permits a complete control over the speed, the acceleration and the deceleration of the shaft. The disc has an effective diameter of 381 mm, which leads to a contact speed of up to 70 m/s at full motor speed. The

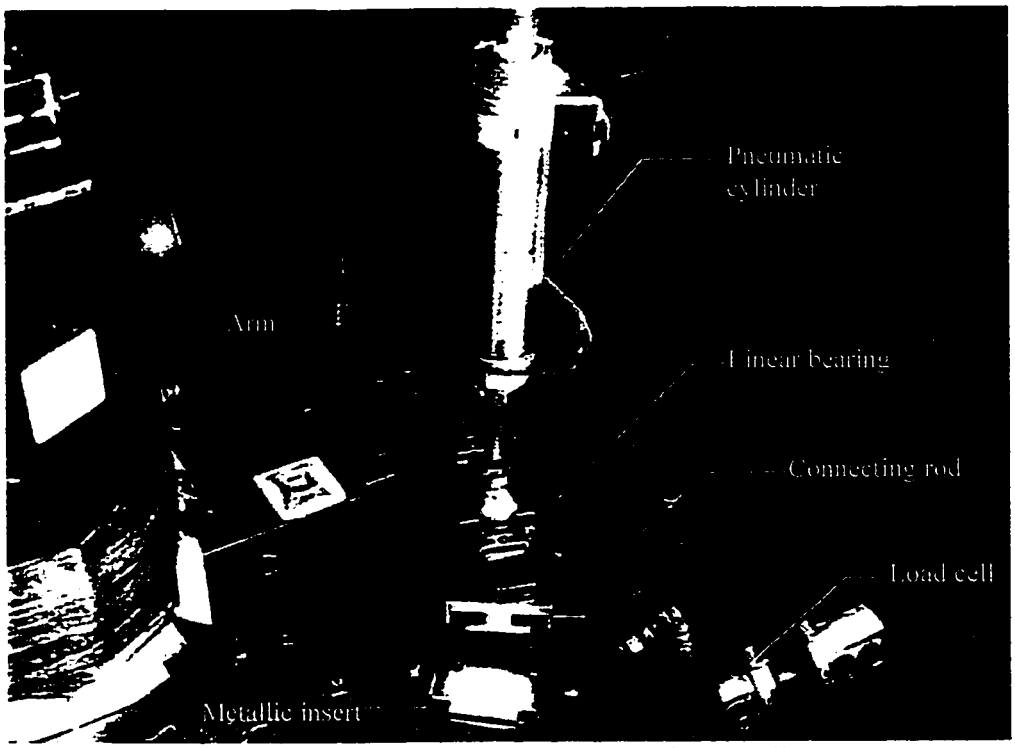

Figure 2.10 Polymer specimen and metallic counterface in discontinuous contact

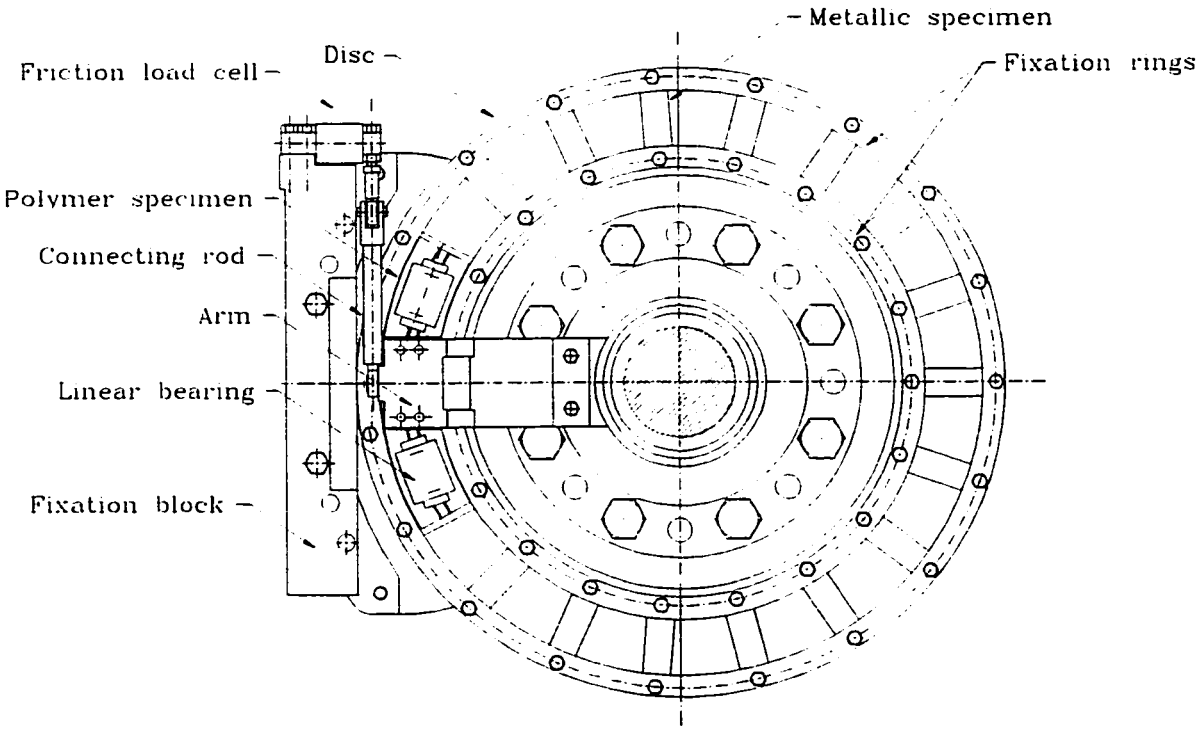

Figure 2.11 The metallic counterface in discontinuous contact

minimum speed is 0.4 m/s. The recommended speed range for smooth running is 1-50 m/s. The linear speed in the inside and outside the contact area varies between ±9% of the mean speed value. The speed calibration is presented in section 2.7.1.

2.2.3.2 Applied load

The load is applied by 2 pneumatic antifriction cylinders which are connected to a 700 kPa (100 psi) compressed air line through 2 servo pressure control cards. Each cylinder can provide up to 145 N (maximum load = 290 N). For higher loads another set of cylinders is used which can provide loads up to 700 N. These cylinders have higher frictional loss and the spring force is much higher than that off the small cylinders. A linear guide bearing is fixed on the polymer specimen fixation plate to minimize the friction between the piston road and the plate (figure 2.3). This eliminates the effect of the applied load on the friction force measurement.

On the other hand, a moment is created between the line of action of the friction load cell and that of the friction force. The individual control of each pneumatic cylinder permits the application of an equivalent moment which neutralizes the effect of the first one on the pressure distribution along the contact surface. The control module is programed to calculate the moment and apply two different forces on each pistons.

The pneumatic cylinders and the pressure control cards specifications are presented in Appendix II. A loading calibration test is conducted for both cylinder sizes with the pressure control system to insure accurate load application (see section 2.7.3)

2.2.3.3 Contact area and Pv value

The contact area is maintained at about 2380 mm^2 in both continuous and discontinuous contact. In discontinuous contact, the polymer specimen length (210 mm)

always insures a minimum of three inserts in contact with a mean contact length of about 70 mm. The contact pressure is calculated with the relation:

$$P = \frac{W}{A_{app}} \quad (MPa) \qquad \textbf{2.1}$$

Where W is the load (N), and A_{app} is the apparent area of contact (mm^2). Table 2.1 presents the Pv values used in the present document.

Table 2.1 Pv values for different speeds and loads in $MPa.m.s^{-1}$

Load (Contact pressure MPa)	**Pv value**					
	2 m/s	4 m/s	6 m/s	8 m/s	16 m/s	30 m/s
30 N (0.013)	0.026	0.052	0.078	0.104	0.208	0.39
60 N (0.025)	0.052	0.104	0.156	0.208	0.416	0.78
90 N (0.038)	0.078	0.156	0.234	0.312	0.624	1.17
120 N (0.050)	**0.101**	**0.202**	**0.303**	**0.404**	**0.808**	**1.51**
150 N (0. 063)	0.13	0.26	0.39	0.52	1.04	1.95
180 N (0.076)	0.156	0.312	0.468	0.624	1.25	2.34
200 N (0.084)	**0.168**	**0.336**	**0.504**	**0.672**	**1.34**	**2.52**
210 N (0.088)	0.176	0.352	0.528	0.704	1.41	2.64
240 N (0.101)	0.202	0.404	0.606	0.808	1.62	3.03
270 N (0.113)	0.226	0.452	0.678	0.904	1.81	6.78
290 N (0.121)	0.242	0.484	0.726	0.968	1.94	3.63

2.2.4 Measured parameters

In friction and wear tests, the main parameters that are generally reported are the coefficient of friction, the wear rate and the temperature of the contact. The friction

coefficient is calculated using Coulomb law of friction (C_f = F / W), the wear rate is measured by weight and the contact surface temperature is measured using thermocouples. A thermocouple type J is installed at the bottom of the machine head to monitor the temperature of the tapered bearing which would be the most affected by any mechanical problem, excessive preloading or vibration in the machine.

2.2.4.1 Friction force

The friction force (F) is measured using 150 lb (667 N) bending beam load cell which is fixed to the machine frame. The load cell is connected to the arm through a flexible connecting rod mechanism (figure 2.3). The connection between the arm and the load cell is designed in such a way that the line of contact is always perpendicular to the resultant friction force on the arm. The maximum output torque of the motor shaft is about 47.5 N.m which leads to a maximum friction force of 250 N. The calibration of the friction measurements is presented in section 2.7.2. The friction load cell specifications is presented in Appendix II.

2.2.4.2 Wear rate

The wear rate is measured by weight using a 0.1 mg precision balance. The polymer surface is cleaned before and after each test using a pressurized air jet. Due to the specimen dimensions in discontinuous contact, a larger balance is used which has a precision of 0.01 g. The density of the polymer ρ is used to determine the volumetric wear rate as follows:

$$k = \frac{\Delta m}{\rho \, W \, v \, t} \qquad 2.2$$

Where Δm is the mass loss (kg) during the test period t (sec).

2.2.4.3 Contact temperature

In continuous contact, the metallic surface temperature and the heat flux are measured using 3 groups of thermocouples type K (Ni-Cr and Ni-Al). Each group consists of 3 thermocouples distributed at 120 ° along the effective circumference; the first group is fixed inside the metallic specimen at 0.4 mm from the surface, the second group is fixed directly under the metallic surface whereas the last group is fixed under the isolating film adjacent to the second group as shown in figure 2.12. The first 2 groups are used to detect the difference between the temperature measured adjacent to the surface and directly under the metallic specimen. The last 2 groups are used to calculate the heat flux through the asbestos film. Another thermocouple is installed 2 mm above the metallic surface to measure the air temperature. The complete heat transfer analysis is presented in section 3.2.2.

The thermocouples are connected, through 9 thermocouples amplifiers (10 mV / °C), to a 10 contacts slip ring fixed on the shaft end as shown in figure 2.13. Amplifying the temperature signals before the slip ring insures a lower noise on the signals. The thermocouples and amplifiers specifications are presented in Appendix II. The calibration of the thermocouples is presented in section 2.7.4.

In discontinuous contact, The metallic surface temperature is measured using 9 thermocouples type K. The first 5 thermocouples are fixed under 5 different inserts where the other 4 are fixed under the isolating asbestos film of the adjacent inserts.

It is very difficult to measure the polymer surface temperature due to its low thermal conductivity and high wear at high speeds. Also, the film transfer affects the temperature measurement on the metallic surface. To study those effects, fine thermocouples are embedded in the polymer surface at 1 mm from the surface of contact. This technique is used in evaluation tests only to investigate the difference between the metallic and the polymer surface temperatures measured for different polymers at different speeds (see section 3.3.2).

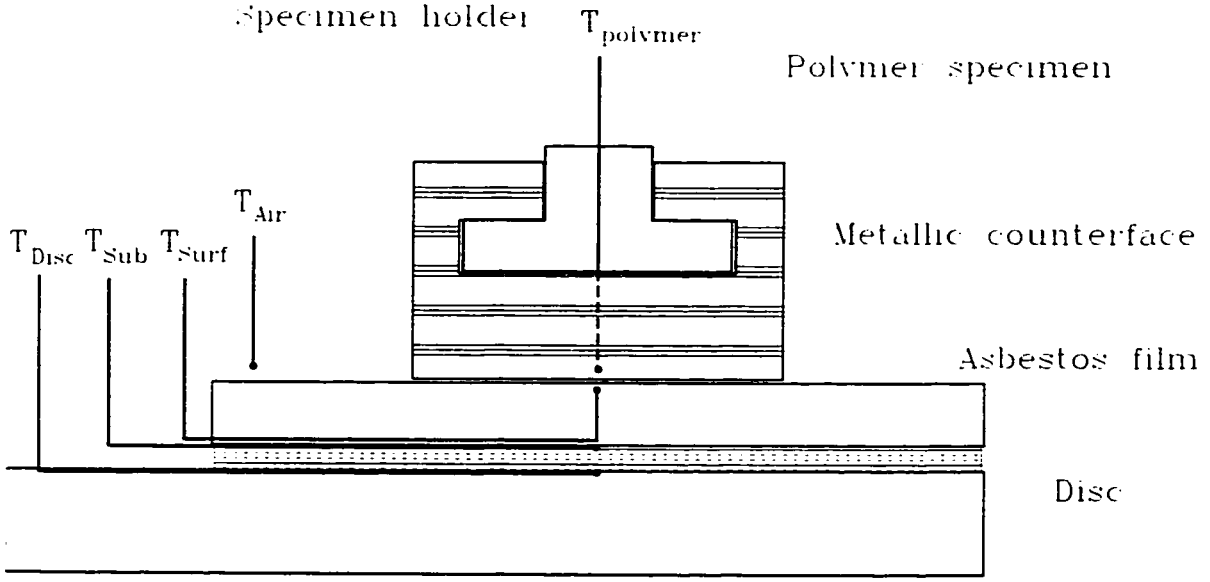

Figure 2.12 Temperature measurement of the metallic counterface

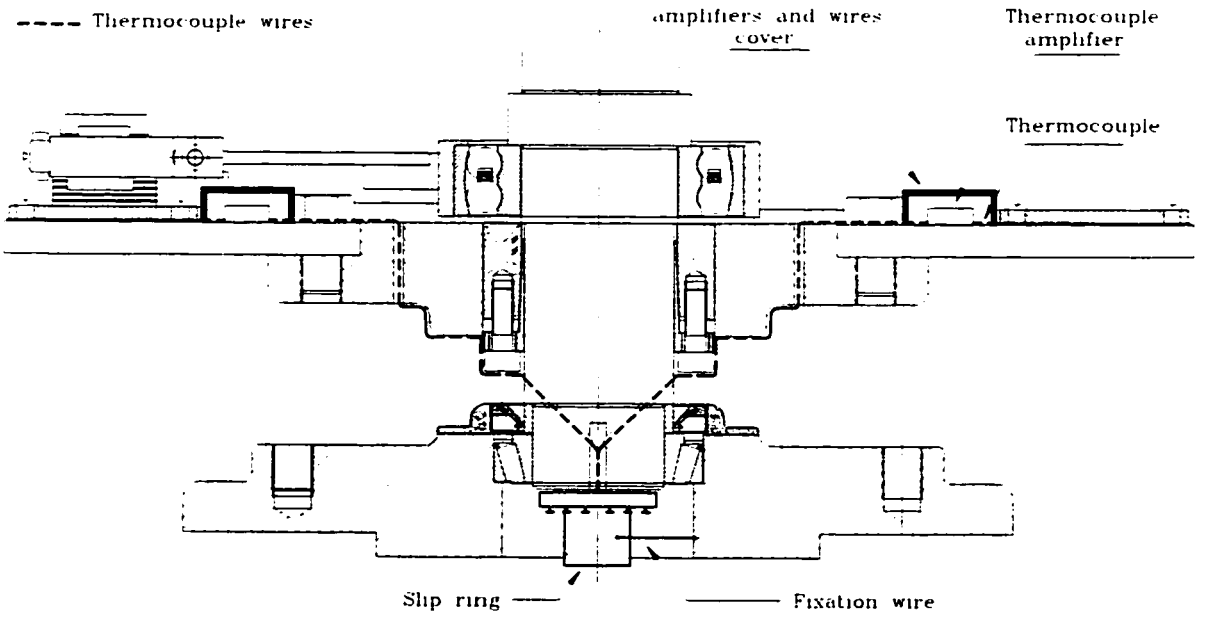

Figure 2.13 Thermocouples wires and slip ring

2.2.5 Other applications

This tribometer has also the capacity to run under lubricated conditions with and without abrasive particles. A system of water lubrication is installed and was tested under variable flow rates. A spray nozzle with mixed air and water inlet insures both the flow rate control and a homogeneous distribution of water through the requested area as shown in figure 2.14. The calibration of this system is presented in section 2.7.5.

A system of abrasive particles feed is also installed on the machine head as shown in figure 2.15. The abrasive particles feed is controlled manually for both lubricated and unlubricated contact. Due to the humidity effect in lubricated system, certain modification were necessary to eliminate the risk of blocking the outlet of the abrasive hose.

2.3 Polymer specimens

The polymers tested are UHMWPE(Ramex from Symplastics), Acetal homopolymer (Delrin from Dupont), Nylon 6/6 (Comco Nylon-GP from Commercial Plastics) and PTFE (Teflon from Dupont). General properties of the tested materials are found in table 2.2, and the manufacturers reported no additives or fillers in any material.

In continuous contact, the polymer specimens are prepared from a 1.2 m slides with 19 mm x 38 mm cross section. They are cut to 70 mm long specimens and machined to have the cross section shown in figure 2.16. The polymer specimens have a contact area of 2380 mm^2 with a surface roughness of about R_a = 1 μm.

In discontinuous contact, the polymer specimens are cut from the same slides to have 210 mm length and 34 mm width. Then they are machined to have the same cross section as in continuous contact. The specimen and the preform die (figure 2.17) are then heated for

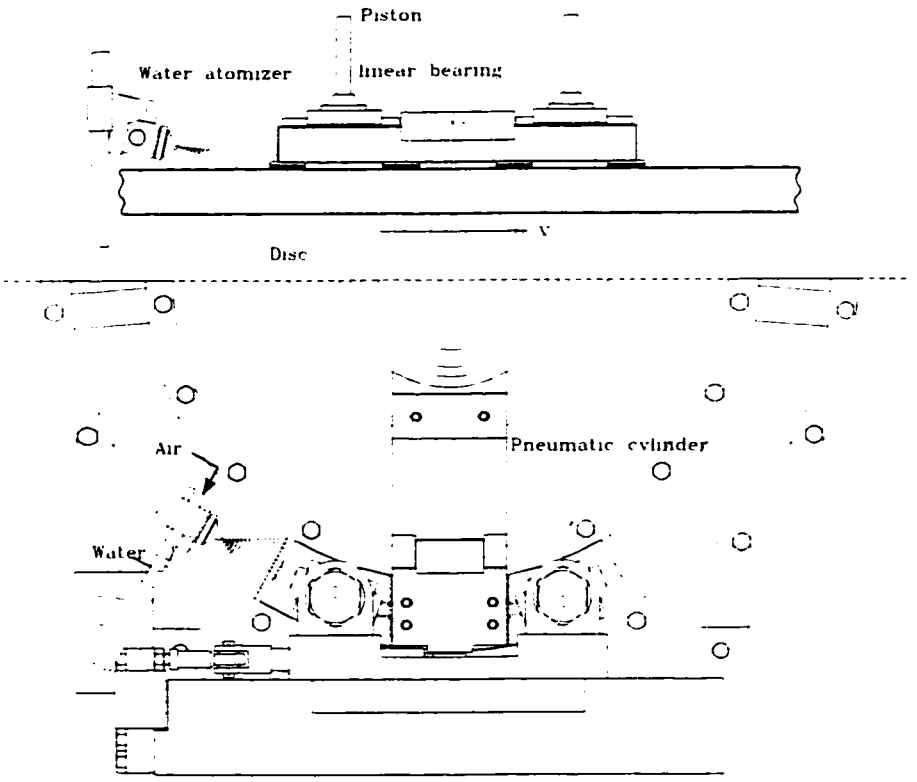

Figure 2.14 Schematic representation of the water lubrication system

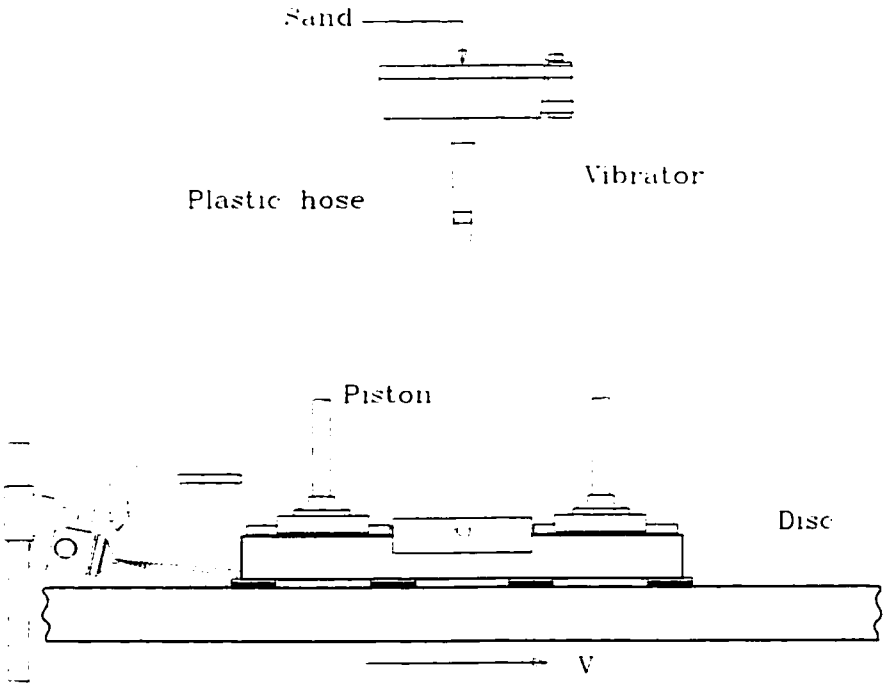

Figure 2.15 Schematic representation of the water lubrication system with abrasives

Table 2.2 General properties of tested materials from manufacturer

Properties	PTFE	Acetal	UHMWPE	Nylon 6/6
Specific gravity	2.17	1.42	0.93	1.14
Tensile strength at yield, MPa	9	68 [r]	20	81
Tensile strength at break, MPa	28 [r]	69	42	83
Percentage Elongation, % at break	275	75	325	90
Izod impact strength, J/m (at 23 °C)	---	240 [r]	No break	---
Notched	160	123	1600	107
Young's modulus, MPa (at 23 °C)	0.35	3.0 [r]	0.53	2.6 [r]
Flexural modulus, GPa (at 23 °C)	0.62	2.8	0.76	2.8 [r]
Hardness, Shore D	52 [r]	81 [r]	65	80 [r]
Hardness, Rockwell R	58	120	52	120
Heat deflection temp. °C, 1.85 MPa	56	136	45	90
0.45 MPa	121	172	70	235
Melting temperature, °C	325	175	135	255
Glass transient temperature T_g °C	127 [r]	-60 [r]	-120 [r]	57-80 [r]
Specific heat kJ / kg °C	1.05	1.47 [r]	2.01	1.67 [r]
Coef. of linear expansion, x 10^5 °C^{-1}	8.5	11.3	18	8
Thermal conductivity W/m.°C	0.25	0.38	0.42 [r]	0.24 [r]
Maximum useful temperature* °C	280 [r]	130 [r]	125 [r]	80 [r]
Water absorption, % wt. in 24 h	0.01	0.25	None	1.2

(r) From different references (*) Recommended in tribological applications

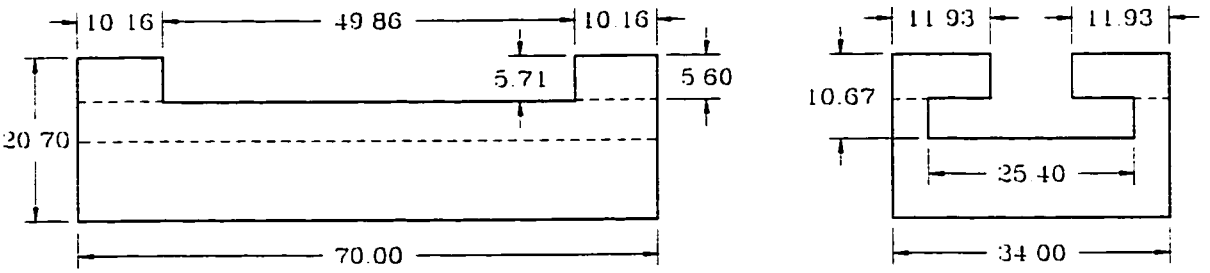

Figure 2.16 Dimensions of the polymer specimen

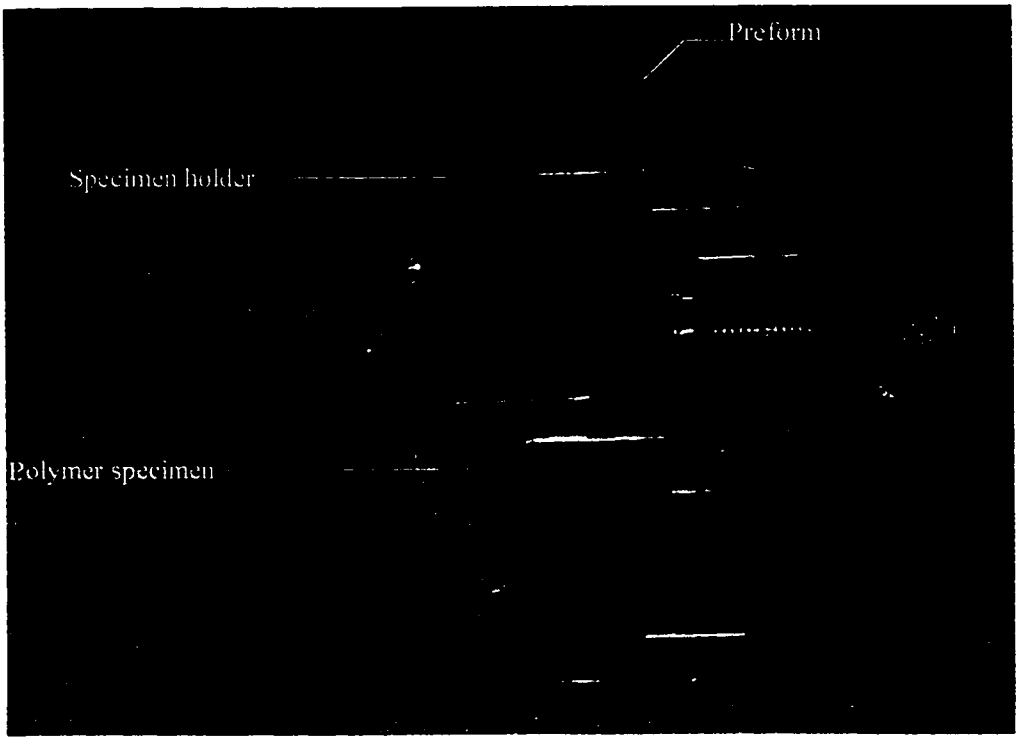

Figure 2.17 The polymer specimen bent in the preform die

two hours to a preselected temperature for each material. Then the polymer is bent in the preform die to have an arc with an mean radius of 190.5 mm. The polymer fixation plate is inserted in the specimen groove and the die, with the specimen bent inside, is left to regain the ambient temperature inside the furnace.

2.4 Calibration

2.4.1 Motor speed and controller

Tests has been conducted on the machine speed and the controller of the DC motor to calibrate the running speed. A stroboscope was used to calibrate the rotating speed of the disc and there was no difference between the stroboscope and the machine readings. The precision of the stroboscope is ±1 r.p.m. (i.e. ±0.02 m/s).

For the motor control system, the machine was tested for more than 18 months before the present tests. The motor was run for more than 300 hr. ($\sim 2 \times 10^7$ rev.) and no problems were detected for either speed, acceleration or deceleration control.

2.4.2 Friction load cell

The friction load cell was tested using the mechanism shown in figure 2.18. The pressure control card are presented in figure 2.19. Standard weights were used for the load cell calibration in both loading and unloading. The load cell output voltage (V_f) to the load measured (W) is presented by the relation:

$$W = 44.48\ V_f - 22.25 \qquad \textbf{2.3}$$

The load cell precision was found to be about ± 0.02 N.

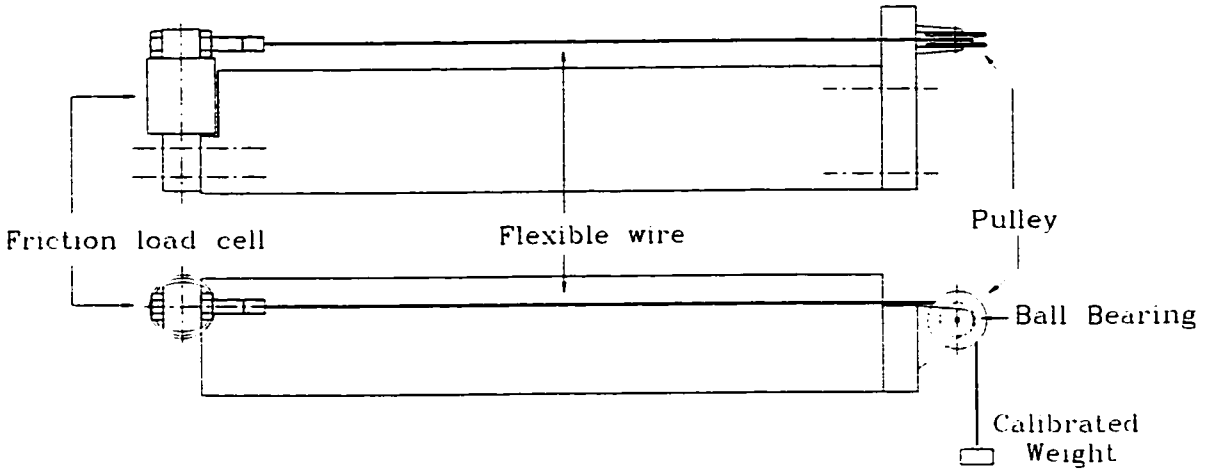

Figure 2.18 Schematic representation of the calibration mechanism for the load cell

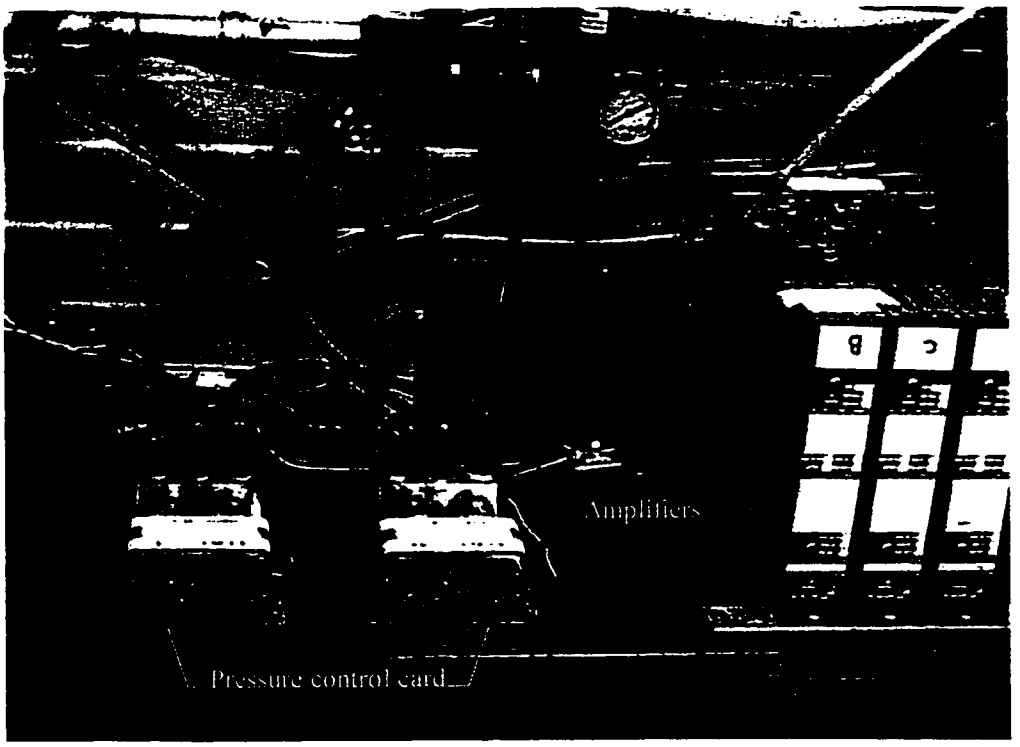

Figure 2.19 Pressure control cards and amplifiers

2.4.3 Load control

The pneumatic pistons applying the load were calibrated using the friction load cell as shown in figure 2.20. To simulate the dynamic loading induced by vibration in the system, a high stiffness spring is used to calibrate the pistons. In this calibration tests, a sinusoidal wave loading was added to the applied voltage (V_i) with a 5 Hz frequency and variable amplitudes from 0 to 0.5 volts. Figure 2.21 and 2.22 presents the relation between the output voltage of the pressure control card (V_o) and the load measured by the load cell for the small pistons. Figure 2.23 and 2.24 presents the same relation for the large pistons with static loading and dynamic loading with 0.5 volt amplitude.

It was found that in general, the difference in loading and unloading values measured by the load cell is minimized in dynamic loading. In the small pneumatic cylinders, the relation between load and output voltage is perfectly linear and the error between loading and unloading values is negligible. In the large pneumatic cylinders, the error between loading and unloading is very high at low loads, whereas at high loads this error becomes negligible. It was recommended to use the small cylinders for loads up to 270 N. For higher values the use of the large cylinders insures a precise loading especially with the dynamic effect induced due to vibrations. In friction and wear tests the weight of the polymer specimen with the holder and the arm is included in the applied load.

2.4.4 Thermocouples

The thermocouples with their specific amplifiers were calibrated in a standard oil bath system. This system provides a calibration temperature range of 20 to 100 °C. An example of such calibration is presented in figure 2.25. Although the precision of each thermocouple provided from the manufacturer is 2.2 °C, the difference in the readings of different thermocouples at high temperature could reach values up to 10 °C. This demonstrates the importance of using the mean values of three thermocouples for each

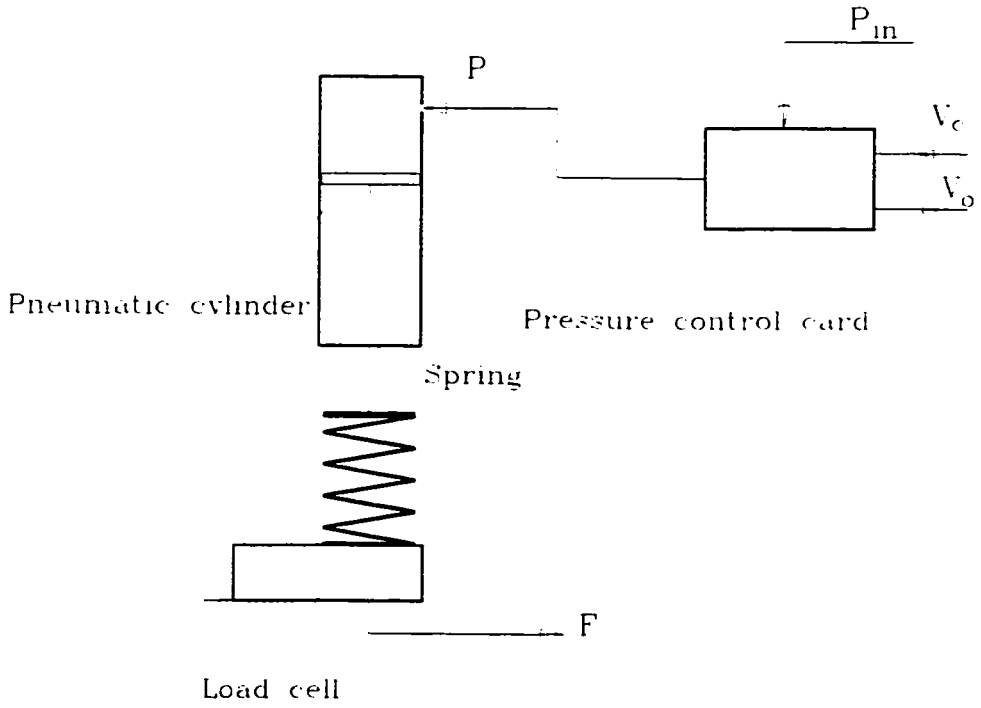

Figure 2.20 Schematic representation of the calibration mechanism for load application

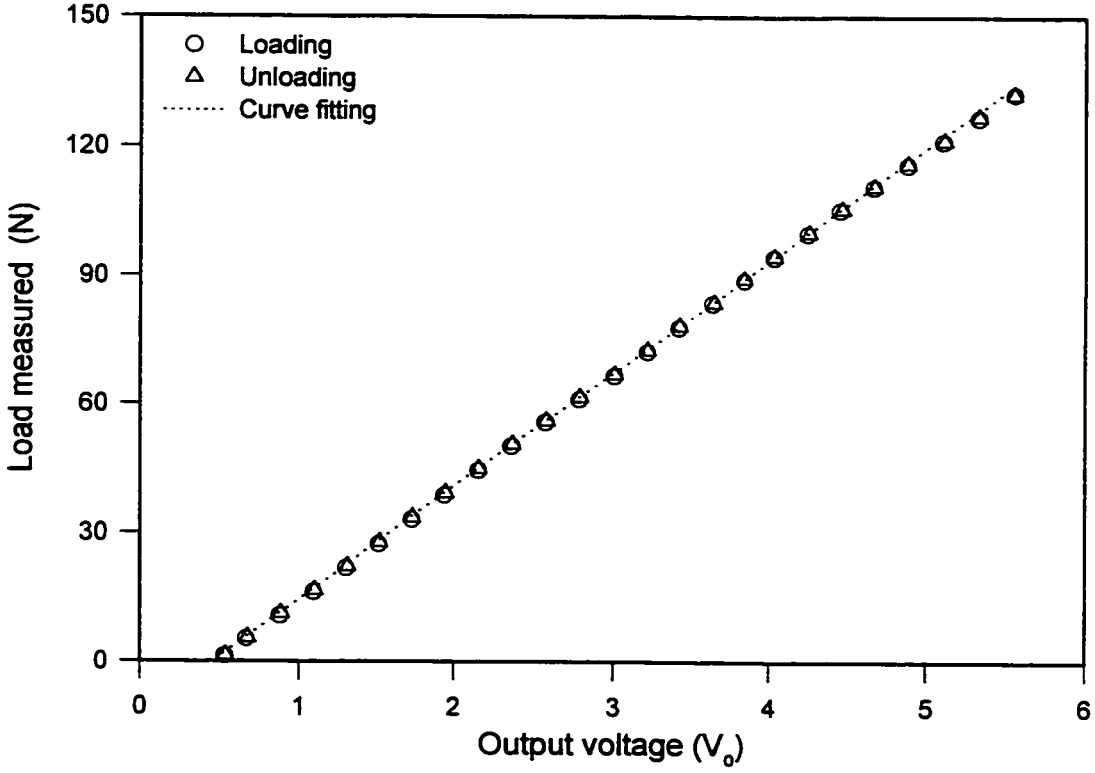

Figure 2.21 Calibration of small pneumatic cylinder 1

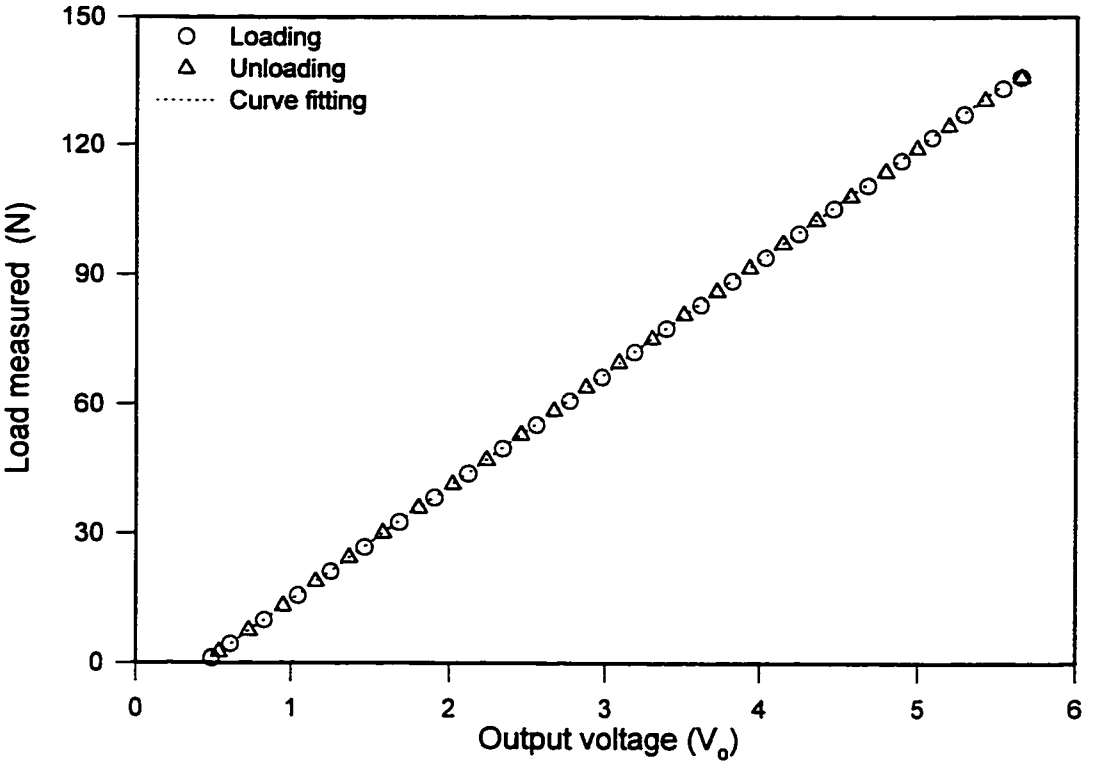

Figure 2.22 Calibration of small pneumatic cylinder 2

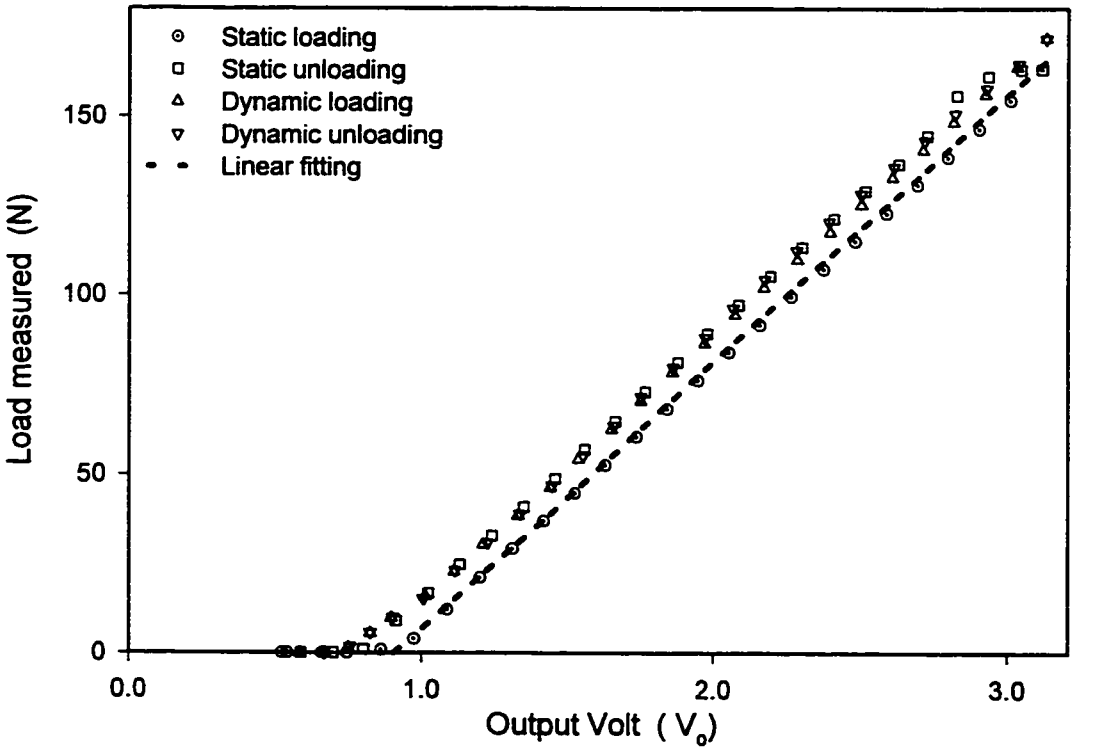

Figure 2.23 Calibration of large pneumatic cylinder 1

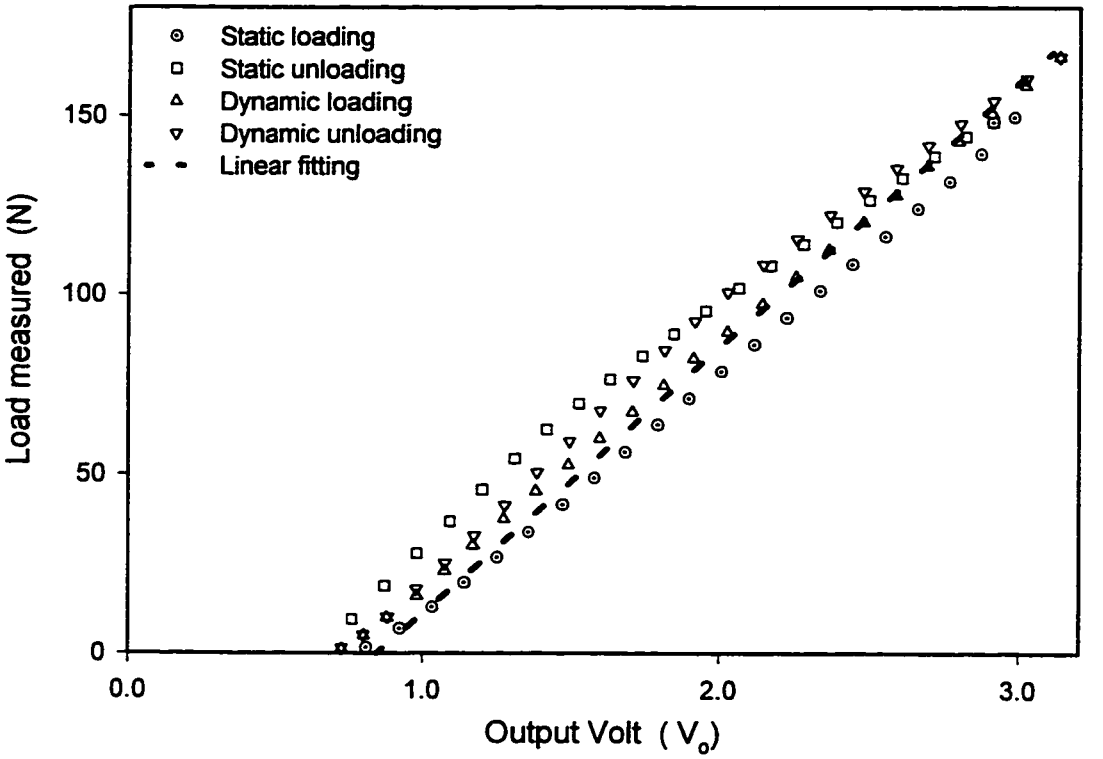

Figure 2.24 Calibration of large pneumatic cylinder

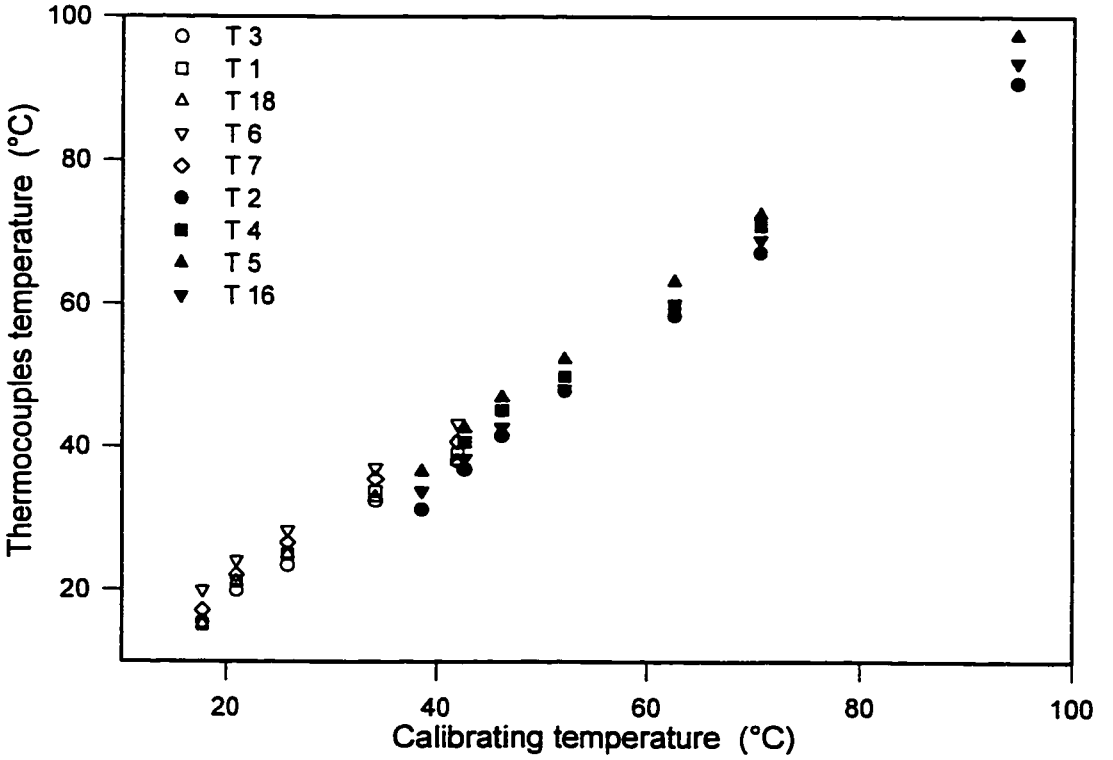

Figure 2.25 Thermocouples calibration (with amplifiers)

temperature measurement. It is to note that some thermocouples were eliminated after the calibration.

2.4.5 Lubrication

The lubrication system of the machine was calibrated using a graduated jar. The flow rate was measured by calculating the time necessary to obtain 200 ml of water in the jar for a certain air and water pressures. Figure 2.26 presents the results of the flow calibration. In this calibration, the area covered by the sprayed liquid must not exceed the contact surface width; this was taken to be the criterion for the maximum flow rate. It is to note that the lubricated tests are performed at speeds varying from 2 to 60 m/s and loads varying from 100 to 600 N. The performance of the load application, speed control and the lubrication system was satisfactory

2.5 Conclusion

The tribometer was calibrated, tested and found to be satisfactory for friction and wear testing under high speed of up to 60 m/s and loads of 600 N with the necessary rigidity and dynamic stability. The system has the capacity to withstand long duration tests with large contact area (7000 mm^2) for both continuous and discontinuous contact.

The load application control and the friction and temperature measurements are calibrated and found to be reliable with the necessary precision required for such machines. Two different set of pneumatic cylinders are installed and calibrated for low and high load applications. The system computer allows an on line control and monitoring of the load, the coefficient of friction and the temperature distribution at different points of contact. It is also equipped with safety features for high wear rates and to monitor excessive temperature rise, high friction force and bearing temperatures.

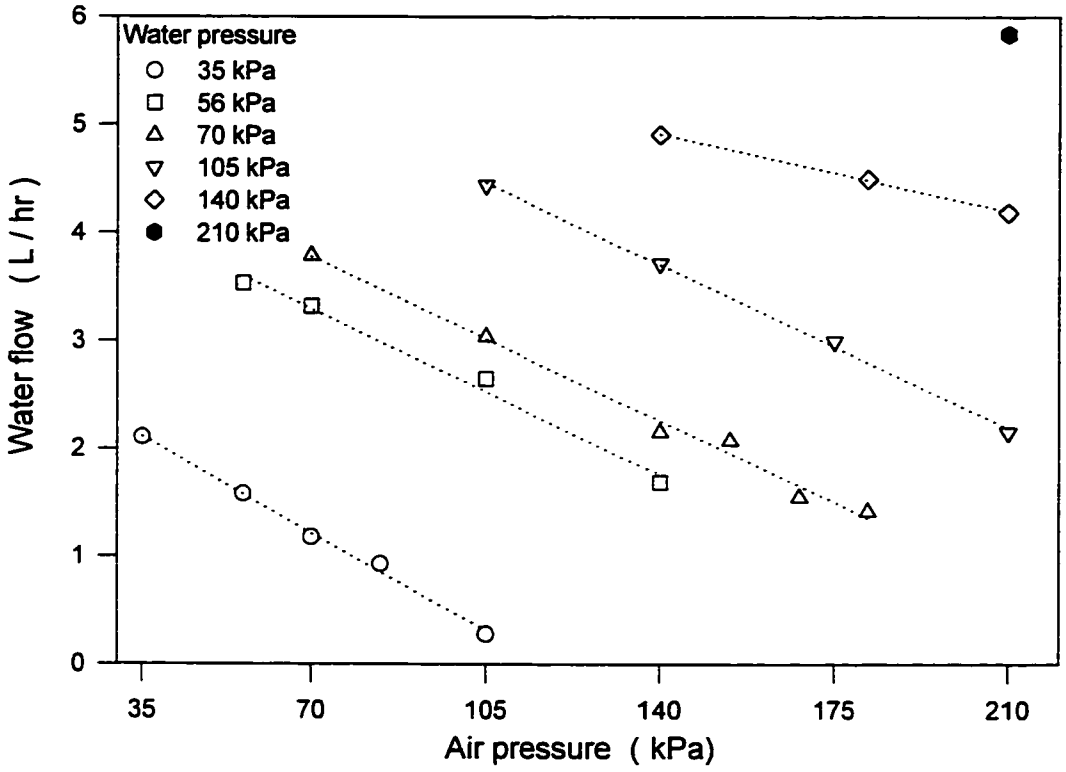

Figure 2.26 Calibration curves for water atomizer

The machine has also the capacity to work under lubricated conditions with and without abrasive particles. A chart is prepared for water lubrication control using the inlet air and water pressure. This lubrication system with abrasives was used in various industrial tests which are not reported due to the confidential aspect of the project.

Although the machine is designed mainly to test polymer-metal contact, it has the capacity to test any combination of materials. Many dry and lubricated sliding applications can be studied using the tribometer such as: snowmobile sliders, disc brakes, wheels on pavement and thrust bearings.

CHAPTER III
THERMAL ANALYSIS

3.1 Introduction

In high speed applications the contact temperature has a predominant effect on friction and wear characteristics of polymers. The rate of heat generation increases with increasing speed and load. Due to the low thermal conductivity of polymers, high temperature is generally developed in the contact surface. This temperature rise will eventually decrease the elastic modulus of the material which in turns increases the real contact surface and decreases its rigidity. This change in surface characteristics affect dramatically the friction coefficient and wear mechanisms in the contact zone.

One of the most sophisticated problems in tribological applications is the contact temperature measurement. This is due to the large number of parameters which affect the heat generation and dissipation in the contact. In chapter I, theoretical models have been presented which are combined to experimental measurements to evaluate the contact temperature in a specific application. The parameters used in those models are deduced for specific geometries of the surface in contact. There is no general model that predicts the contact temperature in any application.

In this chapter, a one dimensional thermal analysis is presented for the calculation of the contact temperature in the tribometer. The energy equation derived is applied on the friction and the metallic temperature measurements, obtained at different test conditions, to validate the measurement approach. Another measurement technique is also used to investigate the real contact temperature.

3.2 Heat transfer energy equation

The first objective of this analysis is to develop a simplified heat transfer equation which can be used to evaluate the friction and temperature measurements performed on the tribometer. The energy equation deduced will also be used to compare the conduction and convection terms in the heat transfer energy. The problem considered here is applied on the continuous contact case.

The metallic surface, with high width to thickness ratio (~12:1), is in contact with the polymeric specimen over a 2380 mm² surface area. The polymer specimen is considered as an intermittent source of heat in contact with a metallic surface. Due to the high difference in thermal diffusivity, the heat generated is considered to be completely absorbed by the metallic surface. The heat energy is dissipated from the metallic surface by convection to the surroundings and by conduction to the disc through the isolating asbestos film.

3.2.1 Transient heat transfer problem

To solve the energy equation certain conditions are to be considered. In this part, the problem of the transient heat source is analyzed to determine the expected variation of the contact temperature per disc revolution.

The polymer specimen is represented by a heat source (Q) of surface area (A), in contact with a metallic surface of width (B) and thickness (t_m) over a length (l) at a speed (v) as shown in figure 3.1. In the contact zone, the surface temperature rise from the value T_{in} to T_{max}. In the no-contact zone, the temperature drop from T_{max} to T_{in} as shown in figure 3.2. The energy equation in transient condition, presented by Eckert (1972), is solved using the following assumptions:

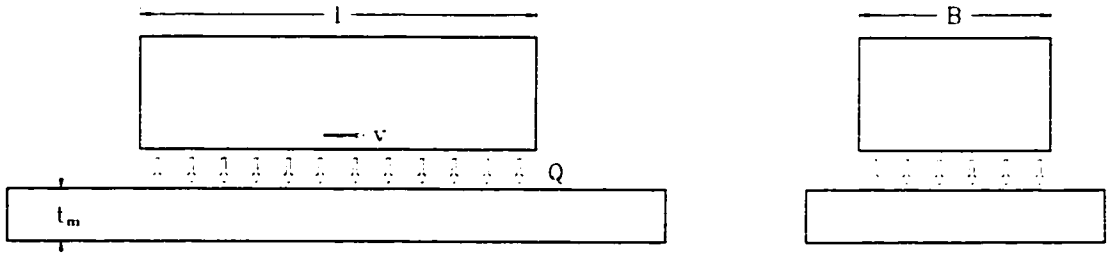

Figure 3.1 Moving heat source in contact with metallic counterface

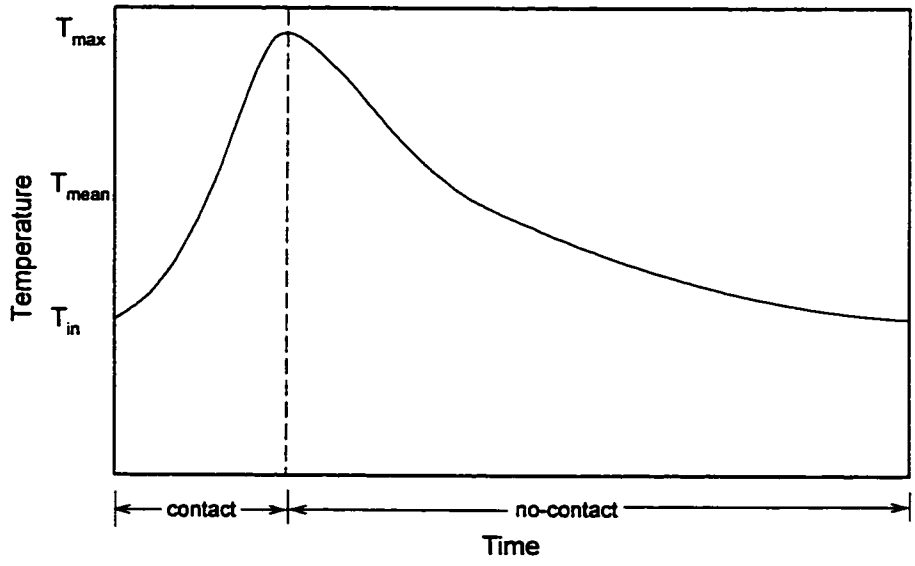

Figure 3.2 Schematic representation of the temperature rise in the contact

- Semi-infinite body (to be validate)
- Constant heat flux ($Q = C_f W v$)
- Constant k, ρ, c_p with temperature
- No heat convection in the contact zone during the contact
- The heat is homogeneously distributed on the contact surface

Using these assumptions, the temperature rise (ΔT) after a contact time (τ) at a distance (x) under the metallic surface is given by the relation:

$$\Delta T = T_x - T_{in} = 1.065 \frac{q}{k_m} \sqrt{\alpha_m \tau} \left(1 - \frac{x}{2.81 \sqrt{\alpha_m \tau}}\right) \qquad \textbf{3.1}$$

Where $q = Q/A$, k_m and α_m are respectively the thermal conductivity and diffusivity of the metallic surface. Hence, the maximum surface temperature rise can be given by:

$$\Delta T_{max} = T_{max} - T_{in} = 1.065 \frac{q}{k_m} \sqrt{\alpha_m \tau} \qquad \textbf{3.2}$$

The depth of penetration of the temperature x_{max}; i.e. the thickness at which no temperature rise will occur per disc revolution, is given by:

$$x_{max} = 2.81 \sqrt{\alpha_m \tau} \qquad \textbf{3.3}$$

Example: In a typical continuous contact test the sliding speed is 10 m/s, and the applied load is 200 N with a contact length of 70 mm. The coefficient of friction is measured and found to be 0.36. The friction heat generated and the contact time are:

$$q = \frac{C_f W v}{A} = 3.0 \times 10^5 \ W/m^2 \quad , \quad \tau = \frac{l}{v} = 0.007 \text{ sec}$$

For steel with 1% C: $k_m = 43$ W/m°C and $\alpha_m = 1.17 \times 10^{-5}$ m^2/sec

Applying equations 3.2 and 3.3, the temperature rise and the depth of penetration are:

$$\Delta T_{max} = 2.13 \ ^\circ C \quad , \quad x_{max} = 0.8 \ mm$$

It is clear from this example that the maximum possible temperature rise of a point on the contact surface will be very small compared to the mean metallic surface temperature. Hence, the steady state energy equation can be solved with the assumption of a uniformly distributed heat source on the metallic counterface surface A_m.

On the other hand the transient temperature rise is concentrated on a thin film representing 1/4 the thickness of the metallic counterface. This confirm the assumption of semi-infinite body used in this analysis. This temperature rise will not influence the readings of the thermocouples installed under the metallic surface.

3.2.2 One dimensional energy equation

Before analyzing the energy equation for heat transfer under high speed contact, the following assumptions are considered:

- First, assuming that the heat source is uniformly distributed along the contact length, as discussed in section 3.2.1, the problem can be considered as a two dimensional problem.

- Then, assuming that the heat source width gives a uniformly distributed temperature along the width of the metallic specimen, the problem is furthermore simplified to one dimension.

- The metallic specimen has a homogenous temperature distribution over the surface. The temperature of the bolt head in contact with the surface of the metallic specimen is equal to the temperature under the metallic specimen.

- The air flow on the metallic surface is purely turbulent due to the disc rotation and infinite direction of air circulation.

- No contact resistance; i.e. the contact temperature is the same on both materials surface.

Applying the preceding assumptions, the heat balance can be given by the relation:

Heat generated (H_g) = Heat dissipated (H_d) + variation in internal energy (H_i)

where H_i is the variation in the internal energy of the metallic specimen. Taking H_{cond} and H_{conv} to be heat dissipated through conduction and convection respectively, we obtain the following relations:

$$H_g = F\,v \quad , \quad H_d = H_{conv} + H_{cond} \quad , \quad H_i = \rho_m\, C_p\, V_m \frac{dT_m}{d\tau} \qquad \textbf{3.4}$$

where V_m is the volume of the metallic counterface and T_m is its mean temperature. Using the temperature notation presented in figure 2.3 we obtain:

$$H_{conv} = h\, A_m\, (T_{surf} - T_{air}) \quad , \quad H_{cond} = k_{asb}\, A_m \frac{(T_{sub} - T_{disc})}{t_{asb}} \qquad \textbf{3.5}$$

The energy equation becomes:

$$F\,v = h\, A_m\, (T_{surf} - T_{air}) + k_{asb}\, A_m \frac{(T_{sub} - T_{disc})}{t_{asb}} + \rho_m\, C_p\, V_m \frac{dT_m}{d\tau} \qquad \textbf{3.6}$$

3.2.3 Simplified energy equation

The difference between the metallic surface temperature T_{surf} and the temperature measured under the surface T_{surb} is very small. This can be verified by a simple calculation

of the difference between the thermal resistance of the asbestos film and that of the metallic one as follows:

$$q_{cond} = k_m \frac{(T_{surf} - T_{sub})}{t_m} = k_{asb} \frac{(T_{sub} - T_{disc})}{t_{asb}} \qquad \textbf{3.7}$$

Using the thermal conductivities and thickness of both surfaces we obtain:

$$\frac{T_{surf} - T_{sub}}{T_{sub} - T_{disc}} = \frac{k_{asb}\, t_m}{k_m\, t_{asb}} = \frac{0.17 \times 6.35}{43 \times 2.5} = 0.01$$

In the following analysis both temperature will be taken equal to T_m. On the other hand, the precision in internal energy calculation is extremely low since the interval of temperature measurement is 1 second and the precision is 1 °C. An order of magnitude analysis shows that the error in internal energy calculation is between 100 to 2000% of the heat generated for the application load and speed range. Only steady state conditions will be studied in this analysis; i.e. when the metallic surface temperature stabilizes. Hence, the heat balance at steady state conditions can be written in the form;

$$F\, v = h\, A_m\, (T_m - T_{air}) + k_{asb}\, A_m \frac{(T_m - T_{disc})}{t_{asb}} \qquad \textbf{3.8}$$

In the calculation of the conduction term, the heat conducted from the metallic specimen to the disc through the bolts was neglected. In the following calculations, using the fourth assumption, the ratio between the heat conducted through the bolts and that through the asbestos film is calculated and a correction factor is added to the conduction term. Using the turbulent flow assumption, the coefficient of heat convection is calculated from the relations:

$$h = \frac{Nu}{L} \times k_{air} \quad , \quad Nu = 0.037\, Re_L^{4/5} \times Pr_{air}^{1/3} \quad , \quad Re_L^{4/5} = \frac{v\, L}{\nu_{air}} \qquad \textbf{3.9}$$

The characteristic length (L) is taken as the mean circumference of the metallic ring (π D_{mean}) The air constants k_{air} , Pr_{air} and ν_{air} are taken from tables at T = 23 °C (Eckert 1972). The steel and asbestos thermal properties are taken from the same reference and the metallic surface is calculated. The heat transfer relation for the frictional contact in the tribometer can finally be given by the relation:

$$F\ v = 0.55\ v^{4/5}\ (\ T_m - T_{air}\ ) + 14.36\ (\ T_m - T_{disc}\ ) \qquad \textbf{3.10}$$

Measuring the friction force permits the calculation of the left side of the equation (heat generation), where measuring the air temperature, T_{sub} and T_{disc} permits the calculation of the right side of the relation (heat dissipation). Therefore, the temperature measurements could be verified by the friction force measurement and vis versa.

3.3 Measurements

To verify the temperature and heat flow measurements precision and reliability, tests has been performed on different polymers for different speeds. Two group of tests are performed; the first to investigate the accuracy of the force and the temperature measurements, the second to measure the polymer surface temperature in order to investigate the real contact temperature.

3.3.1 Metallic surface temperature

The objective of these tests is to evaluate the accuracy of the friction and metallic surface temperature measurements. First, the friction force and the metallic surface temperature are measured in variable speed tests for different polymers. The results are then substituted in the energy equation to calculate the heat generated and the heat dissipated by

both conduction and convection. This group of tests are performed under constant load of 200 N. The initial speed is 2 m/s and increased by 2 m/s each 10 minutes. The polymer specimens are described in section 2.3.

Figure 3.3 presents the surface temperature and coefficient of friction of PTFE specimen sliding on steel in a variable speed test. Figure 3.4 presents the variation of the generated and dissipated heat as calculated from equation 3.10. The transient zone, which corresponds to the variation in internal energy, is demonstrated in the second figure by the gap between the frictional heat and total heat transfer curves. When the temperature stabilizes the gap between the two curves is minimized and is in the order of 2 to 5 % at medium speeds. The difference between the heat generated and the heat dissipated decreases with increasing speed. On the other hand the conduction term is much more important at low speeds whereas the convection term becomes more important at high speeds.

This test was repeated for UHMWPE, Acetal and Nylon 6/6 specimens. The UHMWPE and Acetal tests had the same results as PTFE. In the case of Nylon 6/6 the maximum speed is lower (figure 3.5) and the gap between the heat balance curves is larger and does not decrease at high speed as shown in figure 3.6 (see section 3.3.2). The tests also confirmed that the difference between T_{surf} and T_{sub} is in the order of thermocouples accuracy.

Another group of tests are performed under constant speed of 2, 8 and 16 m/s for the same materials. Figure 3.7 presents the variation of the generated and dissipated heat in the test conducted on UHMWPE specimen sliding on steel at 8 m/s. Figure 3.8 presents the same results for Acetal sliding against steel at 16 m/s. The figures demonstrate the correlation between the generated and dissipated heat curves which confirms the reliability of the measurements especially at high sliding speed.

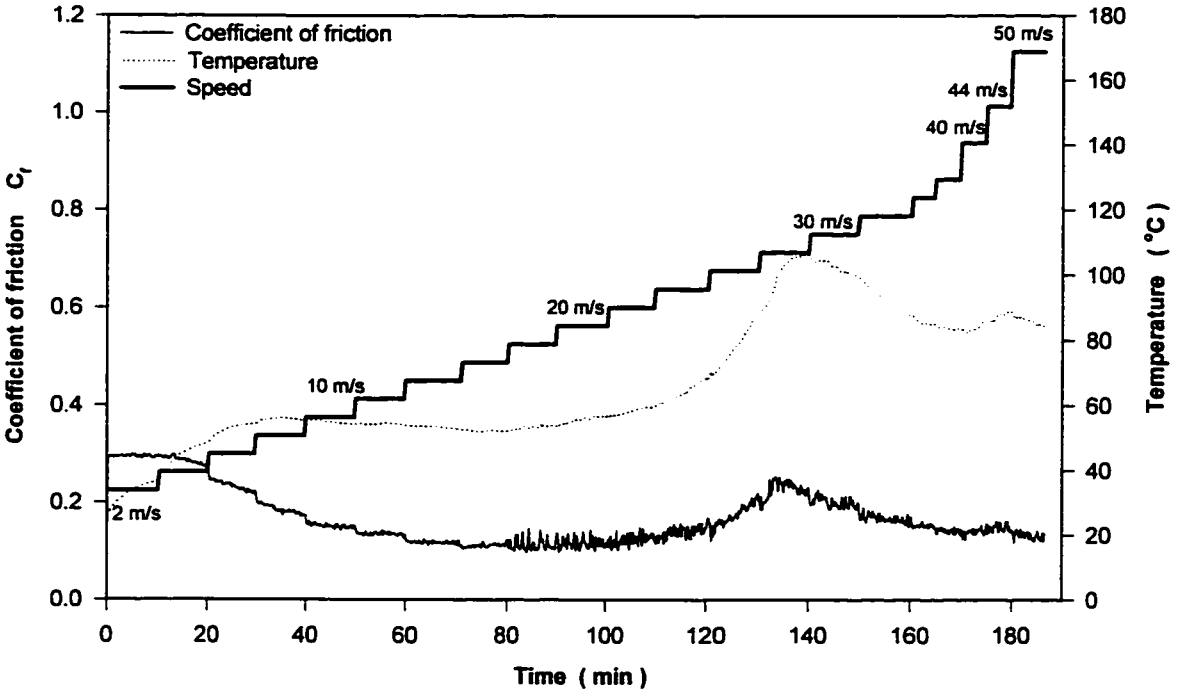

Figure 3.3 Friction coefficient and temperature distribution for PTFE sliding on steel under 200 N load

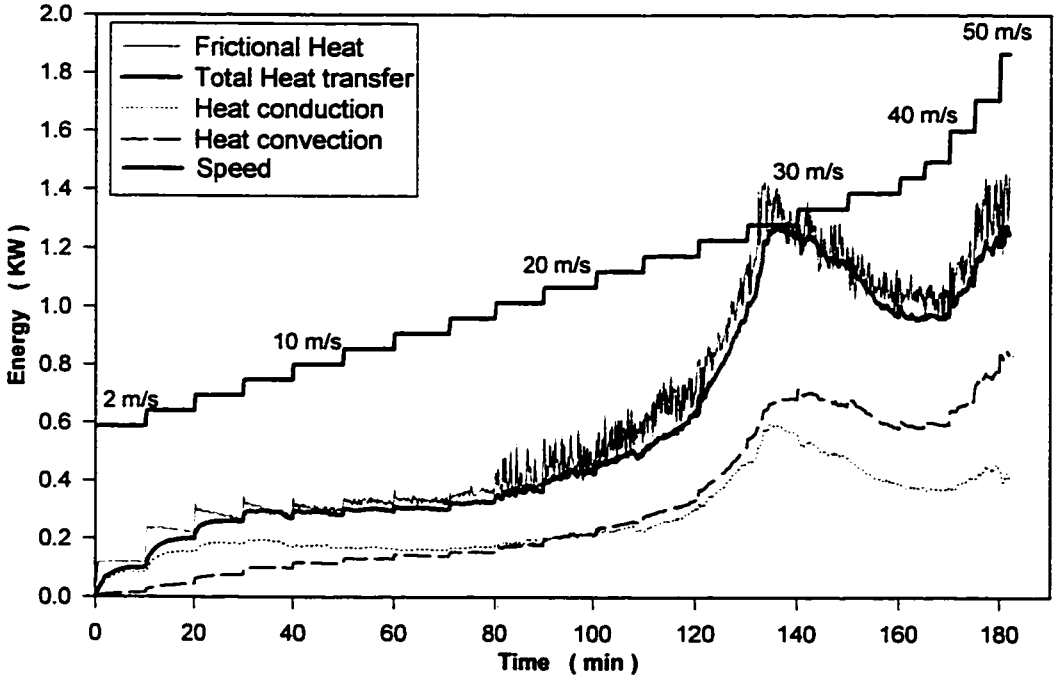

Figure 3.4 Energy distribution for PTFE sliding on steel under 200 N load

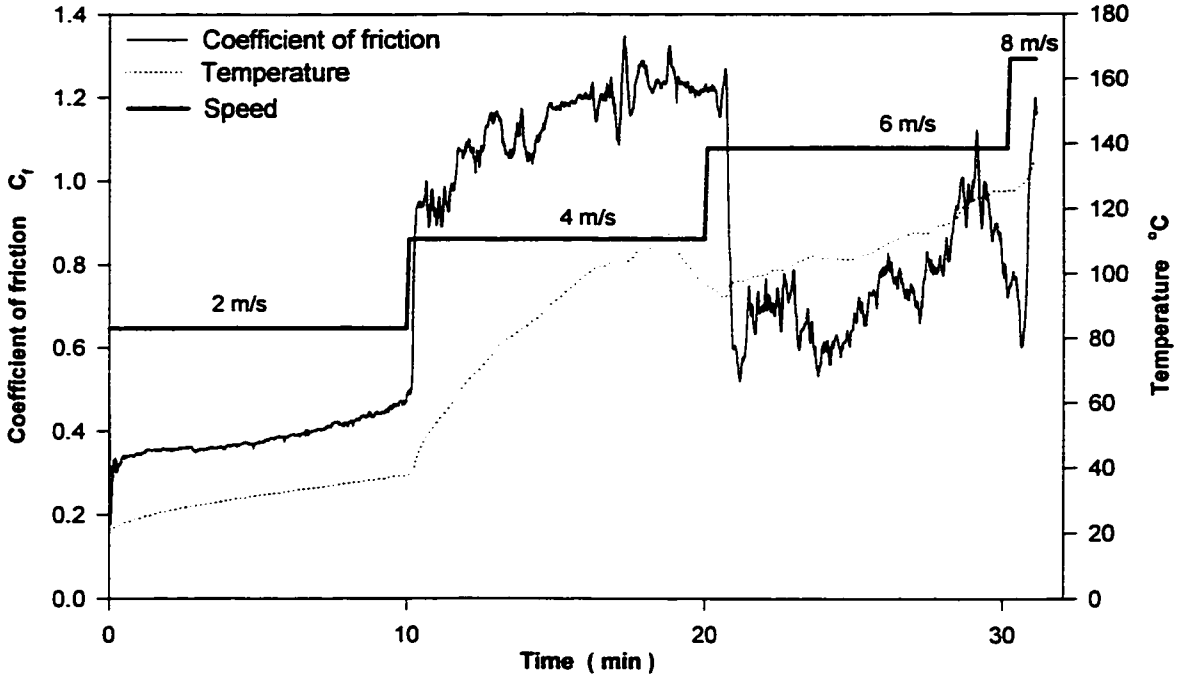

Figure 3.5 Friction coefficient and temperature distribution for Nylon 6/6 sliding on steel under 200 N load

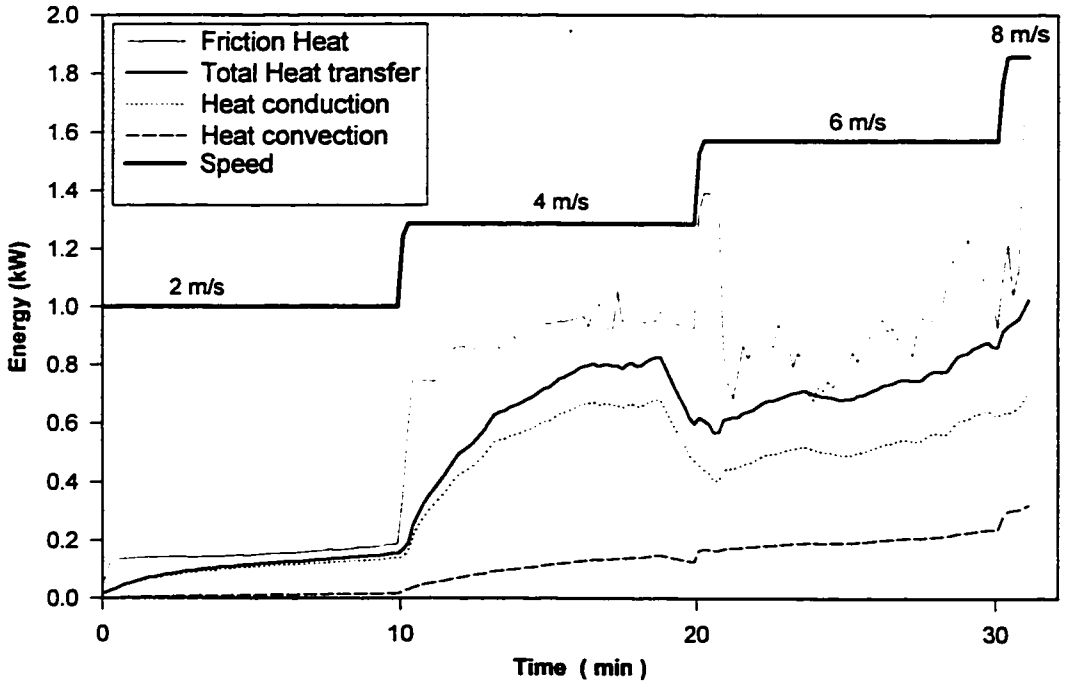

Figure 3.6 Energy distribution for Nylon 6/6 sliding on steel under 200 N load

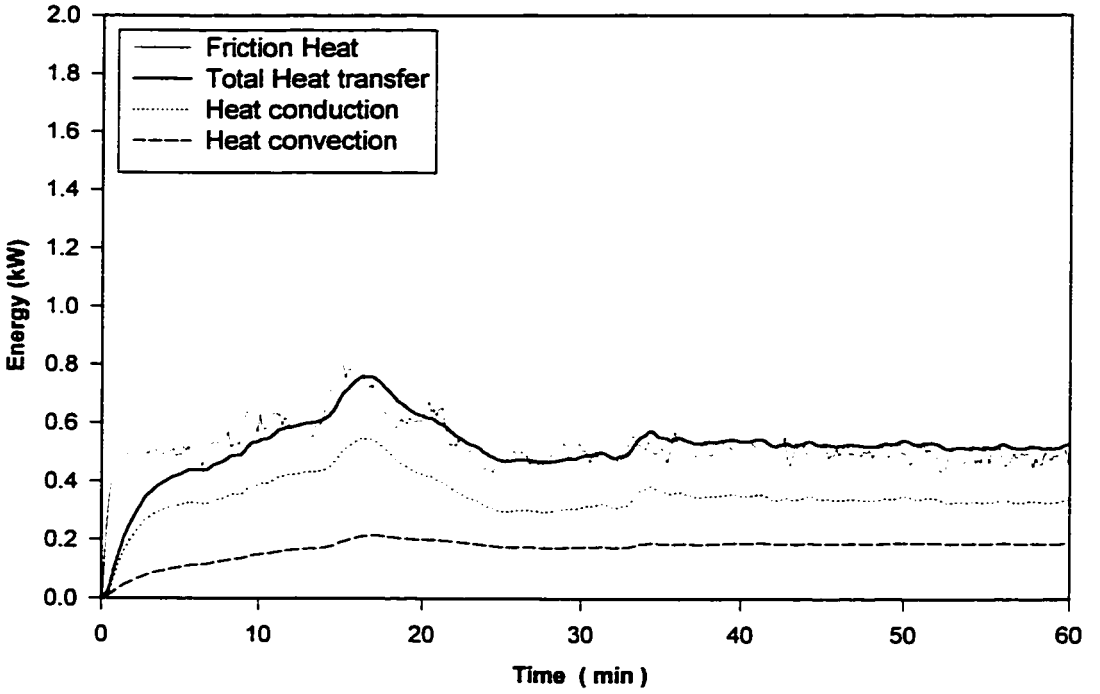

Figure 3.7 Energy distribution for UHMWPE sliding on steel at constant speed of 8 m/s under 200 N load

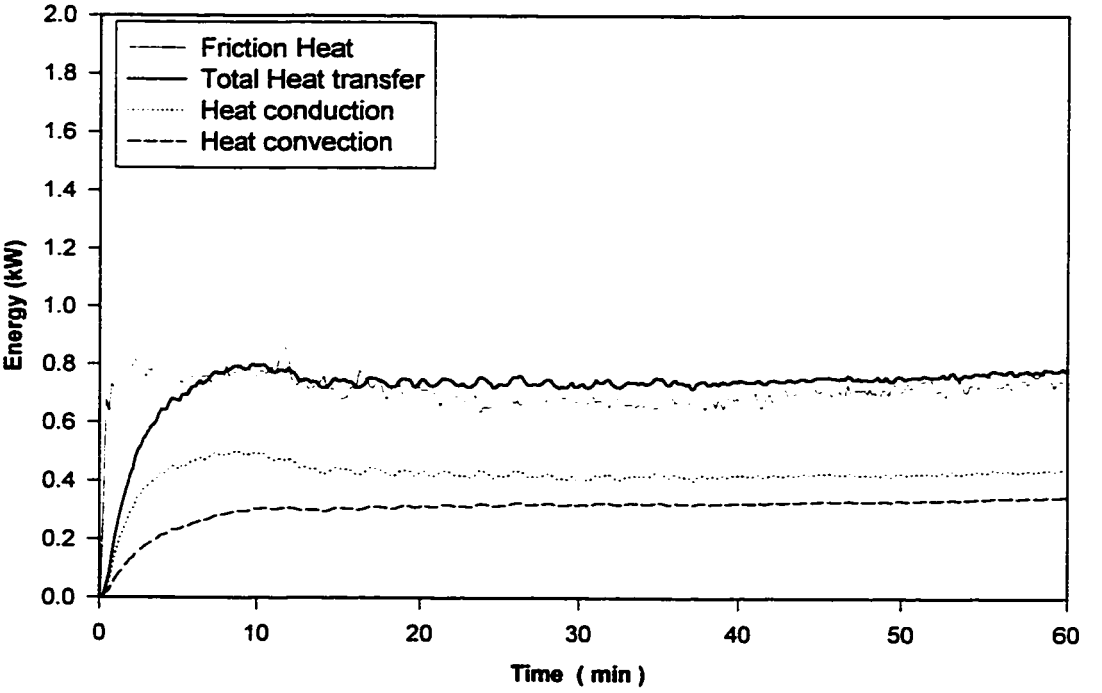

Figure 3.8 Energy distribution for Acetal sliding on steel at constant speed of 16 m/s under 200 N load

3.3.2 Polymer surface temperature

In these tests the real contact temperature is evaluated by measuring the polymer surface temperature in the contact zone. The objective of these tests is to compare the temperature measured under the metallic surface with the real contact temperature and to study the effect of speed on the accuracy of the temperature measurements. This group of tests are performed under constant load of 200 N and constant speed of 6, 8, 10 and 16 m/s.

In each test a fine thermocouple type K is inserted in the polymer specimen 1 mm from the surface of contact as shown in figure 2.3. The test is conducted at constant speed, and the polymer specimen is left to worn until the thermocouple touch the metallic surface.

Figure 3.9 presents the metallic and polymer surface temperature of UHMWPE specimen sliding on steel at 10 m/s where figure 3.10 presents the same results for Acetal at 16 m/s. Both curves revealed a small difference between the polymer and metallic surface temperature in the order of 2 - 3 °C in steady state condition; this difference in polymer to metallic temperature is in the order of the thermocouples accuracy. The polymer, being always in the contact zone, its surface temperature should be equal to the maximum temperature of the metallic surface. When the thermocouple reaches the metallic surface, as a result of the polymer wear, a sudden increase is detected due to the metal to metal contact.

Similar test is conducted for PTFE at 8 and 16 m/s. The difference between the polymer and metallic surface temperature is slightly larger (4 - 6 °C) as shown in figure 3.11 for the 8 m/s test. This is attributed to the polymer film deposition on the metallic surface which acts as a thin isolating film.

On the other hand, a similar test is conducted for Nylon 6/6 sliding on steel at 8 m/s.

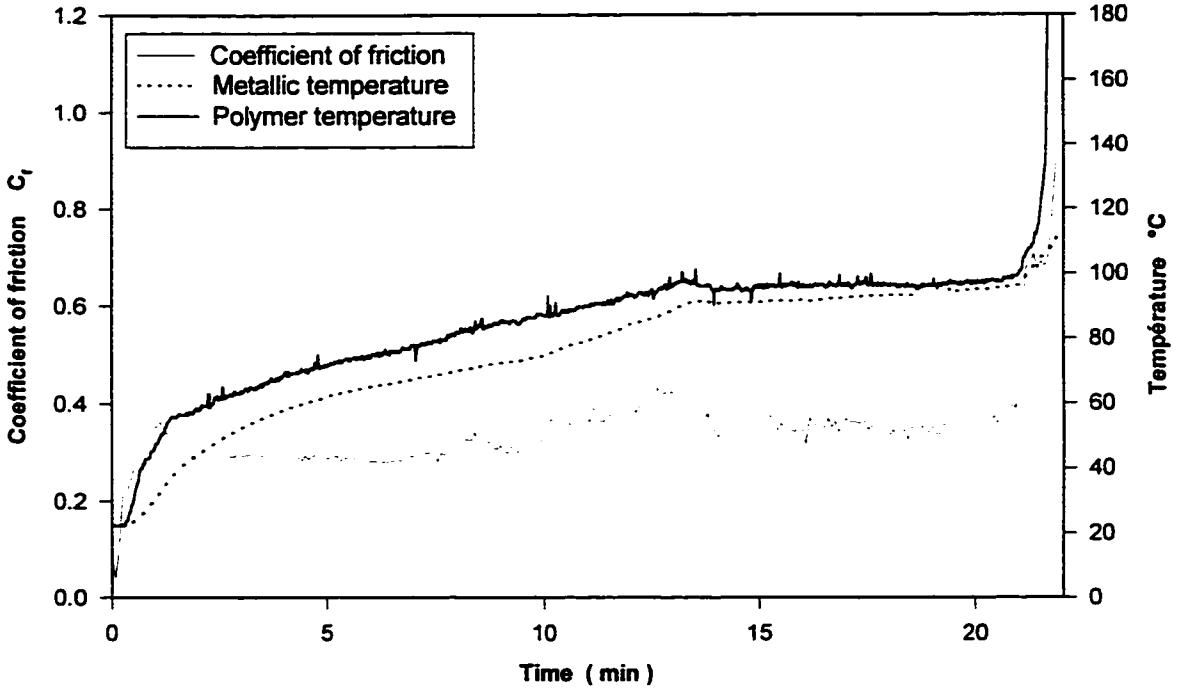

Figure 3.9 Polymer and metallic surface temperature for UHMWPE sliding on steel at constant speed of 10 m/s under 200 N load

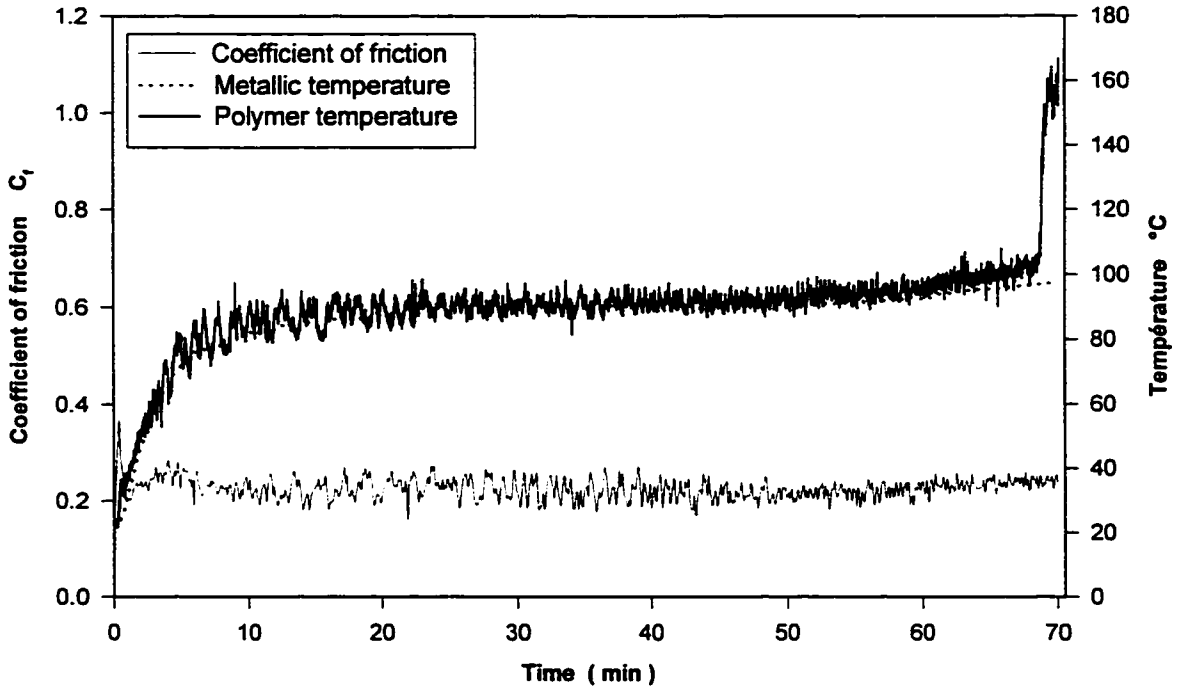

Figure 3.10 Polymer and metallic surface temperature for Acetal sliding on steel at constant speed of 16 m/s under 200 N load

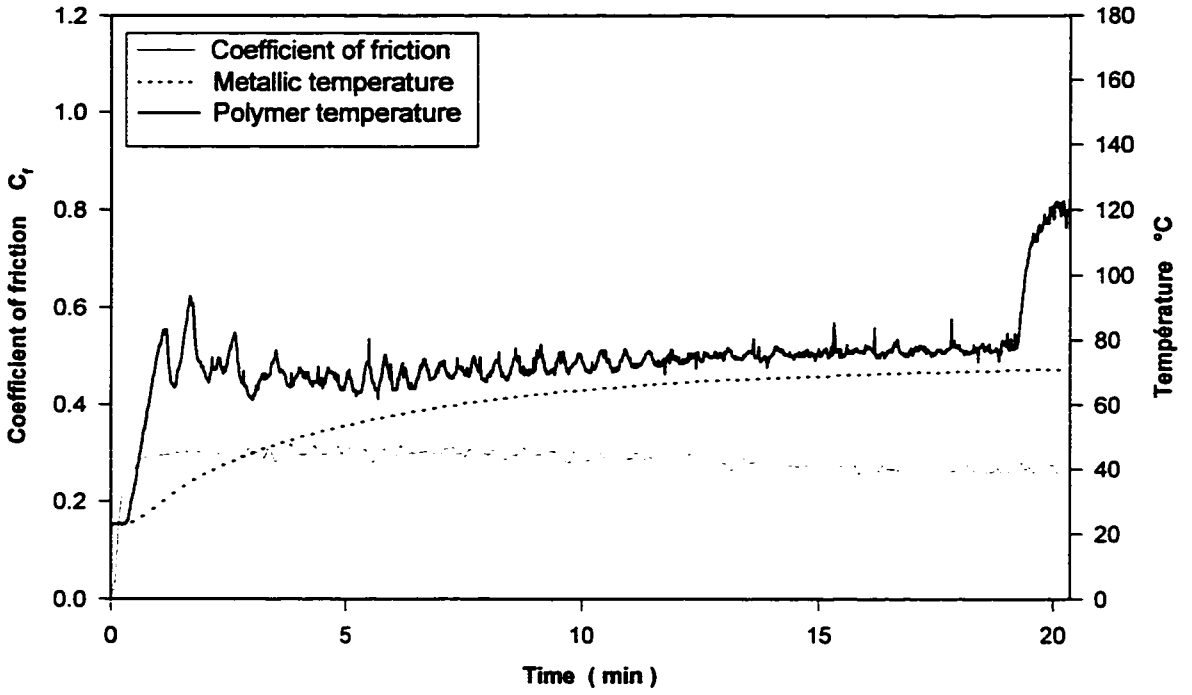

Figure 3.11 Polymer and metallic surface temperature for PTFE sliding on steel at constant speed of 8 m/s under 200 N load

The test shows much greater difference between the polymer and metallic surface temperature as shown in figure 3.12. It is also noted that the metallic surface temperature was about 120°C when surface melting was observed on the polymer surface. It is suggested that for Nylon 6/6 sliding contacts the film deposition is much larger and isolates completely the two surfaces. The test is repeated at 6 m/s and the same observations are noted as shown in figure 3.13.

Spalding [61] studied the friction and mechanical melting mechanism for Vinylidene chloride copolymers and measured lower temperature values on the metallic surface than the melting temperature of the polymer. He concluded that higher temperature are developed under the polymer surface which causes subsurface cracks and failure leading to higher film deposition and subsurface melting. He demonstrated his conclusion with a simple thermal energy calculation to prove the possibility of higher temperature developed under the polymer surface. Although our results can not confirm directly the same mechanism for Nylon 6/6, both theories lead to the conclusion that the surface temperature measurement are very much affected by the film deposition.

3.4 Conclusion

A simplified energy equation of heat transfer was developed which can be used to validate the temperature measurements of the tribometer. The equation developed was applied on the friction and temperature results obtained for different polymers in contact with steel at different sliding speeds. The correlation between the heat generated and the heat dissipated demonstrated the accuracy of the friction and temperature measurements in the cases where limited film deposition in likely to occur. The error was in the range of 2 - 5 %. The accuracy of the temperature measurement increases with increasing the sliding speed. This equation also permits the calculation of the heat dissipated by conduction and

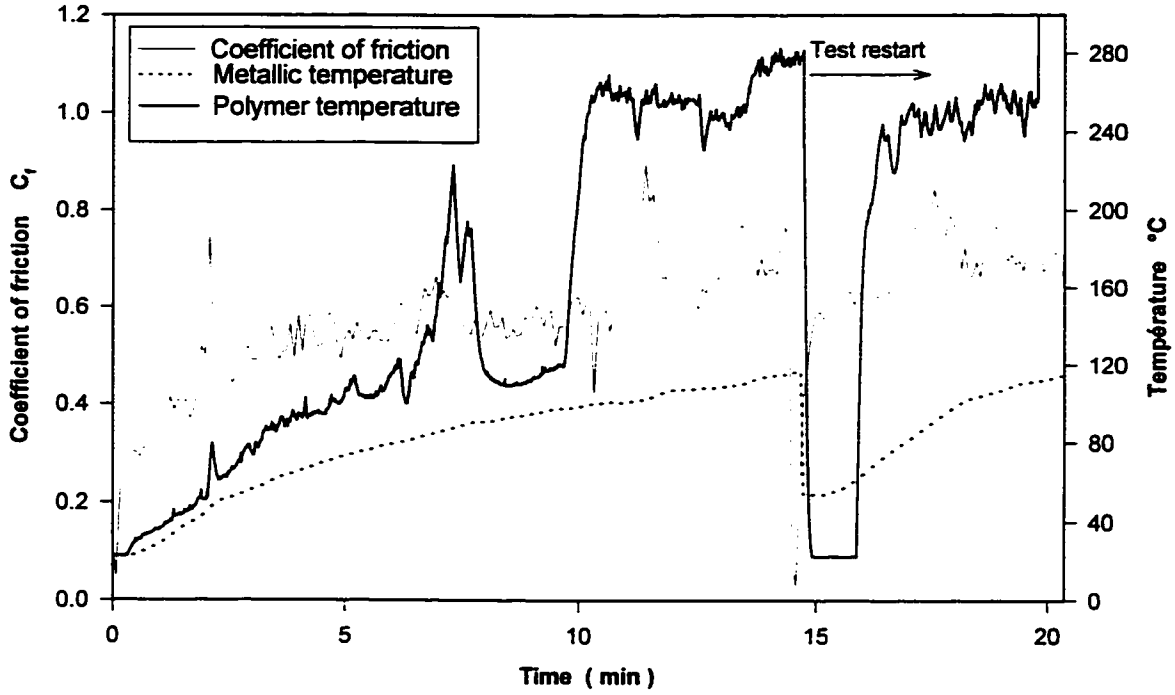

Figure 3.12 Polymer and metallic surface temperature for Nylon 6/6 sliding on steel at constant speed of 8 m/s under 200 N load

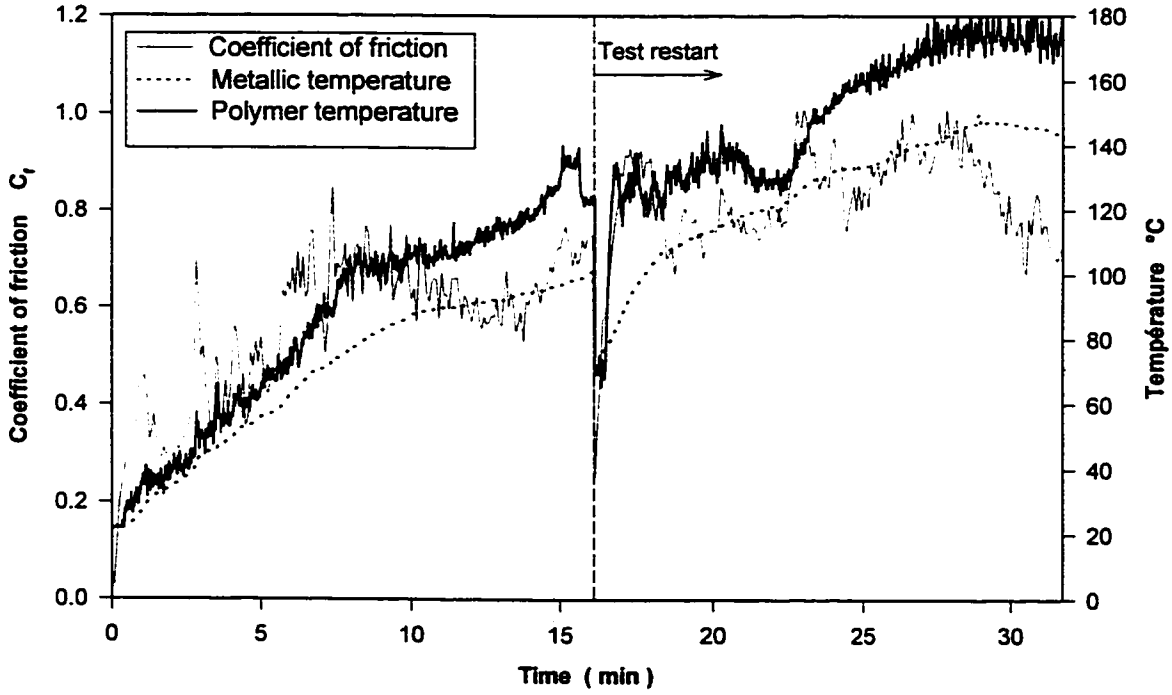

Figure 3.13 Polymer and metallic surface temperature for Nylon 6/6 sliding on steel at constant speed of 6 m/s under 200 N load

convection which may help in the detection of certain errors in the temperature measurements.

In another test group, a fine thermocouple is inserted under the polymer specimen surface. The polymer specimen is left to worn until the thermocouple touch the metallic surface in order to evaluate the real contact temperature. For UHMWPE and Acetal, The tests confirmed that the difference between the temperature measured under the metallic specimen and the actual contact temperature is in the order of the thermocouples accuracy (2°C), whereas for PTFE it is slightly higher.

For Nylon 6/6, the surface temperature measurement is much affected by the film deposition. Surface and/or subsurface melting is likely to occur at high sliding speed and the thick film deposition would affect largely the accuracy of the temperature measurement.

CHAPTER IV

CONTINUOUS CONTACT TESTS

4.1 Introduction

From the literature review of polymers friction and wear characteristics, it was concluded that there is a lack of information about the tribological behavior of polymers at high speed especially near their melting temperature. On the other hand, there is no available information on the effect of the contact surface at high speed sliding where the wear mechanism would affect the friction and wear properties of the materials.

Previous research work at moderate speed revealed the distinction of some polymers such as UHMWPE, PTFE Acetal and Nylon 6/6 in tribological applications. At high sliding speed, a model of a thermal control regime of friction is proposed, in which the coefficient of friction decreases with increasing the sliding speed and load. This model was only applied to a limited number of materials which do not include UHMWPE, PTFE or Acetal and with a relatively small contact surface. The difference in wear mechanisms of different polymers is not considered at such high sliding speeds.

Tests are conducted on four different polymers to study their friction and wear properties at high sliding speed and load in continuous contact with a contact area of 2380 mm^2. The polymers tested are UHMWPE, PTFE, Acetal and Nylon 6/6. First, variable speed tests are performed to study the variation of the friction coefficient with speed and to determine the polymers Pv limits. Then, constant speed tests are performed to determine the coefficient of friction and the specific wear rate of each material for a specific speed and load and to study the wear mechanisms of each polymer at different speeds. Finally, variable load tests are performed to study the variation of the friction coefficient with load.

4.2 Variable speed tests

In these tests, the load is maintained constant during the test where the speed is increased in a given interval till a very high wear rate or severe surface melting occurs. This speed is called the material speed limit for the corresponding load. The product of the maximum speed and the load per unit area is referred as the Pv limit of the material.

4.2.1 Objectives

The objective of these tests is to study the variation of the coefficient of friction with speed and temperature for each material. Also, to determine the limiting speed of each material and compute its Pv limit. The Pv values obtained will be correlated to those obtained in variable load tests for materials analogy.

4.2.2 Tests procedures

Primary tests on different material are conducted to determine the period at which temperature stability occurs and to reduce the test period. A time increment of 10 minutes was chosen. On the other hand, the optimum speed increment is found to be 2 m/s, although in some tests the speed increment was 1 m/s. Table 4.1 presents the different variable speed tests conducted on the 4 materials and their speed limits. The first test group is conducted at 120 N with initial speed of 2 m/s. Before each test, both surfaces are cleaned using carbon tetrachloride and pressurized air jet. The test is stopped when a high wear rate or severe surface melting occurs. The relation between speed, coefficient of friction and contact temperature are plotted against the running time. After the test, the metallic surface finish is restored; the major particles of the molten polymer are collected manually, then the surface is machined as described in section 2.3.1. The same tests are then repeated at 200 N for the 4 polymers to study the effect of the load on the coefficient of friction and the limiting speed.

Table 4.1 Variable speed tests in continuous contact (A = 2380 mm^2)

Test No	Material	Load N	Speed m/s	Duration min.	Speed Limit	Notes
Load 120 N, speed increment of 1 or 2 m/s each 10 minutes						
1	PTFE	120	1 - 50	370	> 50 m/s	↑
2	PTFE	120	2 - 54	170	> 54 m/s	↑
3	Acetal	120	1 - 56	320	> 56 m/s	↑
4	UHMWPE	120	2 - 34	165	32 m/s	↑↑↑
5	UHMWPE	120	1 - 23	225	22 m/s	↑↑↑
6	Nylon 6/6	120	2 - 10	45	8 m/s	↑↑↑
7	Nylon 6/6	120	1 - 9	88	8 m/s	↑↑↑
Load 200 N, speed increment of 2 m/s each 10 minutes						
8	PTFE	200	2 - 50	185	> 50 m/s	↑
9	Acetal	200	2 - 24	115	22 m/s	↑↑
10	UHMWPE	200	2 - 10	50	8 m/s	↑↑↑
11	Nylon 6/6	200	2 - 8	32	6 m/s	↑↑↑

↑ high wear rate
↑↑ very high wear rate leading to test termination
↑↑↑ Severe wear with surface melt leading to test termination

4.2.3 120 N tests

Figure 4.1 shows the variation of the friction coefficient and the contact temperature with time and speed in a variable speed test of UHMWPE sliding against steel at 120 N load. The coefficient of friction increases with speed, up to 4 m/s, and then decreases. When the speed reaches 32 m/s, the coefficient of friction begins to increase till the temperature reaches 55 °C after which the coefficient of friction increases rapidly, the temperature rises to 150°C and surface melting occurs on the polymer surface. In the repeated test, the coefficient of friction began to increase at 22 m/s where the contact temperature was about 80 °C. The speed limit is taken to be about 26 m/s. The same trend is found with Nylon 6/6 (figure 4.2); the coefficient of friction is generally higher and the temperature at which the friction coefficient starts to increase rapidly is between 85° and 110 °C. The speed limit is between 8 and 10 m/s.

On the other hand, the speed limits were not attained in the tests conducted on Acetal and PTFE for up to 50 m/s and more. Figure 4.3 and 4.4 shows the variation of the friction coefficient and contact temperature with time and speed in PTFE and Acetal tests respectively. First, the coefficient of friction initially increases, similar to UHMWPE and Nylon, and then it starts to decrease with speed up to the maximum value where the test was stopped. The coefficient of friction reached values as low as 0.03 at high speed for both materials. This values are confirmed using the simplified energy equation. It is suggested that these low friction values result from the formation of an air film under the contact together with the high frequency and low amplitude vibrations created by the frictional contact.

4.2.4 200 N tests

Figure 4.5 shows the variation of the friction coefficient and contact temperature with time and speed in a variable speed test of Acetal sliding against steel at 200 N load. The coefficient of friction increases with speed, up to 6 m/s, and then decreases as seen with 120

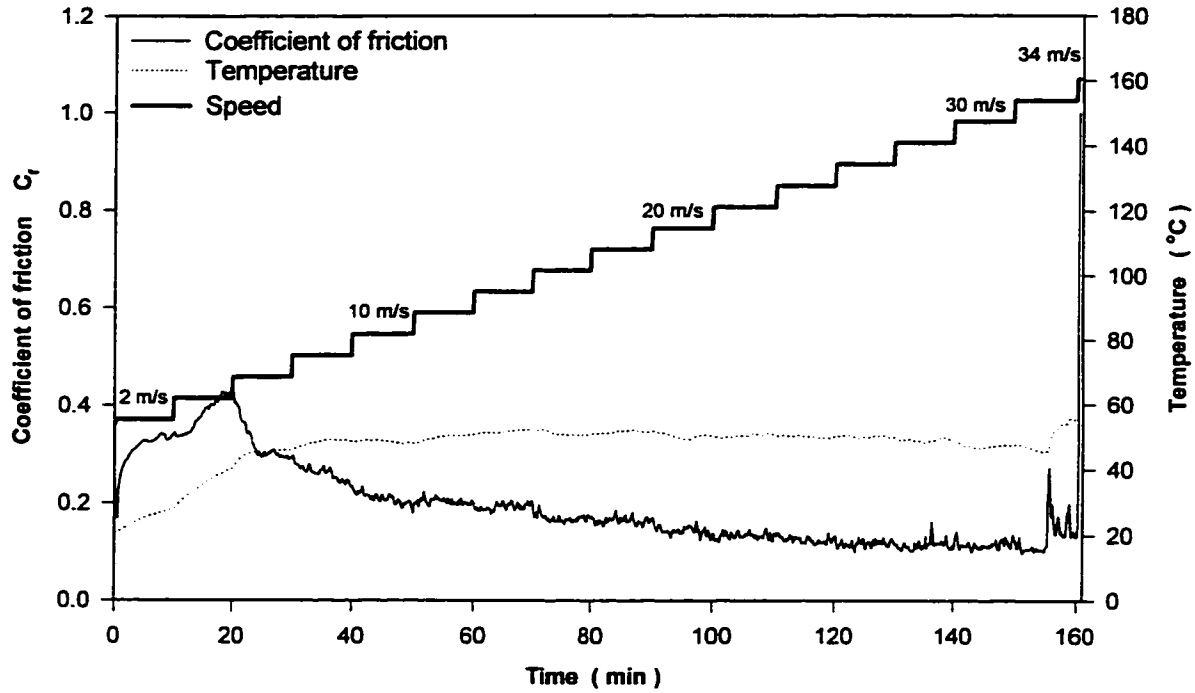

Figure 4.1 Friction coefficient and contact temperature of UHMWPE sliding against steel at variable speed test under 120 N load

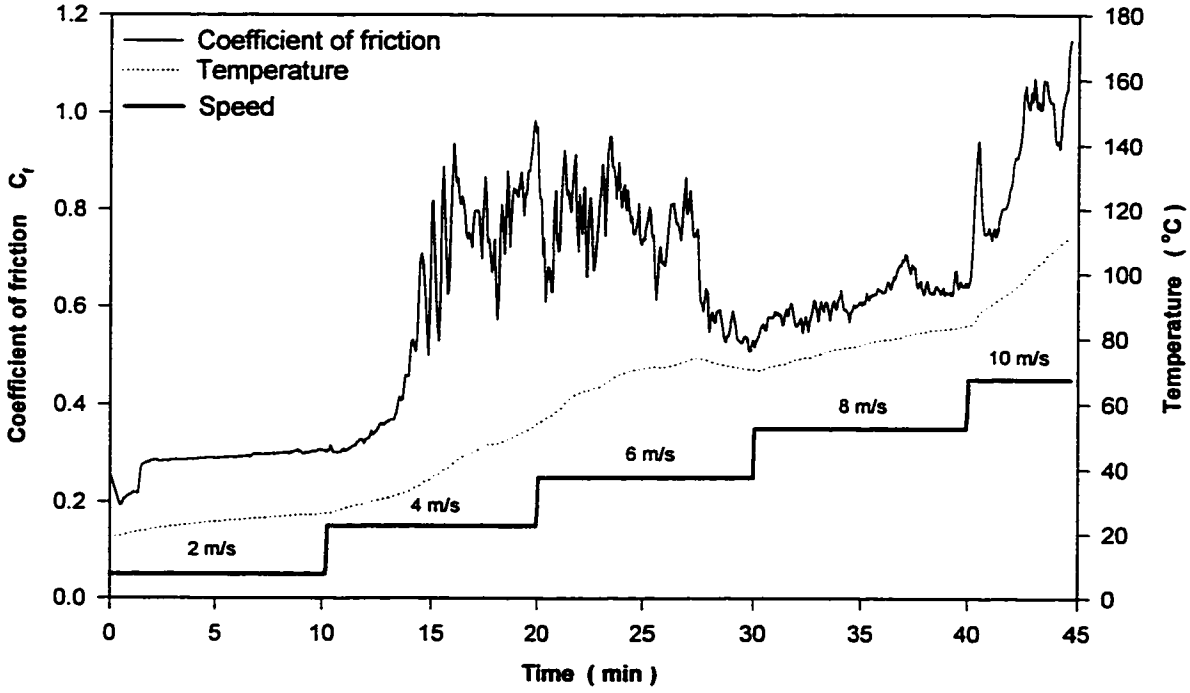

Figure 4.2 Friction coefficient and contact temperature of Nylon 6/6 sliding against steel at variable speed test under 120 N load

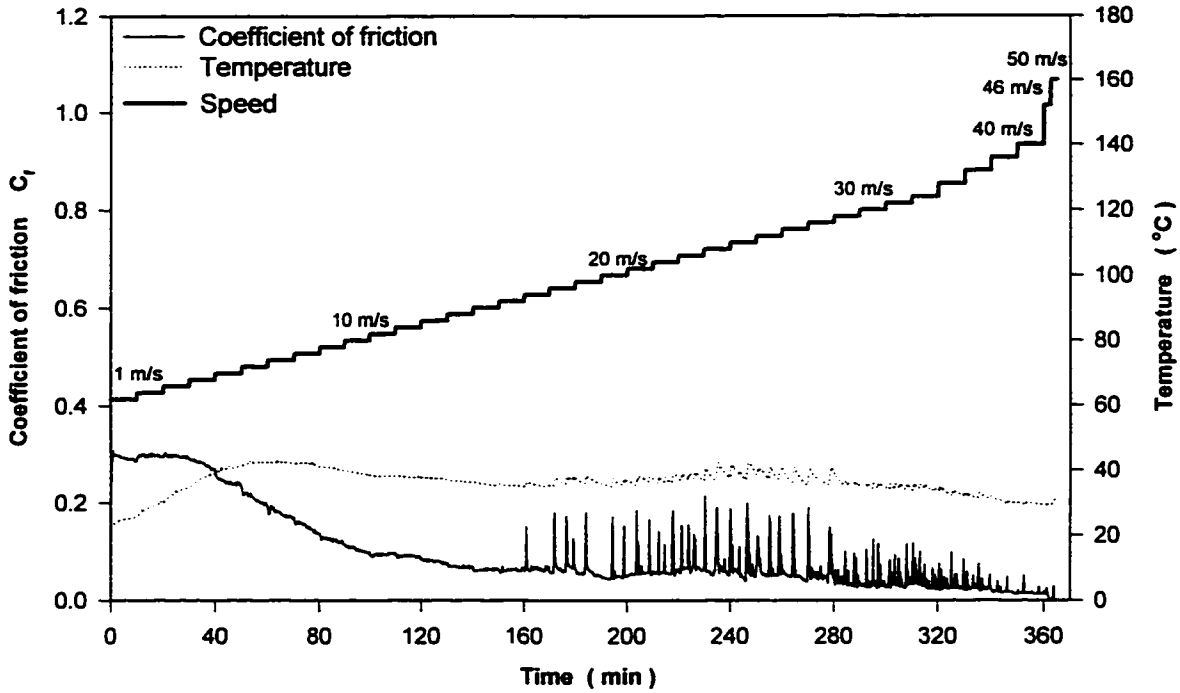

Figure 4.3 Friction coefficient and contact temperature of PTFE sliding against steel at variable speed test under 120 N load

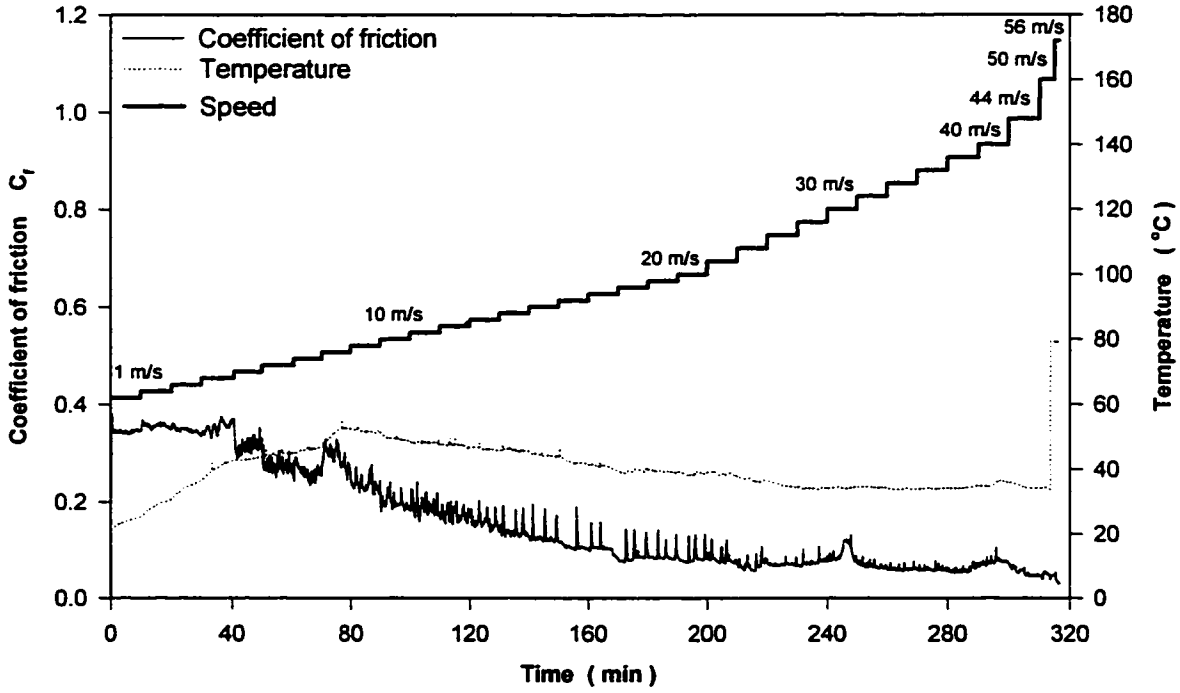

Figure 4.4 Friction coefficient and contact temperature of Acetal sliding against steel at variable speed test under 120 N load

N load tests. When the speed reaches 24 m/s, the test is stopped due to a very high wear rate. For UHMWPE (figure 4.6) and Nylon 6/6 (figure 4.7) the maximum speed is lower than that at low speed tests, the coefficient of friction is generally higher whereas the temperature at which the friction coefficient starts to increase is the same. On the other hand, the speed limits are not attained in the tests conducted on PTFE, for up to 50 m/s, as in low load tests (figure 4.8).

4.2.5 Discussion

Figures 4.9 and 4.10 resume the variation of the friction coefficient with speed for different materials at low and high load tests respectively. From these tests, it is found that the PTFE has the lowest coefficient of friction at both high and low loads. The material maintains its stability up to the maximum tests speed of 50 m/s. Acetal has a relatively low coefficient of friction. The material maintains its stability up to 50 m/s at 120 N test but the wear rate was high at 200 N test. UHMWPE has a moderate coefficient of friction but it increases dramatically with the contact temperature when approaching its speed limit. Nylon 6/6 has both the highest coefficient of friction and the lowest speed limit in all tests.

In general, the coefficient of friction decreases with increasing speed with a peak value at a specific speed for each material. On the other hand, the coefficient of friction is relatively higher at high loads. The performance of PTFE and Acetal can be related to their mechanical stability at relatively elevated temperatures.

It is clear from those tests that, at large contact surfaces, the coefficient of friction does not decrease at higher speed and load when exceeding their speed limits. This may be related to the large contact surface and the nonuniform wear distribution along the surface which limits the lubrication effect of the molten surface. Also, the real surface of contact increases due to the high temperature developed leading to a significant increase in the adhesion force.

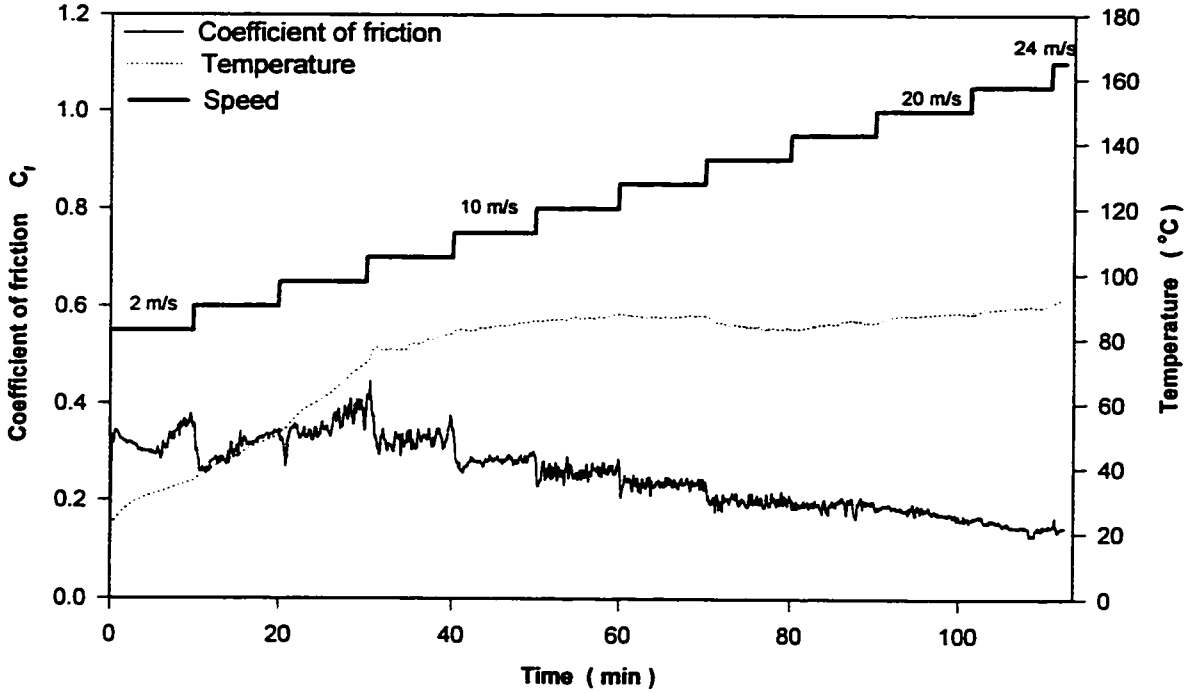

Figure 4.5 Friction coefficient and contact temperature of Acetal sliding against steel at variable speed test under 200 N load

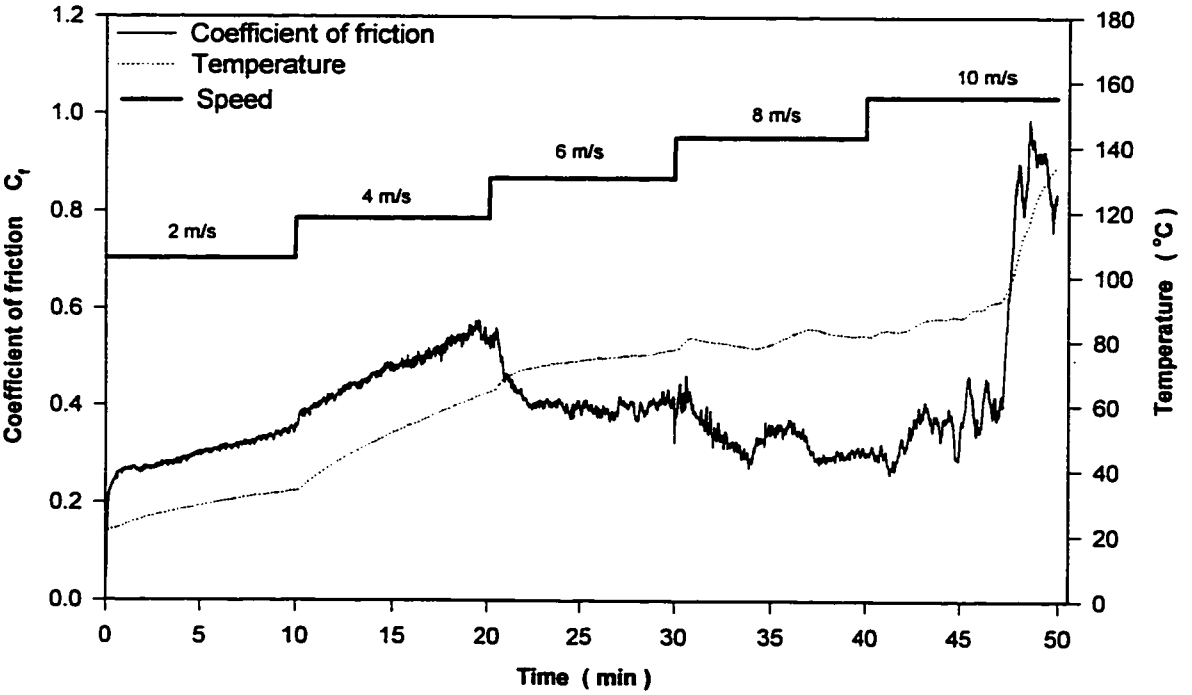

Figure 4.6 Friction coefficient and contact temperature of UHMWPE sliding against steel at variable speed test under 200 N load

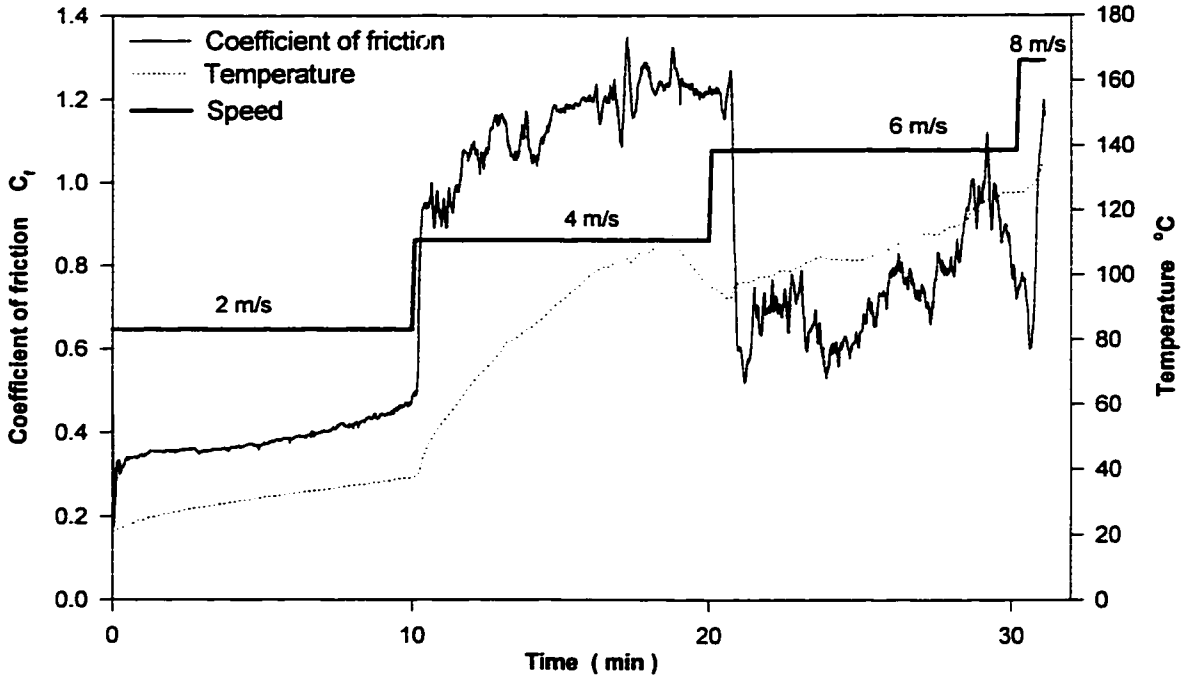

Figure 4.7 Friction coefficient and temperature distribution for Nylon 6/6 sliding on steel under 200 N load

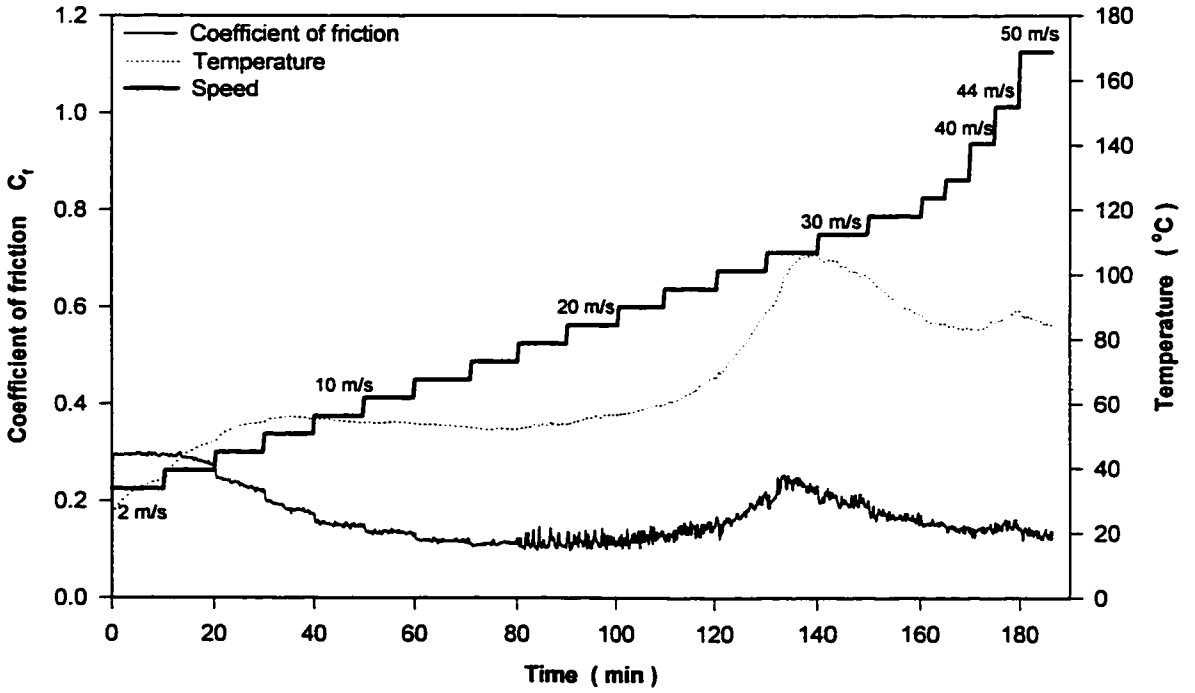

Figure 4.8 Friction coefficient and temperature distribution for PTFE sliding on steel under 200 N load

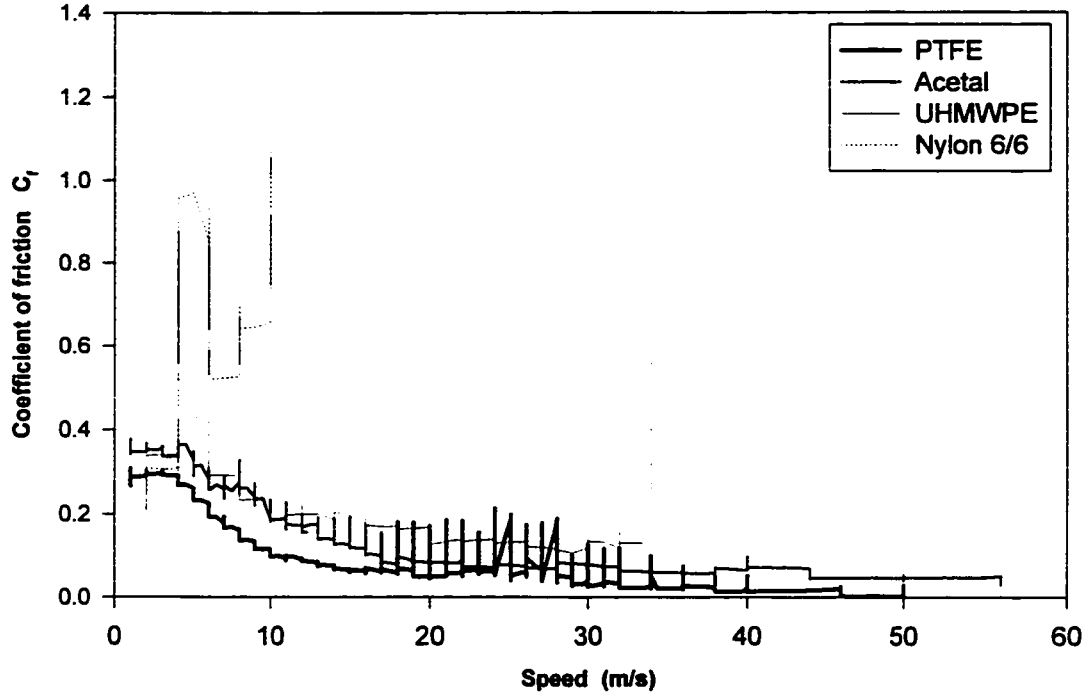

Figure 4.9 The variation of the friction coefficient with speed for different materials sliding against steel in variable speed tests under 120 N load

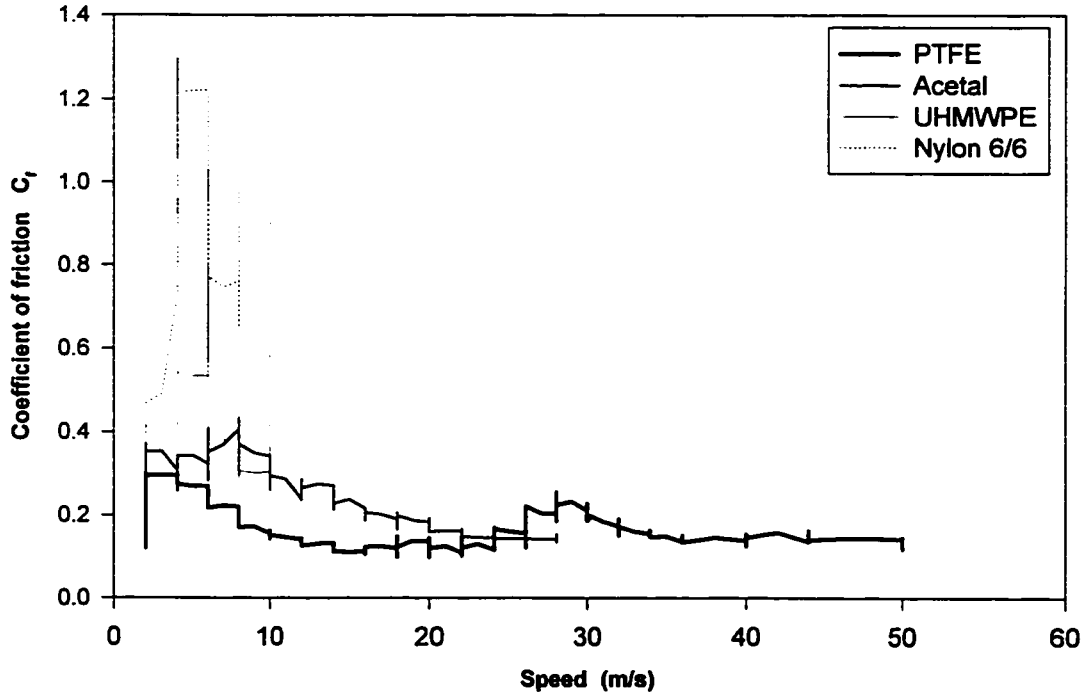

Figure 4.10 The variation of the friction coefficient with speed for different materials sliding against steel in variable speed tests under 200 N load

The temperature measurement revealed a significant error when the sliding speed exceeds 50 m/s. This was detected when the contact temperature revealed a sudden and substantial rise when this speed is exceeds. Using the heat balance, it was found that this was not associated with an adjacent increase in the heat generation. This may be the result of the inertia or other dynamic forces on the thermocouples and their amplifiers.

4.3 Constant speed and load tests

In these tests the load and speed are maintained constant. The variation of the coefficient of friction and the temperature with time is monitored. The wear rate is measured by weight. The polymer and metallic surfaces are investigated to study the wear mechanisms of different materials at different speeds.

4.3.1 Objectives

The objective of these tests is to determine the coefficient of friction and the specific wear rate of each material for a specific speed and load, and to study the wear mechanisms of each polymer at different speeds.

4.3.2 Tests procedures

Before each test, both surfaces are cleaned using carbon tetrachloride and pressurized air jet. The polymer specimen weight is measured using a precision balance (±0.1 mg). Tests are performed at a constant load of 200 N for two periods of one hour each at speed 4, 6, 8, 16 and 30 m/s tests, and 2 hours period for the 2 m/s test. During the tests the load and speed are maintained constant. The test is stopped if high wear rates or severe surface melting occurs. The relation between the coefficient of friction and the contact temperature are plotted against the running time.

After the test, photographs are taken for both surfaces. The polymer surface is then cleaned using pressurized air jet, and the weight is remeasured. The polymer specimen is reinstalled in the machine and the test is repeated. After the second weight measurement, the metallic surface finish is restored as described earlier in section 4.2.2.

4.3.3 Results

Table 4.2 presents the different speed and load tests conducted on the 4 materials. The speed, duration and wear loss of each test are reported. Figure 4.11 shows the variation of the friction coefficient and contact temperature with time in a typical constant speed and load test of UHMWPE sliding against steel at 200 N load and 8 m/s. When the test was repeated, surface melting occurred and the test was stopped. Other examples are found in figure 4.12 and 4.13 showing the same relation for Acetal at 16 m/s and PTFE at 30 m/s respectively. For UHMWPE, Acetal and PTFE, the coefficient of friction increases at the first period of the test then stabilizes with the temperature. When the test speed is higher than the polymer speed limit, the temperature increases continuously till surface melting occurs.

For Nylon 6/6 the coefficient of friction increases constantly in all tests. At 2 m/s the friction coefficient increases up to a value of 1.2 as shown in figure 4.14, but the low surface temperature maintains the material stability with a low wear rate. At 4 m/s the wear rate increases dramatically at the end of the test depositing a thick film on the metallic surface. The test was stopped for an excessive wear rate. At speed 6 m/s and over surface melting occurs with thick film deposit. This may explain the low contact temperature detected on the metallic surface during polymer surface melting as discussed in section 3.3.2.

4.3.4 Discussion

Table 4.3 resumes the friction and temperature results of the constant speed and load tests. The coefficient of friction and the contact temperature reported are the mean values

Table 4.2 Constant speed and load tests in continuous contact (A= 2380 mm^2)

Test No	Material	Load N	Speed m/s	Duration min.	w loss g	Wear 10^{-5} mm^3/N.m
12	PTFE	200	2	120	2.82	45.1
13	PTFE	200	2	120	2.27	36.3
14	Acetal	200	2	120	1.17	28.6
15	Acetal	200	2	120	0.13	3.18
16	UHMWPE	200	2	120	0.03	1.12
17	UHMWPE	200	2	120	<0.01	<0.4
18	Nylon 6/6	200	2	60	0.0297	1.81
19	Nylon 6/6	200	2	60	0.0237	1.45
20	PTFE	200	4	60	1.8036	28.8
21	PTFE	200	4	60	0.7886	12.6
22	Acetal	200	4	60	1.7897	43.7
23	Acetal	200	4	60	0.1351	3.30
24	UHMWPE	200	4	60	0.0032	0.12
25	UHMWPE	200	4	60	0.0013	0.05
26	Nylon 6/6	200	4	16.5	0.0145	1.61
27	PTFE	200	6	60	3.7594	40.0
28	PTFE	200	6	60	2.1113	22.5
29	Acetal	200	6	60	0.4365	7.11
30	Acetal	200	6	60	0.2595	4.24
31	UHMWPE	200	6	62	4.34	"
32	UHMWPE	200	6	60	3.7590	96.4
33	Nylon 6/6	200	6	27	12.79	" "

Table 4.2 (Continue) Constant speed and load tests for continuous contact

Test No	Material	Load N	Speed m/s	Duration min.	w loss g	Wear 10^{-5} mm^3/N.m
34	PTFE	200	8	60	5.17	41.4
35	PTFE	200	8	60	5.02	40.2
36	Acetal	200	8	60	0.30	3.67
37	Acetal	200	8	60	0.18	2.20
38	UHMWPE	200	8	60	0.08	1.49
39	UHMWPE	200	8	28	3.86	↑↑↑
40	Nylon 6/6	200	8	18	14.59	↑↑↑
41	PTFE	200	16	60	5.4902	22.0
42	PTFE	200	16	60	4.0781	16.3
43	Acetal	200	16	60	2.0796	12.7
44	Acetal	200	16	60	3.6252	22.2
45	UHMWPE	200	16	16	13.427	↑↑↑
46	Nylon 6/6	200	16	3.5	11.271	↑↑↑
47	PTFE	200	30	60	5.0270	10.7
48	PTFE	200	30	60	7.3931	15.8
49	Acetal	200	30	13	19.128	↑↑↑

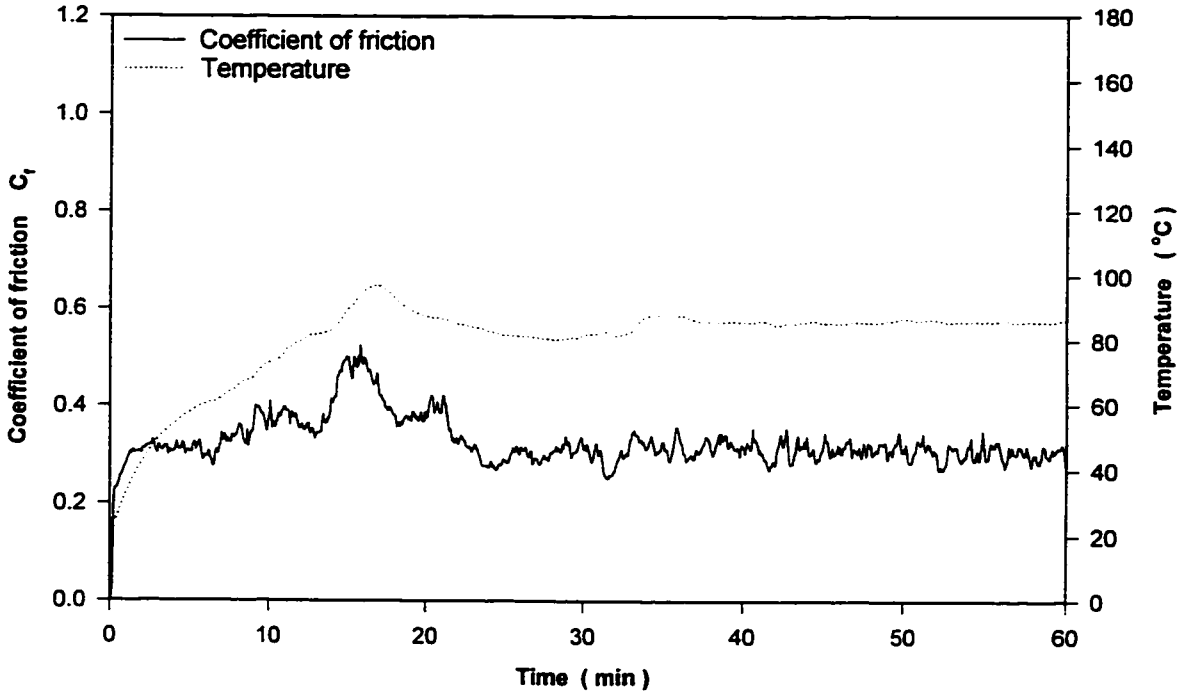

Figure 4.11 Friction coefficient and contact temperature of UHMWPE sliding against steel at 8 m/s under 200 N load

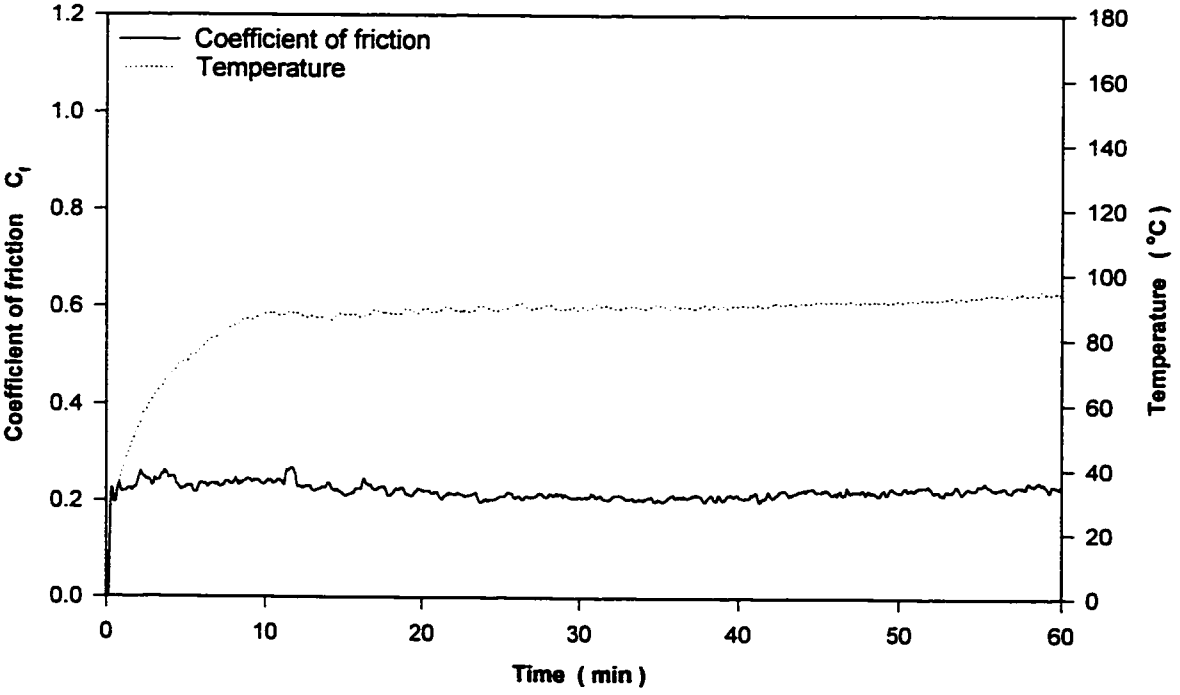

Figure 4.12 Friction coefficient and contact temperature of Acetal sliding against steel at 16 m/s under 200 N load

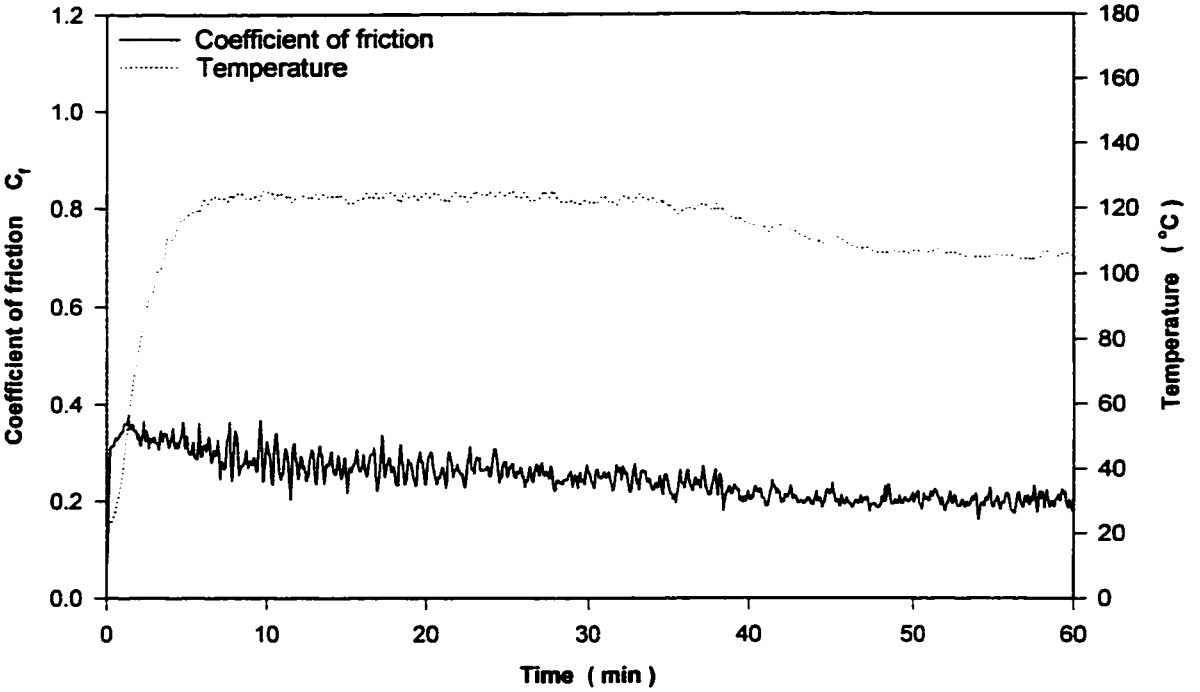

Figure 4.13 Friction coefficient and contact temperature of PTFE sliding against steel at 30 m/s under 200 N load

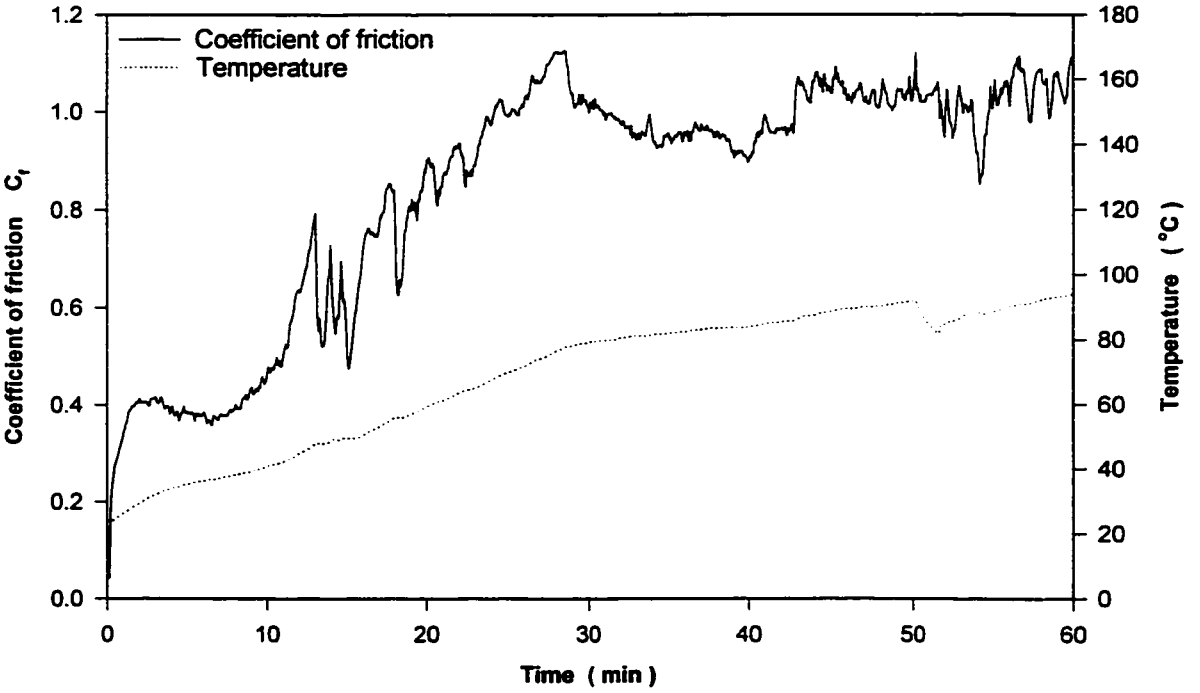

Figure 4.14 Friction coefficient and contact temperature of Nylon 6/6 sliding against steel at 2 m/s under 200 N load

Table 4.3 Mean coefficient of friction and surface temperature in constant speed and load tests for continuous contact (A = 2380 mm^2)

		PTFE		Acetal		UHMWPE		Nylon 6/6	
		C_f	Temp. (°C)	C_f	Temp. (°C)	C_f	Temp. (°C)	C_f	Temp. (°C)
2 m/s	Test 1	0.271	38	0.478	56	0.267	40	0.850	70
	Test 2	0.247	39	.580	61	0.310	45	0.790	67
4 m/s	Test 1	0.238	48	0.490	76	0.441	73	1.01*	84*
	Test 2	0.146	42	0.635	96	0.346	60	1.15**	100**
6 m/s	Test 1	0.258	60	0.238	57	0.450*	79*	0.685*	94*
	Test 2	0.198	53	0.449	92	0.980**	140**	0.901**	131**
8 m/s	Test 1	0.226	60	0.410	95	0.328*	82*	0.560*	88*
	Test 2	0.210	58	0.430	100	0.810**	138**	0.850**	123**
16 ms	Test 1	0.251	93	0.222	88	0.331*	80*	0.750*	85*
	Test 2	0.132	59	0.253	90	0.730**	144**	1.10**	135**
30 m/s	Test 1	0.247	114	0.177*	70*				
	Test 2	0.203	106	0.690**	108**				

For materials where melting occurs during the first test period:

* Estimated value during normal running

** Estimated value during polymer melting

computed for each test period. Table 4.4 presents the analysis of the friction, temperature and wear results for the test period with higher stability. Figure 4.15 resumes the relation between the mean coefficient of friction and speed for all the materials. The relation between the wear rate and speed is presented in figure 4.16.

Studying the wear rate of different materials, it is found that PTFE has the highest wear rate. Its transfer film is unstable and transforms easily to a smooth powder form debris allowing a low coefficient of friction and high wear rate with a very fine surface finish on both surfaces as shown in figures 4.17 and 4.18. Acetal has a relatively high wear rate. The wear mechanism is very similar to that of PTFE as seen in figure 4.19 and 4.20, although the wear rate is much lower. UHMWPE has the lowest wear rate. Its smooth and thin film transfer is rigidly attached to the surface covering surface imperfections and leading to a moderate coefficient of friction. Figure 4.21 shows the metallic surface after 2 hours in a 4 m/s test with UHMWPE. The film transfer is completely transparent and it is very difficult to scratch it from the surface. This film rigidity is maintained till the contact temperature reaches 80 °C, where a sudden increase in the wear rate is detected leading to surface failure. This is demonstrated by small cavities induced due to local melting as shown in figure 4.22. Nylon 6/6 has a relatively low wear rate. The film transfer is very limited at low speeds. At 4 m/s and over, the film deposit increases and the counterface surface becomes highly altered as shown in figure 4.23. The thick film deposit creates large wear tracks on the polymer surface, as shown in figure 4.24, and a substantial increase in the friction coefficient.

The coefficient of friction detected for PTFE is in the range of that obtained in variable speed tests. For Acetal the coefficient of friction is higher than that obtained in variable speed tests for low speeds, whereas at high speeds it is practically the same. On the other hand, the values obtained in constant speed and load tests are relatively high for UHMWPE where it is much higher for Nylon 6/6 especially at low speeds. It is clear for both materials, that the initial coefficient of friction at the beginning of the tests is almost the same as variable speed tests. As the contact temperature increases, the coefficient of friction

Table 4.4 Analyzed coefficient of friction, surface temperature and wear rate in constant speed and load tests for continuous contact

	PTFE						UHMWPE				
Speed (m/s)	2	4	6	8	16	30	2	4	6	8	16
Mean C_f	0.27	0.15	0.20	0.21	0.13	0.25	0.27	0.35	0.45*	0.33	0.33*
Max. C_f	0.30	0.32	0.36	0.33	0.25	0.38	0.54	0.58	1.09	0.53	0.9
Min. C_f	0.24	0.07	0.12	0.14	0.11	0.18	0.20	0.23	0.28	0.20	0.17
S_d C_f	0.01	0.04	0.03	0.04	0.01	0.04	0.03	0.06	0.2*	0.05	0.2*
Mean Temp.	38	42	53	58	59	114	40	60	79*	82	80*
Max. Temp.	40	39	73	63	64	127	47	84	146	97	157
S_d Temp.	1.7	5.2	6.5	6.2	3	15	4.7	14.1	25*	13	27*
Δ w (gr.)	2.27	0.79	2.11	5.02	4.08	5.03	<0.01	0.0013	3.759	0.08	13.4
k	36.3	12.65	22.53	40.2	16.3	10.7	<0.4	0.05	96.4 ↑	1.49	120 ↑
	Acetal						**Nylon 6/6**				
Speed (m/s)	2	4	6	8	16	30	2	4	6	8	16
Mean Cf	0.58	0.49	0.24	0.43	0.22	0.18	0.85	1.01*	0.69*	0.58*	0.78*
Max. Cf	0.71	0.76	0.62	0.56	0.28	0.69	1.15	1.33	1.16	0.85	1.20
Min. C_f	0.35	0.26	0.21	0.33	0.02	0.06	0.34	0.35	0.27	0.38	0.48
S_d C_f	0.03	0.08	0.02	0.05	0.02	0.06	0.24	0.24*	0.12*	0.08*	0.25*
Mean Temp.	61	76	57	99	88	70*	70	84*	90*	88*	76*
Max. Temp.	70	106	111	111	96	109	94	109	140	124	139
S_d Temp.	11	17.5	18.0	15	11	19*	21	22.5*	26*	25*	34*
Δ w	0.13	0.14	0.26	0.18	2.08	19.1	0.024	0.015	12.8	14.6	11.3
k	3.18	3.42	4.24	2.20	12.7	538 ↑	1.45	1.61↑	580↑	750↑	1500↑

Temp. → Contact temperature in °C,

Δ w → Weight loss in gr.,

k → Specific wear rate in 10^{-5} $mm^3/N.m$

↑ → Very high wear rate and/or surface melting leading to test termination

* → Values affected by test termination (high wear rate and/or surface melting)

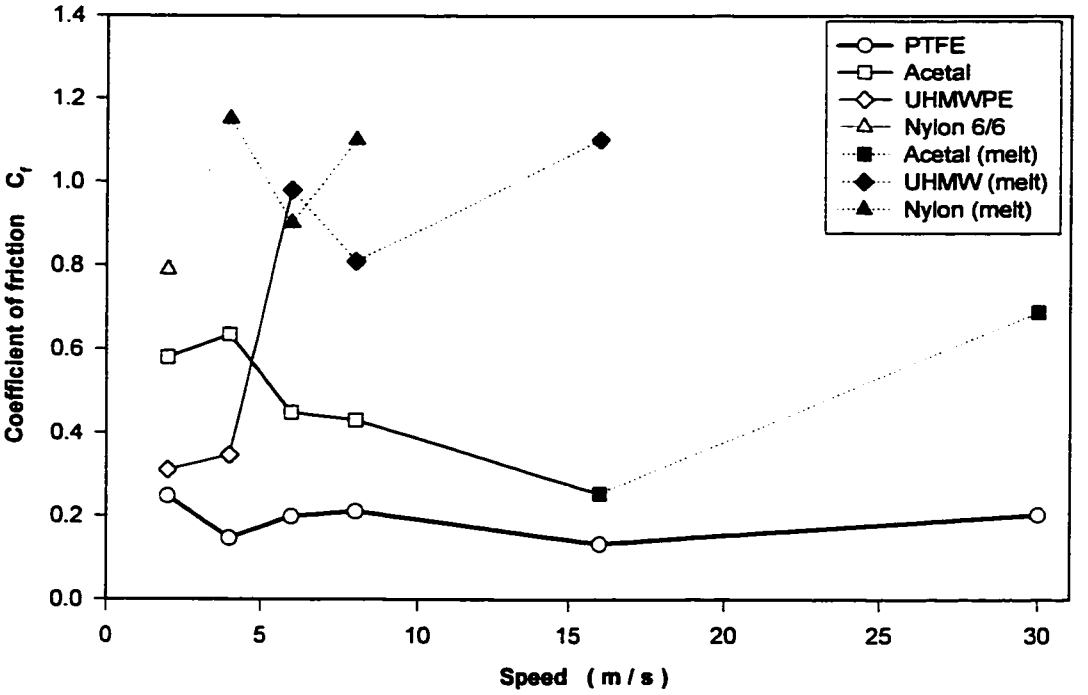

Figure 4.15 The friction coefficient of different materials sliding against steel at different speeds under 200 N load

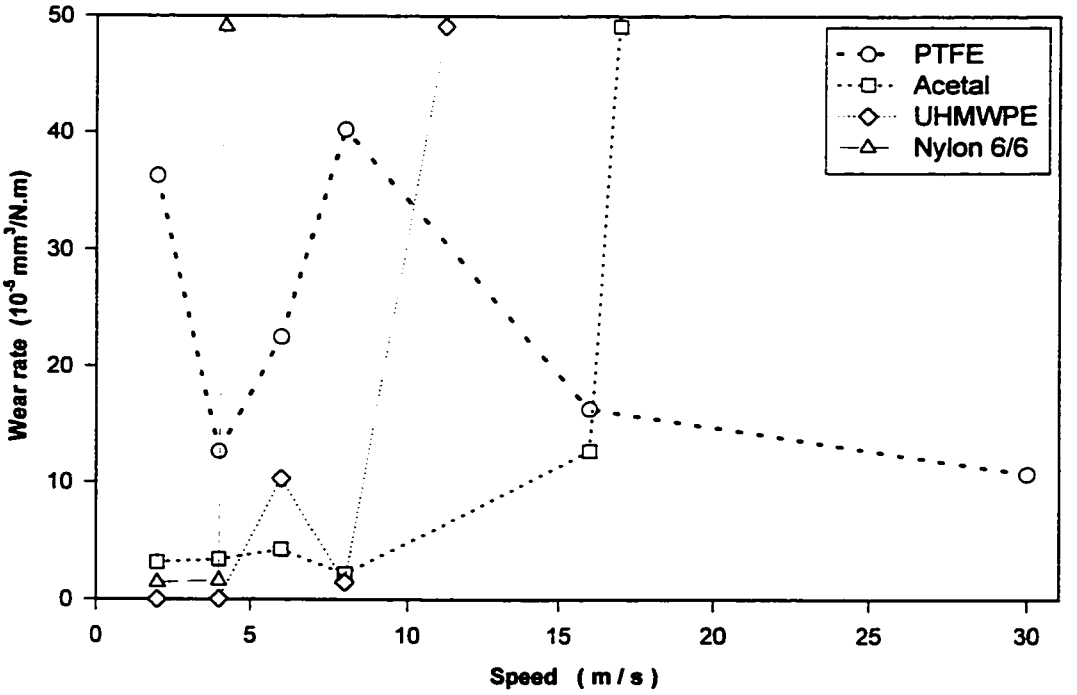

Figure 4.16 The wear rate of different materials sliding against steel at different speeds under 200 N load

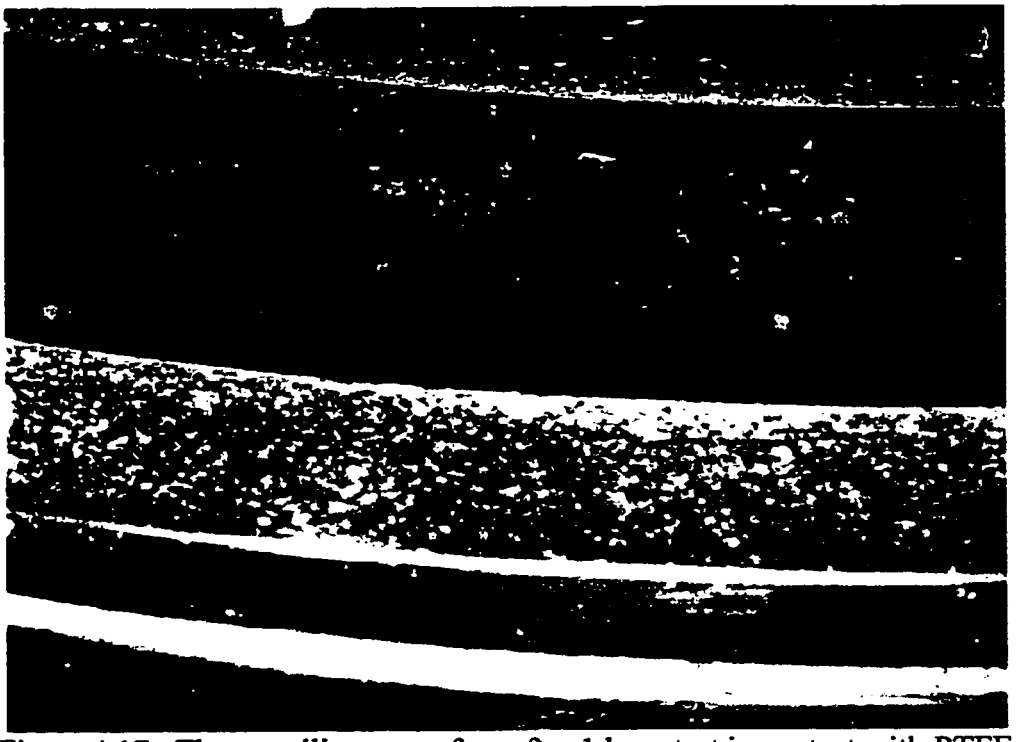

Figure 4.17 The metallic counterface after 1 hour test in contact with PTFE at 8 m/s under 200 N load

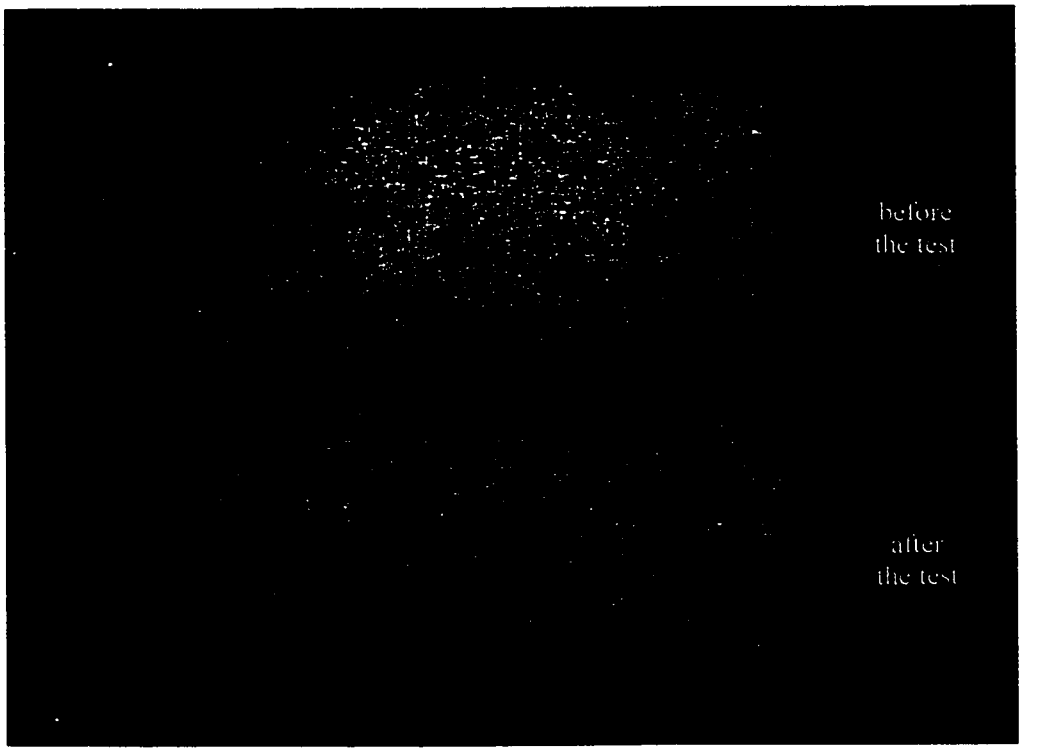

Figure 4.18 PTFE specimen surface before and after 16 m/s test under 200 N load

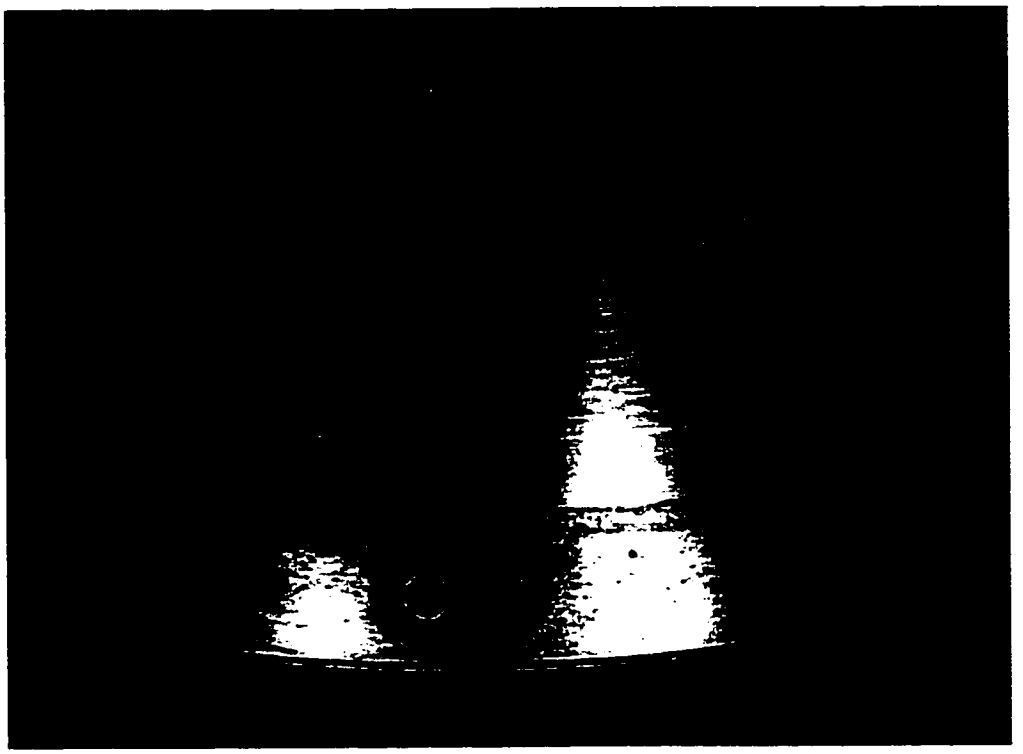

Figure 4.19 The metallic counterface after 1 hour test in contact with Acetal at 8 m/s under 200 N load

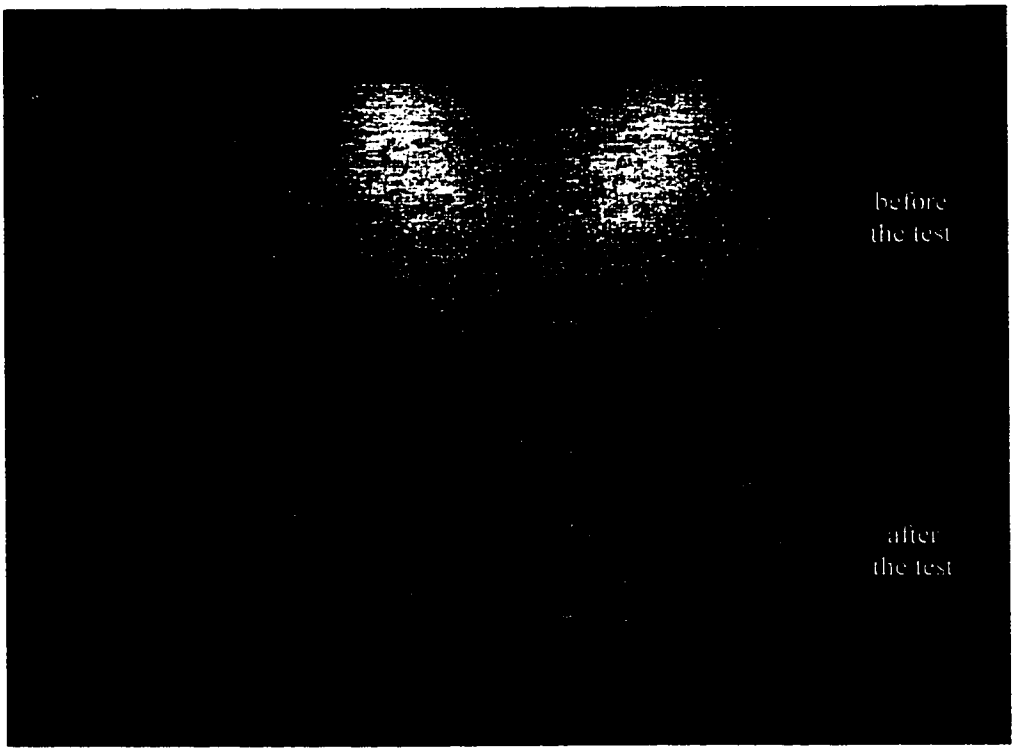

Figure 4.20 Acetal specimen surface before and after 16 m/s test under 200 N load

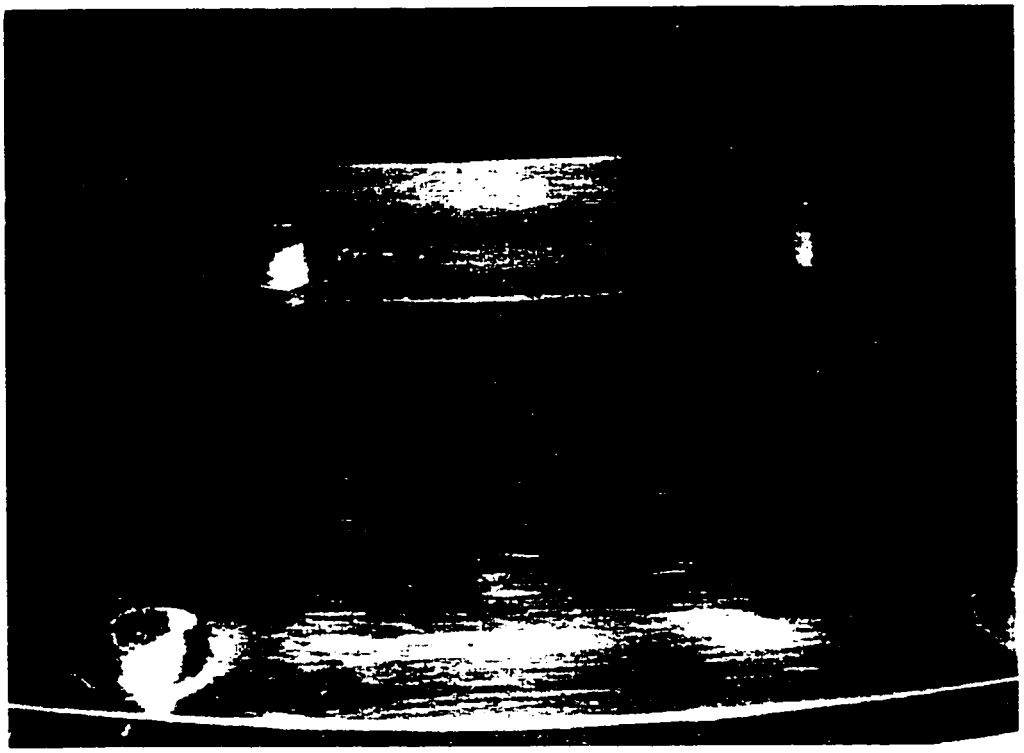

Figure 4.21 The metallic counterface after 2 hours test in contact with UHMWPE at 4 m/s under 200 N load

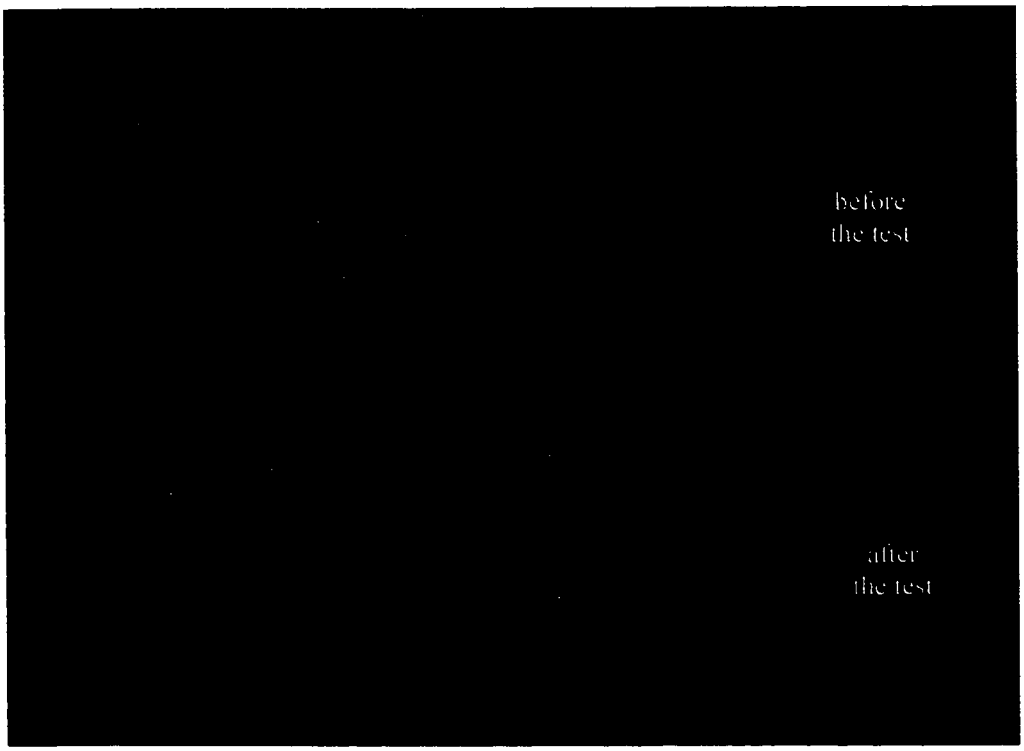

Figure 4.22 UHMWPE specimen surface before and after 16 m/s test under 200 N load

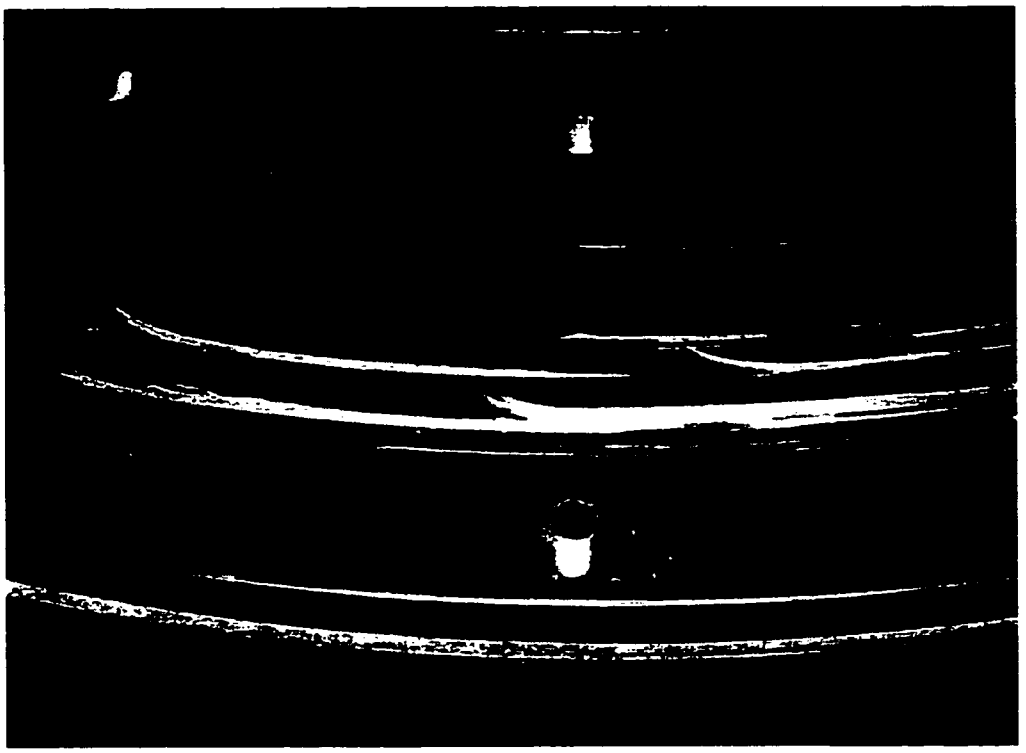

Figure 4.23 The metallic counterface after 1 hour test in contact with Nylon 6/6 at 8 m/s under 200 N load

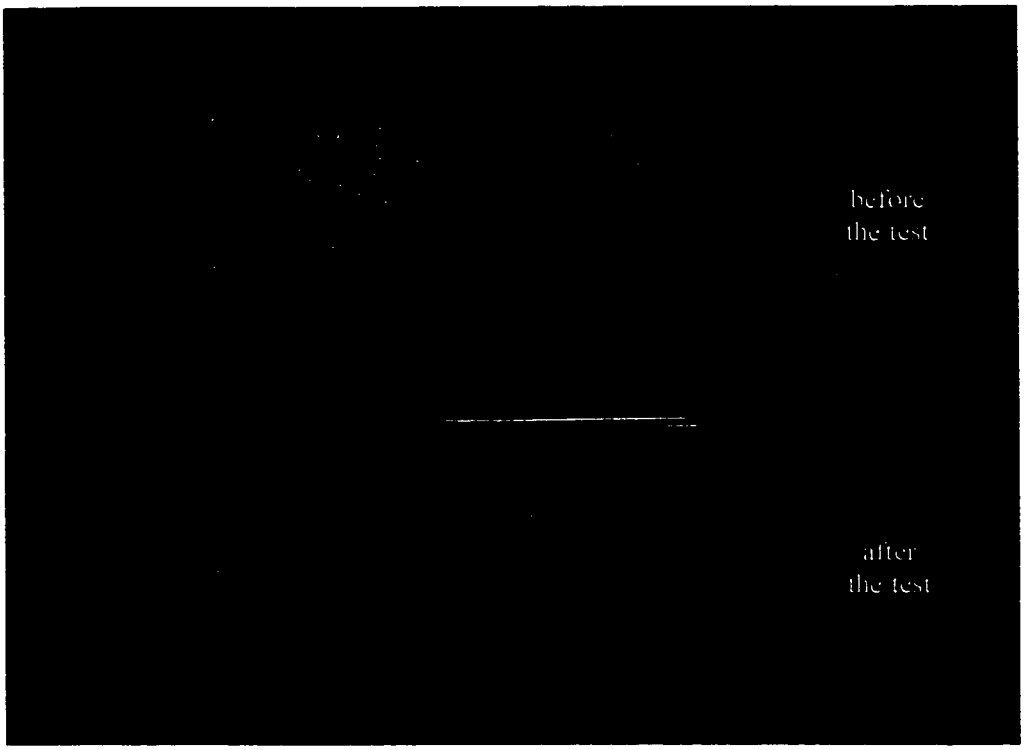

Figure 4.24 Nylon 6/6 specimen surface before and after 8 m/s test under 200 N load

becomes much larger. The low coefficient of friction detected at short duration tests with Nylon 6/6 may be related to the material high rigidity and surface hardness which reduces the real surface of contact. It is suggested that, after a certain test period, subsurface fatigue may occur due to the high contact pressure developed, leading to higher wear rate with surface deformation. This mechanism also increases the coefficient of friction, and therefore the contact temperature. On the other hand, when the surface temperature reaches the glass transition temperature, which is between 50 ° and 80 °C for Nylon 6/6, the substantial decrease of the polymer surface rigidity would increase the real contact area. This would lead to an increase in the adhesion component of the friction coefficient.

Generally, the coefficient of friction decreases with increasing speed until the contact temperature reaches a certain value. This temperature is in the range of the maximum useful temperature of each material reported in table 2.2, except for Acetal which can withstand relatively higher temperature. On the other hand, the wear rate decreases with increasing speed up to the limiting speed of each material.

4.4 Variable load tests

In these tests the speed is maintained constant where the load is increased in a given interval till a very high wear rate or severe surface melting occurs. In this case, the Pv limit is the product of the maximum load and the running speed per unit area.

4.4.1 Objectives

The objective of these tests is to study the variation of the coefficient of friction with the load for each material. Also, to determine the Pv limit of each material and compare it with the values obtained in variable speed tests.

4.4.2 Tests procedures

Before each test both surfaces are cleaned as described earlier. The initial load is 30 N. During the tests, the load is increased by 30 N each 10 minutes at 16 m/s. The relatively high load increment is selected to avoid excessive wear rates before the end of the test period. Table 4.5 presents the different variable load tests conducted on the 4 materials and their load limits. The test is stopped when high wear rates or severe surface melting occurs. The relation between the load, the coefficient of friction and the contact temperature are plotted against the running time. After the test, the metallic surface finish is restored as described in section 4.2.2. Tests are repeated at 30 m/s to study the effect of the speed on the coefficient of friction and the limiting load.

4.4.3 Results and discussion

Figure 4.25 shows the variation of the friction coefficient and contact temperature with time and load in a variable load test of UHMWPE sliding against steel at 16 m/s. The coefficient of friction decreases slightly with increasing the load. When the load reaches 210 N, the coefficient of friction begins to increase till the temperature reaches 80 °C after which the coefficient of friction increases rapidly, the temperature rises to 150°C and surface melting occurs on the polymeric surface. For Nylon 6/6, the coefficient of friction increases slightly with increasing the load up to 90 N as shown in figure 4.26, and then a sudden increase in the friction coefficient is detected and surface melting occurs.

On the other hand, the load limits were not attended in the tests conducted on PTFE for up to 290 N as shown in figure 4.27. First, the coefficient of friction initially decreases, similar to UHMWPE, and then it starts to increase with increasing the load above 270 N. For Acetal, the coefficient of friction remains relatively constant with increasing the load, as shown in figure 4.28, but the wear rate increases rapidly at 270 N.

Table 4.5 Variable load tests in continuous contact (A = 2380 mm^2)

Test No	Material	Load N	Speed m/s	Duration min.	Load Limit	Notes
Speed 16 m/s, speed increment of 30 N each 10 minutes						
50	PTFE	30-290	16	105	> 290 N	—
51	Acetal	30-290	16	93	240 N	↑↑
52	UHMWPE	30-210	16	75	180 N	↑↑↑
53	Nylon 6/6	30- 90	16	33	60 N	↑↑↑
Speed 30 m/s, load increment of 30 N each 10 minutes						
54	PTFE	30-270	30	90	270 N	↑
55	Acetal	30-180	30	66	150 N	↑↑↑
56	UHMWPE	30- 90	30	32	60 N	↑↑↑
57	Nylon 6/6	30- 90	30	32	60 N	↑↑↑

↑ high wear rate

↑↑ very high wear rate leading to test termination

↑↑↑ Severe wear with surface melt leading to test termination

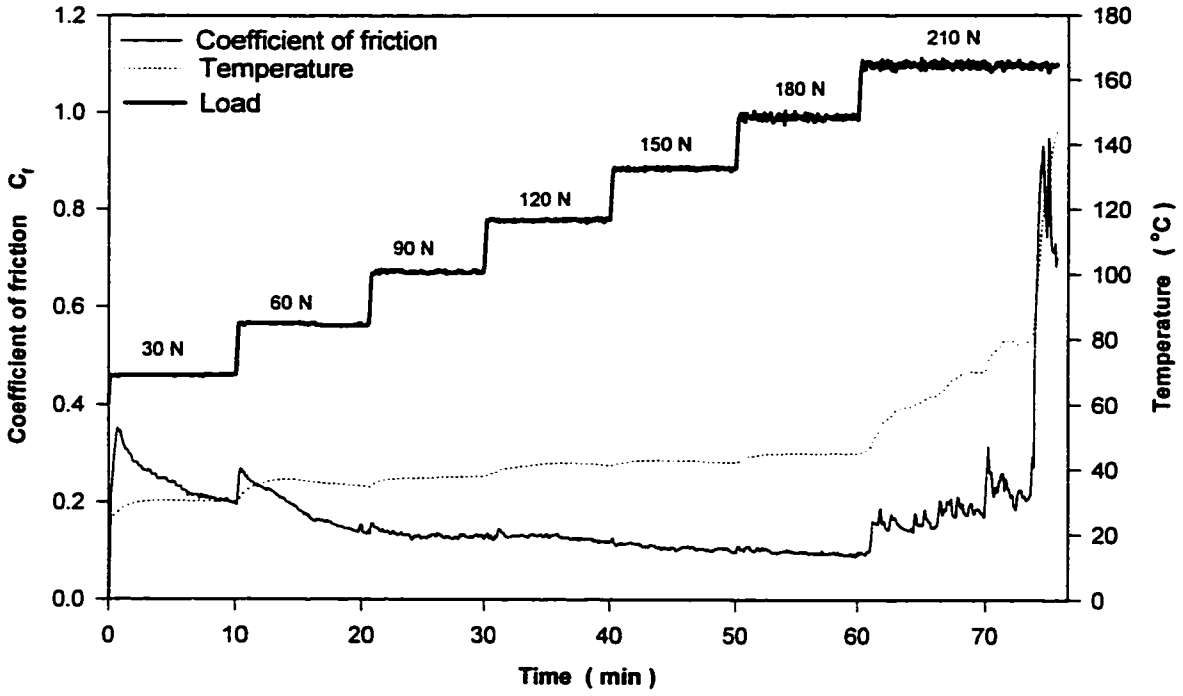

Figure 4.25 Friction coefficient and contact temperature of UHMWPE sliding against steel in a variable load test at 16 m/s

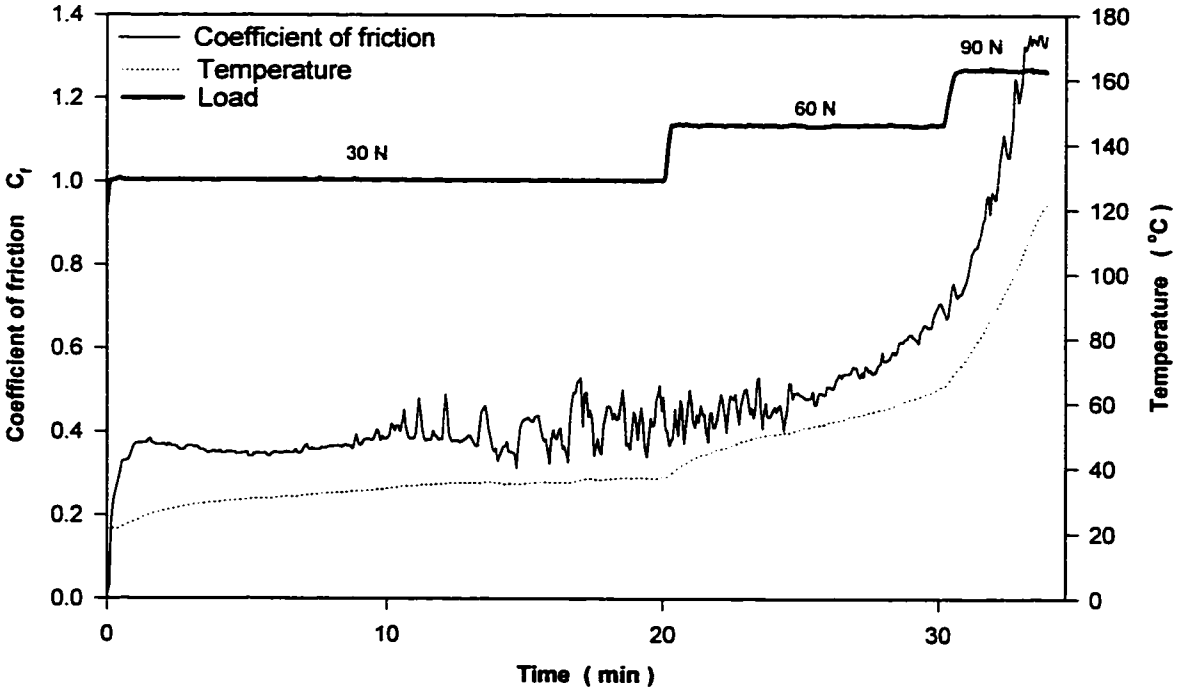

Figure 4.26 Friction coefficient and contact temperature of Nylon 6/6 sliding against steel in a variable load test at 16 m/s

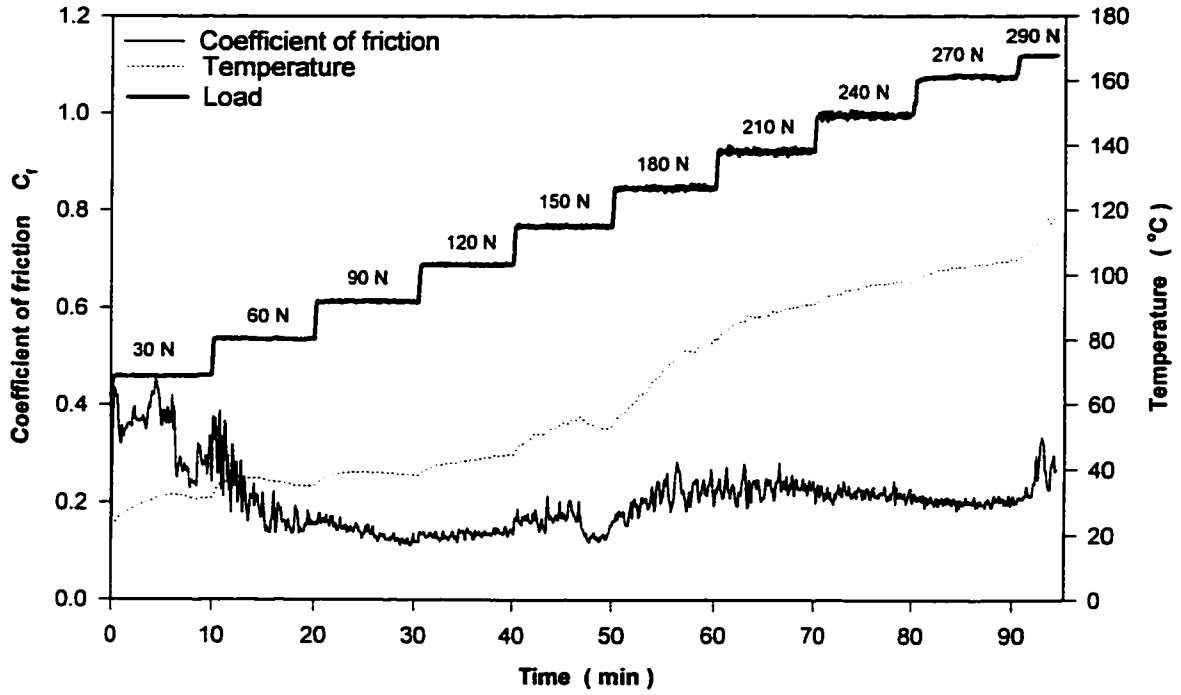

Figure 4.27 Friction coefficient and contact temperature of Acetal sliding against steel in a variable load test at 16 m/s

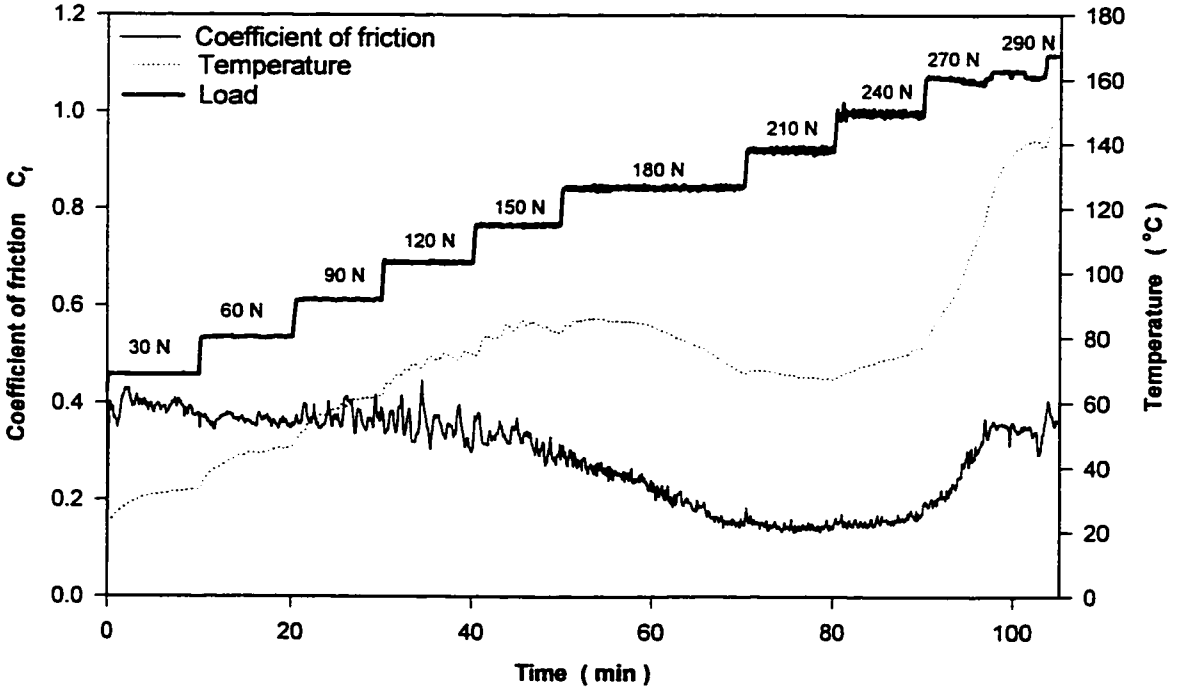

Figure 4.28 Friction coefficient and contact temperature of PTFE sliding against steel in a variable load test at 16 m/s

Figure 4.29 shows the variation of the friction coefficient and contact temperature with time and load in a typical variable load test of Acetal sliding against steel at 30 m/s. The coefficient of friction is very low and remains constant with increasing the load up to 150 N. At 180 N high wear rate is detected. For UHMWPE the same trend is observed where the temperature increase begins at 90 N as shown in figure 4.30. Nylon 6/6 has the same load limit as UHMWPE but a very high wear rate is detected before surface melting occurs (figure 4.31). On the other hand, a slight decrease in the friction coefficient is detected with load increase for PTFE up to 270 N (figure 2.32).

The Pv limits calculated from variable load and variable speed tests are presented in table 4.6. Figure 4.33 presents the different load and speed limits for each material. It is clear that PTFE has the highest Pv limit followed by Acetal, UHMWPE where Nylon has the lowest Pv values. On the other hand, the values detected are usually much higher than those found in literature. It is suggested that the relatively large contact surface with moderate contact pressure are responsible for such high values. It is important to mention here that the Pv values reported are for material comparison and not to be taken as recommended values. The variation of the Pv limit with speed needs further investigations.

4.5 Conclusion

Tests were conducted on four different materials in contact with steel counterface at relatively large surfaces of contact. Those tests demonstrated that PTFE has the lowest friction coefficient and the highest Pv limits but with a relatively high wear rate at moderate speeds. The PTFE shows a very high stability up to the maximum speed at both high and low loads with Pv values exceeding largely the limits found in literature. The film transfer of this material decreases the adhesion force between both surfaces in contact. In addition, the film detaches easily from the surface and acts as smooth lubricant which leads to a high wear rate but with a very low coefficient of friction.

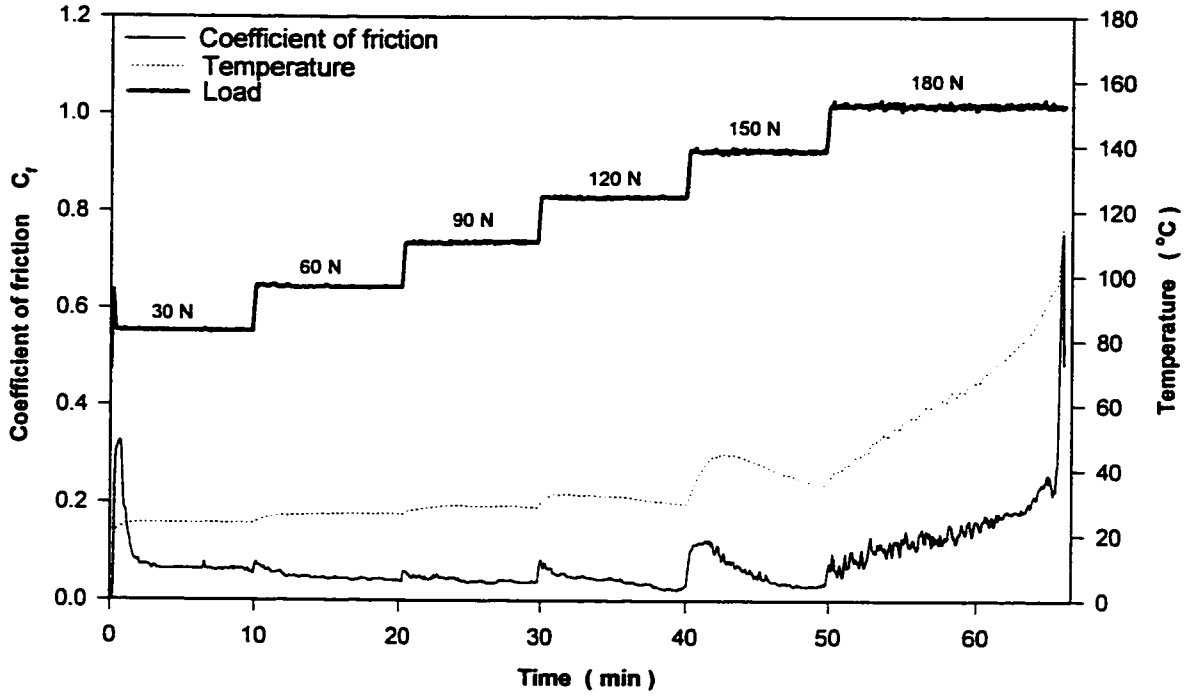

Figure 4.29 Friction coefficient and contact temperature of Acetal sliding against steel in a variable load test at 30 m/s

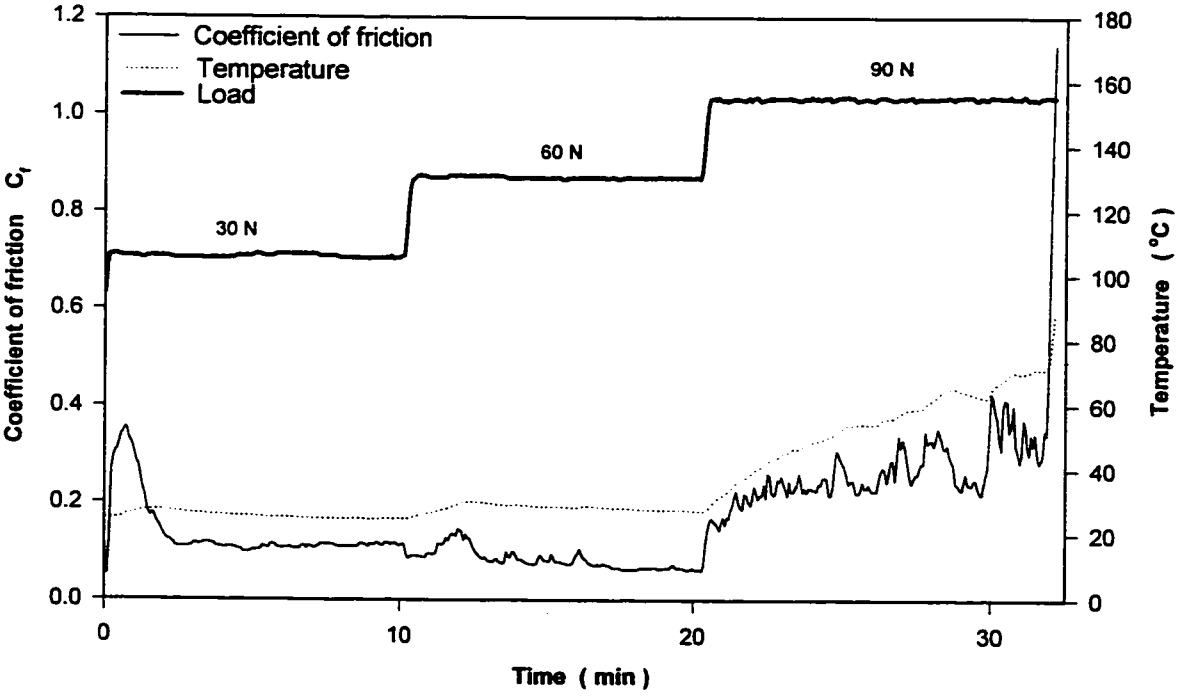

Figure 4.30 Friction coefficient and contact temperature of UHMWPE sliding against steel in a variable load test at 30 m/s

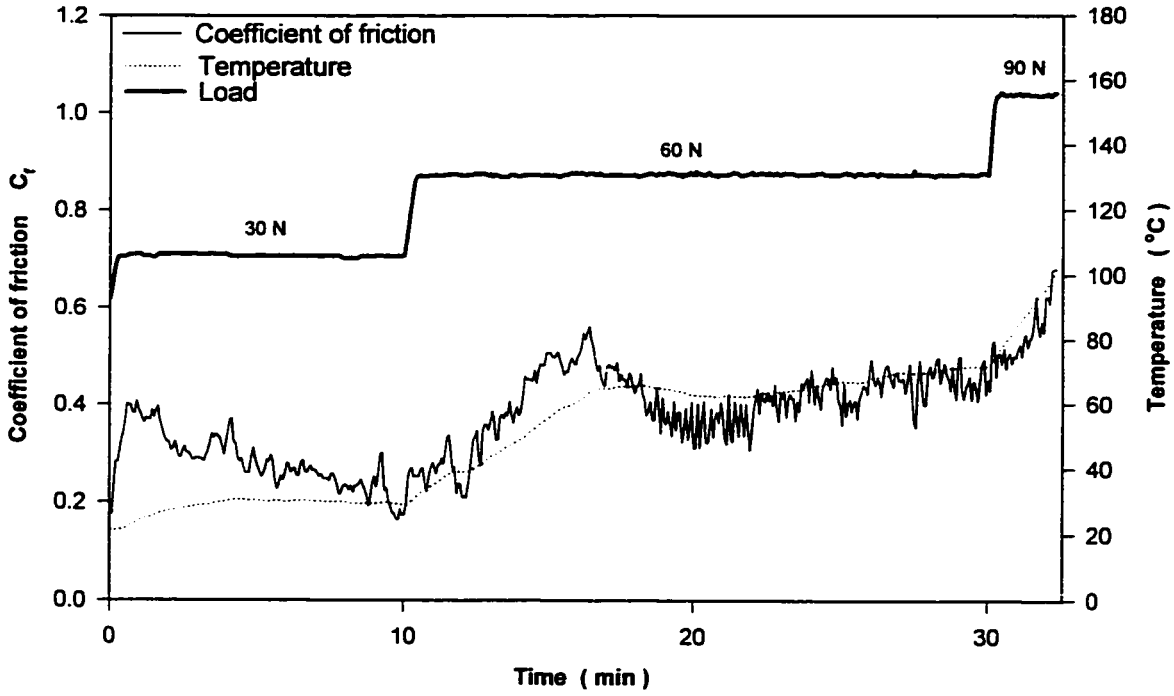

Figure 4.31 Friction coefficient and contact temperature of Nylon 6/6 sliding against steel in a variable load test at 30 m/s

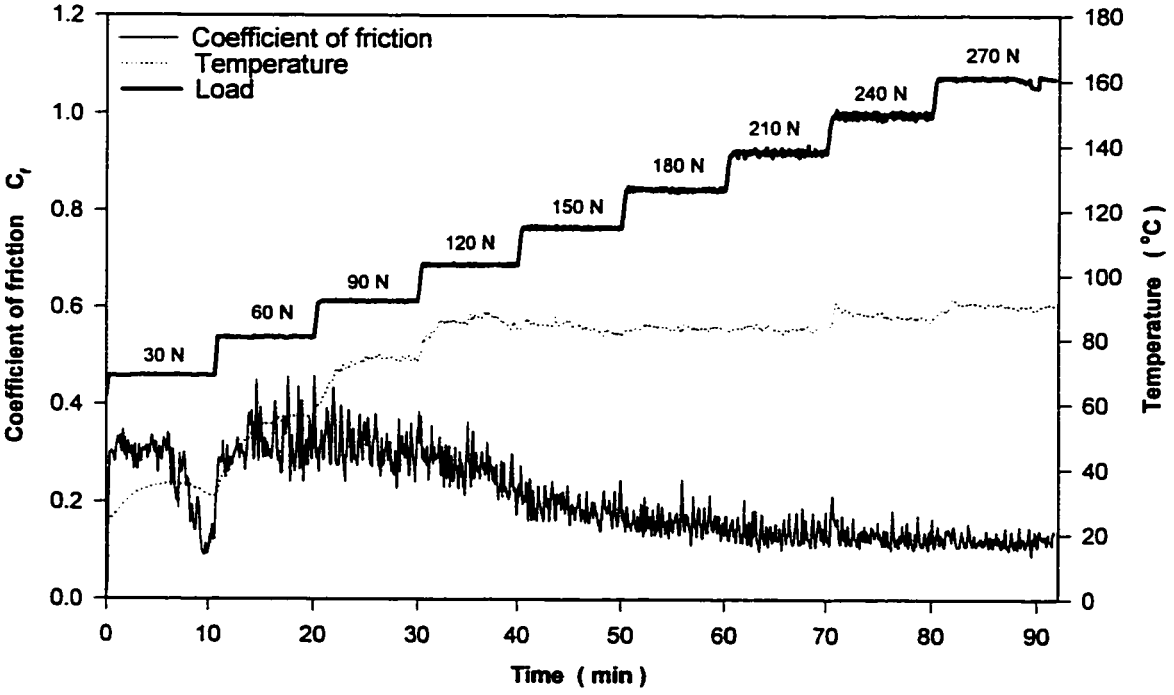

Figure 4.32 Friction coefficient and contact temperature of PTFE sliding against steel in a variable load test at 30 m/s

Table 4.6 Pv limits in continuous contact tests (A = 2380 mm^2)

Materials	Speed m/s	Load N	W x v N.m/s	Pv Limit MPa.m.s^{-1}
PTFE	50*	200	10 000*	---
PTFE	30	270	8100*	---
PTFE	50*	120	6 000*	---
PTFE	16	290*	4640*	---
Acetal	56*	120	6720*	---
Acetal	30	150	4500	1.875
Acetal	22	200	4400	1.83
Acetal	16	240	3840	1.60
UHMWPE	26	120	3120	1.30
UHMWPE	16	180	2880	1.2
UHMWPE	30	60	1800	0.75
UHMWPE	8	200	1600	0.66
Nylon 6/6	30	60	1800	0.75
Nylon 6/6	6	200	1200	0.5
Nylon 6/6	16	60	960	0.40
Nylon 6/6	8	120	960	0.40

* The material maintain its stability at the maximum applied speed or load (i.e. no Pv limit)

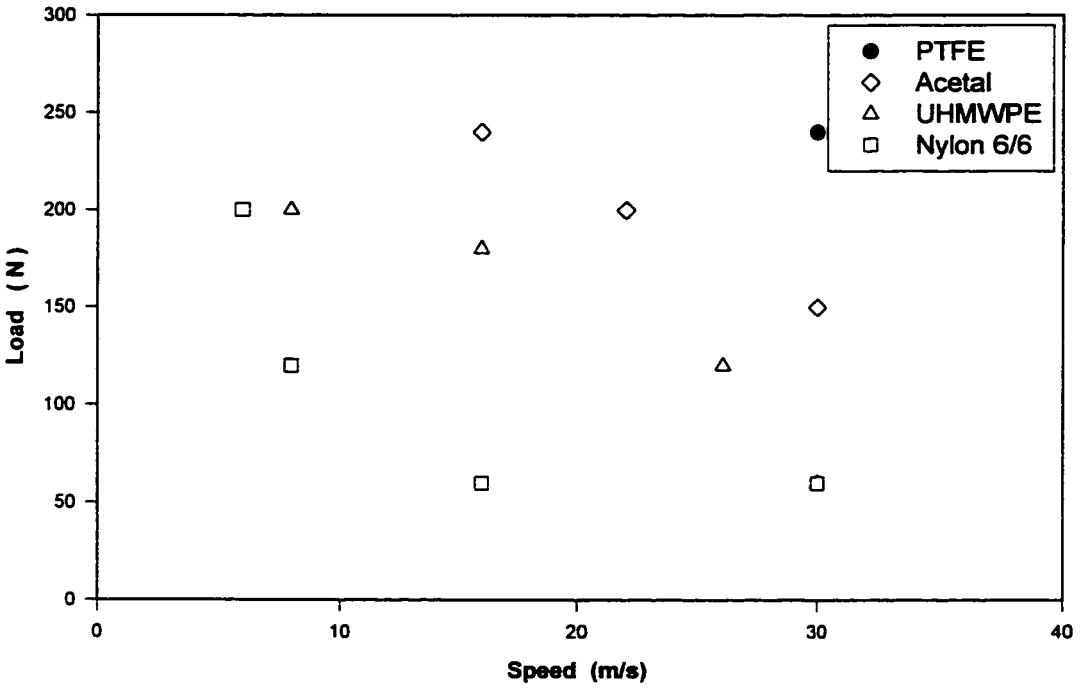

Figure 4.33 Load and speed limits for different materials

Acetal has also a relatively low coefficient of friction with relatively high Pv limits. Its wear mechanism is similar to PTFE. However, it is suggested that its higher surface hardness and lower melting temperature lead to a lower wear rate and higher coefficient of friction with respect to PTFE.

UHMWPE exhibits the minimum wear rate at moderate speeds but with lower Pv limits than PTFE and Acetal. This material embeds a very thin film which adheres rigidly to the metallic surface. This leads to a relatively low coefficient of friction and a very low wear rate. On the other hand, its relatively low Pv limits can be related to the material low melting temperature. The material maintains its consistency up to very high contact temperature although very high wear rate and severe surface damage occurs.

Nylon 6/6 has both the highest coefficient of friction and the lowest Pv limits. At low speed sliding, no film transfer is detected on the metallic surface. This material rigidity and high surface hardness may be the cause of its high coefficient of friction at low speeds.

The performance of those materials was directly related to the nature of the transfer film deposits at different speeds and their mechanical characteristics' stability at different contact temperatures.

Studying the effect of the contact surface, it is found that the wear mechanisms of the different materials are practically the same as found in literature for small contact surfaces. However, the surface deformation and the wear particles are much larger; this leads to large changes in the counterface surface profile and increase the wear rate and the coefficient of friction. On the other hand, the molten film, developed when exceeding the polymer melting point, does not decrease the coefficient of friction; this may limit the application of the thermal control friction theory for large contact surfaces.

Usually, at high speed sliding, the coefficient of friction decreases with increasing speed up to the materials Pv limits. Very low coefficient of friction are recorded at high sliding speed. Studying the effect of the applied load on the friction coefficient, at high sliding speed, it is found that the effect is not conclusive and depends on the material in contact. On the other hand, the wear rate decreases with increasing the sliding speed up to the Pv limits. It is also concluded that the wear rate decreases with increasing the contact temperature.

CHAPTER V

DISCONTINUOUS CONTACT TESTS

5.1 Introduction

Many high speed tribological applications include discontinuous contact. This contact is characterized by higher dynamic loading and impact on both surfaces. This may affect largely the wear mechanisms and friction force. In such application, the use of polymers is highly recommended due to their capacity of absorbing shock loading. In polymers, the film deposition could be highly affected by dynamic loading. There is no available information about the tribological behavior of polymers at discontinuous contact.

In this chapter tests are conducted on four different polymers to study their friction and wear properties at high sliding speed and load for discontinuous contacts. Those tests are also conducted to test the capacity of the tribometer in discontinuous contact. The polymers selected are UHMWPE, PTFE, Acetal and Nylon 6/6. The effect of speed and the discontinuous contact on the friction coefficient and wear mechanisms is studied. In addition, the limiting Pv value is investigated for each material and compared with that obtained in continuous contact.

5.2 Variable speed tests

In these tests the load is maintained constant where the speed is increased in a given interval till a very high wear rate or severe surface melting occurs. This speed is called the material speed limit and its product with the applied load per unit area is referred as the Pv limit of the material for discontinuous contact. The apparent area of contact is 2380 mm^2 as in continuous contact.

5.2.1 Objectives

The objective of these tests is to study the variation of the coefficient of friction with speed and temperature for each material in discontinuous contact. The Pv limit of each material is also evaluated and compared with continuous contact results.

5.2.2 Tests procedures

The test procedure is the same as in continuous contact tests: surface cleaning, initial loading with 200 N at 2 m/s, speed increment of 1 m/s each 10 minutes and test stop when high wear rate or severe surface melting occurs. The relation between speed, coefficient of friction and contact temperature is plotted against the running time. After the test, both surfaces are photographed and the metallic surface finish is restored in two steps; first manually using abrasive papers to clean the metallic insert sides and corners, then using the same procedure as in section 4.2.2.

5.2.3 Results

Table 5.1 presents the different variable speed tests conducted on the 4 materials and their speed and Pv limits in discontinuous contact. Figure 5.1 shows the variation of the friction coefficient and contact temperature with time and speed in a typical variable speed test of UHMWPE sliding against steel. At 4 m/s, when the temperature reaches 80 °C, the coefficient of friction starts to increase rapidly from 0.3 to 0.7 where the temperature reaches 180 °C. When the speed is increased to 5 m/s the coefficient of friction starts to decrease slightly where the material maintains its stability with a relatively high wear rate. When the speed reaches 7 m/s, the coefficient of friction and the wear rate increase dramatically leading to a substantial surface melting. For Nylon 6/6, the coefficient of friction and the contact temperature start to increase at 2 m/s and then decrease at 3 m/s as shown in figure 5.2. At 4 m/s the friction coefficient and contact temperature increase dramatically.

Table 5.1 Variable speed tests in discontinuous contact (A = 2380 mm^2)

Test No	Material	Load N	Speed m/s	Duration min.	Limits m/s	Pv Limits MPa.m.s^{-1}
58	Acetal	200	2 - 6	50	5	0.42
59	PTFE	200	2 - 12	104	11	0.92
60	Nylon 6/6	200	0 - 4	27	3	0.25
61	UHMWPE	200	0 - 7	52	6	0.5

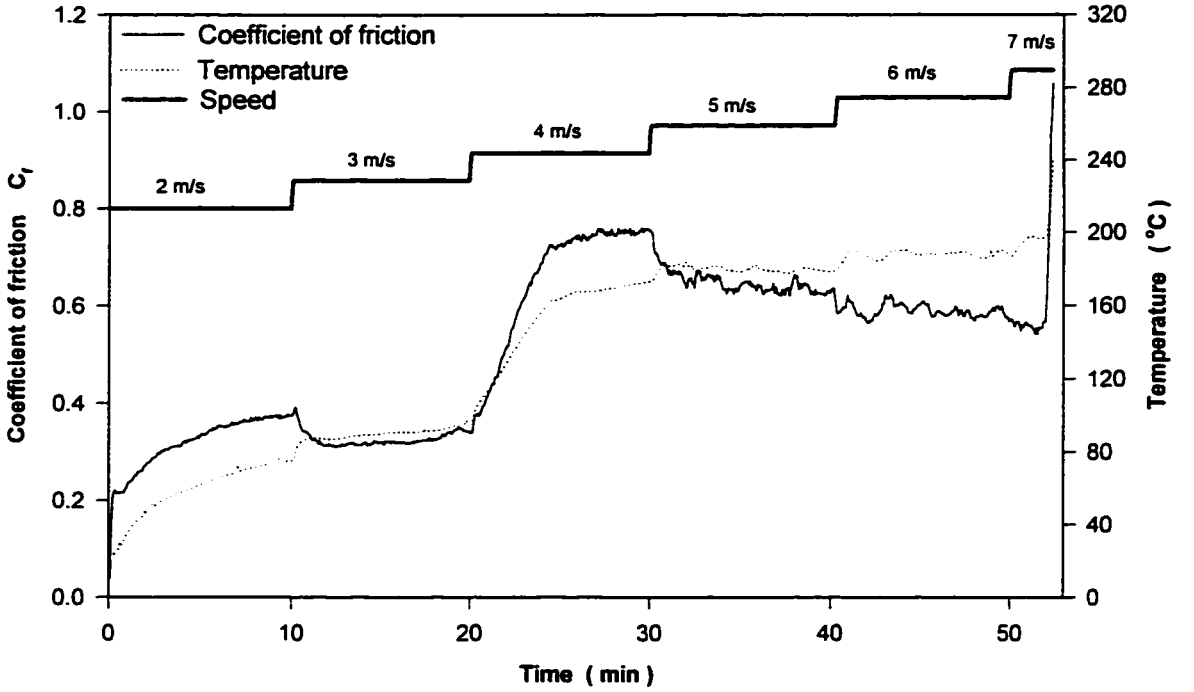

Figure 5.1 Friction coefficient and contact temperature of UHMWPE sliding against steel in discontinuous contact at variable speed test under 200 N load

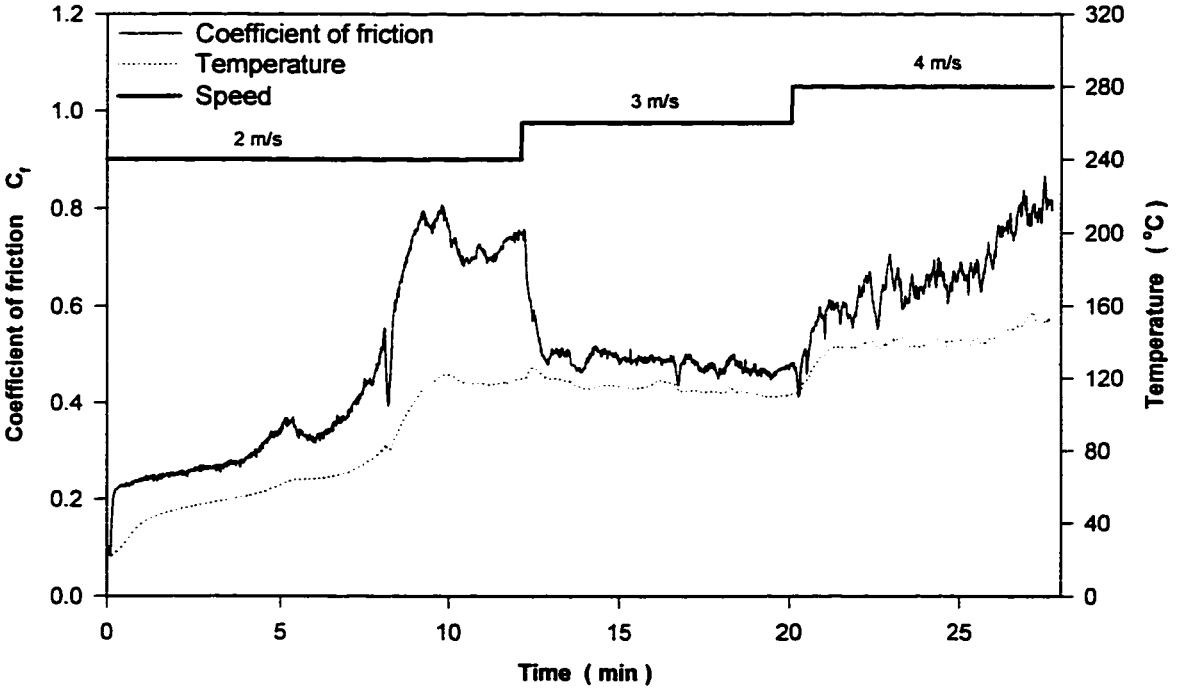

Figure 5.2 Friction coefficient and contact temperature of Nylon 6/6 sliding against steel in discontinuous contact at variable speed test under 200 N load

The coefficient of friction for PTFE is relatively low and increases slightly with speed up to 8 m/s. Then a sudden increase in temperature and coefficient of friction is detected to reach a peak value and then stabilize at 160 °C with a coefficient of friction of 0.3 as shown in figure 5.3. The temperature and the coefficient of friction maintain their stability with increasing speed up to 12 m/s where they start to increase dramatically and surface melting occurs. The temperature reaches values up to 400 °C where surface melting is demonstrated by a large cavity but with high surface smoothness. On the other hand, Acetal maintains a moderate friction coefficient, decreasing slightly with speed from 0.4 to 0.3, up to 6 m/s where it starts to increase with a very high wear rate as shown in figure 5.4. Figure 5.5 resumes the relation between the friction coefficient and speed for different materials.

5.2.4 Discussion

From the preceding tests, it is found that PTFE and Acetal have similar coefficient of friction which is slightly higher than that detected at continuous contact tests. Nylon has slightly lower coefficient of friction in discontinuous contact whereas UHMWPE exhibits a relatively higher coefficient of friction with very high contact temperatures.

The estimated Pv limits for all materials at discontinuous contact are much lower than in continuous contact as shown in table 5.1. This is attributed to the lower metallic counterface surface which limits the heat dissipation in both conduction and convection. UHMWPE demonstrated a remarkable stability at high contact temperature and its speed limit exceeds that of Acetal. PTFE has the highest Pv limits whereas Nylon 6/6 has the lowest as in continuous contact.

The wear mechanism detected when exceeding the UHMWPE speed limit is much different from that detected at continuous contact. The polymer specimen has a very smooth surface as shown in figure 5.6. No smears or cavities are detected on the polymer surface as in continuous contact. Thick film deposition is found around the metallic inserts having

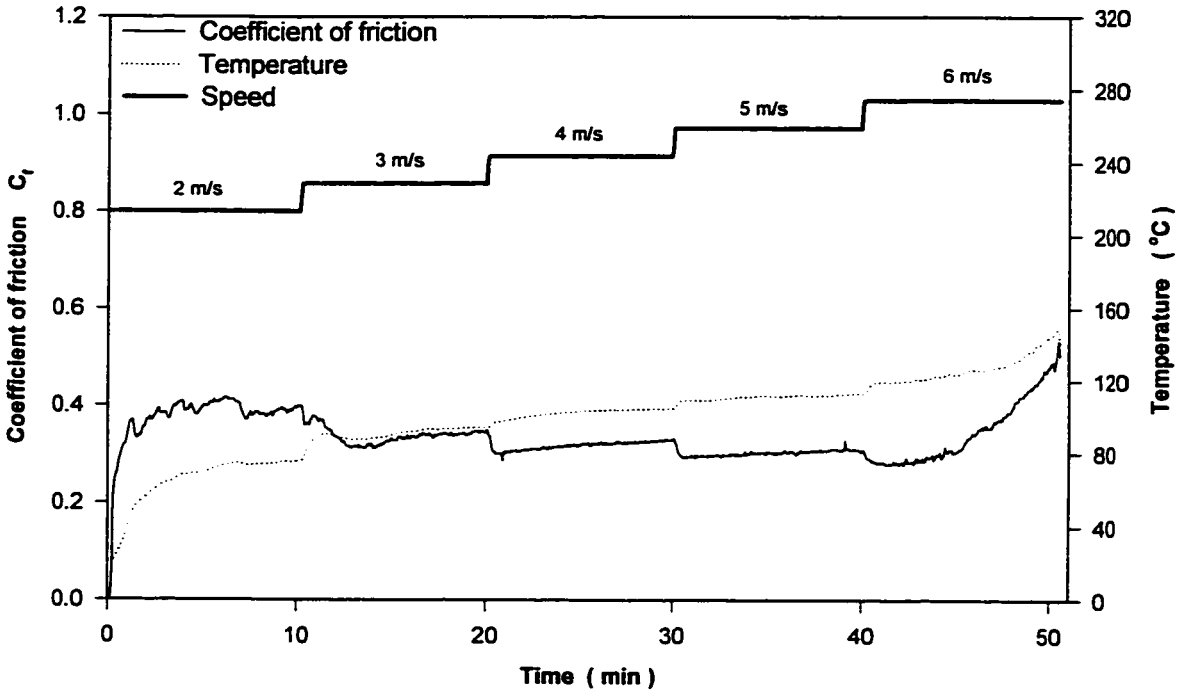

Figure 5.3 Friction coefficient and contact temperature of Acetal sliding against steel in discontinuous contact at variable speed test under 200 N load

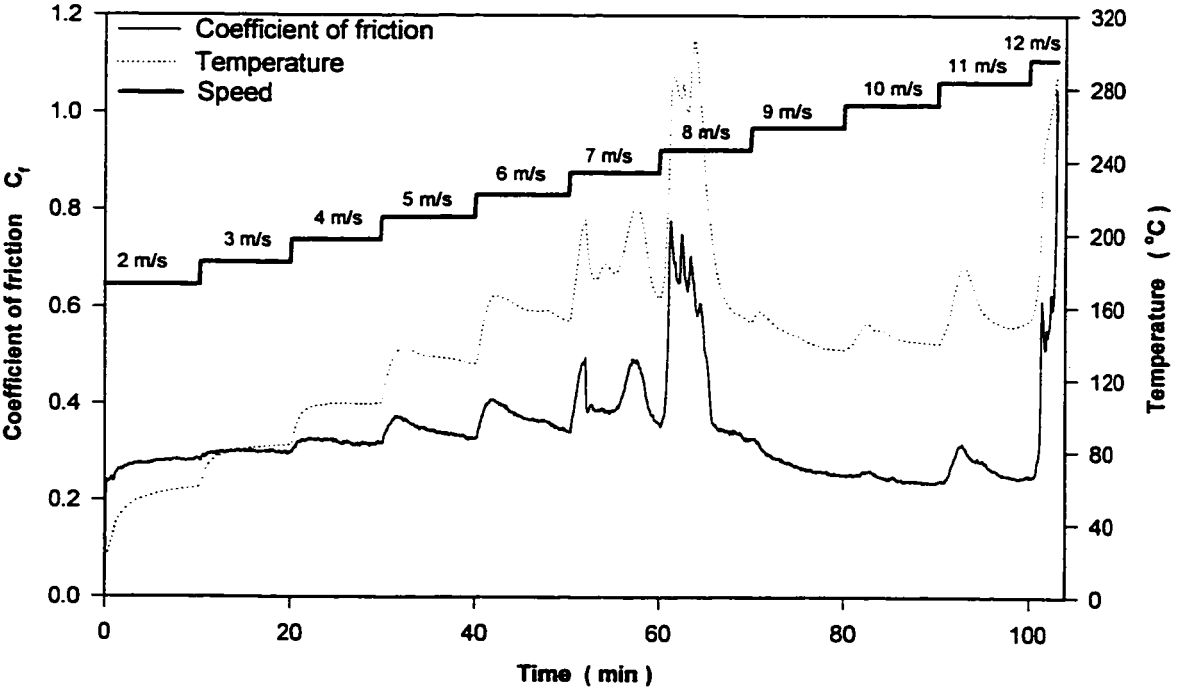

Figure 5.4 Friction coefficient and contact temperature of PTFE sliding against steel in discontinuous contact at variable speed test under 200 N load

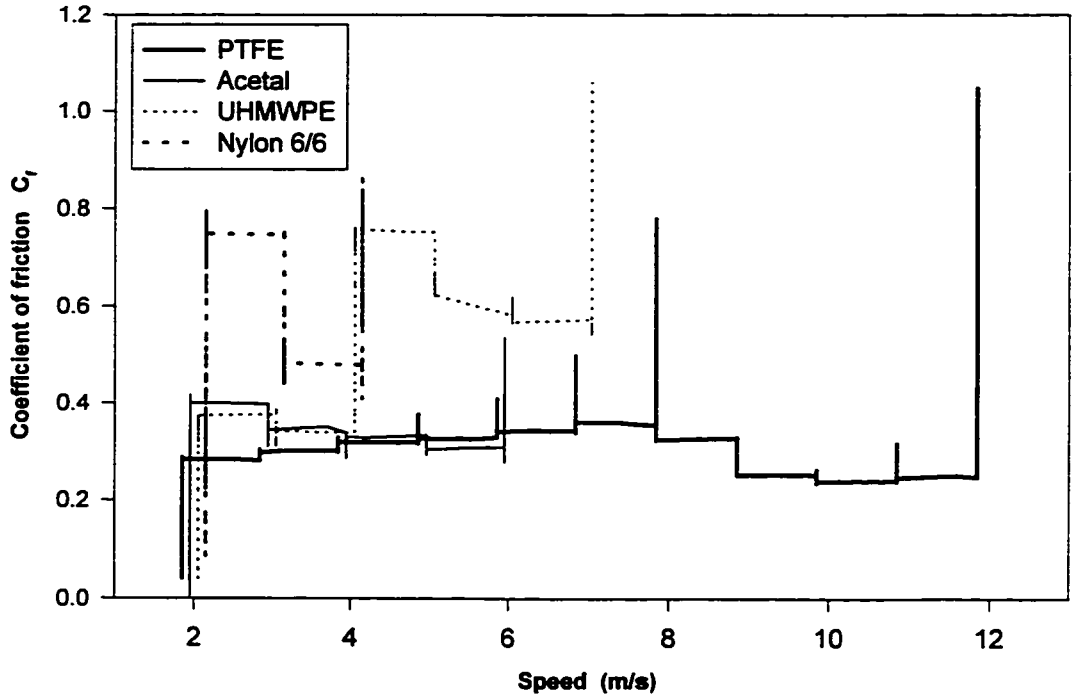

Figure 5.5 The variation of the friction coefficient with speed for different materials sliding against steel in variable speed discontinuous contact tests under 200 N load

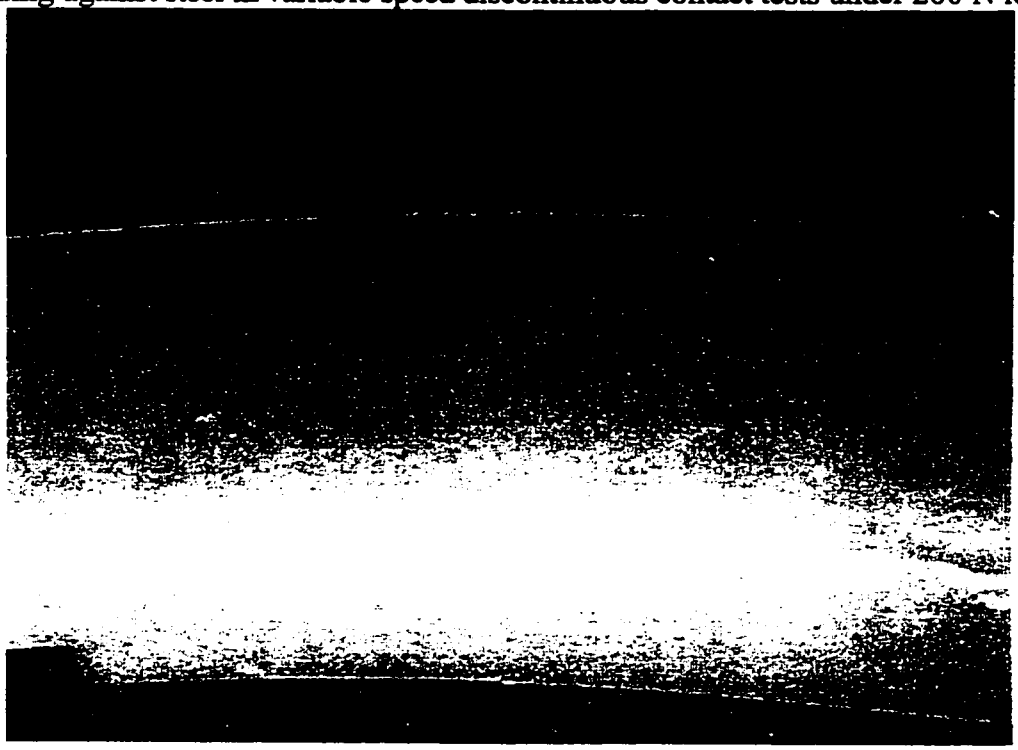

Figure 5.6 UHMWPE specimen surface after variable speed test under 200 N load in discontinuous contact

different degree of transparency as shown in figure 5.7. On the other hand, a large cavity is detected on the PTFE specimen surface after the test, which is the result of surface melting as shown in figure 5.8. Fine debris is found on the metallic surface as shown in figure 5.9. Nylon 6/6 demonstrates the same wear mechanisms and surface failure as in continuous contact which is represented by thick film deposition on the metallic surface as shown in figure 5.10. For Acetal, the surface distortion is slightly higher and a fine powder debris is found on the metallic inserts as with PTFE.

5.3 Constant speed and load tests

In these tests the load and speed are maintained constant. The variation of the coefficient of friction and the temperature with time is monitored. The wear rate is measured by weight. The polymer and metallic surfaces are investigated to study the wear mechanisms of different materials at different speeds for discontinuous contact.

5.3.1 Objectives

The objective of these tests is to determine the coefficient of friction, the specific wear rate and the different wear mechanisms of each material at different speeds for discontinuous contact and compare it with that of continuous contact.

5.3.2 Tests procedures

Tests are performed at a constant load of 200 N for two periods of one hour each at 2 and 5 m/s. The same test procedures are maintained as in continuous contact; surface cleaning, polymer specimen weight measurement, constant load and speed test for one hour, weight remeasured, test restarted with the same specimen for the same load and speed for another hour. After the test, the metallic surface finish is restored as in section 5.2.2.

Figure 5.7 The metallic counterface after variable speed test in contact with UHMWPE under 200 N load in discontinuous contact

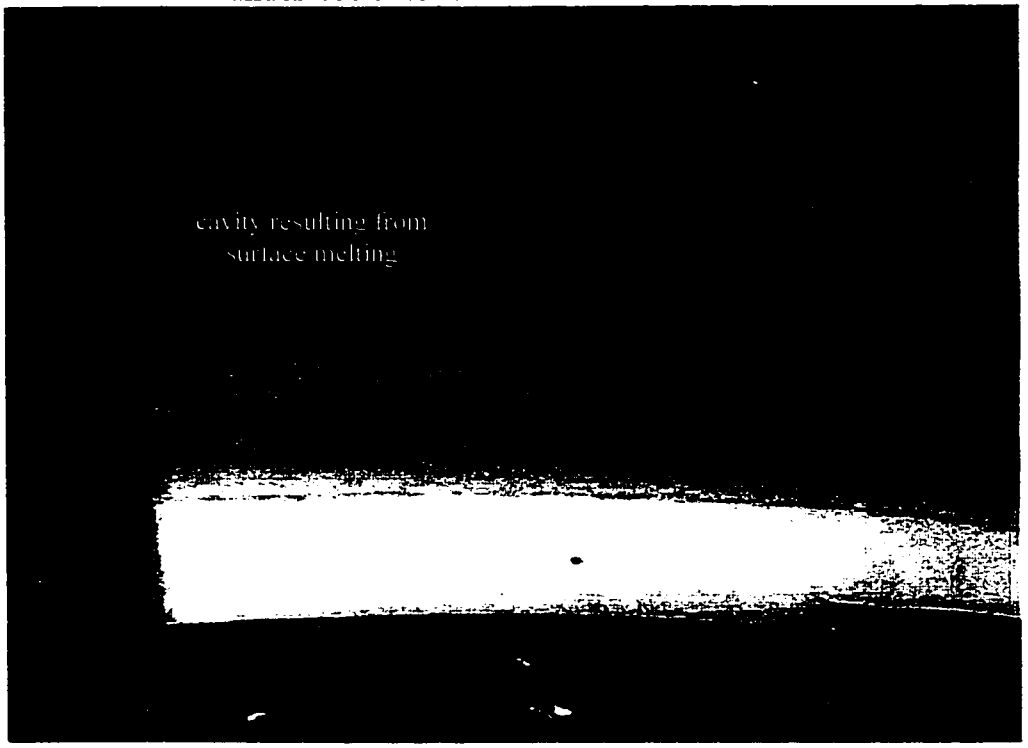

Figure 5.8 PTFE specimen surface after variable speed test under 200 N load in discontinuous contact 200 N load

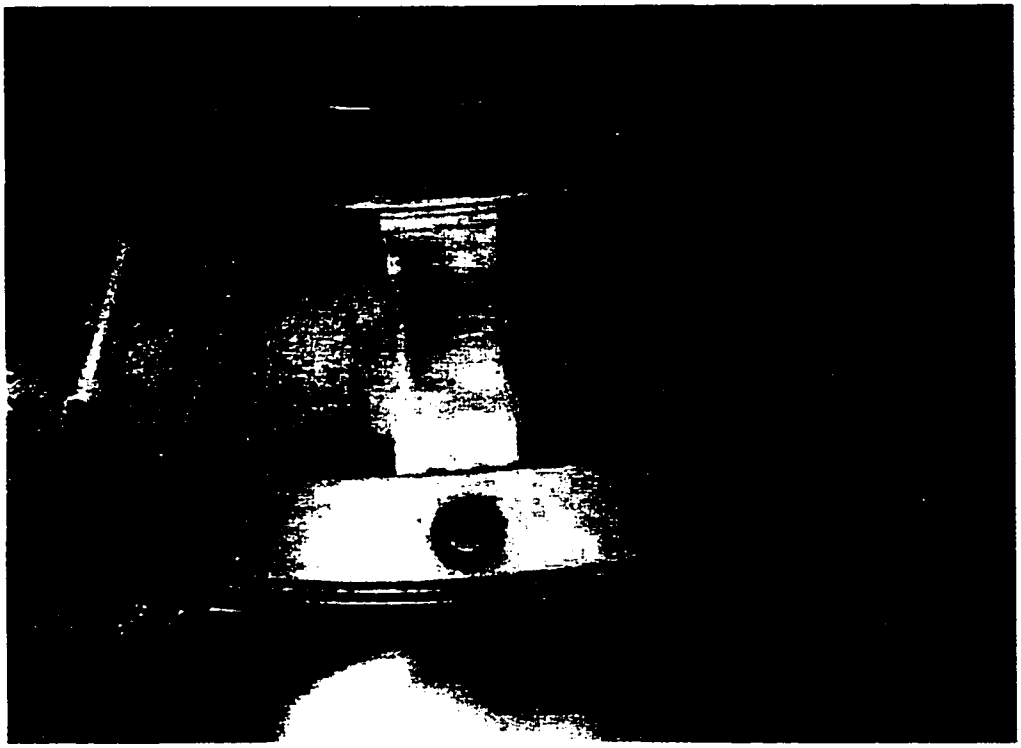

Figure 5.9 The metallic counterface after variable speed test in contact with PTFE under 200 N load in discontinuous contact

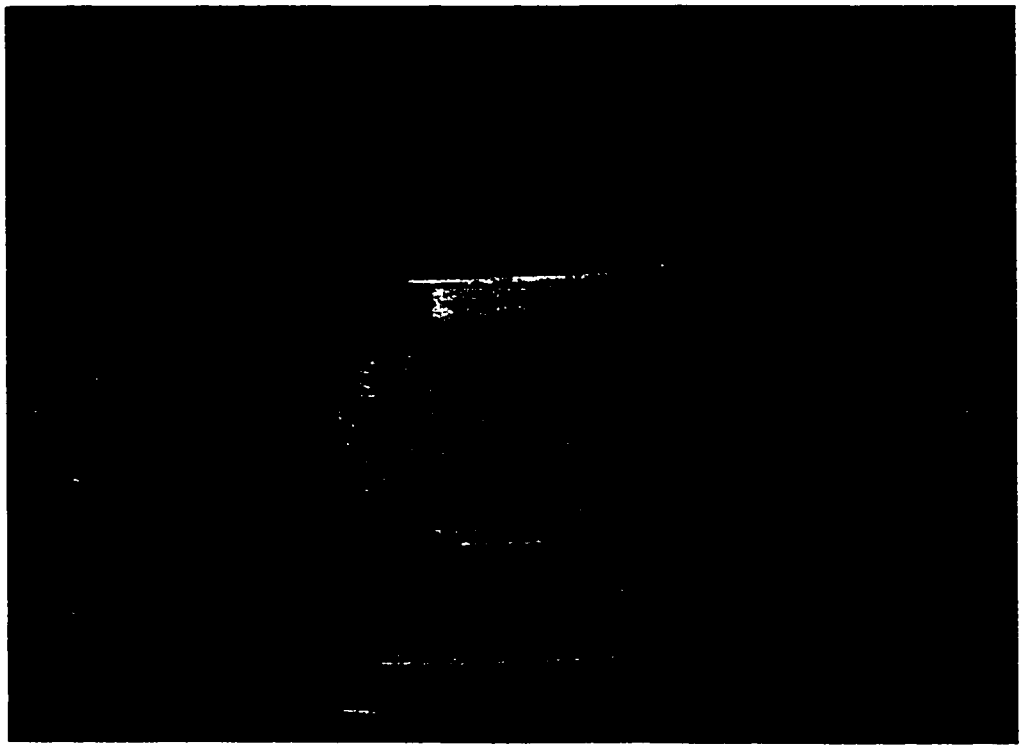

Figure 5.10 The metallic counterface after variable speed test in contact with Nylon 6/6 under 200 N load in discontinuous contact

5.3.3 Results

Table 5.2 presents the different constant speed tests conducted on the 4 materials. The speed, duration and wear loss of each test are reported. Figure 5.11 shows the variation of the friction coefficient and contact temperature with time in a typical constant speed test of Nylon 6/6 sliding against steel at 200 N load and 2 m/s. Another example is found in figure 5.12 showing the same relation for PTFE at 5 m/s. Generally the coefficient of friction increases at the first period of the test then stabilizes with the temperature for all materials. When the test speed is higher than the polymer maximum speed, the temperature increases continuously till surface melting occurs.

For UHMWPE at 5 m/s, the coefficient of friction initially increases to stabilize at 0.7 with a contact temperature of 180 °C. The wear rate is very high and a phase transformation is detected as shown in figure 5.13. This figure, illustrating an UHMWPE specimen in contact with steel inserts, shows the formation of a transparent zone near the contact surface after 50 minutes. The transparent zone is the result of the transformation from semi-crystalline to amorphous state. Figure 5.14 shows the same zone ten minutes later; the transparent zone increases and a general deformation of the polymer specimen is detected.

Figure 5.15 resumes the relation between the mean coefficient of friction and speed for all the materials. The relation between the wear rate and speed is presented in figure 5.16. The coefficient of friction, the contact temperature and the wear rate for the different materials are presented in table 5.3.

5.3.4 Discussion

Studying the wear rate of different materials at 2 m/s tests, it is found that PTFE has the highest wear rate followed by Acetal and Nylon 6/6 as in continuous contact. UHMWPE exhibits a very low wear rate which is not detected using a 0.01 g precision balance.

Table 5.2 Constant speed tests in discontinuous contact (A = 2380 mm^2)

Test No	Material	Load N	Speed m/s	Duration	w loss g	Wear 10^{-5} mm^3/N.m
62	PTFE	200	2	60	2.25	72.0
63	PTFE	200	2	60	2.04	65.3
64	Acetal	200	2	60	0.10	4.88
65	Acetal	200	2	60	0.11	5.37
66	UHMWPE	200	2	60	0.02	1.49
67	UHMWPE	200	2	60	0.01	<0.8
68	Nylon 6/6	200	2	60	0.05	3.05
69	Nylon 6/6	200	2	60	0.02	1.21
70	PTFE	200	5	60	3.55	45.4
71	PTFE	200	5	60	3.68	47.1
72	Acetal	200	5	60	20.88	408
73	Acetal	200	5	60	25.72	503
74	UHMWPE	200	5	60	31.82	950
75	Nylon 6/6	200	5	15	18.86	1840

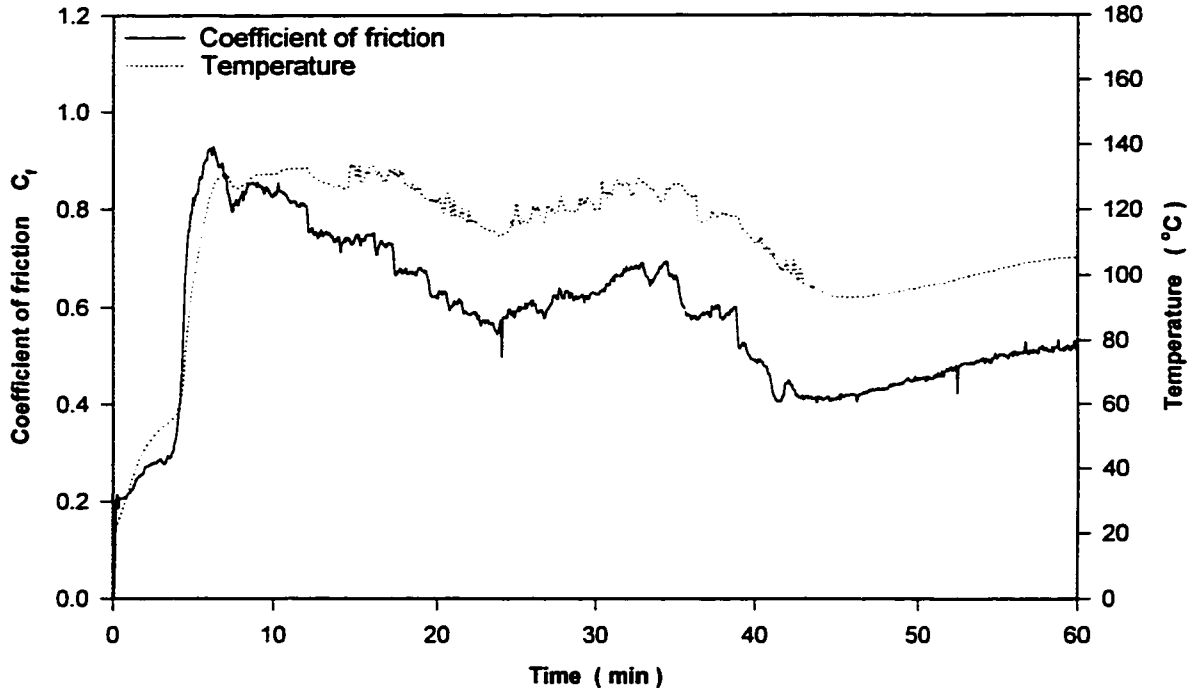

Figure 5.11 Friction coefficient and contact temperature of Nylon 6/6 sliding against steel in discontinuous contact at 2 m/s under 200 N load

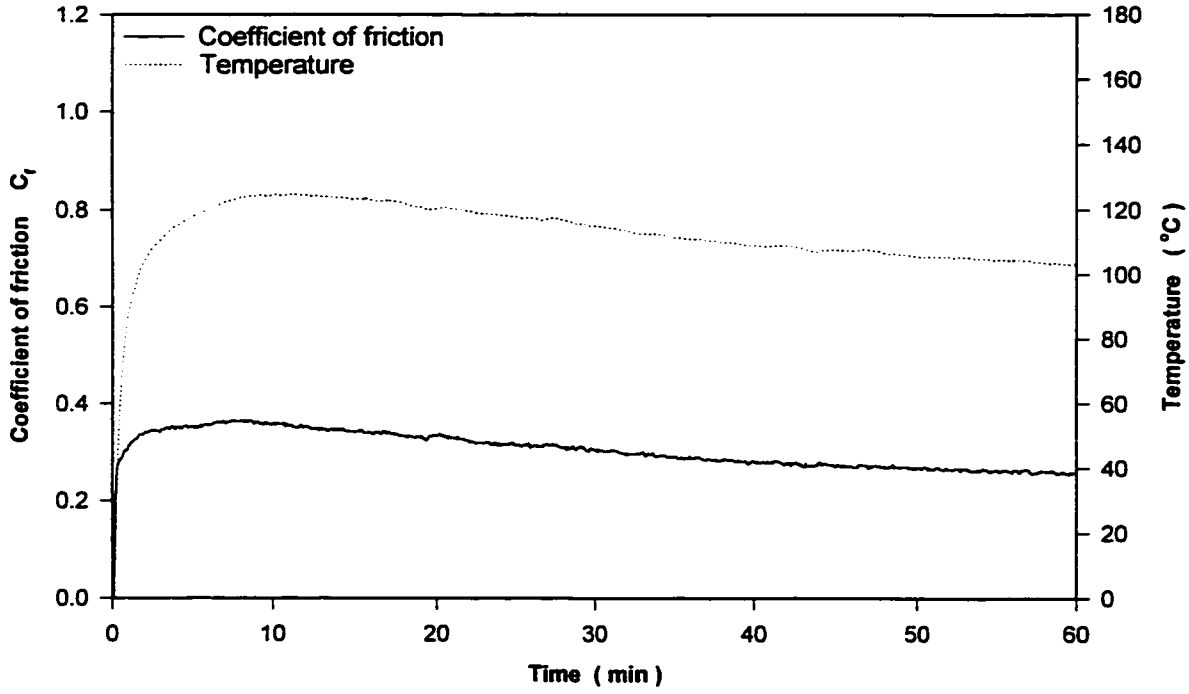

Figure 5.12 Friction coefficient and contact temperature of PTFE sliding against steel in discontinuous contact at 5 m/s under 200 N load

Figure 5.13 UHMWPE specimen after 50 min. in contact with steel inserts in discontinuous contact test at 5 m/s under 200 N load

Figure 5.14 UHMWPE specimen after 60 min. in contact with steel inserts in discontinuous contact test at 5 m/s under 200 N load

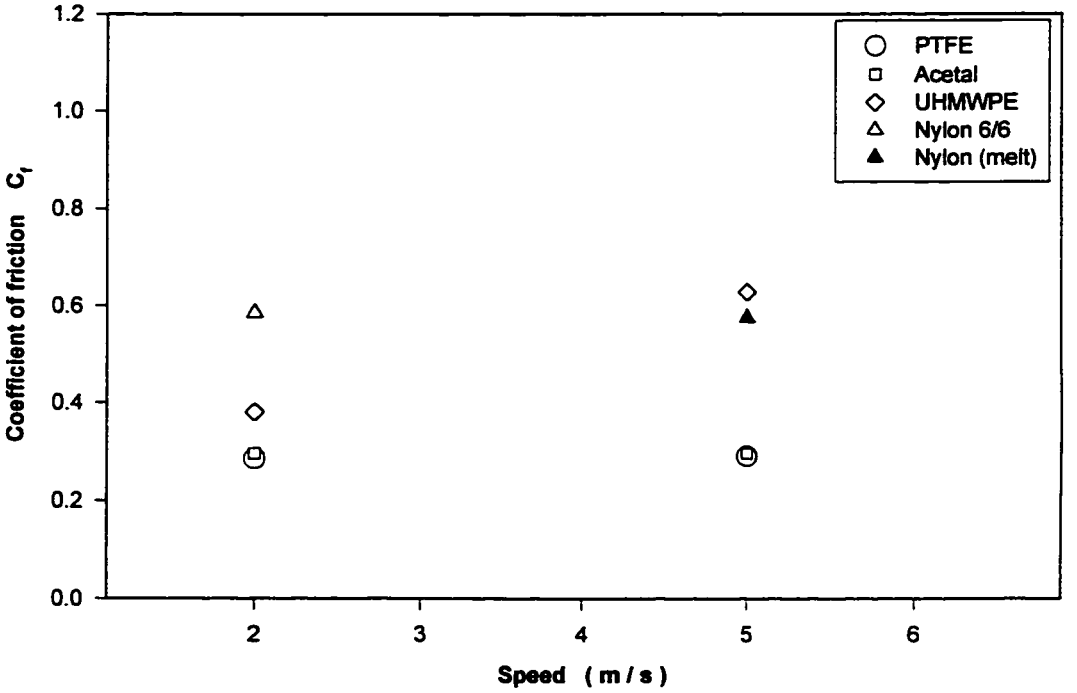

Figure 5.15 The friction coefficient of different materials sliding against steel in discontinuous contact at different speeds under 200 N load

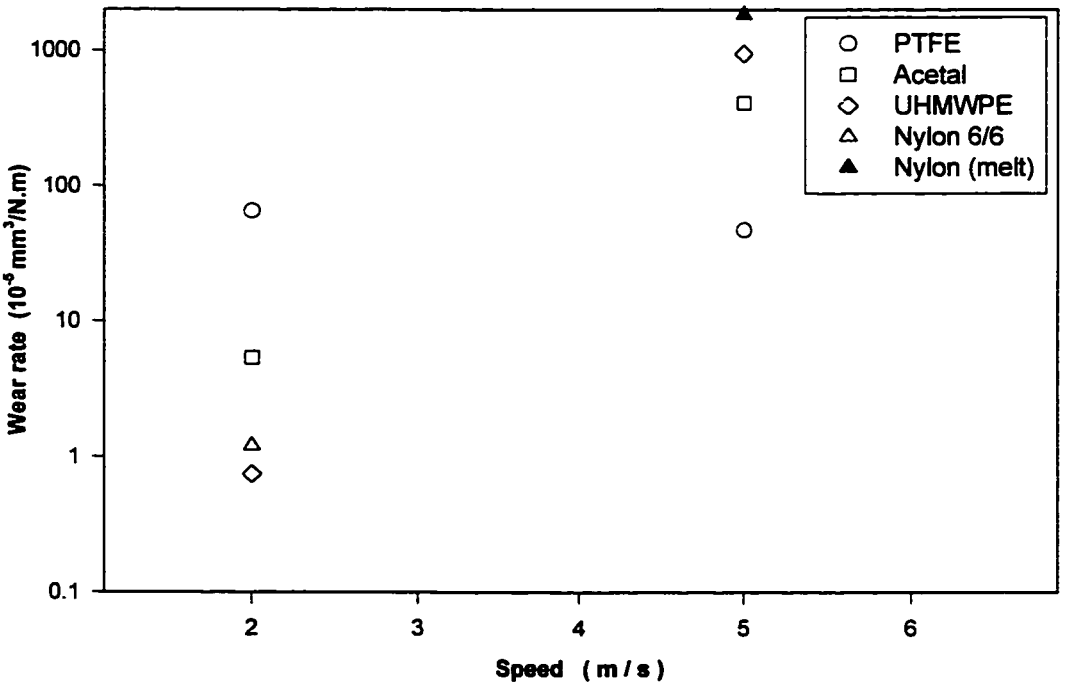

Figure 5.16 The wear rate of different materials sliding against steel in discontinuous contact at different speeds under 200 N load

Table 5.3 Coefficient of friction, contact temperature and wear rate in discontinuous contact

	PTFE		Acetal		UHMWPE		Nylon 6/6	
Speed (m/s)	2	5	2	5	2	5	2	5
Mean C_f	0.285	0.290	0.295	0.295	0.380	0.628	0.585	0.575*
Max. C_f	0.320	0.370	0.500	0.390	0.430	0.735	0.945	0.810*
Min. C_f	0.270	0.245	0.195	0.240	0.240	0.260	0.220	0.410*
S_d C_f	0.005	0.03	0.03	0.02	0.025	0.08	0.15	0.07*
Mean Temp.	65.2	109	65.3	100	72.0	170	111	128*
Max. Temp.	78.0	125	80.25	111	98.0	188	136	158*
S_d Temp.	3.00	2.90	6.25	12.0	5.90	20.2	19.5	10.8*
Δ w	2.04	3.68	0.11	25.72	<0.01	31.82	0.02	18.86*
k	65.3	47.1	5.37	408	<0.75	950	1.21	1840 ↑

Temp. → Temperature in °C,

Δ w → Weight loss in gr.,

k → Specific wear rate in 10^{-5} $mm^3/N.m$

↑ → Very high wear rate and/or surface melting leading to test termination

* → Values affected by test termination (high wear rate and/or surface melting)

The transfer film detected is the same as in continuous contact for all materials, but with higher wear rates. At 5 m/s tests, the wear rate decreases for PTFE where it increases for all the others; a very high wear rate is detected for Acetal and UHMWPE and surface melting occurs with Nylon 6/6.

The coefficient of friction detected for all materials is in the range of that obtained in variable speed tests. Generally, the coefficient of friction is higher than that of continuous contact except for Nylon 6/6. It is suggested that the uniform distribution of the contact pressure eliminates the possibility of the high pressure which may develop in continuous contact as described in section 4.3.4. Furthermore, the polymer surface temperature stabilizes much slower than the metallic surface. It is suggested that this may contribute in the delay detected between metallic surface reaching the polymer melting temperature and the actual surface melting. Nevertheless, the unique performance of UHMWPE at contact temperature higher than its melting point needs further investigation.

5.4 Conclusion

Tests were conducted on four different materials in contact with steel counterface at a relatively large surface in discontinuous contact. It is concluded that in general, the coefficient of friction is slightly higher in discontinuous contact except for Nylon 6/6, whereas the Pv limits are much lower. This can be related to the lower metallic contact surface which limits the heat dissipation in both conduction and convection. PTFE has the highest Pv limit followed by UHMWPE, Acetal and finally Nylon 6/6.

Studying the wear rate of different materials at low speed, it is found that PTFE has the highest wear rate followed by Acetal, Nylon 6/6 where UHMWPE exhibits a very low wear rate. The wear mechanisms are the same as in continuous contact for all materials, but with higher wear rates. At high speed tests, the wear rate decreases for PTFE where it

increases for all the others. The unique performance of UHMWPE at contact temperature higher than its melting point needs further investigation.

It is suggested that the wear mechanisms of polymers when exceeding their Pv limits would affect greatly the performance of the machine components involved. For PTFE and Acetal, the material may wear rapidly with relatively small debris or melt without depositing a film on the counterface surface; this would not affect the counterface materials and might take certain time before contact failure occurs. For UHMWPE, the material maintains its stability for a certain time, after which a very high wear rate occurs and large particles are smeared out from the surface. The particles adhere to the counterface surface and both surfaces may weld together after the machine is stopped. As for Nylon 6/6, the large film deposited on the counterface surface, with high polymer surface distortion induce high vibrations in the system which may cause mechanical problems. The large film deposited may also be projected from the surface, which may cause certain damage to other components of the machine.

CONCLUSIONS

A tribometer is designed for testing the friction and wear of polymer-metal contact at high sliding speed. The machine has the capacity to withstand long duration tests with large contact surfaces (7000 mm^2) for both continuous and discontinuous contact. The system control is calibrated, tested and found to be satisfactory for friction and wear testing under high speed of up to 60 m/s and loads of 600 N with high rigidity and dynamic stability. The machine has also the capacity to work under lubricated conditions with and without abrasive particles. Two different sets of pneumatic cylinders are installed and calibrated for low and high load applications. The system computer allows an on line control and monitoring of the load, the coefficient of friction and the temperature distribution at different points of contact. It is also equipped with safety features for high wear rates and to monitor excessive temperature rise, high friction force and bearing temperatures.

Although the machine is designed mainly to test polymer-metal contact, it has also the capacity to test any combination of materials with minor changes in specimen fixations. Many dry and lubricated sliding applications can be studied using the new tribometer such as disc brakes, wheels on pavements, snowmobile sliders and thrust bearings in hydrodynamic or hydrostatic regimes.

A simplified equation is developed to calculate the heat generated by friction and dissipated by conduction and convection. The equation is used to validate the temperature measurements of the tribometer by applying it on friction and temperature data from different tests. The correlation between the heat generated and the heat dissipated demonstrated the accuracy of the friction and temperature measurements in the cases where limited film deposition in likely to occur. The accuracy of the temperature measurement increases with increasing the sliding speed. Another technique is used to measure the contact temperature.

A fine thermocouple is inserted under the polymer specimen near the surface to evaluate the actual contact temperature. The tests confirmed that the difference between the temperature measured under the metallic specimen and the actual contact temperature is in the order of the thermocouples accuracy which is ± 2°C. On the other hand, thick film deposition would affect largely the accuracy of the temperature measurement.

Tests were conducted on four different materials in contact with steel counterface at relatively large surfaces in continuous contact. Those tests showed that PTFE has the lowest friction coefficient and the highest Pv limit wich exceeds largely that reported in literature. The film transfer of this material decreases the adhesion force between both surfaces in contact. In addition, the film detaches easily from the surface, resulting in high wear rate, and acts as a smooth lubricant which leads to a very low coefficient of friction.

Acetal has also a relatively low coefficient of friction with relatively high Pv limits. Its wear mechanism is similar to PTFE. However, it is suggested that its higher surface hardness is responsible for its lower wear rates and higher coefficient of friction with respect to PTFE.

UHMWPE exhibits the minimum wear rate at moderate speeds but with lower Pv limits than PTFE and Acetal. This material deposes a very thin film which adherers strongly to the metallic surface. This leads to a relatively low coefficient of friction and a very low wear rate. On the other hand, its relatively low Pv limits can be related to the material low melting temperature. The material maintains its consistency up to very high contact temperature although very high wear rate and severe surface damage occurs.

Nylon 6/6 has both the highest coefficient of friction and the lowest Pv limits. At low sliding speed, no film transfer is detected on the metallic surface. This material rigidity and

high surface hardness may be the cause of its high coefficient of friction at low speeds. On the other hand, subsurface melting is likely to occur at high sliding speed and the thick film deposition affects largely the temperature measurement.

In general, at high sliding speed, the coefficient of friction and the wear rate decrease with increasing speed up to the material Pv limit. Also, the Pv limits calculated are much larger than that reported in literature. The performance of those materials was directly related to the nature of the transfer film deposed at different speeds and their mechanical characteristics stability at different contact temperatures. Very low coefficient of friction are recorded at high sliding speed. The effect of the applied load on the friction coefficient at high sliding speed is not conclusive and depends on the materials in contact. It is also concluded that the wear rate decreases with increasing the contact temperature.

When exceeding the polymer Pv limit, it is found that the coefficient of friction does not decrease and very high wear rates occur. This contradiction with the thermal control regime of friction model may be attributed to the large contact surface and the nonuniform wear distribution along the surface which limits the lubrication effect of the molten surface. Also, the real surface of contact increases due to the high temperature developed leading to a significant increase in the adhesion force.

In discontinuous contact, the coefficient of friction is slightly higher than that in continuous contact, except for Nylon 6/6, whereas the Pv limit is much lower. This can be related to the lower metallic contact surface which limits the heat dissipation in both conduction and convection. This reveals the importance of the contact surface on determining the polymer Pv limits. On the other hand, the wear mechanisms are the same as in continuous contact for all materials, but with higher wear rates. PTFE had the highest Pv limit followed by UHMWPE, Acetal and finally Nylon 6/6. The unique performance of

UHMWPE at discontinuous contact, when the contact temperature exceeds its melting point, needs further investigations.

Finally, it is suggested that the wear mechanisms of polymers when exceeding their Pv limits would affect greatly the performance of the machine components involved. For PTFE and Acetal, the material may wear rapidly with relatively small debris or melt without depositing a film on the counterface surface; this would not affect the counterface materials and might take certain time before contact failure occurs. For UHMWPE, the material maintains its stability for a certain time, after which a very high wear rate occurs and large particles are smeared out from the surface. The particles adhere to the counterface surface and both surfaces may weld together after the machine is stopped. As for Nylon 6/6, the large films deposited on the counterface surface with high polymer surface distortion induce high vibrations in the system which may cause mechanical problems. The large film deposited may also be projected from the surface, which may cause certain damage to other components of the machine.

FUTURE WORK

There are clearly many tests and analysis which can be conducted to study the friction and wear behavior of polymers at high sliding speed. The following are some proposed future works to complete the friction and wear analysis at high sliding speed presented in the present document:

- Performing tests at various contact area from 200 to 7000 mm^2 to study the effect of the contact area on the friction and wear of polymers at high sliding speed.

- Performing tests at applied loads of 300 to 600 N to investigate the effect of both speed and load on the Pv limit of different polymers. The larger pneumatic cylinders can be used. A power transmission ratio of 2:1 is needed to increase the friction torque capacity of the system.

- Measuring the polymer surface temperature in discontinuous contact tests to compare the polymer and metallic surface temperatures and to investigate the performance of UHMWPE at surface temperature higher than its melting temperature.

- Developing a similar simplified energy equation for discontinuous contact and applying it on the friction and temperature data to evaluate the effect of the nature of contact on the heat dissipation.

- Performing dynamic mechanical thermal analysis (DMTA) on the polymers to study the effect of the variation of the elastic modulus with temperature on the friction coefficient.

The contact temperature has predominant effect on the tribological behavior of polymers. It is proposed to install a controlled temperature casing for the tribometer to realize tests at moderate speeds and controlled temperature. The temperature range needed is between -20 °C and 200 °C.

It is also proposed to develop a generalized form of the heat transfer equation which would include the heat convection of the disc to the surroundings. This equation would provide a direct relation between the friction coefficient and the contact temperature for different speeds and loads.

REFERENCES

AKKOK, M., ETTLES, C.M. and CALABRESE, S.J. (1987 Jul.). Parameters affecting the kinematic friction of ice. Journal of Tribology, 109, 552-561.

An American national standard: Surface roughness, ANSI/ASME B46.1-1985.

ANDERSON, J.C. (1982). High density and ultra-high molecular weight polyethylene: their wear properties and bearing applications. Tribology International, 15, 43-47.

ARCHARD, J.F. (1959). The temperature of rubbing surfaces. Wear, 2, 438-455.

ATKINSON J.R., BROWN, K.J. and DOWSON, D. (1978). The wear of Ultrahigh-Molecular-Weight Polyethylene Part I: The wear of isotropic Polyethylene against dry stainless steal in unidirectional motion. Journal of Lubrication Technology, 100, 208-218.

BARRETT, G.W., STACHOWIAK, G.W. and BATCHELOR, A.W. (1992). Effect of roughness and sliding wear on the wear and friction of UHMWPE. Wear ,153, 331-350.

BEJAN, A. (1989 Feb.). The fundamentals of sliding contact melting and friction. Journal of Heat Transfer, 111, 13-20.

BENABDALLAH, S.H. (1991(a)). The running-in and steady-state coefficient of friction of some engineering thermoplastics. Polymer Engineering and Science, 33, 2, 70-74.

BENABDALLAH, S.H. and TREHEUX, D. (1991(b)). Friction and wear of ultrahigh molecular weight polyethylene against various new ceramics. Wear, 142, 43-56.

BICEGO, V., FIGARI, A. and POLETTI, G. (1981 Jul.). Lubrication of a melting slider under nonisothermal conditions. Journal of Lubrication Technology, 103, 436-442

BLANCHET, T.A. and KENNEDY, F.E. (1989). The development of transfer films in ultrahigh molecular weight polyethylene/stainless steel oscillatory sliding. STLE, Tribology Transactions, 32, 3, 371-379.

BLAU, P.J. (1989). Static and kinetic friction coefficients for selected materials. Friction, lubrication and wear technology, ASM Handbook, 18, 70-75.

BLOCK, H. (1937). General discussion on lubrication. Institution of mechanical engineers, London,, 2, 222.

BÖHM, H., BETZ, S. and BALL, A. (1990). The wear resistance of polymers. Tribology International, 23, 6, 399-406.

BOWDEN, F.P., and PEKSSON, P.E. (1961). Deformation, heating and melting of solids in high-speed friction. Proc. Roy. Soc., A, 260, 433-458.

BRISCOE, B. J., POGOSIAN, A. K. and TABOR, D. (1974). The friction and wear of high density polyethylene: the action of lead-oxide and copper-oxide fillers. Wear, 27, 19-34.

BROWN, K.J., ATKINSON, J.R. and DOWSON, D.(1982). The wear of Ultrahigh-Molecular-Weight Polyethylene Part I: The effects of reciprocating motion, orientation in the Polyethylene and preliminary study of the wear of polyethylene against itself. Journal of Lubrication Technology, 104, 17-22.

BUDINSKI, K.G.(1989). Laboratory testing methods for solid friction. Friction, lubrication and wear technology, ASM Handbook, 18, 45-58.

BURTON, R.A. (1980). Thermal deformation in frictionally heated contact. Wear, 59, 1-20.

BYETT, J.H. and ALLEN, C. (1992). Dry sliding wear behavior of polyamide 66 and polycarbonate composites. Tribology international, 25, 4, 237 - 246.

CHALLEN, J.M. and DOWSON, D. (1976). The calculation of interfacial temperatures in a pin on disc machine. Proc. Of the 3rd Leeds-Lyon Symp. on tribology, Wear of non-metallic Materials, Mechanical Engineering Publications, London, 87-93.

CLARK, D.T. and FEAST, W.J.. (1978). Polymer Surfaces, John Wiley & Sons Ltd.

CLARKE, C.G. and ALLEN, C. (1991). The water lubricated sliding wear behaviour of polymeric materials against steel. Tribology International, 24, 2, 109-115.

COOPER, J.R. and DOWSON, D.(1991). Birefringent studies of polyethylene wear specimens and acetabular cups. Wear, 151, 391-402.

COOPER, J.R., DOWSON, D. and FISHER, J.(1993). Macroscopic and microscopic wear mechanisms in Ultra-high molecular weight Polyethylene. Wear, 163, 378-384.

DEANIN, R.D. and PATEL, L.B. (1980). Structure, properties and wear resistance of polyethylene. ASM Materials Science Seminar, Pittsburgh, Pensylvinia, 569- 583.

DOWSON, D., ATKINSON, J.R. and BROWN, K. (1974). The wear of high molecular weight polyethylene with particular reference to its use in artificial human joints, Polymer Science and Technology, 5B, 533-551.

DOWSON, D. and HARDING R.T.(1982). The wear characteristics of Ultrahigh-Molecular-Weight Polyethylene against a high density alumina ceramic under wet (distilled water) and dry conditions. Wear, 75, 313-331.

DUMBLETON, J. H. and SHEN, C. (1976). The wear behavior of ultrahigh molecular weight polyethylene. Wear, 37, 279-289.

ECKERT, E.R. and DRAKE, R.M. (1972). Analysis of heat and mass transfer. Mc Graw-Hill.

EISS N.S., WOOD, K.C., HEROLD, J.A. and SMYTH, K.A. (1976 Apr.). Model for the transfer of polymer to rough, hard surfaces. Journal of Lubrication Technology, 101, 212-218

EISS, N. (1983). Wear of nonmetallic materials. CRC Handbook of lubrication, II, CRC press, 185-200.

Engineering plastics (1987). Engineering materials handbook, vol. 2, ASM international.

ETTLES, C.M. (1985 Oct.). The thermal control of friction at high sliding speed. ASME/ASLE Joint Lubrication Conference, Atlanta, 85-Trib-37, 1-7.

ETTLES, C.M. (1985). Heat generation and friction in rotating bands. ASLE Transactions, 29, 3, 312-320.

ETTLES, C.M., (1985). Possible flash temperatures in slider and recording disk transient contact. ASLE Transactions, 29, 3, 321-328

ETTLES, C.M. (1986). Polymer and elastomer friction in the thermal control regime. ASLE Transactions, 30, 2, 149-159.

ETTLES, C.M. and JUI, H.S.(1988). The influence of frictional heating on the sliding friction of elastomers and polymers. Journal of Rubber Chemistry and Technology, 61, 119-136.

ETTLES, C.M. and HARDIE, C.E. (1988 Oct.). The friction of some Polymers and Elastomers at high values of Pressure x Velocity. Journal of Tribology, 110, 678-684.

EVANS, D.C. and SENIOR, G.S. (1982). Self-lubricating materials for plain bearings. Tribology International, 15, 43-248.

FOWLER, A.J. and BEJAN, A. (1993). Contact melting during sliding on ice, International Journal of Heat and Mass Transfer , 36, 5, 1171-1179.

FUSARO, R.L. (1982). Geometrical aspects of the tribological properties of graphite-fibber-reinforced polyimide composites .National Aeronautics and Space Administration, TM-82757.

FUSARO, R.L. (1983). Friction, wear, transfer, and wear surface morphology of Ultrahigh-Molecular-Weight Polyethylene. ASLE/ASME Lubrication conference, ASLE Preprint No. 83-LC-3A-2.

FUSARO, R.L. (1990). Self-lubricated polymer composites and polymer transfer film lubrication for space applications. Tribology International, 23, 2, 105-122.

HARSCHNITZ, R., SCHEETZ, H. and HARTING, S. M. (1992 Feb.) Plastics for high temperature bearing and wear applications. International congress & exposition, Detroit, Michigan, paper 920505.

HOLMBERG, K. and WICKSTRÖM, G. (1987). Friction and wear tests of polymers. Wear, 115, 95-105.

HORNBOGEN, E. and SCHÄFER, K. (1980). Fundamentals of friction and wear of materials. ASM Materials Science Seminar, Pittsburgh, Pensylvinia, 409-438.

HUTCHINGS, I.M. (1992). Tribology: the friction and wear of engineering materials. CRC press.

JONES, W.R. and HADY, W.F. (1981). Effect of γ irradiation on the friction and wear of Ultrahigh Molecular Weight Polyethylene. Wear, 70 , 77-92.

KENNEDY, F.E. (1981 Jan.). Surface temperatures in sliding systems. Journal of Lubrication Technology, 103, 90-96.

KRAFFT, J. M. (1955 Oct.). Surface friction in ballistic penetration. Journal of Applied Physics, 26, 10, 1248-1253.

KRASNOV, A. P., MAKINA, L.B. and MIT, V.A. (1996 Jan.). Tribochemical view on friction ultra-high molecular weight polyethylene (UHMWPE) in different media. Tribology: Solving friction and wear problems, 10th international colloquium. Stuttgart, Ostfilden, Germany.

LANCASTER, J.K. (1971). Estimation of the limiting Pv relationships for thermoplastic bearing materials. Tribology International, 4, 82-86.

LANCASTER, J.K. (1972). Polymer-based bearing materials: The role of fillers and fibre reinforcement. Tribology International, 5, 49-255.

LANCASTER, J.K. (1973). Dry bearings : A survey of materials and factors affecting their performance. Tribology International, 6, 219-251.

LLOYD, A.I. and NOËL, R.E.J. (1988). The effect of counterface roughness on the wear of UHMWPE in water and water-in-oil emulsion. Tribology International, 21, 83-88.

MARCUS, K., BALL, A. and ALLEN, C. (1991). The effect of grinding direction on the wear of the transfer film formed during the sliding wear of ultrahigh molecular weight polyethylene. Wear, 151, 323-336.

MARCUS, K. and ALLEN, C. (1993). Effect of fillers on the friction and wear behavior of ultrahigh molecular weight polyethylene during water-lubricated reciprocating sliding. Wear, 163, 1091-1102.

MARSCHER, W. D. (1982). Thermal versus mechanical effects in high speed sliding. Wear, 79, 129-143.

MARTINELLA, R., GIOVANARDI, S. and PALOMBARINI, G. (1989). Wear of ultrahigh molecular weight polyethylene sliding against surface-treated Ti6A14V, AISI 316 Stainless Steel and Vitallium. Wear, 133, 267-279.

MC LAREN, K.G. and TABOR, D. (1965). Friction of Polymers and engineering materials: Influence of speed, temperature and lubricants. Wear, 8, 79-83.

MENS, J.W.M. and Gee, A.W. J. (1991). Friction behavior of 18 polymers in contact with steel in environment of air and water. Wear, 149, 255-268.

MONTGOMERY, R.S. (1976). Friction and wear at high sliding speeds. Wear, 36, 275-298.

OKSANEN, P. and KEINONEN, J. (1982). The mechanism of friction of ice. Wear, 78, 315-324.

PADOVAN, J. and PADOVAN, P.(1994). Modeling wear at intermittently slipping high speed interfaces. Journal of Computers and Structures, 52, 4, 792-812

RAMASUBRAMANIAN, N., KRISHNAMURTHY, R. and MALHOTRA S.H. (1993). Tribological characteristics of filled Ultrahigh-Molecular-Weight Polyethylene, Wear, 162, 631-635.

SEEDHOM, B.B., DOWSON, D. and WRIGHT, V. (1973). Wear of solid phase formed high density polyethylene in relation to the life of artificial hips and knees wear. Wear, 24,. 35-51.

SLIFKA, A.J., CHAUDHURI, D.C., COMPOS, R. and SIEGWARTH, J.D. (1993). A tribometer for measurements in hostile environments. Wear , 170, 39-44.

SPALDING, M.A., HYUN, K.S., JENKINS, S.R. and KIRKPATRICK, D.E. (1995 MID-Dec.). Coefficients of dynamic friction and the mechanical melting mechanism for vinylidene chloride copolymers. Polymer Engineering and Science, 35, 23, 1907-1916.

ASTM standard test method for static kinetic coefficients of friction of plastic film and sheeting. ASTM D-1894-93.

ASTM standard test method for kinetic coefficient of friction of plastic solids. ASTM D-3028-93.

ASTM standard test method for wear testing with pin-on-disk apparatus. ASTM G-99-95.

STIFFLER, A. K. (1984 Jul.). Friction and wear with fully melting surface. Journal of Tribology, 106, 416-419.

SVIRIDENOK, A. and MESHKOV, V.V. (1996 Jan.). On friction behavior of polymers and composites at high -speed sliding.Tribology: Solving friction and wear problems, 10th international colloquium. Stuttgart, Ostfilden, Germany.

TANAKA, K. and UCHIYAMA Y. (1974). Friction, wear and surface melting of crystalline polymers. Polymer Science and Technology, 5B, 499-531.

TANAKA, K.(1980). Friction and wear of semicrystalline polymers sliding against steel under water lubrication. Journal of Lubrication Technology, 102, 526-533.

TETREAULT, D.M. and KENNEDY F.E. (1989). Friction and wear behavior of ultra high molecular weight polyethylene on Co-Cr and Titanium alloys in dry and lubricated environments. Wear, 133, 295-307.

THORP, J.M. (1981). A novel tri-pin-on disc tribometer designed to retain lubricants. Tribology International, 14, 121-125.

THORP, J.M. (1982). Abrasive wear of some commercial polymers. Tribology International, 15, 59-68.

THORP, J.M. (1982). Friction of some commercial polymer-based bearing materials against steel. Tribology International, 15, 69-74.

WATANABE, M. and YAMAGUCHI, H. (1986). The friction and wear properties of nylon. Wear, 110, 379-388.

WILSON, W.R. (1976 Jan.). Lubrication by a melting solid. Journal of Lubrication Technology, 98, 22-26

WOLVERTON, M.P., THERBERGE, J.E. and MCCADDEN, K.L. (1983). Tribological properties of reinforced and lubricated thermoplastic composites at elevated temperatures. 38th Annual Conference, Reinforced Plastics/ Composites Institute, The society of the Plastic Industry Inc., 15-B, 1-8

YOON, E., KONG, H., KWON, O. and OH, J. (1997). Evaluation of frictional characteristics for a pin-on-disc apparatus with different dynamic parameters. Wear, 203-204, 341-349.

APPENDIX I

THERMAL CONTROL REGIME THEORY

To clarify the thermal control of friction theory, Ettles (1985) considered Blok's model (1937) of a heat source Q (W/m^2) traveling a half space at a certain speed v (m/s). The temperature rise ΔT can be presented by,

$$\Delta T = 2\ Q\ (\frac{t}{\pi\ k_c\ \rho\ c})^{1/2} \qquad \text{A.1}$$

Where t(s) is the contact period. For a contact length B (m), the equation becomes,

$$\Delta T = 2\ Q\ (\frac{B\ /\ v}{\pi\ k_c\ \rho\ c})^{1/2} \qquad \text{A.2}$$

where k_c is the coefficient of thermal conductivity (W/m °K), ρ is the density (kg/m^3) and c is the specific heat (J/kg °K)

In friction the source strength Q is given by $Q = C_f\ P\ v$, so that the maximum flash temperature of the contact, and assuming all heat flows to the half-space, can be given by,

$$\Delta T_{max} = 2\ C_f\ P\ (\frac{B\ v}{\pi\ k_c\ \rho\ c})^{1/2} \qquad \text{A.3}$$

The partitioning of heat into the slider and the counterface has been the subject of many investigations. Usually a partition factor K is used to define a flux $K\ C_f\ P\ v$ entering the counterface. In moderate sliding speed applications this factor is found to be about 0.5. In the case of a thermal controlled regime at high Peclet number, $Pe = (\rho\ c\ /\ k_c)\ (v\ B\ /\ 4)$, most of the heat generated is dissipated by the moving counterface and the partition factor K approaches unity (Ettles, 1986). Also in thermoplastics contact, where a film deposition

on the metallic surface is likely to occur, the value of k μ c are always attributed to the polymeric surface. Several authors developed Block's model for different configurations and boundary conditions. In Archard (1959) model the average flash temperature of the contact is given by,

$$\Delta T_{av} = 1.22\ C_f\ P\ (\frac{B\ v}{\pi\ k_c\ \rho\ c})^{1/2} \qquad \textbf{A.4}$$

Applying Archard equation to high speed contact of a nylon block on steel counterface, and assuming reasonable value of friction coefficient, Ettles obtained values of ΔT_{av} in the order of 600 °C which exceeds by 335 °C the Nylon melting point. Knowing that all the parameters in the equation are fixed, the only available option is a decrease in the friction coefficient.

Applying the theory of thermal controlled friction, and assuming that a maximum allowable temperature in a sliding contact can be characterized by T_f and that the surface temperature of the approaching track is T_a, a relation between coefficient of friction and Pv in the form $\mu = f(P\ v^{1/2})$ is established as follows,

$$\mu = C\ (\frac{\pi\ k_c\ \rho\ c}{B\ v})^{1/2}\ (\frac{T_f - T_a}{P}) \qquad \textbf{A.5}$$

where C is a constant depending on the geometry of the contact.

The characteristic temperature was defined as the surface temperature above which the material cannot remain in the contact surface, since it is easily abraded and removed by shearing. This implies that T_f is the softening temperature of the material. In polymers, this temperature is usually in the order of the surface melting temperature (Ettles, 1988).

On the other hand, Ettles (1988) stated that the sudden increase of friction coefficient,

detected just before the thermal control regime, could be the result of the increase of the contact area, eventually to the apparent area.

In later research Ettles (1988) presented a more general form of the equation, relating directly the friction coefficient with load and speed, in the form:

$$C_f = I\, v^a\, W^b \qquad \textbf{A.6}$$

Where I is a correction factor, a and b are constants depending on the materials and the nature of the surfaces in contact.

A schematic representation of the relation between friction coefficient, speed and load, in a thermal controlled regime, is represented in figure 1.18. Examples applied to different materials are presented in figures 1.19-1.24.

The value of P is a very important part of the relation. This value, which determines the relation between μ and W in the thermal control regime theory, depends on the nature of contact.

For full contact friction (ex: projectile in rotating bands) the value of P approaches the uniaxial yield strength of the material so that $P = W/A_{app}$.

where: A_{app} is the apparent area of contact.

Applying the equation given by Block & modified by Ettles, the Coefficient of friction becomes inversely proportional to the load applied; i.e. $C_f \propto W^{-1}$

In completely plastic contact the value is taken as the surface hardness $P = P_H$

For partial contact this value depends on the number of points or asperities in contact and their hardness P_H so that

$$W = \pi/4\ B^2\ P_H\ n \qquad \text{or} \qquad B = (4\ W/\pi\ P_H\ n)^{1/2}$$

where: B is the diameter of the contact area and the contact length

n is the number of asperities in contact.

Then, for partial contact: $C_f \propto P_H^{-3/4} . (n/W)^{-1/4}$ or P_H is constant, hence: $C_f \propto W^{-1/4}$

In his study of the parameters affecting the kinematic friction on ice, Akkok (1987) have used the previous equation in the form:

$$C_f = \frac{C\ (T_f - T_a)}{P} \left(\frac{k\ \rho\ c}{v\ b}\right)^{1/2} \qquad \textbf{A.7}$$

He then used the partial contact form which is:

$$C_f = \frac{1.88\ (T_f - T_a)}{P_H^{3/4}} \left(\frac{k\ \rho\ c}{v\ b}\right)^{1/2} \left(\frac{n}{W}\right)^{1/4} \qquad \textbf{A.8}$$

The value of n used is unity since this gives the simplest and best results as presented in previous work by Ettles (1985) and others. He compared his results with those theoretical models and found a fair agreement. Then he derived another general model in the form:

$$C_f = D\ v^d\ W^e\ (T_f - T_a)^f\ (k\ \rho\ c)^g \qquad \textbf{A.9}$$

He applied it in the contact of different materials on Ice (steel, rubber, nylon and glass). He found that all exponential coefficients vary significantly depending on both slider and contact materials.

Using finite difference model, Ettles proved the theory of limited maximum temperature after which the coefficient of friction becomes a dependent parameter.

APPENDIX II

INSTRUMENTATIONS

DC Motor:

Model: brushless DC drive 184 T from POWERTEC

Power: 15 HP

Speed: 0 - 3600 rpm

Torque: 47.5 N.m (35 lb.ft) maximum

Control: DIGIMAX IV micro-processor

Pneumatic pistons

Large pistons:

Model: 1 1/16" adjustable stroke SR 092-AV from BIMBA

Spring force: 13.3 N retracted and 26.7 N extended

Power factor: load (N) = 6.2 x air pressure (kPa)

Small pistons:

Model: Airpel Anti-stiction air cylinder E16 x 2.0N from FAUVER

Spring force: 0.27 N (retracted or compressed)

Power factor: load (N) = 2.2 x air pressure (kPa)

Servo pressure control card:

Model: SPCJR - 0E10 - 0G100 from BUZMATICS Incorporation

Voltage input: 0 - 10 V

Output range: 0 - 700 kPa (0 - 100 psi)

Linearity: 0.1% full scale

Friction load cell:

Model: Low profile bending beam load cell LCDA-150 from OMEGA

Capacity: 150 lb (667 N)

Accuracy: 0.037% full scale

linearity: 0.03% full scale

Slip ring:

Model: SR 10 from MICHIGAN scientific corporation

RPM: 6000

Acquisition card:

Model: AT-MIO-64E-3 from National Instruments corporation

speed: 333 kHz

Thermocouples:

Model: Type J (Fe and Cu-Ni), from OMEGA

Range: 0 - 750 °C

Precision: ±2.2 °C

Amplifier: Type J (10 mV / °C)

Model: Type K (Ni-Cr and Ni-Al), from OMEGA

Range: -200 °C to 1250 °C

Precision: ±2.2 °C

Amplifier: Type K (10 mV / °C)

Linear bearing:

Model: RSR 9WVMUU + 80 LM from THK

Air Atomizer:

model: 1/8 J - SUJ13A flat spray from Brooks

Air pressure: 69 - 690 kPa (10- 100 psi)

Water pressure: 69 - 414 kPa (10- 60 psi)

output range: 2.4 - 15.4 L/hr (0,53 - 3,41 gph)

Air pump:

Model:	1/3 HP from WEG
Power:	1/35 HP
Speed:	1745 rpm
Intake:	150 mm (8") diameter
Output:	150 mm (8") diameter

IMAGE EVALUATION
TEST TARGET (QA-3)

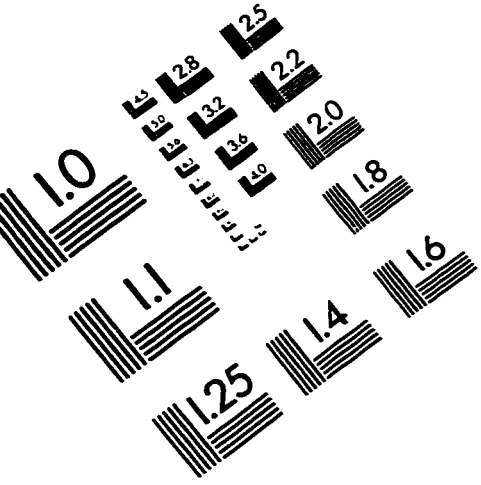

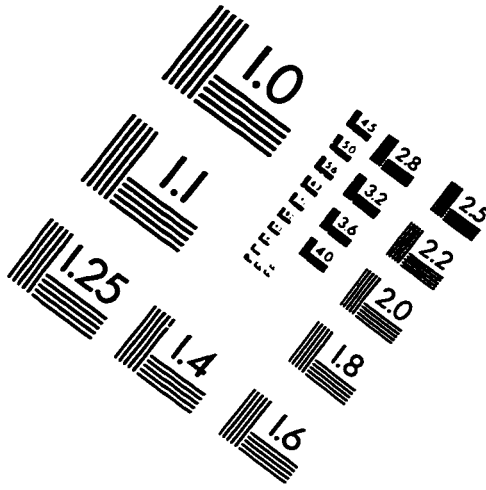

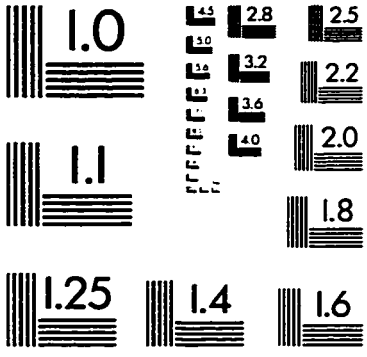

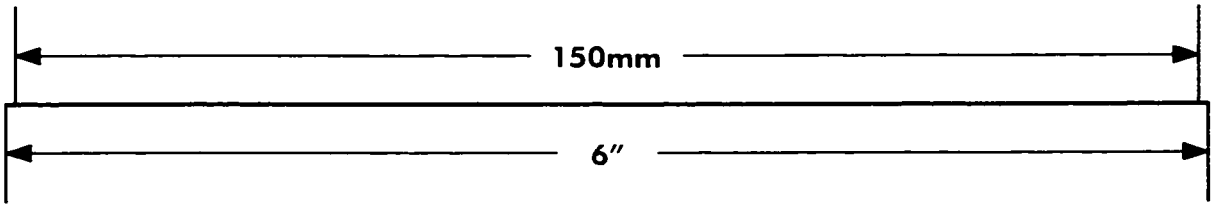

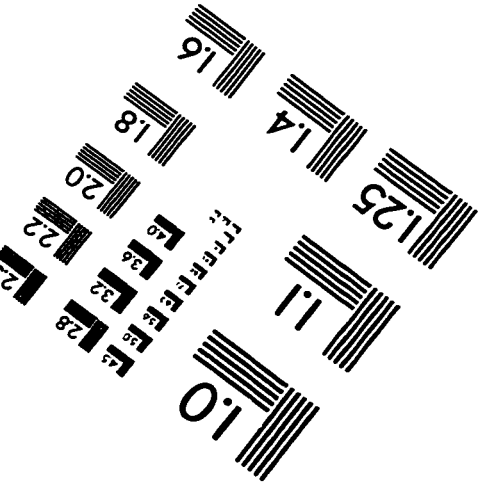

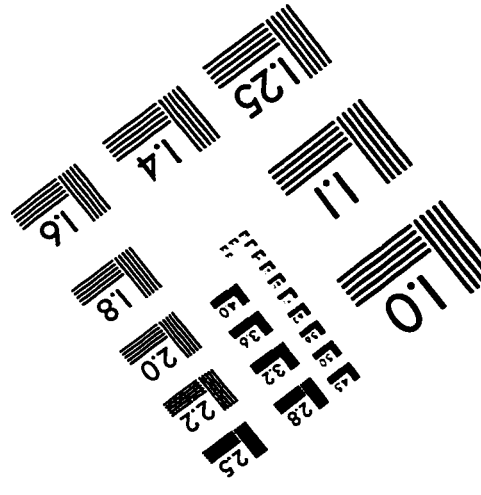

APPLIED IMAGE, Inc
1653 East Main Street
Rochester, NY 14609 USA
Phone: 716/482-0300
Fax: 716/288-5989